Indian and Northern Affairs Canada
Affaires indiennes et du Nord Canada

Contributions to the Geology of the Northwest Territories

VOLUME 3

Canada

1988

Volume 3

Contributions to the Geology of the Northwest Territories

Managing Editor, W.A. Padgham
NWT Geology Division
Northern Affairs Program
Yellowknife, NWT

©Minister of Supply and Services Canada 1988.
Available by mail from: NWT Geology Division,
Department of Indian Affairs and Northern Development,
Box 1500, Yellowknife, N.W.T. X1A 2R3.

Published under the authority of the
Hon. Bill McKnight, P.C., M.P.,
Minister of Indian Affairs and Northern Development,
Ottawa, 1988.

QS-Y040-030-EE-A1

90-01942/

This is the first volume of Contributions to be fully refereed, in accordance with the suggestion of academic representation on the Northwest Territories Mineral Exploration Liaison Committee (NWT MELC). Reviewers of the papers published herein include two or more of the following:

Dr. L.B. Aspler	Ottawa
Dr. R.W. Boyle	GSC, Ottawa
Mr. J.A. Brophy	NWT Geology Division, Yellowknife
Dr. E.M. Cameron	GSC, Ottawa
Prof. W.K. Fyson	University of Ottawa
Dr. W.A. Gibbins	NWT Geology Division, Yellowknife
Prof. A.M. Goodwin	University of Toronto
Dr. C.W. Jefferson	GSC, Ottawa
Dr. A.S. Judge	GSC, Ottawa
Prof. W.F.S. Kidd	State University of New York, Albany
Dr. J. King	GSC, Ottawa
Prof. R. Kretz	University of Ottawa
Prof. A.E. Lalonde	University of Ottawa
Prof. R. St.J. Lambert	University of Alberta
Prof. R.D. Morton	University of Alberta
Dr. W.A. Padgham	NWT Geology Division, Yellowknife
Dr. S.M. Roscoe	GSC, Ottawa
Prof. D.W.G. Smith	University of Alberta
Dr. D.L. Trueman	Highwood Resources, Vancouver
Dr. G.M. Yeo	GSC, Ottawa

The NWT Geology Division and the authors of the papers contained in this volume thank the referees for their valuable assistance.

Arnold Enge, John Brophy and Diane Gault assisted with proofreading. Northern Affairs Program Drafting Section staff redrafted some diagrams. Outcrop Ltd. staff provided valuable advice and assistance towards the design of the volume.

It is recommended that references to this volume be made as follows: Authors, 1988 Title, *in* Contributions to the Geology of the NWT, Vol. 3. NWT Geology Division, Yellowknife, NWT.

INTRODUCTION

This third volume of Contributions to the Geology of the NWT comprises papers written by researchers under contract to the Geology Division of the Northern Affairs Program (NAP) in Yellowknife. Such papers were previously included with the NAP's annual Mineral Industry Reports, but the volume of material currently being generated justifies a separate publication. The articles in this volume were submitted to fulfill program-funded contracts, but we would like to take this opportunity to encourage submissions for Volume 4 from other sources, especially from industry geologists whose experience exploring for mineral deposits in the NWT would make their contributions particularly valuable. Submissions in either official language should be forwarded to W.A. Padgham, Chief Geologist, Northern Affairs Program, Box 1500, Yellowknife, NWT X1A 2R3.

Ce troisième volume des contributions à la géologie des TNO comprend des études écrites par les chercheurs sous contrat au Programme des Affaires du Nord (PAN) en poste à Yellowknife. Ces études étaient auparavant incluses dans les Rapports de l'Industrie du Minéral publiés annuellement par le PAN. Cependant, le volume de matériel présentement généré justifié une publication séparée. Nous voulons profiter de cette occasion pour encourager tous les chercheurs, spécialement les géologues de l'industrie privée, à soumettre des articles de façon à completer un quatrieme volume. Les articles peuvent être soumis dans l'une ou l'autre des langues officielles a W.A. Padgham, Géologue en Chef, Programme des Affaires du Nord, C.P. 1500, Yellowknife, TNO, X1A 2R3.

CONTENTS

Stratigraphy and Structure of Tent Outlier, Nonacho Basin, District of Mackenzie
Lawrence B. Aspler 1

Geochemistry of Slave Province Volcanic Rocks: Yellowknife Belt
A.M. Goodwin 13

Stratigraphy and Structure of the Early Proterozoic Wilson Island Group of Great Slave Lake
B.J. Johnson 27

The Formation of Gold Deposits with Particular Reference to Archean Greenstone Belts and Yellowknife
I Geological Boundary Conditions and Metal Inventory
R. Kerrich and W.S. Fyfe 37

The Formation of Gold Deposits with Particular Reference to Archean Greenstone Belts and Yellowknife
II Source of hydrothermal fluids, alteration patterns and genetic models
R. Kerrich and W.S. Fyfe 63

Thrusting Between the Cameron River Greenstone Belt and the Sleepy Dragon Metamorphic Complex, Slave Province, District of Mackenzie
Timothy M. Kusky 97

The Petrotectonic Environment of Basalts of Point and Redrock Lakes, Slave Province NWT
Karen St. Seymour, Paul Budkewitsch and Stephen Kumarapeli 103

An Archean Ultramafic Lamprophyre, Yellowknife: Implications for Tectonics and Source Regions
Dave R. Webb and Robert Kerrich 115

Phosphate Mineralogy of the Yellowknife Pegmatite Field
M.A. Wise, R.E. Meintzer and P. Cerny 123

Geophysics and Permafrost
W.J. Scott 131

Contribution to the Geology of the Northwest Territories, Volume 3, 1988, NWT Geology Division, INAC, Yellowknife.

Stratigraphy and Structure of Tent Outlier, Nonacho Basin, District of Mackenzie

Lawrence B. Aspler
39 Muriel Ave., Ottawa, Ontario

Abstract

Mapping at a scale of 1:50,000 has confirmed that lower greenschist grade sedimentary rocks exposed in two belts between Tent and Whitefish Lakes, although highly strained, are part of the Nonacho Group. Lithostratigraphic correlation of units in the outlier is based on lithologic criteria, position of individual units in a sequence and comparison with those areas in the main basin in which low strain protolith can be traced into high strain equivalents. Basement rock types include amphibolite grade, isoclinally folded para (?) gneisses and a variety of pre- and post-isoclinal folding granitoid rocks. The basement/Nonacho unconformity is obscured by faults, typical of the high-strain western margin of the basin. Conglomeratic rocks are assigned to the basal breccia/conglomerate member of the Hjalmar Formation, and consist of angular to subrounded clasts of basement derivation set in an arkose matrix. Arkoses with local single pebble layers, heavy mineral bands and centimetre to decimetre scale pelitic layers represent the monomictic pebbly sandstone member of the Tronka Chua Formation. The Chief Nataway Formation consists of centimetre to decimetre scale mudstone/sandstone rhythmites. By analogy to better preserved equivalents in the main basin, this fining upward megasequence is inferred to represent a depositional system including talus slope, alluvial fan, braided stream, and lacustrine facies.

Structural trends in basement are generally concordant with contacts against the Nonacho Group, and strike northeast, with near-vertical dips. Narrow mylonite zones display gently plunging stretching lineations. Reliable kinematic indicators (C/S fabrics, shear bands, type 1 and type 2 asymmetric pull-aparts) are sparse but consistent, tentatively suggesting sinistral strike slip. Sheared rocks in the Catholic Lake area, previously reported to be rhyolites, are considered here to be mylonites developed at the expense of basement gneisses and granitoid rocks. Evidence of the earlier structural history preserved in Nonacho strata of the main basin (D_1 and D_2) was destroyed by pervasive D_3 overprinting in Tent Outlier. Primary layering is transposed to S_3 and all units display a strong S_3 fabric. Near-vertical northeast striking basement cover faults are considered to have been sites of (tentatively) sinistral strike slip. As with basement, kinematic indicators within the sediments are sparse but consistent and include C/S fabrics, type 2 asymmetric pull-aparts, shear bands, displaced broken clasts in conglomerates and foliation fish. D_4 structures include local open folds which crumple previously near-vertical layers about near-horizontal axial surfaces. The main manifestation of D_5 is a conjugate set of brittle strike slip faults (NNW-trending sinistral, NE-trending dextral). The two main belts of Nonacho strata in the outlier are not considered the limbs of a single fold, as has been previously suggested, but as discrete slivers, dismembered and rotated by a vertical component of the predominantly strike slip displacement.

Introduction

Presented herein are the results of 1:50,000 scale mapping of Tent Outlier, Nonacho Basin undertaken in the 1986 field season (Figs. 1, 2, Aspler 1987). Previous investigations of the outlier include a 1:1,000,000 scale reconnaissance by Wright (1967) and descriptions of isolated localities by Roscoe (1986). Regional analysis of Nonacho Basin was undertaken by Aspler (1985a, b). The goals of the present project were: 1) to test if the lower greenschist grade, siliciclastic rocks exposed between Tent and Whitefish Lakes (Fig. 2) are part of the Nonacho Group; 2) to establish if the stratigraphic and structural analysis determined for the main part of the basin is valid in the outlier and 3) to sample heavy mineral bands from beach and fluvial sandstones for ongoing regional studies concerning the detrital zircon geochronology of Nonacho Basin, the economic potential of paleoplacer deposits in Nonacho Basin, and the geological significance of regional variations in the opaque and translucent heavy mineral suite.

Tectonic Setting

Nonacho Basin is interpreted to have formed due to sinistral strike slip along a series of north-northeast trending faults concentrated on its western border (Aspler 1985a, Aspler and Donaldson 1985). The regional significance of the basin is as yet uncertain. Aspler and Donaldson (1984) suggested that it may have formed as a foreland molasse due to continental collision to the southeast, in western Churchill Structural Province or in Trans- Hudson Orogen. However, recent studies by Culshaw (1986), Hanmer (1986a), Hoffman (1987), Hoffman *et al.* (1986), James (1986), Thompson *et al.* (1986), Grotzinger *et al.* (1987), Henderson *et al.* (1987), and Van Breeman *et al.* (1987) indicate that

Figure 1: *Tent Outlier, Nonacho Basin with respect to elements of the northwestern Canadian Shield.*

the Proterozoic re-activation of the Thelon Tectonic Zone was a major event, possibly manifesting oblique eastward underplating of Slave Craton beneath Churchill Province. Hence Nonacho Basin may have formed due to collision from the west (Hoffman 1987) reflecting the sideways escape of the northwest Churchill Province from impacting of Slave Craton against the northern Churchill Province. This is analogous to the propagating extrusion tectonics model of Tapponnier *et al.* (1982) in which slivers of Indochina are regarded as having escaped sideways from between the 'jaws' of India and Eurasia. The strike-slip faults that generated Nonacho Basin may be comparable to those in the Indochina Sea.

Stratigraphic Setting

The Nonacho Group consists of talus cone, alluvial fan, fluvial, pond, fan delta, beach, eolian and lacustrine sediments deposited on an erosional surface cut into Archean and Aphebian rocks. Sedimentation was in a system of rhomb, wedge and rectangular semi-independent sub basins. Marked thickness changes of individual stratigraphic units (Fig. 3) reflect both the terrigenous depositional system and the rugged basement topography generated in a strike slip setting (see Fig. 8 of Sporli 1980). The basin developed an active western margin, in which continuous faulting maintained a rugged high gradient

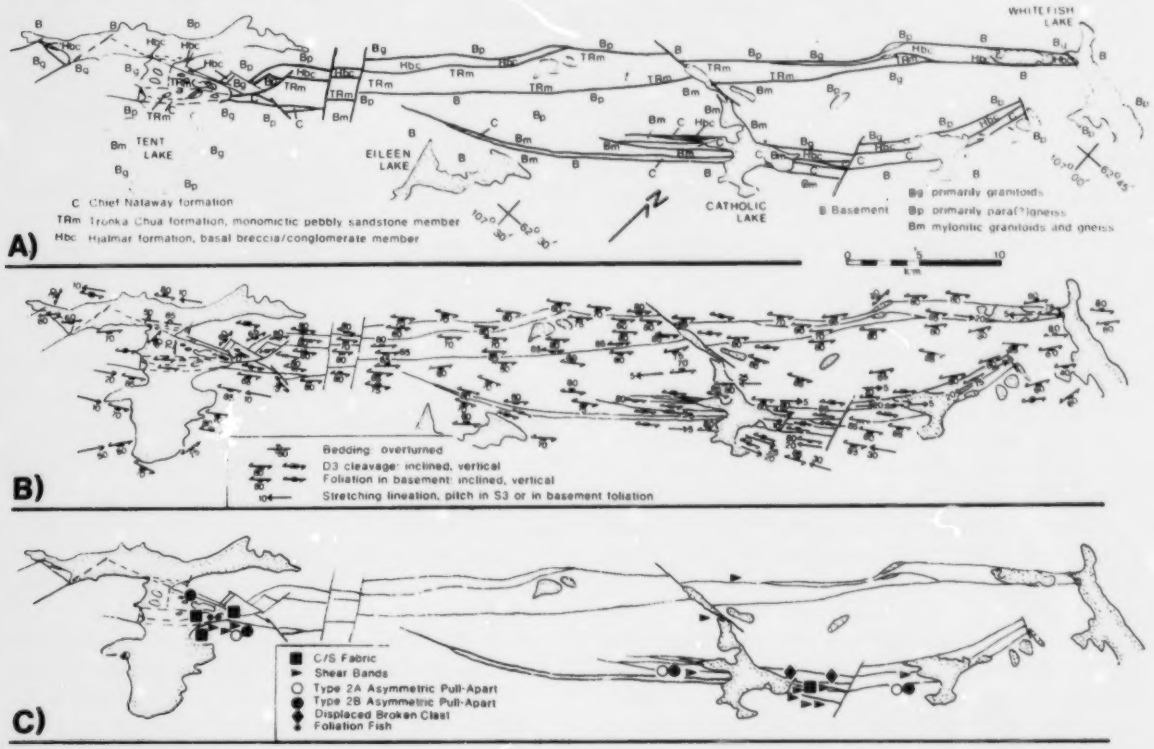

Figure 2: *Generalized Geology of Tent Outlier (After Aspler 1987). A) lithologic units; B) structural data; C) type and distribution of kinematic indicators (all indicate sinistral shear, see Figs. 5, 6, 7, and 8 for examples).*

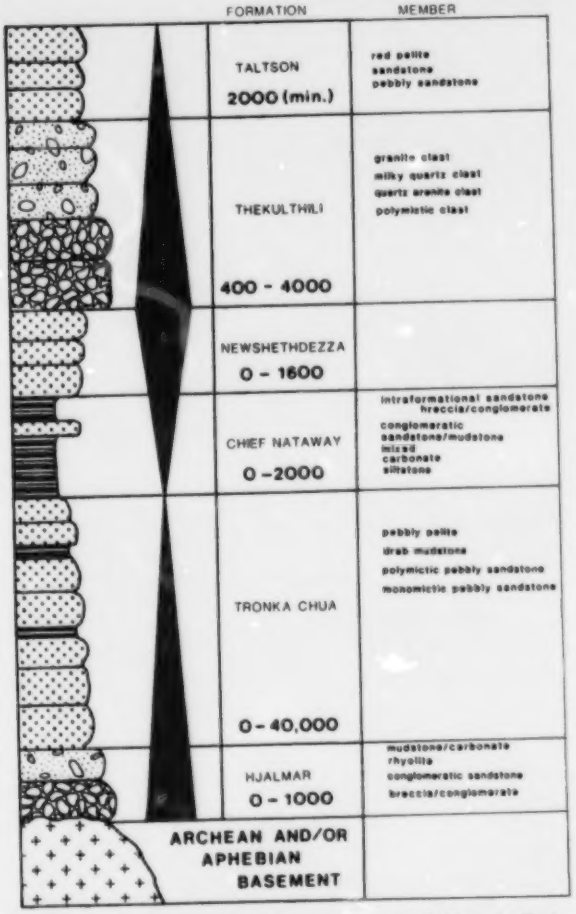

Figure 3: *Stratigraphy of the Nonacho Group, main Nonacho Basin (after Aspler 1985a,b). In Tent Outlier only the Hjalmar, Tronka Chua and Chief Nataway Formations are represented. Large black arrows refer to fining upward and coarsening upward megasequences. Crosses: basement; open spheroids: conglomerate; stippled: sandstone; black: mudstone. Thicknesses are in metres.*

paleotopography, and a passive eastern margin of low gradient (Aspler 1985a, Aspler and Donaldson 1986a). An extreme longitudinal thickness of greater than 40,000 m accumulated as sites of sedimentation moved northward along strike-slip faults that form the western margin of the basin: the basin floor acted as a conveyer belt such that there was longitudinal stacking of depositional units, like shingles on a roof (see Fig. 7 of Crowell 1982a, Fig. 9 of Crowell 1982b, Fig. 6 of Crowell 1985, Christie-Blick and Biddle 1985). It should be emphasized that this cumulative thickness does not represent the depth to basement at any one site.

Three megasequences (Fig. 3) represent 1) fault induced basin initiation, followed by erosional retreat of source areas (Base of Hjalmar Formation to top of Tronka Chua Formation); 2) sudden fault induced basin deepening and infilling (base of Chief Nataway Formation to top of Newshethdezza Formation); and 3) relative tectonic quiescence and backwasting (base of Thekulthili Formation to top of Taltson Formation).

Structural Setting

Steeply dipping NNE-striking faults concentrated on the western side of the basin are considered to have been the main loci of sinistral strike slip; cross faults that bring basement into contact with the Nonacho Group probably had a more significant dip slip component. Bulk strain is generally low, except adjacent to major brittle-ductile shear zones. However the sediments have been polydeformed (Table 1) and structural patterns are complex (Aspler 1985a,b,).

Map Units in Tent Outlier

Basement

Basement was mapped only where it borders the Nonacho Group, and was not rigorously subdivided. However, several potential map units were encountered, and are described below.

The oldest unit that can be placed in a stratigraphic order is a sequence of amphibolite grade gneissic rocks (para?) that consist of quartzo-feldspathic and amphibolite domains alternating on various scales (Fig. 4a). It is uncertain to what extent compositional layering represents bedding of a supracrustal protolith versus reflecting the transposition of initially oblique mafic dykes within a uniform quartzo-feldspathic protolith. Locally observed were narrow tabular amphibolite bodies which are slightly oblique to the compositional layering, suggesting that before transposition, the compositional layering was already present. Possible equivalents are the Tsu Lake gneiss of Bostock (1981) and the Rutledge Lake complex of Culshaw (1984).

After isoclinal folding the gneissic rocks were intruded by a suite of granitoids. Relationships between the gneiss and the granitoid rocks range from unintruded gneiss, to gneiss with abundant granitic dykes to granitoid rocks with rafts of gneiss (Fig. 4b) to homogeneous granitoid rock. Strain of the granitoid rocks is variable, ranging from pristine undeformed granite to ultramylonite. Mylonitic rocks, previously considered as rhyolites (Roscoe 1986) are discussed below (see Basement Deformation).

Nonacho Group

Because the outlier is a zone of high strain, bedding is transposed into D_3 foliation and few primary sedimentary structures are preserved. For detailed descriptions and sedimentologic analysis of correlative units in zones of low strain elsewhere in the basin, see Aspler (1985) and Aspler and Donaldson (1985). Lithostratigraphic correlation of the highly deformed units in the outlier is based on lithologic criteria, the position of individual units in a sequence of units, and comparison with those areas in the main basin in which low strain protolith can be traced into high-strain equivalents.

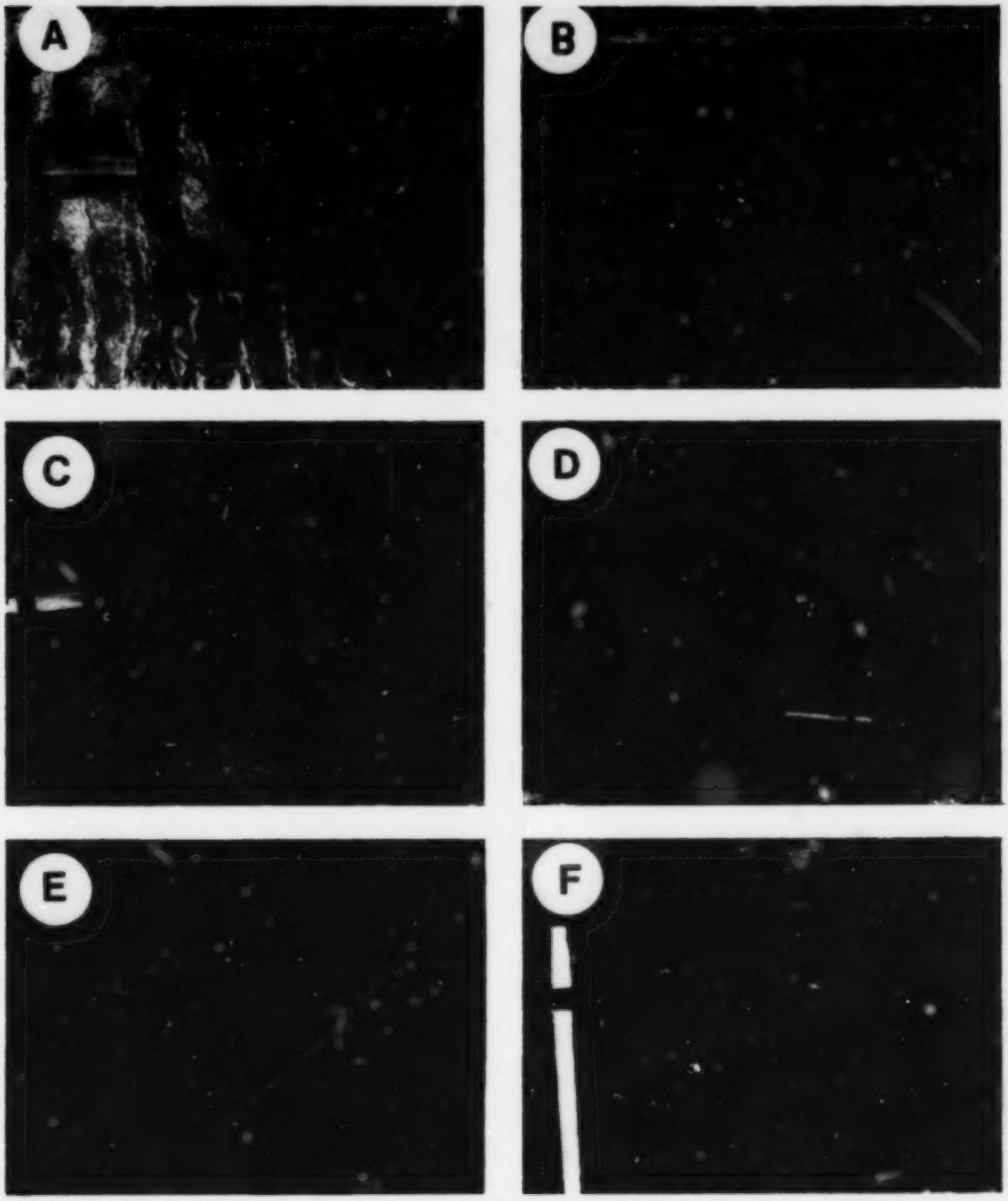

Figure 4: *Map units, Tent Outlier. A) Basement para (?) gneiss. B) Basement; amphibolite rafts within granite. C) Hjalmar Formation conglomerate; granitic clasts strained and aligned along S_3. D) Hjalmar Formation conglomerate with bedding defined by variation in clast size and percentage, transposed to S_3. E) Tronka Chua Formation sandstone, with millimetre scale penetrative D_3 fabric (from upper left to lower right are glacial striae). F) Chief Nataway Formation sandstone/mudstone laminates; transposed parallel to S_3.*

Within the outlier, Nonacho Group strata form two main belts: a western one that extends from Tent Lake to Whitefish Lake; and an eastern one, from west of Eileen Lake to south of Whitefish Lake. A narrow discontinuous third belt is exposed along the eastern shore of the west arm of Tent Lake (Fig. 2).

Hjalmar Formation

Conglomeratic rocks of Tent Outlier are assigned to the basal breccia/conglomerate member of the Hjalmar Formation (Hbc, Fig 1). Typical of the high-strain western margin of the basin, the unconformity with basement is obscured by faulting (see Aspler 1985a, Aspler and Donaldson 1986b for details of the unconformity).

The conglomerates consist of angular to subrounded clasts up to 1 m, set in an arkose matrix (Fig. 4C). Clast/matrix ratios vary from 9/1 to 4/6. Clasts are aligned along, and define, the penetrative D_3 fabric. Rare decimetre scale sandstone layers, subtle differences in clast size or clast/matrix ratio locally define bedding (Fig. 4D). The conglomerate ranges from monomictic, with clasts of one granitic rock type, to oligomictic, containing foliated and unfoliated granitoid clasts, amphibolite, and milky quartz. The clasts are entirely of basement derivation; the conglomerates lack the diversity of pristine sedimentary and volcanic clasts typical of the Thekulthili Formation higher in the section. By analogy to better preserved equivalent rocks in the main basin, the conglomerates are inferred to be primarily talus cone and proximal alluvial fan deposits.

The conglomerates form the westernmost deposits of the two main belts of Nonacho strata. They also constitute the narrow western belt in the west arm of Tent Lake. Generally the conglomerates appear as a discrete uniformly massive unit. However, east of the west arm of Tent Lake, are thick (several ten's of metres) sandstone interbeds that resemble sandstones of the Tronka Chua Formation. These are inferred to be minor interfan stream deposits. They are considered as part of the Hjalmar Formation because they are interbedded with conglomerate, are discontinuous, and can be traced along strike into conglomerate. Similarly, local pelite beds exposed in a narrow wedge south of the southwest arm of the unnamed lake between Catholic and Whitefish Lakes are interpreted as minor interfan pond deposits and part of the Hjalmar Formation.

Tronka Chua Formation

Arkoses assigned to the monomictic pebbly sandstone member of the Tronka Chua Formation (TRm, Fig. 2) are characterized by a uniform, millimetre scale penetrative S_3 fabric that obliterates primary structures (Fig. 4E). Vestiges of bedding are locally apparent as bedding/cleavage lineations on S_3 surfaces and, rarely, as transposed heavy mineral bands, centimetre to decimetre scale pelitic layers, or single pebble layers. Most outcrops appear as homogeneous, light grey weathering sandstone with a well developed fissility imparted by S_3. By analogy to better preserved equivalents in the main basin, the sandstones are inferred to be primarily fluvial deposits.

The sandstones are exposed in only the western of the two main belts. They are in contact with, and outcrop east of, the conglomerates except: 1) south of the west arm of Catholic Lake, where the sandstones are in direct fault contact with basement; 2) in a zone north of Tent Lake, where the conglomerates and sandstones are separated by a basement horst; and 3) on an island in north-central Tent Lake where a basement sliver segments sandstone exposures. It is uncertain if the absence of the Tronka Chua Formation in the eastern belt is due to the unit having been wedged out along a fault that brings Chief Nataway Formation sandstone/mudstone laminates into contact with Hjalmar Formation conglomerates, or due to nondeposition of the unit resulting from a primary high gradient alluvial fan to lacustrine facies transition. Although not unequivocal, the local abundance of pebbles and cobbles in the sandy portions of the laminates on the western margin of the eastern belt, favours the latter alternative.

Chief Nataway Formation

Rocks of the Chief Nataway Formation (c, Fig. 2) consist of centimetre to decimetre scale sandstone/mudstone laminates (Fig. 4f). Sandstone/mudstone ratios vary from 3/7 to 6/4. On the western margin of the eastern belt the sandstones locally contain pebbles and cobbles derived from basement. Layering is transposed to S_3; both lithologies bear a penetrative S_3 fabric and are fissile. The laminates are probably sublacustrine turbidites (see Aspler 1985a, Aspler and Donaldson 1985).

In the western of the two main belts, the sandstone/mudstone laminates are bounded on the west by sandstones of the Tronka Chua Formation. The laminates are exposed on a number of small islands in central Tent Lake and continue in a strip to north of Tent Lake for about 5 km, where they are cut out on the east against a fault with basement. In the eastern belt the laminates are in direct contact on the west with Hjalmar conglomerates, possibly reflecting nondeposition of the Tronka Chua Formation (see above). South of Catholic Lake, the unit was mapped as discrete, isolated slivers bounded by mylonitic basement rocks.

Diabase Dykes

Near-vertical, north-northwest trending diabase dykes cut both basement and Nonacho Group sediments, the largest of which is on the east shore of the southwest arm of Tent Lake. The dykes are unmetamorphosed and undeformed, clearly crosscutting penetrative fabrics in the

Nonacho Group. Similar dykes in the main basin comprise the Sparrow Diabase Dyke Swarm (McGlynn *et al.* 1974). The dykes are oriented normal to the extension direction of the inferred regional strain ellipsoid and hence may represent a late stage manifestation of the same sinistral shear couple that generated Nonacho Basin.

Although the Sparrow Swarm is parallel to the better known Mackenzie Swarm, the two are not considered equivalent because: 1) the Sparrow Swarm is older (Ar/Ar minimum of 1700 my, McGlynn *et al.* 1974, versus 1200 my for the Mackenzie Swarm, eg. Fahrig *et al.* 1981); 2) the Sparrow dykes do not have the marked aeromagnetic expression of the Mackenzie dykes (Geological Survey of Canada Map 1566A); and 3) although generally unstrained, the Sparrow dykes are locally deformed and display a cleavage (McGlynn *et al.* 1974, Bostock 1984, Culshaw 1984, Aspler 1985, Fig. III - 32A).

It is uncertain which of the two dyke swarms, if not both, are represented in Tent Outlier. Because the large dyke exposed on the east shore of the southwest arm of Tent Lake does display a positive aeromagnetic anomaly, it may be part of the Mackenzie Swarm.

Structure of Tent Outlier

Basement Structure

A protracted basement structural history is indicated by isoclinal folds and layer transposition of the gneisses, intrusion by granitoid bodies, and subsequent strain of the gneisses and the granitoids. Timing of basement deformation is unconstrained, except that the presence of foliated granitic rocks as clasts in Hjalmar conglomerates and the contrast in metamorphic grade between basement (amphibolite) and the Nonacho Group (lower greenschist) indicate a significant pre-Nonacho history. Post-Nonacho basement/cover relations will be discussed below.

Structural trends of basement are generally concordant with outlines of the basin, and strike northeast, with near-vertical dips (Fig. 2B). Close folding about northeast axes results in deviations from the general trend.

Of interest are near-vertical, northeast trending shear zones within basement, particularly those close to contacts with the Nonacho Group. A gently plunging displacement vector is indicated by gently plunging stretching lineations and by near-vertical bulk layering/oblique fabric intersection lineations (Fig. 2b, 5, 6, 7b, d; cf. Brown and Murphy 1982).

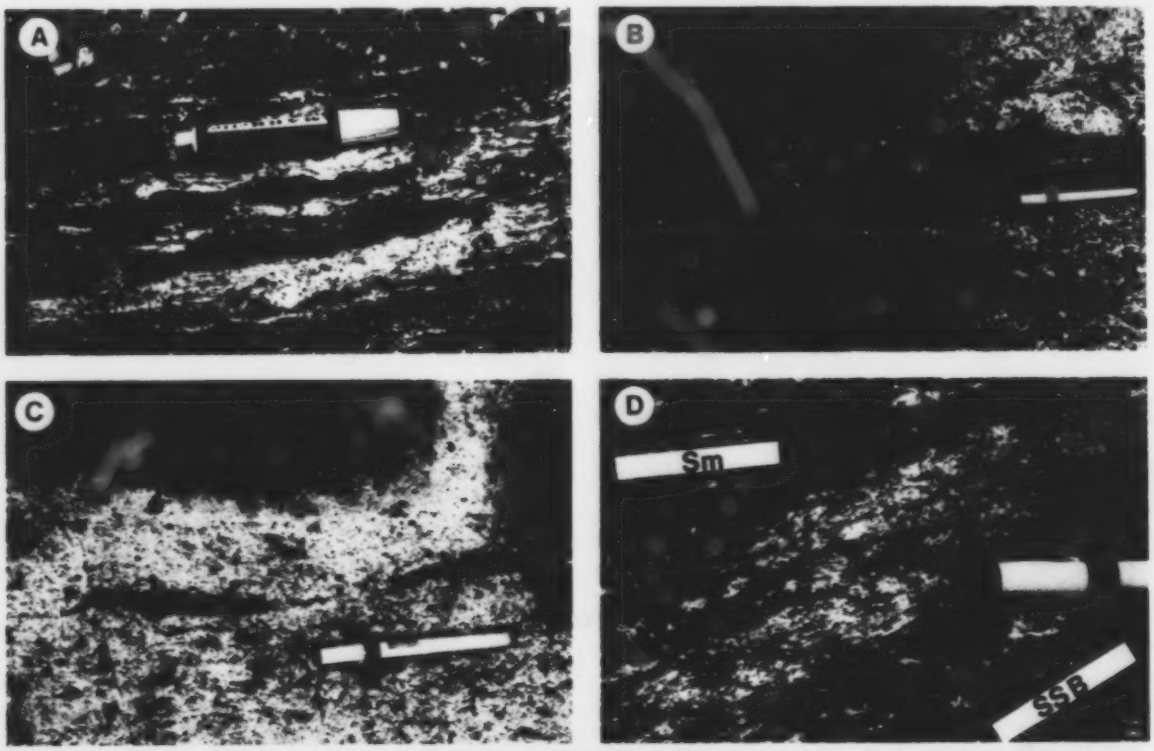

Figure 5: *Kinematic indicators in basement. All views are of near-horizontal surfaces and near-vertical fabrics and suggest sinistral movement. A) Type 2B asymmetric pull-apart (Hanmer 1986b) of amphibolite layer in quartzo-feldspathic matrix (below marker). B) Type 2B asymmetric pull-apart of quartzo-feldspathic layer in amphibolite. Note clockwise back rotation of pull-apart in center of photo. C) Type 2A asymmetric pull-apart; amphibolite in granitic mylonite. D) Shear bands (SSB), oblique to mylonitic fabric (Sm) in granitic mylonite.*

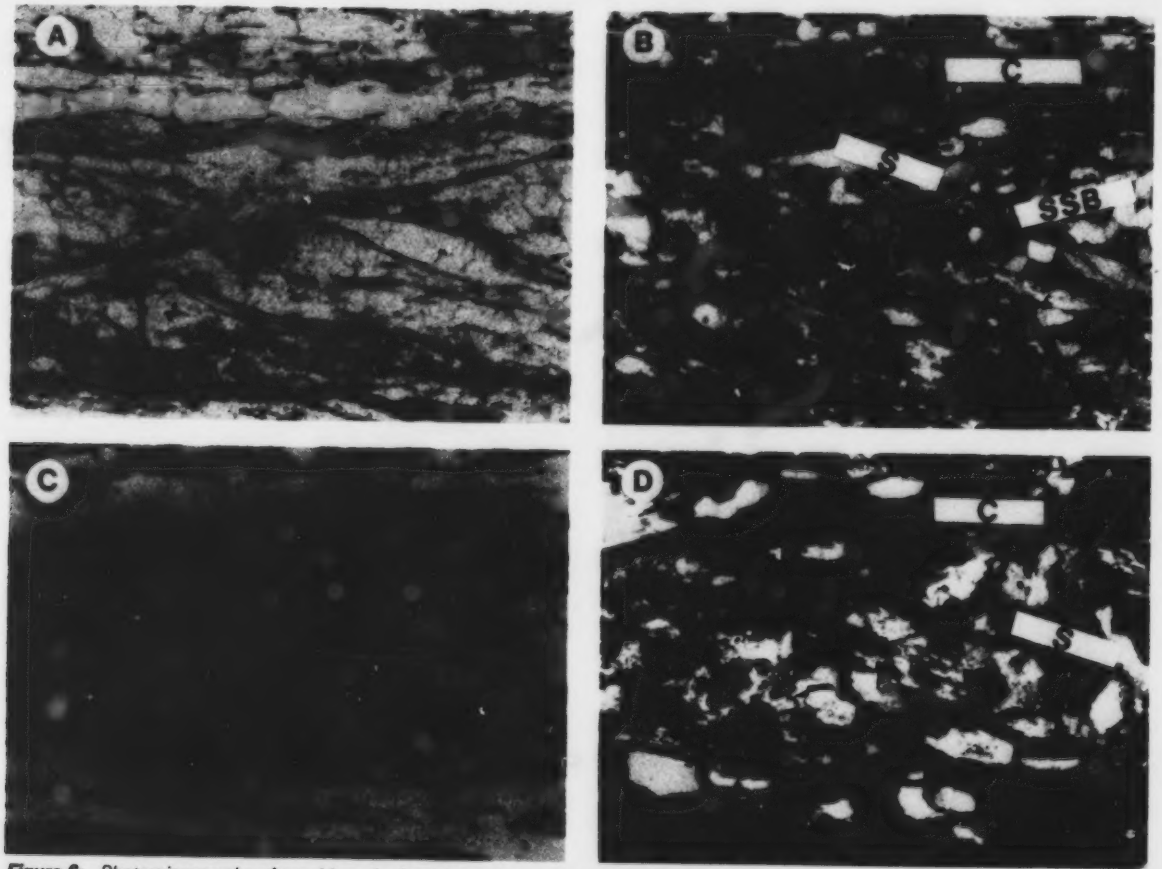

Figure 6: *Photomicrographs of granitic mylonite thin sections cut perpendicular to mylonitic layering and parallel to stretching lineation. A) (plane light) B) (crossed nichols): C, S and sinistral shear band (SSB) (width of view is 2mm). C) (plane light) and D) (crossed nicols) C/S fabric (width of view is 0.5 mm).*

Reliable kinematic indicators are sparse (Fig. 2c) and it is emphasized that the following is a tentative interpretation requiring further testing. Kinematic indicators in basement: S/C fabrics (Berthe *et al.* 1979); shear bands (eg. White *et al.* 1980, Platt and Vissers 1980); Type 1 and Type 2 asymmetric pull-aparts (Hanmer 1986b); consistently suggest sinistral strike slip along near-vertical northeast trending shear zones (Fig. 5, 6, 7).

In the Catholic Lake area, zones of mylonitic basement are not considered as rhyolites within the Nonacho Group as suggested by Roscoe (1986) because: 1) transitions were observed in which virtually pristine granitic protolith can be traced continuously to ultramylonite (Fig. 7c); 2) the finely banded mylonitic rocks have a well developed stretching lineation on foliation surfaces (Fig. 7c); 3) the development of structures such as shear bands (Fig. 7d) and S/C fabrics characteristic of mylonitic rocks; and 4) the rocks in question do not resemble rhyolites elsewhere in the basin (rhyolite member, Hjalmar Formation, Aspler 1985a). Basement rocks that form the strip separating the two main belts of Nonacho strata are not inherently different than those which surround the sediments (cf. Roscoe 1986).

Nonacho Group Structure

In Tent Outlier, the overprint of D_3 is sufficiently pervasive so as to destroy any evidence of the earlier structural history that is preserved in the main basin (Table 1). As described above, all Nonacho map units have been transposed to S_3 and bear a strong S_3 cleavage (Fig. 4), Contacts with the Nonacho Group and basement are generally concordant with S_3; with northeasterly trends and near-vertical dips (Fig. 2). Slight variation in dip of S_3 about the vertical may reflect original heterogeneous strain and/or be a product of D_4 folding about near-horizontal axial surfaces.

Of particular concern is the nature of basement/cover faulting. A gently plunging displacement vector is suggested by shallow plunges of locally developed stretching lineations in conglomerates (Fig. 2b) and by steeply plunging bulk layering/ oblique fabric intersections (Fig. 8). As with basement, kinematic indicators are sparse (Fig. 2c), but again a tentative conclusion of sinistral strike slip is advanced because of the consistent sense given by available kinematic indicators, which include C/S fabrics, Type 2 asymmetric pull-aparts, foliation fish (as defined by Hanmer 1986b) and displaced broken clasts in conglomerates (Fig. 8).

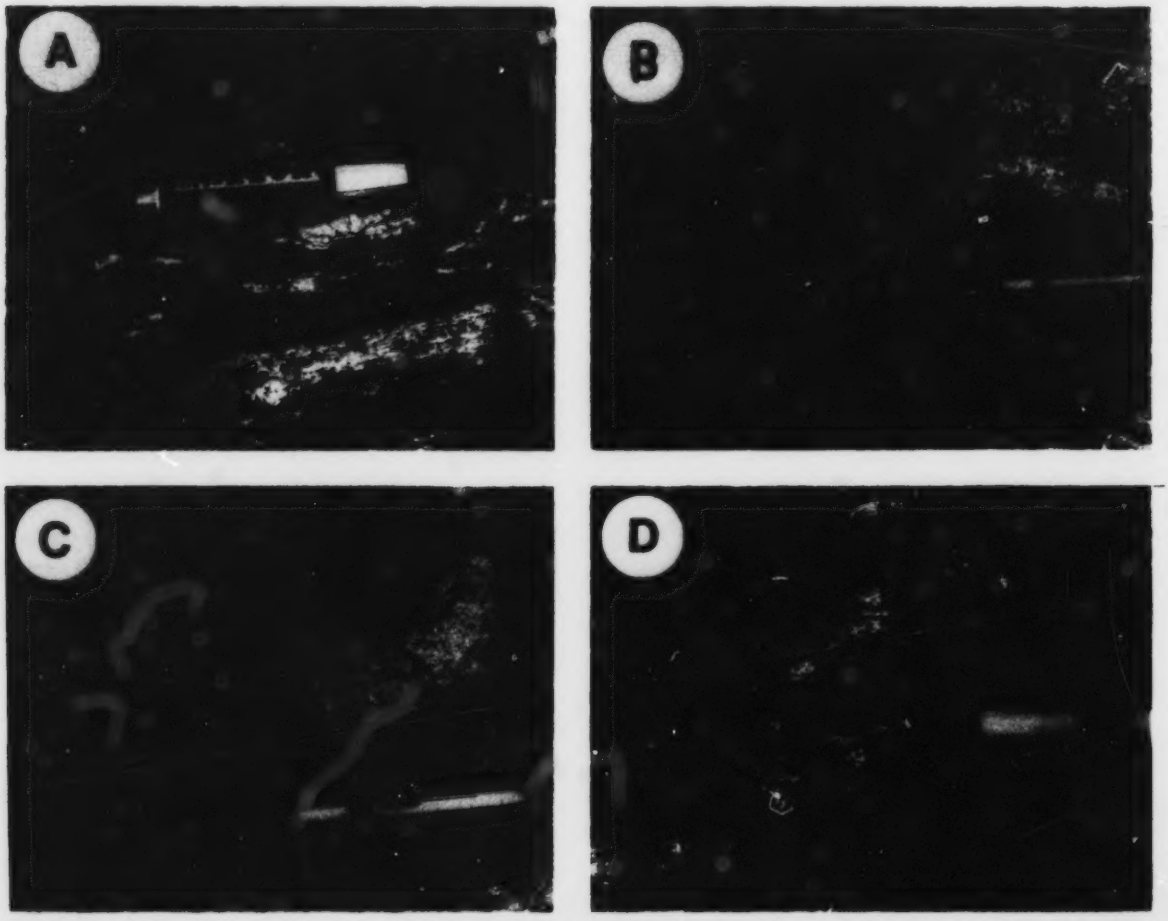

Figure 7: *Granitic mylonite, Catholic Lake. A) Coarse-grained equigranular granitic protolith. B) Near-vertical mylonitic layering surface with near-horizontal stretching lineation. C) Protomylonite on right passing to mylonite and ultramylonite on left. D) Granitic protomylonite with sinistral shear bands from upper right to lower left of photo (same outcrop as C).*

In the main basin, the oblique angle between S_3 and related shear zones, and the sigmoidal pattern of S_3 between shear zones, were used as evidence to suggest heterogeneous sinistral shear (Aspler 1985a,b, Aspler and Donaldson 1985, Table 1). This pattern was not observed in Tent Outlier: S_3 maintains consistently northeast trends parallel to sheared contacts with basement. This may reflect a degree of higher strain in the outlier, with S_3 having rotated about a near-vertical axis into parallelism with the shear zones, but also may be due to a greater component of shear zone parallel flattening (transpression) which would have resulted in a diminished initial S_3/shear zone angle (see Sanderson and Marchini 1984). Strain gradients in the main basin are manifested by an increase in the intensity of S_3 development and a decrease in minor-fold interlimb angle, in addition to a decrease in S_3/shear zone angles. Similar gradients were not observed in Tent Outlier, although adjacent to shear zones there is a local abundance of quartz veins transposed parallel to S_3, and S_3 surfaces in sandstones and pelites take on a phyllonitic sheen. Commonly, basement rocks in sheared contact with the Nonacho Group are not obviously highly deformed, suggesting that strain has been concentrated in the less competent sediments.

The two main belts of Nonacho strata were previously interpreted as the limbs of a single fold (Wright 1967). Younging indicators are not preserved within the two main belts. However, in both the sequence is of (from west to east): basement to conglomerate (with low clast diversity) to sandstone and/or to sandstone/mudstone laminates. This sequence is comparable to transitions in the main basin (where positive younging data are abundant) in which conglomerates of the Hjalmar Formation (characterized by a low clast diversity, in contrast to the Thekulthili Formation) pass upsection to sandstones of the Tronka Chua Formation and to sandstone/mudstone laminates of the Chief Nataway Formation. The stratigraphy in the two belts is not symmetric about a central axis, as is required by the fold hypothesis. North and south of Catholic Lake, the eastern belt is internally segmented: elongate wedges of Nonacho Group alternate with slices of mylonitic basement. Furthermore, the fold

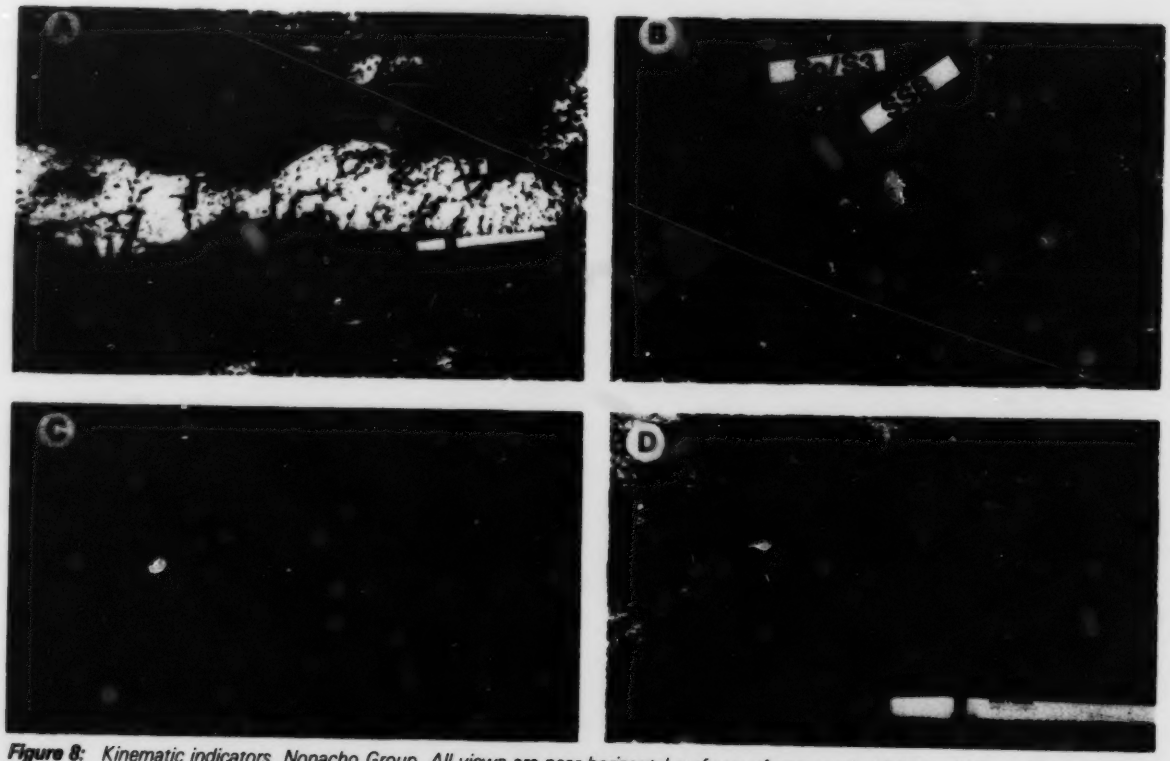

Figure 8: *Kinematic indicators, Nonacho Group. All views are near-horizontal surfaces of near-vertical fabrics. A) Type 2B asymmetric pull-apart, quartz vein in conglomerate. B) Sinistral shear bands (SSB) cutting across So/S_3 fabric, Chief Nataway argillites. C) Granitic clast in conglomerate with a pre-existing foliation along which segments show dextral offset and counterclockwise rotation, possibly analogous to antithetic microfaults in displaced broken grains (see Simpson and Schmid, 1983, Simpson 1984, and Takagi 1986) formed in sinistral bulk shear. D) Sigmoidal shaped lense (above pen) in argillite with sigmoidal internal fabric oblique to bulk fabric; possibly analogous to foliation fish in mylonites (see Hanmer 1986b) and indicating sinistral shear.*

closure indicated by Wright (1967) does not appear to exist: although outcrop is poor south of Whitefish Lake, both belts appear to terminate without joining.

The two belts are interpreted here as eastward young-ing monoclinal panels. They are regarded as discrete slivers that were dismembered and rotated due to a vertical component of the predominantly strike slip displacement. In strike slip terrains, even a minor dip slip component along master faults can generate significant basement uplifts and the development of flower structures (Rod 1956, Sanderson and Marchini 1984, Christie-Blick and Biddle 1985, Harding 1985, Harding *et al.* 1985, Stanstreet *et al.* 1986). Strata adjacent to such uplifts may undergo extreme rotations about horizontal axes and become physically segmented, yet never be part of a single coherent flexure. Figure 9 is a conceptual model to illustrate the inferred geometry in the present example. Both belts are considered to have rotated eastward away from basement uplifts, forming half flower structures. Although younging indicators are sparse in the third belt, exposed on the western extreme of the outlier, the belt appears to young to the west. This suggests that the strip has been rotated westward, and forms the western segment of a complete flower structure. The degree to which a component of flattening across the shear zones may have enhanced rotation and the development of near-vertical attitudes (see Fyson 1987) is unknown.

The cross faults that define the northern limits of the two main belts (Fig. 2) are not well constrained, owing to poor outcrop in the vicinity of Whitefish Lake (see Aspler 1987 for details). However, the interpretation is based on a well exposed example of a high a[illegible]le cross fault that serves to terminate the western belt on its [illegible]outhern end, near the south-central shore of Tent Lake. There, basement gneiss and massive granitoid rocks abut against northeast trending sandstones and sandstone/mudstone laminates along a northwest trending reverse fault that dips 40° south at its eastern end and 80° south at its western end. The southern termination of the eastern belt is different, with the faults that bound the Nonacho Group slivers merging into one another at a low angle.

The effect of D_4 is relatively minor and is manifested by local open folds of previously near-vertical strata about near- horizontal axial surfaces. Conjugate brittle strike slip faults are the main manifestation of D_5: NNW-trending sin-

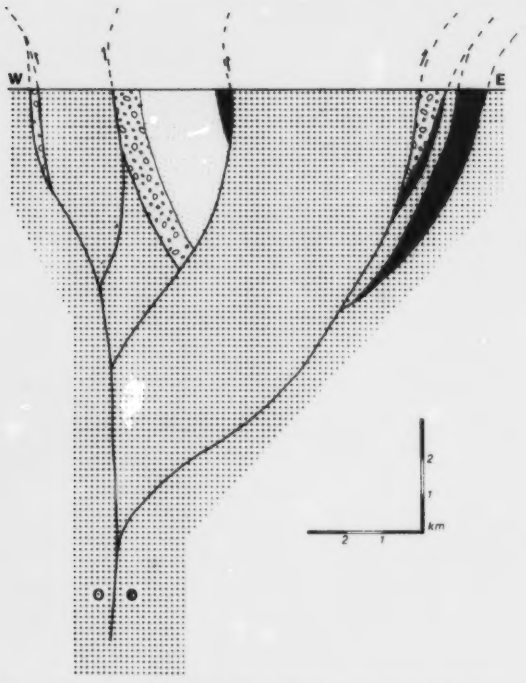

Figure 9: *Flower structure, Tent Outlier. The two main belts are inferred to be eastward younging monoclinal panels that have rotated eastward away from basement uplifts. The narrow western belt is west younging and is inferred to have rotated westward and to represent the partly preserved segment of a full flower structure. Composite cross section is based on sections in Aspler (1987). Note that the manner in which the faults merge at depth is speculative. Crosses: basement; spheroids and stippled: Hjalmar Formation; stippled: Tronka Chua Formation; black: Chief Nataway Formation.*

istral and NE-trending dextral. The faults truncate all earlier structures (with the possible exception of D_4 folds). Because they crosscut near-vertical features, apparent offsets approximate true offsets. In contrast to D_3 faults, breccia zones are common.

Relationship of Tent Outlier to Main Nonacho Basin

Tent Outlier comprises the northernmost known exposures of Nonacho Basin. It is separated from another outlier, centered on Jones Lake to the southwest, by about 4.5 km. The narrow, westward younging belt of Hjalmar conglomerate and sandstone that extends discontinuously along the southwest arm of Tent Lake (Fig. 2A) may continue into Jones Outlier. Spot observations in Jones Outlier indicate a sequence (from east to west) of basement to low clast diversity conglomerate to sandstone to pelite (see also Stockwell *et al.* 1967). This sequence may represent the more fully preserved western segment of a symmetric flower structure only partly preserved in Tent Outlier. The eastern boundary of the westward younging belt in Tent Outlier is a shear zone along which the two outliers may have been sinistrally offset (Roscoe 1986).

Conclusions

Highly strained, lower greenschist facies grade conglomerates, sandstones and sandstone/mudstone laminates in Tent Outlier are part of the Nonacho Group and are assigned to the Hjalmar, Tronka Chua and Chief Nataway Formations respectively. The rocks are inferred to be talus, alluvial fan, fluvial and lacustrine deposits.

Although kinematic data are sparse, they consistently indicate sinistral strike slip along the main northeast trending faults that border and transect the basin; a conclusion that requires further testing.

Rather than representing the limbs of a single fold, the two main belts of Nonacho strata within the outlier are reinterpreted as representing the segmented and rotated margins of flower structures formed due to basement uplifting along predominantly strike-slip master faults.

Acknowledgements

This project was funded by INAC (Yellowknife) contract YK-86-87-054. W.A. Padgham, Chief Geologist, INAC Yellowknife, is thanked for field and moral support. I benefited from discussions with W.K. Fyson and S.M. Roscoe. At different times during the field season able assistance was provided by Gordon Bailey, William Donaldson, Lloyd Drygeese and C. Diane Gault. Expediting was by C. Diane Gault, Martin Irving and Ken Leishman. Wayne Degan is thanked for superior Beaver piloting. W.K. Fyson, C.W. Jefferson and S.M. Roscoe are thanked for their constructive criticisms of the paper. Help given by C.W. Jefferson during preparation of the final manuscript is appreciated.

References

Aspler, L.B., 1985a. Geology of Nonacho Basin (Early Proterozoic) NWT. Unpublished PhD thesis, Carleton University, Ottawa Ontario, 385p.

Aspler, L.B., 1985b. Geological maps of Nonacho Basin, (1:125,000 and 1:250,000). INAC Open File, EGS 1985-7.

Aspler, L.B., 1987. Geological map: Tent Outlier, Nonacho Basin (1:50,000). INAC Open File, EGS 1987-2.

Aspler, L.B., and Donaldson, J.A., 1984. Oblique-slip sedimentation and deformation in Nonacho Basin (Early Proterozoic) Northwest Territories, Canada. American Association of Petroleum Geologists Bulletin, 68, p. 449.

Aspler, L.B., and Donaldson, J.A., 1985. The Nonacho Basin (Early Proterozoic), Northwest Territories, Canada: Sedimentation and deformation in a strike-slip setting. In Biddle, K.T., and Christie-Blick, N., Eds., Strike-slip Deformation, Basin Formation, and Sedimentation. Society of Economic Paleontologists and Mineralogists Special Publication 37, p. 193-209.

Aspler, L.B., and Donaldson, J.A., 1986a. Contrasting styles of lacustrine sedimentation, Nonacho Basin (Early Proterozoic) NWT: asymmetric paleotopography of a strike-slip basin. Geological Association of Canada Program With Abstracts, 11, p. 42.

Aspler, L.B., and Donaldson, J.A., 1986b. Paleoclimatology of Nonacho Basin (Early Proterozoic), Northwest Territories, Canada. Palaeogeography, Palaeoclimatology, Palaeoecology, 56, p. 17-34.

Berthe, D,M. Choukroune, P., and Jegouzo, P., 1979. Orthogneiss, mylonite and non coaxial deformation of granites: the example of the South Armorican Shear Zone. Journal of Structural Geology, 1, p. 31-42.

Bostock, H.H., 1981. A granitic diapir of batholithic dimensions at the west margin of the Churchill Province. In Current Research, Part B., Geological Survey of Canada Paper 81-1B, p. 73-82.

Bostock, H.H., 1984. Preliminary geological reconnaissance of the Hill Island Lake and Taltson Lake areas, District of Mackenzie. In Current Research Part A, Geological Survey of Canada Paper 84-1A, p. 165-170.

Brown, R.L., and Murphy, D.C., 1982. Kinematic interpretation of mylonitic rocks in part of the Columbia River fault zone, Shuswap terrane, British Columbia. Canadian Journal of Earth Sciences, 19, p. 456-465.

Crowell, J.C., 1982a. The tectonics of Ridge Basin, southern California. In Crowell, J.C., and Link, M.H., Eds. Geologic History of Ridge Basin, Southern California. Pacific Section, Society of Economic Paleontologists and Mineralogists, p. 89-97.

Crowell, J.C., 1982b. The Violin Breccia, Ridge Basin, southern California. In Crowell, J.C., and Link, M.H., Eds. Geologic History of Ridge Basin, Southern California. Pacific Section Society of Economic Paleontologists and Mineralogists, p. 89-97.

Crowell, J.C., 1985. The recognition of transform terrane dispersion within mobile belts. In Howell, D.G. Ed., Tectonostratigraphic Terranes of the Circum-Pacific Region. American Association of Petroleum Geologists Earth Science Series 1, p. 51-61.

Christie-Blick, N., and Biddle, K.T., 1985. Deformation and basin formation along strike-slip faults. Biddle, K.T., and Christie-Blick, N. Eds. Strike-slip Deformation, Basin Formation, and Sedimentation. Society of Economic Paleontologists and Mineralogists Special Publication 37, p. 1-34.

Culshaw, N.G., 1984. Rutledge Lake, Northwest Territories; a section across a shear belt within the Churchill Province. In Current Research Part A, Geological Survey of Canada Paper 84-1A, p. 331-338.

Culshaw, N.G., 1986. Proterozoic basement tectonics along the western edge of the Thelon Tectonic Zone (NWT) – compressional and transcurrent structures – a result of oblique convergence? Geological Association of Canada Program With Abstracts 11, p.60.

Fahrig, W.F., Christie, K.W., and Jones, D.L., 1981. Paleomagnetism of the Bylot Basins: evidence for continental extensional tectonics. In Campbell, F.H.A. ed., Proterozoic Basins of Canada. Geological Survey of Canada Paper 81-10, p. 303-312.

Fyson, W.K., 1987. A succession of quartz veins in Archean metaturbidites, Yellowknife Bay, Slave Province. Canadian Journal of Earth Sciences, 24, p. 698-710.

Geological Survey of Canada, 1981. Magnetic Anomaly Map of Lockhart River Northwest Territories (1:1,000,000) Geological Survey of Canada Map 1566A.

Grotzinger, J.P., McCormick, D.S., and Pelechaty, S.M., 1987. Progress report on the stratigraphy, sedimentology, and significance of the Kimerot and Bear Creek groups, Kilohigok Basin, District of Mackenzie. In Current Research Part A, Geological Survey of Canada Paper 87-1A, p. 219-238.

Hanmer, S.K., 1986a. The Great Slave Lake Shear Zone, NWT: southeast boundary of the Slave Craton. In Current Activities Forum, 1986, Program With Abstracts. Geological Survey of Canada Paper 86-8, p.4.

Hanmer, S.K., 1986b. Asymmetrical pull-aparts and foliation fish as kinematic indicators. Journal of Structural Geology, 8, p. 111-122.

Harding, T.P., 1985. Seismic characteristics and identification of negative flower structures, positive flower structures and positive structural inversion. American Association of Petroleum Geologists Bulletin, 69, p. 582-600.

Harding, T.P., Vierbuchen, R.C., and Christie-Blick, N., 1985. Structural styles, plate-tectonic settings, and hydrocarbon traps of divergent (transitional) wrench faults. *In* Biddle, K.T., and Chritsie-Blick, N. Eds. Strike-slip Deformation, Basin Formation, and Sedimentation. Society of Economic Paleontologists and Mineralogists Special Publication 37, p. 51-78.

Henderson, J.B., McGrath, P.H., James, D.T., and Macfie, R.I., 1987. An integrated geological, gravity and magnetic study of the Artillery Lake area and the Thelon Tectonic Zone, District of Mackenzie. In Current Research Part A, Geological Survey of Canada Paper, 87-1A, p. 803-814.

Hoffman, P.F., Culshaw, N.G., Hanmer, S.K., LeCheminant, A.N., McGrath, P.H., Tirrul, R., and Van Breeman, O. 1986. Is the Thelon Front (NWT) a suture? Geological Association of Canada Program with Abstracts, 11, p. 82.

Hoffman, P.F., 1987. Continental Transform Tectonics: Great Slave Lake Shear Zone (Ca, 1, 9 Ga), Northwest Canada, Geology, 15, p. 785-788.

James, D.T., 1986. Geology of the Moraine Lake area District of Mackenzie; Part 2: a transect across part of the Thelon Tectonic Zone. In Current Research Part A, Geological Survey of Canada Paper 86-1A, p. 417-421.

Mandl, G. 1987. Tectonic Deformation by Rotating Parallel Faults: The "Bookshelf" Mechanism, Tectonophysics, 141, p. 277-316.

McGlynn, J.C., Hanson, G.N., Irving, E., and Park, J.K., 1974. Paleomagnetism and age of Nonacho Group sandstones and age of Sparrow Dykes, District of Mackenzie. Canadian Journal of Earth Sciences, 11, p. 30-42.

Platt, J.P. and Vissers, R.L.M., 1980. Extensional Structures in Anisotropic Rocks. Journal of Structural Geology, 2, p. 397-410.

Rod, E., 1956. Strike-slip faults of northern Venezuela. American Association of Petroleum Geologists Bulletin, 40, p. 457-476.

Roscoe, S.M., 1986. Felsic volcanic rocks in the Nonacho Group near Whitefish Lake, District of Mackenzie. In Current Research Part A, Geological Survey of Canada Paper 86-1A, p. 787-789.

Sanderson, D.J., and Marchini, W.R.D., 1984. Transpression. Journal of Structural Geology, 6, p. 449-458.

Simpson, C., 1984. Borrego Springs-Santa Rosa mylonite zone: a Late Cretaceous west-directed thrust in southern California. Geology, 12, p. 8-11.

Simpson, C., and Schmid, S.M., 1983. An evaluation of the sense of movement in sheared rocks. Geological Society of America Bulletin, 94, 1281-1288.

Sporli, K.D., 1980. New Zealand and oblique-slip margins: tectonic development up to and during the Cainozoic. In Ballance, P.F., and Reading, H.G., Eds. Sedimentation in Oblique-slip Mobile Zones, International Association of Sedimentologists Special Publication 4, p. 147-170.

Stanistreet, I.G., McCarthy, T.S., Charlesworth, E.G., Myers, R.E., and Armsrtrong, R.A., 1986. Pre-Transvaal wrench tectonics along the northern margin of the Witwatersrand Basin, South Africa. Tectonophysics, 131, p. 53-74.

Stockwell, C.H., Henderson, J.F., Brown, I.C., Wright, G.M., and Barnes, F.Q., 1967. Geology, Reliance, District of Mackenzie. Geological Survey of Canada Map 1123A.

Takagi, H. 1986. Implications of mylonitic microstructures for the geotectonic evolution of the Median Tectonic Line, Central Japan. Journal of Structural Geology, 8, p. 3-14.

Tapponnier, P., Peltzer, G., Leidain, A.Y., Armijo, R., and Cobbold, P., 1982. Propagating extrusion tectonics in Asia: new insights from simple experiments with plasticine. Geology, 10, p. 611-616.

Thompson, P.H., Culshaw, N., Buchanan, J.R., and Manoljlovic, P., 1986. Geology of the Slave Province and Thelon Tectonic Zone in the Tinney Hills-Overby Lake (west half) map area, District of Mackenzie. In Current Research Part A, Geological Survey of Canada Paper 86-1A, p. 275-289.

Van Breeman, O., Henderson, J.B., Loveridge, W.D., and Thompson, P.H., 1987. U-Pb zircon and monazite geochronology and zircon morphology of granulites and granite from the Thelon Tectonic Zone, Healey Lake and Artillery Lake map areas, N.W.T. In Current Research Part A, Geological Survey of Canada Paper 87- 1A, p. 783-801.

White, S.H., Burrows, S.E., Carreras, J., Shaw, N.D. and Humphreys, F.J., 1980. On Mylonites and Ductile Shear Zones. Journal of Structural Geology, 2, p. 175-187.

Wright, G.M., 1967. Geology of the southeastern Barren Grounds, parts of the Districts of Mackenzie and Keewatin. Geological Survey of Canada Memoir 350, 91p.

Contribution to the Geology of the Northwest Territories, Volume 3, 1988, NWT Geology Division, INAC, Yellowknife.

Geochemistry of Slave Province Volcanic Rocks: Yellowknife Belt

A.M. Goodwin

Department of Geology, University of Toronto
Toronto, Canada M5S 1A1

Abstract

Systematic sampling and analysis of Yellowknife volcanic rocks have provided mean class compositions and mean compositions by segment, cycle, and formation. The Yellowknife assemblage constitutes a modified bimodal volcanic succession. Ni-Sr plots indicate that Lower Kam lavas are products of mainly fractional crystallization processes, and Upper Kam lavas of mainly partial fusion processes, the respective mantle sources contrasting in Ni-Sr abundances. The bulk of the volcanic components, dominated by basalt and basaltic-andesite, could be products of differentiation processes involving more or less common mantle sources. However, the separate and distinct character of the felsic volcanic components without significant intervening intermediate components suggests a separate origin such as the melting of sialic crust. Further chemical data are required to investigate this possibility.

In general, the Yellowknife volcanic association has trace element characteristics (F1 group) that are considered to be unfavourable for the presence of massive base metal sulfide deposits. However other Slave Province associations include the favourable F3 group of felsic metavolcanics.

Introduction

The Yellowknife Greenstone Belt lies at the western margin of the Yellowknife Supracrustal Basin (Henderson, 1981) a dominantly turbidite-filled Archean repository with subordinate, mainly peripheral, volcanic-rich greenstone belts. The Yellowknife Supracrustal Basin extends 120 km to the east of Yellowknife and 170 km to the north from its southern limit where terminated at a late fault along Hearne Channel of Great Slave Lake. Other greenstone belts bordering this greywacke-mudstone-filled basin include: Clan Lake belt, 50 km north of Yellowknife; Thistlewaite belt, 40 km still further northeast; and Cameron River and Beaulieu River belts respectively 80 and 120 km northeast of Yellowknife, both at or near the eastern margin of the basin. The turbidites, which underlie approximately 90 percent of the Yellowknife Supracrustal Basin, constitute the type sediments of the Yellowknife Supergroup (Henderson, 1970). In all, Slave Province includes at least five such major Archean supracrustal basins of which Yellowknife Basin is the southernmost and High Lake Basin, 700 km to the north, the northernmost.

Numerous granitoid plutons, c. 2650 Ma old, have intruded metasupracrustal rocks of the Yellowknife Basin, commonly folding and contorting them. Metamorphic grade in the basin is typically greenschist to amphibolite facies, rising to upper amphibolite facies near intrusive contacts.

Older granitoid rocks, commonly tonalitic to trondhjemitic gneiss, migmatite, and minor granite and granodiorite, locally with felsic volcanic and metasedimentary enclaves, have been identified in Slave Province, for example, at the northern and southern extremities of the Yellowknife greenstone belt. Structural development of the Yellowknife Supracrustal Basin has been attributed to rifting of this pre-metasupracrustal sialic basement (Henderson, 1981).

Available geochronologic data indicate that Yellowknife sedimentation and volcanism occurred in an abbreviated 20-Ma interval, from 2680 to 2660 Ma ago, upon or near 2700 to 3200 Ma-old sialic crust. This supracrustal accumulation was quickly followed by regional syntectonic plutonism and metamorphism at 2660 to 2620 Ma. Thus complete Yellowknife belt development, occurred in an interval not exceeding 60 Ma (Easton, 1984; Lambert *et al.*, 1984).

Two main types of Archean volcanic successions have been recognized in Slave Province: 1) Yellowknife-type, grossly similar to Superior Province belts, with thick basalt-rich lower phases capped by subordinate intermediate-to-felsic units, and 2) basalt-poor Hackett River-type, dominated by felsic volcanic rocks (Padgham, 1985). Interestingly, komatiite or other ultramafic volcanic rocks have not been positively identified so far in Slave Province.

Slave Province has produced more than 12 million ounces of gold, 88 percent derived from mines in gold-silver-bearing quartz-carbonate-sericite shear zones cutting Yellowknife volcanic rocks. The recently activated Lupin Mine will produce a major part of the province's gold production from amphibolitic silicate-sulfide banded iron formation interstratified with metaturbidites of the Point Lake-

Contwoyto Lake Supracrustal Basin in the centre of the Slave Province. Volcanogenic base metal sulfide deposits have been found in nine volcanic belts of the Slave Province. Of these, the High Lake deposit, in High Lake Supracrustal Basin, centred 600 km north of Yellowknife and 100 km south of Coronation Gulf, contains established reserves of 5.2 million tons grading 3.5% Cu, 2.5% Zn, 0.6 oz/T Ag, 0.2 oz/T Au, and minor Pb. In addition, numerous Li-Be-Sn-W-Ta-bearing pegmatites are present in the province (Padgham, 1985).

The purpose of this study is to chemically characterize the Yellowknife volcanic succession by volcanic class, stratigraphic segment, and belt as a basis for eventual geochemical comparison with other Slave Province greenstone belts and other greenstone terranes.

Yellowknife Volcanic Belt

The north-trending volcanic-rich belt at Yellowknife is 5 km wide and 52 km long. The volcanic rocks form a broad homocline of northeast-trending, near-vertical, southeast-facing units cut by numerous northerly trending, mainly sinistral sub-vertical faults. Of the latter, Kam, West Bay and Akaitcho faults have effected major stratigraphic offsets of up to 5000 m. The resulting structural segments collectively form a continuous stratigraphic section which was previously estimated at 14,000 m (Baragar, 1966), but is now reinterpreted as an off-lapping or shingled sequence that was never more than 10,000 m thick (Helmstaedt and Padgham, 1986). The rocks chemically studied in this report belong to the Kam Group and overlying Banting Group.

The lower contact of the Yellowknife volcanic section, to the west, is about equally shared by faulted and intrusive contacts, the latter against younger granitoid plutons. Only at the northern and southern extremities of the belt is the apparent base of the Kam section preserved and exposed. Thus to the north a substantial area of granitoid gneiss contains presumed pre-Kam felsic metavolcanic enclaves; and to the south a 750 m-thick unit of mafic flows, clastics and felsic volcanic rocks (Octopus Formation) is interpreted as the product of an older volcanic-sedimentary cycle unconformably underlying the Kam Formation (Helmstaedt *et al.*, 1979).

The Kam Formation is composed mainly of mafic lava flows including as previously estimated (Baragar, 1966), massive (43%), pillowed (42%) and variolitic (11%) phases; in addition, felsic tuffs and flows (4%) form a prominent zone (Townsite or Brock Flows) composed of coarse fragmental to densely porphyritic rocks containing at least one pillowed lava flow, at about mid-thickness of the Kam succession. Similar felsic pyroclastic rocks (Banting Formation) unconformably overlie upper Kam mafic volcanic rocks and form the uppermost volcanic division in the belt. On this basis, Baragar (1966) allowed for two volcanic cycles, the lower cycle comprising the Lower Kam and Townsite Flows; and the upper cycle, the Upper Kam lavas (Upper Kam) plus the overlying Banting Formation. Recent work has raised considerable uncertainty as to the true stratigraphic relations of Upper Kam, Banting, and the intervening dominantly metasedimentary Walsh and Jackson Lake Formations (Helmstaedt and Padgham, 1986). However, for present purposes, a straight-forward stratigraphic arrangment will suffice, comprising (Table 1): Lower Kam = segments A + B + Townsite Flows; Upper Kam = segments C, D, E; and Banting Formation = segment F.

As discussed below, Lower Kam division, including Townsite Flows, constitutes the first main mafic-to-felsic volcanic cycle; Upper Kam segments C, D and E^1 constitute the second main cycle; and Upper Kam segment E^2 constitutes a third, subordinate, mafic-to-felsic volcanic cycle. These three volcanic cycles are unconformably overlain by

Table 1: Stratigraphic Division, Thickness, and a Sampling of Yellowknife Greenstone Belt

Formation		Cycle	Segment	Thickness (m)			Sampling			
	Division							No of Samples by:		
				Segment	Formation and Division	Belt	Sample Numbers	Segment	Division	Belt
Banting			F	700	700		43-47	5	5	
Kam	Upper Kam	3	E^2	650			32-35	4		
		2	E^1	650	6800		29-31	3		
			D	2300			b)36-42	7	31	47
							a)22-28	7		
			C	3200		1400	12-21	10		
	Lower Kam	1	Townsite flows	600	6500		10,11	2	11	
			B	3400			5-9	5		
			A	2500			1-4	4		

Banting felsic pyroclastic rocks (segment F) with or without intervening metasediments.

Sampling Procedure

During the 1983 field season, 47 approximately equally spaced volcanic units, mainly lava flows, were sampled across the Yellowknife sequence, including 42 Kam and 5 Banting samples. Each sample is composed of numerous fresh volcanic chips taken at regular intervals either across selected outcrops (35 samples) or of diamond drill core intersections (12 samples). In general, the sampled volcanic units are 350 m apart across the Kam-Banting sequences.

The pattern of sampling closely follows Baragar's (1966) stratigraphic scheme (segments A-F) with the following exceptions: segment B was sampled in 1983 west of, rather than east of, Akaitcho and West Bay Faults; segment F (Banting Formation) was sampled in 1983 exclusively in diamond drill intersections (DDH 1158 and 1157); only the upper part of segment A was sampled in 1983; and finally, Segment D was sampled twice in 1983, once in outcrop (7 samples) and once in two drill intersections, DDH 919 and 1159 (7 samples).

The stratigraphic scheme including formations, segments, cycles and samples are summarized in Table 1.

All samples were crushed and ground for chemical analysis by XRF (Cr, Ni, V, Sr, Zr, Y, Sr, Rb) and INAA (REE, Th, Hf, Ta, Ba, Sc, Co) techniques at the University of Toronto. Major elements were determined by XRF at University of Durham, England, by J.G. Holland. All major element analyses (weight percent) have been recalculated to 100% volatile free. All trace elements are reported in ppm.

The analytical techniques employed and the precision of the results have been described elsewhere (Barnes and Gorton, 1984). The precision of the measurements is estimated to be better than 5% for Zr, La, Sm, Sc, Co, Sr, Rb and most major elements; better than 10% for Hf, Ce, Eu, Yb, Y, V, Cr, Ni and P_2O_5; better than 20% for Th, Nd, Tb and Ba; and worse than 20% for Ta and Ho. Chrondrite values used to normalize the REE abundances are those by Taylor and Gorton (1977).

Stratigraphy

The stratigraphic scheme (formations, segments, cycles) and corresponding sampling are summarized in Table 1. Thus the Kam Formation divides naturally into Lower Kam, 6500 m thick, comprising segments A + B + Townsite Flows; and Upper Kam, 6800 m thick, with segments C, D and E (including E^1 + E^2). Banting Group, 700 m thick, comprises segment F. The volcanic succession also divides naturally into two main mafic-to-felsic cycles and one subsidiary cycle, each cycle marked by comparatively thick uniform basalt flows capped by thin felsic-intermediate

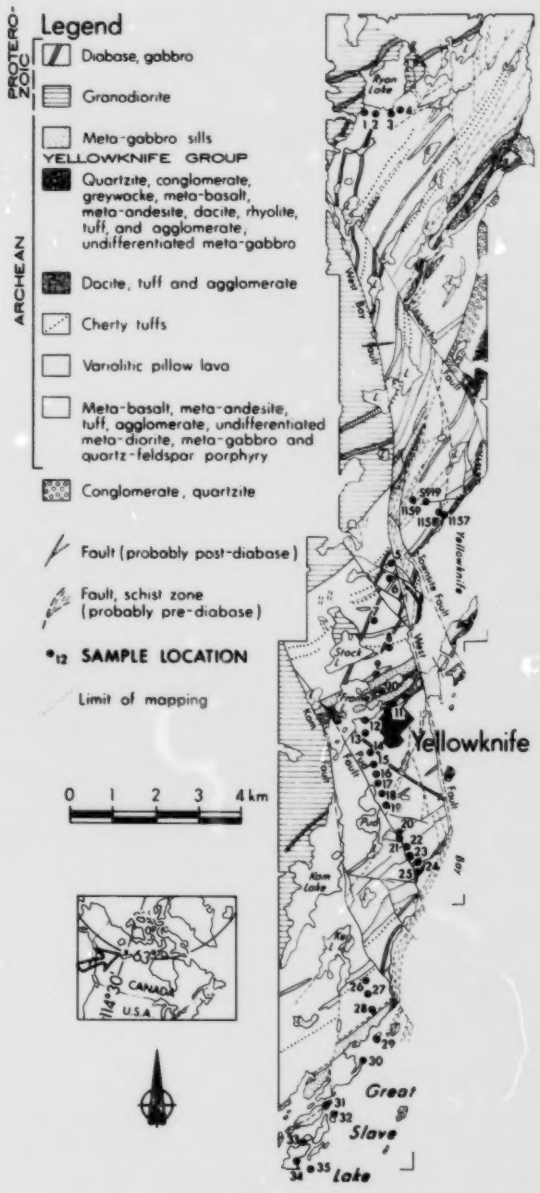

Figure 1: *Generalized geology and sample locations. Yellowknife Greenstone Belt, from Henderson and Brown (1966).*

volcanic units. The present cyclic divisions essentially follow those of Baragar (1966), two points of difference being: 1) Cycle 2 is terminated with segment E^1 rather than with F (Banting), and 2) E^2, previously demarcated chemically though not tabulated independently by Baragar (1966, Fig. 4), is elevated to the status of subsidiary cycle 3. The present scheme thereby divorces Banting felsic volcanic rocks from the Kam succession in recognition of their possible genetic independence (see below).

Table 2: Number of Samples by Class and Stratigraphic Division

	Lower Kam	Upper Kam	Total Kam	Banting	Yellowknife Belt
Basalt	6	23	29	0	29
Basalt-Andesite	3	5	8	0	8
Andesite	0	3	3	1	4
Dacite	2	0	2	4	6
Total	11	31	42	5	47

Classification

A simple SiO_2-based (volatile-free basis) rock classification is used: basalt – < 53%; basaltic andesite – 53-57%; andesite – 57-63%; dacite – 63-70%; and rhyolite – >70%. The possibility of SiO_2 metasomatism, which cannot be entirely excluded, constitutes a limitation of the system. As sampled in 1983, rhyolite is absent in the Yellowknife belt, the highest SiO_2 content recorded being 68.3% (Townsite Flows). This corresponds closely with Baragar's 1966 results.

According the the 1983 sampling, the Yellowknife volcanic succession is composed of the following class percentages, with the number of samples in brackets (Table 2); basalt – 62% (29); basaltic andesite – 17% (8); andesite – 8% (4); and dacite – 13% (6). Baragar's previous estimate (Baragar and Goodwin, 1969), based on greater sampling density (approximately 80 samples) and a normative-based classification, is: basalt – 60%; classes "A + B" – 7%; andesite – 18% and salic – 14%. Assuming that the present classes of basaltic andesite + andesite (= 25%) are equivalent to Baragar's classes "A + B" + andesite (= 25%), then the two results are in close agreement.

Analytical Results

The main chemical results are tabulated in Tables 3, 4, 5. A similar array of chemical results from other greenstone belts in Slave Province may be expected to lead in due course to meaningful province-wide inter-belt geochemical comparisons.

Mean Class (Table 3)

The mean class compositions with standard deviations provide the fundamental chemical framework of the Yellowknife belt. Major element compositions by class compare closely, for the most part, with those previously calculated by Baragar (Baragar and Goodwin, 1969). The notable exception lies in andesite which, according to the 1983 sampling, has significantly higher SiO_2 (62.5 vs 56.7%) and K_2O (1.67 vs. 0.59%); these contrasts are due mainly, though not completely, to different classification systems. Though data for comparison is not abundant, mean trace element compositions based on the 1983 sampling show similar levels of abundances to Baragar's previous calculations in basalt, but substantially higher levels of Ba, Zr and Co in andesite and dacite.

Trace element trends across the 4 classes correspond, for the most part, to those in a standard mafic-to-felsic igneous progression. Thus the mean abundance levels of incompatible elements (e.g. Ba, Sr, Rb, Th) increase; of transition elements (e.g. Ni, Cr, V, Co) decrease; of REE and LREE increase; and of HREE decrease. Basalt-andesite stands in anomalous exception to these trends with respect to both transition elements and REE. It is not known at present whether this is a true expression of this particular class composition, or is simply due to unrepresentative sampling.

Stratigraphic Divisions (Table 4)

Mean compositions by stratigraphic division (Table 4) provides insight into the composition of the volcanic rocks by segment, cycle, division, formation and belt. Segments A, B, C, and D + E[1] (cols. 1, 2, 5 and 6 respectively), which represent the bulk of the Yellowknife mafic volcanic rocks, reveal the following trends: consistently declining FeO, TiO_2 and MnO levels; consistently increasing MgO levels; and inconsistent levels in transition elements and REE. Cycle 3 (col. 8), with high Σ FeO, TiO_2 and MnO levels, very high Σ REE and incompatible element levels, yet unusually low transition element levels, stands apart from these general trends.

Mean Class Composition by Division (Table 5)

Mean class compositions by segment, cycle and formation (Table 5) provide direct comparisons by class across (i.e. from base to top) the stratigraphic column. Similar chemical trends are revealed to those in Table 4. Thus the bulk of the basalts, arranged in sequence (cols. 1, 2, 5, 6), reveal 1) decreasing FeO, TiO_2 and MnO levels, yet 2) increasing MgO level; 3) decreasing Σ REE, Σ LREE and Σ HREE levels, yet 4) generally increasing $[La/Yb]_N$ and $[Sm/Yb]_N$ levels; and 5) inconsistent incompatible and transition element levels.

SiO_2 Histogram (Fig. 2)

A SiO_2 histogram of a) Kam-Banting Formations, b) Lower Kam, and c) Upper Kam (Fig. 2 a,b,c) illustrates the essential bimodal character of the Yellowknife belt volcanic succession. Lower Kam (Fig. 2b) (N.B. including Townsite Flows) with mean SiO_2 = 53.66%, comprises basalt (55%), basaltic-andesite (27%) and some high-SiO_2 dacite (18%), the latter exclusively Townsite Flows. Thus the Lower Kam sequence lacks intermediate SiO_2 values (57-67%). Upper

Table 3: Mean Class Compositions

	Basalt		Basalt-Andesite		Andesite		Dacite	
	Mean	S.D.	Mean	S.D.	Mean	S.D.	Mean	S.D.
N =	29		8		4		6	
wt.%								
SiO_2	51.05	1.43	54.58	1.18	62.63	0.44	65.61	1.95
TiO_2	1.17	0.30	0.80	0.13	0.90	0.16	0.60	0.13
Al_2O_3	13.19	1.09	13.32	2.52	14.92	3.82	16.96	1.41
FeO	13.17	2.72	10.86	1.40	7.24	1.96	4.42	0.25
MnO	0.22	0.03	0.20	0.06	0.13	0.04	0.06	0.01
MgO	7.61	1.65	7.20	1.65	4.68	2.07	1.80	0.37
CaO	10.76	1.96	9.92	1.69	4.33	0.92	3.98	0.76
Na_2O	2.17	0.89	1.94	1.17	3.32	0.81	3.27	0.19
K_2O	0.49	0.37	1.11	1.21	1.67	2.01	3.09	0.30
P_2O_5	0.12		0.07		0.13		0.20	
FeO/MgO	1.60		1.51		1.54		2.46	
$\frac{FeO}{FeO + MgO}$	0.63		0.60		0.61		0.71	
ppm								
La	6.8	4.1	7.8	7.5	27.4	13.5	42.4	8.7
Ce	17.1	10.6	12.7	7.3	48.5	8.9	76.3	13.6
Nd	6.8	3.6	7.2	5.2	20.4	8.0	23.3	8.8
Sm	2.7	1.1	2.2	1.1	4.3	1.0	5.7	1.1
Eu	0.9	0.4	0.6	0.2	1.1	0.2	1.2	0.2
Eu_N	12.4		8.3		15.2		16.6	
Eu^*_N	12.9	5.5	9.5	3.8	16.7	2.1	20.5	3.9
Tb	0.6	0.2	0.4	0.2	0.8	0.3	1.0	0.4
Ho	1.0	0.7	0.7	0.5	1.3	0.5	1.2	0.4
Yb	2.3	0.6	1.8	0.4	1.4	0.9	1.4	1.0
Lu	0.4	0.1	0.3	0.1	0.3	0.1	0.2	0.1
REE[1]	38.6		33.7		105.5		152.7	
LREE[2]	33.4		29.9		100.6		147.7	
HREE[3]	4.3		3.2		3.8		3.8	
$[La/Yb]_N$	2.0	1.0	3.1	3.1 7.6	0.6	30	15	
$[La/Sm]_N$	1.6	0.4	1.9	0.9	3.7	0.9	4.5	0.6
$[Sm/Yb]_N$	1.3	0.4	1.4	0.8	2.3	0.1	6.3	2.9
$[Yb]_N$	10.9	3.0	8.6	1.7	6.5	4.5	6.5	4.8
Eu/Eu^*	1.0		0.9		0.9		0.8	
Th	1.4	1.2	1.4	1.0	7.1	2.1	13.6	2.7
Hf	2.2	1.0	1.6	0.6	4.3	0.9	4.6	0.6
Ta	0.2	0.2	0.2	0.1	0.5	0.2	0.7	0.1
Ba	124	91	22 1	208	494	521	756	206
Sc	37.9	9.4	36.2	7.6	16.8	–	8.8	1.8
Co	53	18	47	19	30	9	15	6
Cr	202	129	392	516	133	56	21	11
Ni	94	32	113	89	66	31	16	10
V	258	39	203	36	134	20	69	11
Zr	82	25	82	51	169	27	189	77
Y	25	6	20	4	23	8	24	16
Sr	111	42	140	113	175	58	223	63
Rb	12	11	29	35	29	44	78	17
Zr/Y	3.3	0.6	3.9	1.6	8.1	2.7	9.1	2.2
Rb/Sr	0.11		0.21		0.17		0.35	
Zr/Hf	37		51		39		41	

Footnotes:

[1] In Tables 3-5 = sum of all nine REE listed in the Table

[2] In Tables 3-5 = sum of La + Ce + Nd + Sm

[3] In Tables 3-5 = sum of Tb + Ho + Yb + Lu

In Tables 3-5, standard N = number of samples: subscript N = chondrite normalized value

Table 4: Mean Compositions by Stratigraphic Division

	Kam Formation												
	Lower Kam				Upper Kam								
	Cycle 1				Cycle 2			Cycle 3					
Segment	A	B	Town-site	Com-plete	C	D+E[1]	Com-plete	Com-plete E[2]	Com-plete	Com-plete	Banting FM. Complete	Upper Kam + Banting	Yellow-knife Complete
Column	1	2	3	4	5	6	7	8	9	10	11	12	13
N	4	5	2	11	10	17	27	4	31	42	5	36	47
wt%													
SiO_2	51.62	52.41	68.18	53.66	51.58	51.81	51.65	51.69	51.66	52.67	64.05	53.55	53.49
TiO_2	1.37	1.10	0.76	1.17	1.02	1.00	1.01	1.38	1.06	1.09	0.55	0.99	1.05
Al_2O_3	11.15	13.45	15.19	12.76	13.33	13.67	13.52	14.15	13.60	13.17	18.37	14.31	13.55
FeO	14.35	12.73	4.43	12.55	12.44	12.28	12.32	13.70	12.51	12.53	4.36	11.43	11.95
MnO	0.27	0.24	0.06	0.23	0.21	0.20	0.20	0.19	0.20	0.22	0.06	0.18	0.21
MgO	6.09	6.50	1.44	5.83	7.12	8.80	8.16	6.36	7.92	6.87	1.92	7.12	6.51
CaO	12.57	10.66	3.20	10.68	11.00	9.22	10.01	8.94	9.87	10.28	4.09	9.10	9.84
Na_2O	1.94	2.25	3.31	2.23	2.79	2.19	2.42	2.07	2.38	2.30	3.06	2.48	2.36
K_2O	0.39	0.54	3.13	0.74	0.42	0.70	0.59	1.31	0.67	0.72	3.39	0.69	0.90
P_2O_5	0.20	0.12	0.29	0.17	0.08	0.12	0.11	0.21	0.12	0.15	0.14	0.12	0.14
Fe/MgO	2.35	1.96	3.07	2.23	1.75	1.40	1.51	2.15	1.59	1.91	2.27	1.68	1.94
$\frac{FeO}{FeO + MgO}$	0.70	0.66	0.76	0.69	0.64	0.59	0.60	0.68	0.61	0.65	0.70	0.62	0.65
ppm													
La	6.2	5.5	41.6	9.4	5.5	8.5	7.3	17.9	8.7	9.1	43.6	13.4	11.6
Ce	17.9	13.0	63.4	20.0	13.3	18.7	16.7	28.4	18.2	19.1	78.5	26.4	23.3
Nd	8.0	6.2	30.2	9.3	6.0	7.6	7.0	12.2	7.7	8.5	22.3	9.7	9.5
Sm	3.1	2.3	6.5	3.0	2.1	2.6	2.4	4.6	2.7	2.8	5.4	3.1	3.0
Eu	1.1	0.8	1.1	1.0	0.7	0.8	0.8	1.2	0.8	0.9	1.2	0.9	0.9
Eu_N	15.1	10.5	15.0	12.8	9.3	11.6	10.7	16.7	11.5	12.2	15.9	12.1	12.5
Eu^*_N	16.9	11.4	24.2	14.9	9.6	12.2	11.2	19.0	12. 2	13.6	18.0	13.0	13.9
Tb	0.8	0.6	0.5	0.7	0.5	0.6	0.5	0.7	0.5	0.6	1.2	0.6	0.6
H_o	1.7	0.9	1.2	1.3	0.6	1.0	0.9	0.8	0.9	1.1	1.4	1.0	1.1
Yb	2.6	2.3	2.6	2.5	2.1	2.0	2.0	2.5	2.1	2.3	0.6	2.1	2.2
Lu	0.4	0.4	0.3	0.4	0.3	0.3	0.3	0.4	0.3	0.3	0.2	0.3	0.3
REE	41.8	32.0	147.4	56.4	31.1	42.1	37.9	68.7	41.9	44.7	154.4	57.5	52.5
LREE	35.2	27.0	141.7	50.8	26.9	37.4	33.4	63.1	37.3	39.5	149.8	52.6	47.4
HREE	5.5	4.2	4.6	4.6	3.5	3.9	3.7	4.4	3.8	4.3	3.4	4.0	4.2
$[La/Yb]_N$	1.8	1.6	10.0	2.5	1.9	3.0	2.6	5.4	3.0	2.8	39.4	7.9	5.4
$[La/Sm]_N$	1.4	1.4	3.9	1.7	1.5	1.9	1.8	2.3	1.9	1.8	4.9	2.3	2.0
$[Sm/Yb]_N$	1.3	1.0	2.7	1.3	1.1	1.5	1.4	2.1	1.5	1.4	8.1	2.4	1.9
Eu/Eu^*	0.9	1.0	0.6	0.9	1.0	1.0	1.02	0.9	1.0	1.0	0.9	1.0	1.0
$[Yb]_N$	12.5	11.0	12.7	11.8	10.1	9.4	9.6	11.2	9.8	10.8	2.8	8.9	10.2
Th	1.4	1.1	11.1	2.2	1.2	2.3	1.9	2.1	1.9	2.1	13.9	3.5	2.9
Hf	2.7	1.9	4.7	2.5	1.7	2.3	2.1	2.7	2.2	2.4	4.5	2.5	2.6
Ta	0.3	0.2	0.8	0.3	0.2	0.3	0.2	0.3	0.2	0.3	0.6	0.3	0.3
Ba	95	185	624	193	100	110	106	300	131	162	910	236	215
Sc	44.3	36.0	7.6	36.5	38.0	33.4	35.1	33.9	34.9	35.7	10.0	31.5	33.9
Co	67	46	12	51	44	49	48	56	49	50	20	45	48
Cr	526	285	5	353	186	219	206	88	191	272	34	170	255
Ni	171	133	9	136	102	109	106	96	105	121	29	95	114
V	298	295	47	271	262	250	254	211	248	260	93	227	248
Zr	92	84	320	111	71	91	84	143	93	102	148	100	105
Y	26	24	40	26	21	20	21	24	21	24	12	20	23
Sr	95	190	147	148	134	102	114	131	116	132	253	135	141
Rb	14	12	96	21	8	15	13	33	16	19	69	23	23
Zr/Y	3.5	3.5	8.0	4.3	3.4	4.6	4.0	5.9	4.4	4.3	12.3	5.0	4.6
Rb/Sr	0.15	0.06	0.65	0.14	0.06	0.15	0.11	0.25	0.14	0.14	0.27	0.17	0.16
Zr/Hf	34	44	68	44	42	40	40	53	42	43	33	40	40

[1]Weighted by number of samples within segments and by stratigraphic thicknesses (Table 1) between divisions.
[2]N = number of samples.

Table 5: Mean Class Compositions by Segment, Cycle and Formation

	Kam Formation											Banting Formation	
	Cycle 1				Cycle 2					Cycle 3			
	Basalt		Basalt Andesite	Dacite	Basalt			Basalt Andesite	Andesite	Basalt	Basalt Andesite	Andesite	Dacite
Segment	A	B			C	D	DH 919						
Column	1	2	3	4	5	6	7	8	9	10	11	12	13
N	3	3	3	2	8	6	6	4	3	3	1	1	4
wt%													
SiO_2	50.23	51.58	54.23	68.17	51.00	51.34	50.11	54.23	62.61	49.99	56.74	62.74	64.36
TiO_2	1.61	1.35	0.70	0.76	1.06	1.01	0.98	0.76	0.97	1.50	1.01	0.67	0.52
Al_2O_3	11.75	13.87	11.78	15.18	13.37	12.82	13.45	13.46	13.11	13.07	17.38	20.40	17.86
FeO	15.05	13.75	11.58	4.42	12.73	12.54	13.25	11.17	8.21	15.66	7.82	4.33	4.39
MnO	0.26	0.27	0.24	0.06	0.21	0.21	0.22	0.20	0.14	0.22	0.11	0.07	0.06
MgO	5.51	5.87	7.53	1.44	7.12	8.35	10.08	7.77	5.68	7.20	3.82	1.71	1.98
CaO	12.81	10.17	11.57	3.20	11.35	10.84	9.74	9.05	4.77	9.14	8.33	3.01	4.37
Na_2O	2.42	2.32	1.60	3.31	2.66	2.25	1.21	2.53	3.66	2.55	0.58	2.29	3.25
K_2O	0.26	0.47	0.69	3.13	0.38	0.51	0.78	0.72	0.67	0.42	3.96	4.65	3.07
P_2O_5	0.16	0.16	0.06	0.29	0.08	0.08	0.16	0.07	0.15	0.21	0.20	0.10	0.16
Fe/MgO	2.72	2.34	1.54	3.20	1.79	1.50	1.37	1.46	1.45	2.17	2.04	2.53	2.24
$\frac{FeO}{FeO + MgO}$	0.73	0.70	0.61	0.76	0.64	0.60	0.57	0.59	0.59	0.69	0.67	0.72	0.72
ppm													
La	6.7	6.5	4.3	41.7	5.4	5.3	6.1	6.0	20.9	15.6	25.1	46.8	42.8
Ce	19.5	16.8	9.1	63.4	12.6	9.5	14.3	15.3	44.2	33.7	12.6	61.3	82.8
Nd	9.1	7.5	4.5	30.2	6.2	3.9	7.1	6.3	16.5	10.0	18.7	37.2	19.9
Sm	3.7	2.6	1.7	6.5	2.1	2.2	2.5	1.9	3.9	4.5	4.9	5.6	5.3
Eu	1.3	0.8	0.6	1.1	0.7	0.7	0.9	0.6	1.1	1.4	0.7	0.8	1.2
Eu_N	17.4	11.5	8.7	15.0	9.6	9.0	12.4	8.8	15.7	19.2	9.3	11.8	17.0
Eu^*_N	19.3	13.7	8.4	24.2	10.4	10.2	12.3	8.3	17.2	19.5	17.5	15.3	18.7
Tb	0.9	0.7	0.4	0.5	0.5	0.5	0.5	0.5	0.7	0.8	0.3	0.9	1.3
H_o	2.0	0.8	0.9	1.2	0.5	0.5	1.6	0.8	1.1	1.0	0	2.0	1.3
Yb	3.0	2.4	2.0	2.6	2.2	2.0	2.1	1.7	1.8	2.8	1.7	0	0.7
Lu	0.5	0.3	0.3	0.3	0.4	0.3	0.3	0.3	0.3	0.4	0.3	0.5	0.1
REE	46.7	38.4	23.8	147.5	30.6	24.9	35.4	33.4	90.5	70.2	64.3	155.2	155.4
LREE	39.0	33.4	19.6	141.8	26.3	20.9	30.0	29.5	85.5	63.8	61.3	150.9	150.8
HREE	6.4	4.2	3.6	4.6	3.6	3.3	4.5	3.3	3.9	5.0	2.3	3.4	3.4
$[La/Yb]_N$	1.7	1.8	1.5	10.5	1.8	1.9	2.0	2.7	7.6	3.8	10.0	–	39.4
$[La/Sm]_N$	1.2	1.5	1.6	3.9	1.5	1.6	1.6	1.8	3.2	2.0	3.2	5.1	4.9
$[Sm/Yb]_N$	1.4	1.1	1.0	2.7	1.1	1.3	1.4	1.3	2.3	1.8	3.2	–	8.1
Eu/Eu^*	1.0	0.8	1.1	0.6	1.08	1.04	1.1	1.1	0.9	1.0	0.5	0.8	0.9
$[Yb]_N$	14.2	11.3	9.5	12.7	10.4	9.7	9.9	8.1	8.7	13.3	4.9	–	2.8
Th	1.5	1.2	1.0	11.1	1.1	1.6	1.2	1.8	6.2	2.4	1.2	9.9	14.9
Hf	3.0	2.3	1.4	4.7	1.8	1.9	2.0	1.7	4.3	3.1	1.4	4.3	4.6
Ta	0.4	0.2	0.2	0.8	0.2	0.2	0.3	0.2	0.5	0.4	0.2	0.5	0.6
Ba	73	184	178	624	101	71	181	136	236	169	691	1253	822
Sc	44.3	37.0	37.7	7.6	40.3	30.8	41.8	34.7	17.4	32.6	37.5	12.0	9.5
Co	62	46	59	12	46	46	64	39	28	62	38	37	16
Cr	92	257	827	5	185	247	210	238	135	104	37	71	25
Ni	84	145	220	9	98	114	109	113	96	117	34	54	23
V	327	332	231	47	266	268	279	249	165	241	122	126	85
Zr	106	98	57	320	72	69	76	67	183	117	203	145	149
Y	29	28	17	40	22	21	20	17	24	24	25	11	12
Sr	96	129	218	147	131	114	78	103	151	148	79	213	263
Rb	3	13	21	96	9	11	18	14	13	8	106	90	64
Zr/Y	3.7	3.5	3.2	8.0	3.4	3.4	3.5	3.8	7.7	4.8	9.0	13.0	12.4
Rb/Sr	0.03	0.10	0.10	0.65	0.07	0.10	0.23	0.14	0.09	0.05	1.34	0.42	0.24
Zr/Hf	35	43	41	68	40	36	38	39	43	38	145	34	12

Kam (Fig. 2c) (N.B. excluding Banting felsic units) with mean SiO_2 = 50.67%, comprises basalt (74%), basaltic-andesite (16%), and andesite (10%). The Upper Kam SiO_2 gap is only 4% (57-61). Finally, Kam + Banting combined (Fig. 2a), with mean SiO_2 = 53.02% comprise basalt (62%), basaltic andesite (17%), andesite (8%), and dacite (13%). Thus the volcanic succession is composed of repeated alternations of thick low-SiO_2 and thin high-SiO_2 units. There is no obvious quantitative relationship between the respective low-SiO_2 and high-SiO_2 parts. Intermediate SiO_2 values (53-63%), though rare, are present in the Yellowknife assemblage which is, therefore, more appropriately classified as a modified biomodal volcanic succession.

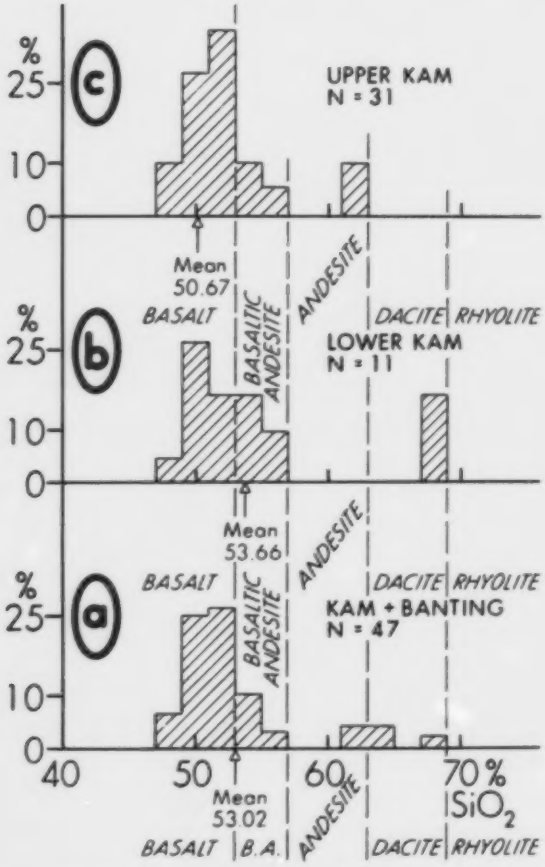

Figure 2: *SiO_2 histogram of 47 Yellowknife samples*

AFM Diagram

The eleven Lower Kam samples display a bimodal distribution. Thus of nine Lower Kam samples (segments A, B in Table 4), eight (#1-8 in Table 1) plot in, or on the boundary of, the tholeiite (TH) field of the AFM diagram (Fig. 3a); and one (#9) falls in the calc-alkaline (CA) field, but close to the TH boundary. The remaining two Lower Kam samples (#10, 11), both of Townsite Flows units, plot well within the CA field.

Thirty-one Upper Kam samples (segments C, D, E^1 and E^2 in Table 4; sample #12-42 in Table 1) plot almost equally in the TH (16 samples) and CA (15 samples) fields (Fig. 3b). The CA components comprise eleven samples (#12, 17-22, 25, 27, 28, 42 of segments C and D) lying close to the TH boundary, and four samples (#29-31, 35 of segments E^1 and E^2) at a greater distance from the F-M tie-line. Finally, the five Banting samples (#43-47 of segment F) occupy the same isolated part of the CA field as do the Townsite Flow samples in Figure 3a.

Comparison with Table 1 reveals that the majority (14 of 18) of Kam CA samples occupy upper stratigraphic positions in their respective segments i.e. segments B (#9), C (#17-21), Da) (#25, 27, 28), Db) (#42), E^1 (#29-31), and E^2 (#35). Thus each of the five segments (B, C,D,E^1 and E^2) represents a chemical compositional gradation with lower thicker TH and upper thinner CA parts. Furthermore the preponderance (15 of 18) of CA units in the Upper Kam division demonstrates an overall TH-CA chemical progression across the entire Kam Group. Furthermore, although most CA units lie close to the TH boundary in proximity to, and in possible genetic relationship with, the accompanying TH units, the seven Townsite and Banting felsic units (Figs. 3a, b) respectively occupy identical, sharply isolated CA positions, thereby allowing of a separate common origin distinct from that of the stratigraphically underlying mafic units.

Ni-Sr (Fig. 4)

A log-log plot of Ni-Sr provides insight into the relationship of incompatible (Sr) and compatible (Ni) elements. Compatible element abundances are controlled mainly by processes of crystallization differentiation whereas those of incompatible elements are influenced mainly by partial fusion. The plot thereby reveals the relative influences of these two main magma-forming processes (Martin, 1985; Jahn *et al.*, 1980).

Fig. 4a shows Ni-Sr plots for the eleven Lower Kam samples. The upper nine plots (>30 ppm Ni) are those of mafic flows in segments A, B whereas the two lower plots (<10 ppm Ni) are those of the felsic Townsite Flows. The pronounced vertical trends, parallel to the compatible element (Ni) axis, is apparent. Considered in more detail, the four segment A samples define a sub-vertical line to the left at about 90 ppm Sr; and the companion four samples from segment B a sub-vertical alignment slightly to the right, with, however, sample #9, which was taken at the stratigraphic top of segment B, significantly offset to the right (400 ppm Sr, 60 ppm Ni) on a line approximately parallel to the incompatible element (Sr) axis. The two felsic Townsite Flow samples plot on the main sub-vertical alignment in the lower

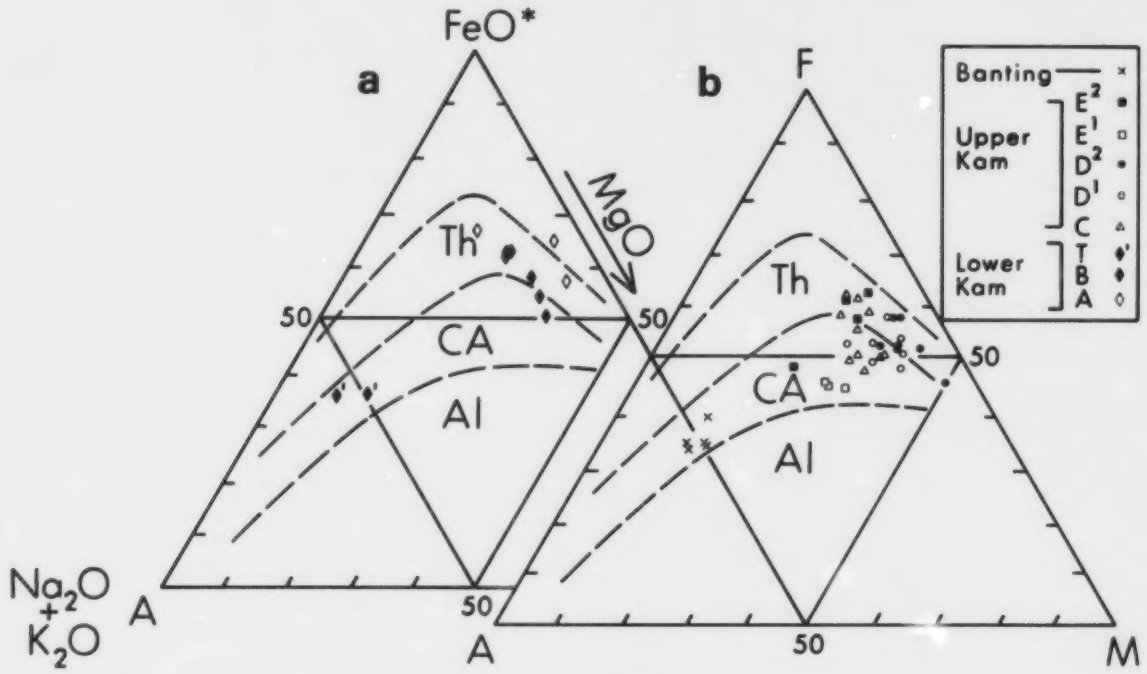

Figure 3: *AFM plot of a) Lower Kam and b) Upper Kam and Banting samples*

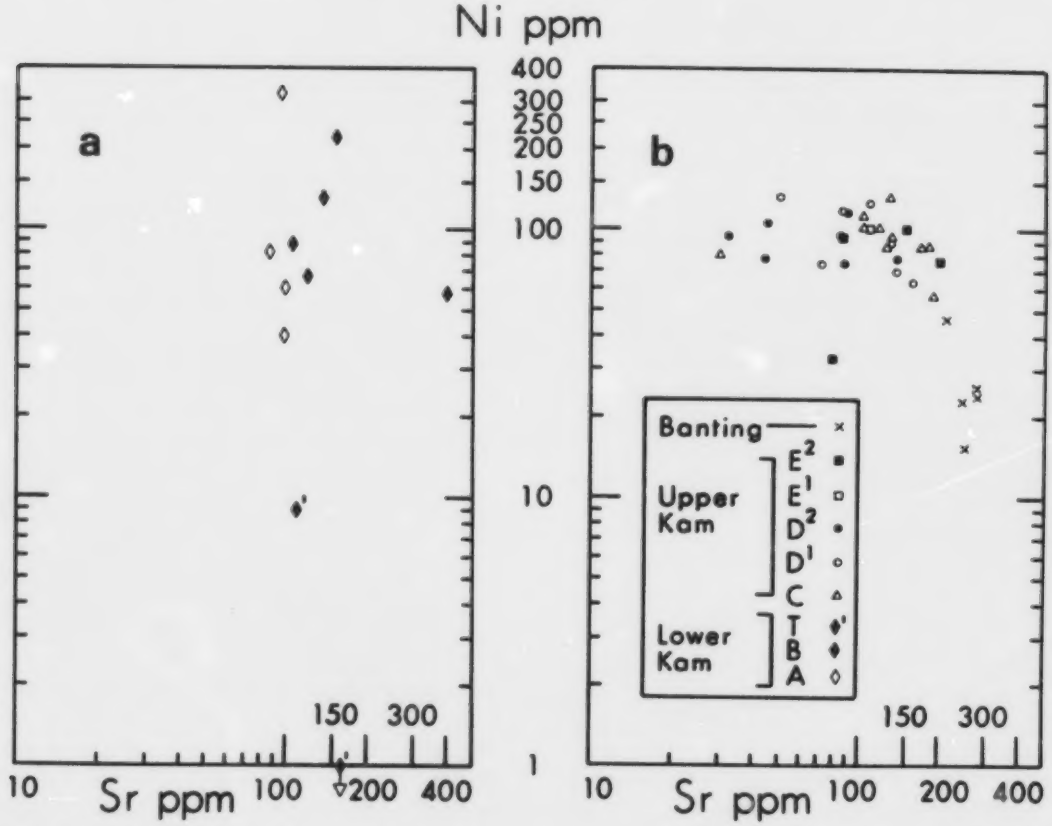

Figure 4: *Ni-Sr log-log plot a) Lower Kam and b) Upper Kam*

part of the diagram, at significantly reduced Ni values compared to the rest of the Lower Kam samples.

Fig. 4b is the comparable Ni-Sr plot for the 31 Upper Kam and 5 Banting samples. All but one (#35 from the top of segment E^2) of the 31 Upper Kam samples plot in a generally subhorizontal oval zone lying between 40-150 ppm Ni and 30-200 ppm Sr that is sub-parallel to the horizontal incompatible element (Sr) axis. Sample #35 plots vertically below this zone (33 ppm Ni and 80 ppm Sr) and close to the sub-vertical trend described by Lower Kam samples (Fig. 4a). The five Banting samples, in contrast, describe a generally vertical trend (200-300 ppm Sr) somewhat offset to the lower right of the main Upper Kam zone, yet with significantly higher Ni-Sr abundances than the two corresponding felsic Townsite Flows (Fig. 4a).

The genetic implications of these contrasting Ni-Sr trends are discussed below. In the meantime, in terms of regional structure, the sharp compositional contrast between Lower Kam (Fig. 4a) and Upper Kam (Fig. 4b) rocks renders unlikely any attempt to stratigraphically correlate these two divisions. Thus the data do not support the proposed mutual stratigraphic correlation on structural grounds (Helmstaedt *et al.*, 1979) of a) Townsite Flows plus associated sill (Lower Kam) and b) Kam Point sill plus felsic fragmental rocks (Upper Kam). Such a correlation would make Lower Kam and Upper Kam volcanic rocks stratigraphic equivalents, a relationship denied by the chemical data.

$[La/Yb]_N$-$[Yb]_N$ (Fig. 5)

This diagram provides a view of light REE (represented by La) and heavy REE (represented by Yb) abundances and corresponding enrichment-depletion trends in the volcanic rocks. In this diagram, a vertical trend parallel to the $[La/Yb]_N$ axis is in the direction of enriched La and depleted Yb contents, whereas a horizontal trend parallel to the $(Yb)_N$ axis represents changes in Yb content alone. Areas I-V represent arbitrary divisions of the general field of Archean volcanic rocks (Goodwin, unpublished). Most tholeiitic basalt-komatiite lavas plot in or close to Area III. The common mafic-felsic volcanic trend in Archean volcanic piles is in a sub-vertical direction from Area III across Area II to Area I. A less common trend in the volcanic piles, but one of metallogenic significance, is sub-horizontally inclined to the upper right from Area III to Areas IV and/or V.

Cycle 1 mafic volcanic samples (I) define an irregular elliptical zone plotting in Area III and the adjoining part of Area II. The two Townsite Flows felsic samples (T) plot vertically above in Area I ($[La/Yb]_N$=10). Cycle 2 mafic volcanic samples (IIa) plot in an enlarged field that incorporates most of that of Cycle 1 mafic lavas, but in addition, extends significantly both below, i.e. lower $[La/Yb]_N$ in Area III, and above, i.e. higher $[La/Yb]_N$ in Area II. The more evolved Cycle 2 andesite flows of segment E^1 (2b) plot

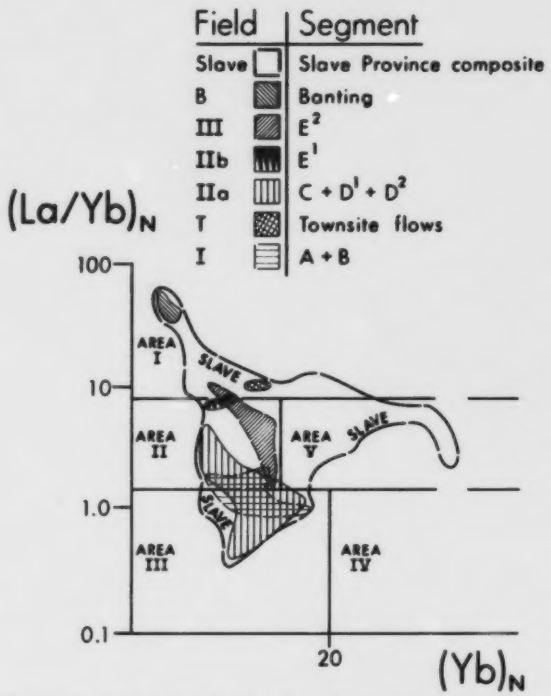

Figure 5: *$[La/Yb]_N$ - $[Yb]_N$ plot of Yellowknife volcanic rocks in relation to Slave Province field*

on the Area I-II boundary close to but slightly offset to the lower left from the Townsite Flows (T). Cycle 3 volcanic samples (III), comprising three basalts and one basaltic-andesite, plot mainly in Area II in a subvertical elliptical field extending from the lower right boundary of Area II to the lower part of Area I. Finally, Banting felsic volcanic samples (B) plot high in Area I, in the extreme upper La/Yb position for the Yellowknife assemblage.

Cycles 1 (segments A + B + Townsite Flows) and 2 (segments C + D + E^1) thereby describe basically similar patterns: 1) stratigraphically lower mafic components have conventionally low $[La/Yb]_N$ = 1.5-2; and 2) upper felsic components have elevated $[La/Yb]_N$ = 8-11. Cycle 3 (segment E^2) pattern is also similar with, however, the mafic components extending to a still higher $[La/Yb]_N$ position. The mafic components of the three cycles thereby display a compositonal progression in the direction of a more evolved (higher $[La/Yb]_N$) components.

In summary, Cycle 1 and Cycle 2 mafic volcanic rocks cover similar fields except for the upper prolongation of Cycle 2. Cycle 3 field has significantly higher $[La/Yb]_N$, in this regard resembling the upper prolongation of Cycle 2. The intermediate-felsic components of the three cycles occupy similar fields at or near the Area I-II boundary. Banting components, in contrast, are the most highly evolved Yellowknife volcanic rocks. The fundamental Yellowknife cyclic pattern is expressed, then, in the rhythmic alternation of lower and higher $[La/Yb]_N$ stratigraphic parts.

Discussion

Petrogenesis

The essential bimodal character of the Yellowknife volcanic succession (Fig. 2) with, however, significant basaltic-andesite and some andesite components, can be interpreted as the products of 1) processes of magma differentiation from a mantle source(s) (i.e. crystallization differentiation and/or partial fusion); 2) involvement of two distinct magma sources, namely mantle and pre-existing continental crust; or 3) some combination of these two. The present data do not provide an unequivocal answer to this fundamental problem of magma genesis. On the one hand, the cyclic development of the bulk of the volcanic components, dominated by basalt and basaltic-andesite components with their conventional TH-CA progressions, could be products of differentiation processes involving more or less common mantle sources. However, the separate and distinct character of the felsic volcanic components, in the volcanic cycles, with only limited intervening intermediate components, suggests a completely separate origin for the felsic volcanic rocks such as the melting of sialic crust. Additional data, especially Sr-Rb and Sm-Nd would be required to resolve this.

Whatever the source of the felsic components, it seems clear that the Lower Kam and Upper Kam mafic components are products of different processes of differentiation, probably involving different mantle sources (Fig. 4). Lower Kam lavas are indicated to be products of fractional crystallization processes of mantle-derived material containing < 300 ppm Ni and 90-150 ppm Sr. Upper Kam lavas, on the other hand, were apparently derived by partial fusion processes from a mantle source with 100-150 ppm Ni and > 30 ppm Sr. Thus there appears to be a fundamental change in both source and process at the Lower-Upper Kam boundary.

A possible solution is provided by a mantle diapir mechanism whereby the earlier mantle source of Lower Kam (Cycle 1) would be overwhelmed by the rising, compositionally changing mantle source of, successively, Cycles 2 and 3. The simplest method of introducing the felsic volcanic components is to allow for periodic fusion of older sialic crust. However, as stated above, other geochemical data are required to test the feasibility of this hypothesis.

Metallogenesis

By way of review, felsic metavolcanics in 13 varied Archean volcanic piles in Superior Province have been divided into 3 major groups based on trace element geochemistry (Lesher *et al.*, 1986) and following the system of Condie (1976), with the following metallogenic aspects:

1. F1 group: dacite and rhyolite. Steep REE patters $[La/Yb]_N$ = 6-34; Yb = 4-3.8; weakly negative to moderately positive Eu anomalies; high Sr and Zr/Y (9-31); low abundances of high field strength (HFS) elements (Th, U, Zr, Hf). Representative horizons have been identified in 7 volcanic piles. None of the F1 group horizons, as known, host base metal sulfide deposits.

2. F2 group: rhyodacite and rhyolite. Gently sloping REE patterns $[La/Yb]_N$ = 2-6, Yb = 1.7-6.0; variable Eu anomalies; moderate Zr/Y (6-11); and intermediate abundances of HFS elements and Sr. Representative horizons have been identified in 4 volcanic piles. Only F2 group horizons in the Sturgeon Lake volcanic pile host base metal sulfide deposits.

3. F3 group: rhyolite and high- SiO_2 rhyolite. Relatively flat REE patterns $[La/Yb]_N$ = 1-5, Yb = 3.4-32, with either a) variable but generally moderately negative Eu anomalies, low Zr/Y (4-7), high Sc, and intermediate HFS element abundances; or b) pronounced negative Eu anomalies. Located so far in 6 volcanic piles. All of the F3 group horizons, with one exception (Garrison in Ontario) host important base metal sulfide deposits.

These results demonstrate the variety of felsic volcanic rocks present in the greenstone belts, and some metallogenic implications. The geochemical variations are attributed mainly to petrogenetic differences. In this regard F3 group volcanic rocks have been attributed to local felsic differentiation in high level magma chambers which also may have influenced the formation of massive base metal sulfide deposits (Campbell *et al.*, 1985).

Figure 5 and Tables 3-5 reveal clearly that Yellowknife volcanic rocks correspond to F1 group, namely those associations in which the felsic components have steep REE patterns, insignificant Eu anomalies, high Sr and Zr/Y, and comparatively low abundances of high field strength elements. According to the model, this association is unfavourable for the presence of massive base metal sulfide deposits.

Figure 5 further shows the field of all available REE analyses from Slave Province including 55 samples from the Cameron River and Beaulieu River greenstone belts and 6 samples from the High Lake belt (unpublished data) located respectively 75 km east and 450 km north of Yellowknife. The composite Slave Province $[La/Yb]_N$ - $[Yb]_N$ field has a significant extension subparallel to the high $[Yb]_N$ axis, which is in the direction of the favourable F3 group of felsic metavolcanics as discussed above. A study of the metallogenic significance and implications of the Cameron River-Beaulieu River data is presently underway.

Conclusions

1. Systematic sampling and chemical analysis of Yellowknife volcanic rocks provide mean class compositions and mean compositions by both stratigraphic division and volcanic cycle in terms of 10 major elements and 23 trace

elements together with conventional element and oxide ratios. This geochemical data base is intended to serve as a basis of comparison with other volcanic belts in Slave Province and beyond.

2. The Yellowknife volcanic sequence comprises 62% basalt, 17% basaltic andesite, 8% andesite and 13% dacite. Rhyolite is apparently absent. The succession constitutes a modified bimodal assemblage.

3. The sequence divides into two main and one subordinate mafic-to-felsic volcanic cycles, each cycle comprising a thick tholeiitic lava flow part capped by thin intermediate-felsic mainly pyroclastic units. The Lower Kam division constitutes volcanic cycle 1; Upper Kam segments C,D and E^1 constitute cycle 2; and Upper Kam segment E^2 constitutes a third, subordinate cycle. These three volcanic cycles are unconformably overlain by Banting felsic pyroclastic rocks (segment F), with or without intervening clastic sediments.

4. The majority of Yellowknife volcanic rocks fall in the tholeiite field or adjoining part of the calc-alkaline field in a normal AFM diagram. In contrast, the felsic pyroclastic units occupy a distant part of the calc-alkaline field without significant intervening representatives. This suggests that the felsic units have a separate origin, possibly related to melting of sialic crust.

5. The relationship of certain incompatible (Sr) and compatible (Ni) elements suggests that Lower Kam volcanic rocks are products of fractional crystallization processes of mantle-derived material containing 300 ppm Ni and 90-150 ppm Sr, whereas Upper Kam lavas were apparently derived by partial fusion processes from a mantle source with 100-150 ppm Ni and 30 ppm Sr. Thus a fundamental change in both source and process is indicated to have occurred at the Lower-Upper Kam boundary. More data are required to further explore this petrogenetic relationship.

6. Yellowknife volcanic rocks clearly correspond to the Lesher *et al.* F1 group of volcanic rocks in which the felsic components have steep REE patterns, insignificant Eu anomalies, high Sr and Zr/Y, and comparatively; low abundances of high field strength elements. This association is considered to be unfavourable for the presence of massive base metal sulfide deposits.

7. However, preliminary data from the Cameron River - Beaulieu River and High Lake volcanic belts show that they include volcanic units that correspond in trace element composition to the F3 group of felsic volcanic horizons which is considered to be favourable to the presence of such base metal deposits.

Acknowledgements

I am grateful to W.A. Padgham for full support in the Yellowknife field area, and to Carol Ellis for her able assistance in the sampling program. S. Shanbhag, University of Toronto, prepared the illustrations. Critical comments by E.M. Cameron and an unknown reviewer are gratefully acknowledged.

References

Baragar, W.R.A. 1966. *Geochemistry of the Yellowknife volcanic rocks*. Can. Jour. Earth Sci.: v. 3, p. 9-30.

Baragar, W.R.A. and Goodwin, A.M. 1966. *Andesites and Archean volcanism of the Canadian Shield*. In Proceedings of the Andesite Conference: edited by A.R. McBirney; Oregon Department of Geology and Mineral Industries: Bulletin 65, p. 121-142.

Barnes, S.J., and Gorton, M.P. 1984. Trace element analysis by neutron activation with a low flux reactor (SLOWPOKE II): results for international standards. Geostandards Newsletter, 8(1), p. 17-23.

Campbell, I.H., McDougal, T.J. and Turner, J.S. 1985. *A note on the fluid dynamic processes which can influence the deposition of massive sulfides*. Economic Geology: v. 79, p. 1905-1913.

Condie, K.C. 1976. *Trace-element geochemistry of Archean greenstone belts*. Earth-Science Reviews: 12, p. 393-417.

Easton, R.M. 1984. *Compilation of geochronologic data for the Yellowknife greenstone belt (85J/8, 85J/I) and vicinity, District of Mackenzie, N.W.T.* In Contributions to the Geology of the Northwest Territories: edited by J.A. Brophy; DIAND, EGS 1984-6, p. 1-20.

Helmstaedt, H., King, J., Goodwin, J.A. and Patterson, J.G. 1979. *Geology of the southwest end of the Yellowknife greenstone belt*. In Proceedings of the Gold.

_____, and Padgham, W.A., 1986. A new look at the stratigraphy of the Yellowknife Supergroup at Yellowknife, N.W.T. – implications for the age of gold-bearing shear zones and Archean basin evolution. Can. Jour. Earth Sci., *23:* 454-475.

Henderson, J.F. and Brown, I.C. 1966. *Geology and structure of the Yellowknife greenstone belt, District of Mackenzie*. Geol. Surv. Canada: Bulletin 141.

Henderson, J.B., 1970. *Stratigraphy of the Archean Yellowknife supergroup; Yellowknife Bay - Prosperous Lake area, District of Mackenzie*. Geol. Surv. Canada: Paper 70-26.

_____ 1981, Archean basin evolution in the Slave Province, Canada; *in* Precambrian Plate Tectonics, ed. A. Kroner; Elsevier, Amsterdam, p. 213-235.

Jahn, B.M., Auvray, B., Blais, S., Capdevila, R., Carnichet, J., Vidal, F., and Hameurt, J., 1980. Trace element geochemistry and petrogenesis of Finnish greenstone belts. Jour. Petrology, *21:* 201-244.

Lambert, R. St. J., Chamberlain, V.E. and Cunningham, M., 1984. *Sm-Nd age and petrogenesis of Yellowknife Group volcanics*, N.W.T. Geol. Assoc. Canada, program with Abstracts: v. 9, p. 81.

Lesher, C.M., Goodwin, A.M., Campbell, I.H. and Gorton, M.P., 1986. *Trace-element geochemistry of ore-associated and barren felsic metavolcanic rocks in Superior Province, Canada*. Can. Jour. Earth Sci., *23:* 222-237.

Martin, H., 1985. Nature, origine et evolution d'un segment de croute continentale archeene: contraintes chimiques et isotopiques. Memoires et Documents du Centre Armoricain d'Etude structurale des Socles, Rennes, France.

Padgham, W.A., 1985. *Observations and speculations on supracrustal successions in the Slave Structural Province*. In Evolution of Archean Supracrustal Sequences: edited by L.D.Ayres, P.C. Thurston, K.D. Card and W. Weber; Geol. Assoc. Canada, Special Paper 28: p. 133-152.

Taylor, S.R. and Gorton, M.P., 1977. Geochemical application of spark source mass spectrography-III. Element sensitivity, precision and accuracy. Geochimica et Cosmchimica Acta, 41: p. 1375-1380.

Contribution to the Geology of the Northwest Territories, Volume 3, 1988, NWT Geology Division, INAC, Yellowknife.

Stratigraphy and Structure of the Early Proterozoic Wilson Island Group of Great Slave Lake

B.J. Johnson

Ottawa-Carleton Centre for Geoscience Studies,
Department of Geology, Carleton University, Ottawa, Ontario

Abstract

The Early Proterozoic (ca. 1.9 Ga) Wilson Island Group is exposed in a fault-bounded belt in the East Arm of Great Slave Lake. Deposition of intercalated basalt flows, felsic flows, volcaniclastic rocks, and fluvial to shallow-marine arkose and conglomerate took place in a tectonically active basin that probably was underlain by extending continental crust. This assemblage grades vertically into sandstone and dolostone of probably marginal- and shallow-marine origin. Dolostone is overlain by sandstone, argillaceous siltstone, concretionary pisolitic ironstone, and mudstone, forming an overall transgressive marine shelf of epicratonic platformal sequence.

Rocks of the Wilson Island Group were deformed and metamorphosed before deposition of the Great Slave Supergroup (Early Proterozoic). East- to southeast-plunging folds and penetrative foliation with a steep down-dip stretching lineation formed in response to north-south compression. These early structures were subsequently deformed by kink folds and dissected by brittle transcurrent faults of the McDonald fault system.

Introduction

The Early Proterozoic Wilson Island Group is a fault-bounded succession of metasedimentary and metavolcanic rocks preserved in the East Arm of Great Slave Lake, District of Mackenzie (Fig. 1). Ubiquitous penetrative deformation and greenschist to amphibolite facies metamorphic grade distinguish the Wilson Island Group from the younger Proterozoic supracrustal successions in the East Arm (Great Slave Supergroup and Et-then Group). Stratigraphic contacts between the Wilson Island Group and the Great Slave Supergroup have been obscured by thrusting, subsequent transcurrent faulting, and erosion (Hoffman, 1980, 1981; Bowring *et al.*, 1984). Demonstrable basement to the Wilson Island Group is nowhere exposed.

The regional geology of the East Arm was first described by Stockwell (1933; 1936a, 1936b). Mapping and stratigraphic studies of rocks in the Wilson Island area were carried out by Reinhardt (1969, unpublished maps). Yeo (1976a, 1976b) reported sedimentological aspects of the Wilson Island Group sandstones, including paleocurrents and geochemical analyses. Hoffman *et al.* (1977) completed 1:50,000 scale mapping of the Proterozoic rocks of the East Arm, and outlined evidence for an unconformable relationship between the Wilson Island Group and the Great Slave Supergroup: clasts of strongly deformed metasedimentary rocks of probable Wilson Island Group provenance within a conglomerate near the base of the Sosan Group (lowermost Great Slave Supergroup). This conglomerate is exposed on an island, 6.5 kilometres south of Wilson Island (Fig. 1b).

A U-Pb zircon age of 1928 ± 11 Ma (Bowring *et al.*, 1984) was determined from samples of a felsic dike that intrudes clastic and volcanic units in the lower part of the Wilson Island Group succession. Extrusive equivalents of the dike occur within this succession.

Detailed mapping during 1984 and 1985 has yielded new stratigraphic and structural information. Results and implications of this work are summarized in this report.

Stratigraphy and Depositional History

The Wilson Island Group is exposed in a northeast-trending belt that extends from the Outpost Islands to Basile Lake (Fig. 1). Incomplete stratigraphic successions are well exposed on Wilson Island, and on the mainland around Basile Bay. The rocks at Basile Bay have been displaced northeastward relative to those on Wilson Island, along the dextral McDonald-Wilson Fault (Hoffman *et al.*, 1977). In both areas the strata generally dip sub-vertically and face northwestward; the lithologies at the top of the section on Wilson Island closely resembly those in the lower part of the Basile Bay section. The Wilson Island and Basile Bay packages therefore appear to represent, respectively, lower and upper parts of a continuous succession.

Informal names for some of the mappable rock units are capitalized in the following descriptions.

Wilson Island: Mixed Clastic/ Volcanic Assemblage

An assemblage of mafic and felsic volcanic rocks intercalated with medium- and coarse-grained clastic sedimen-

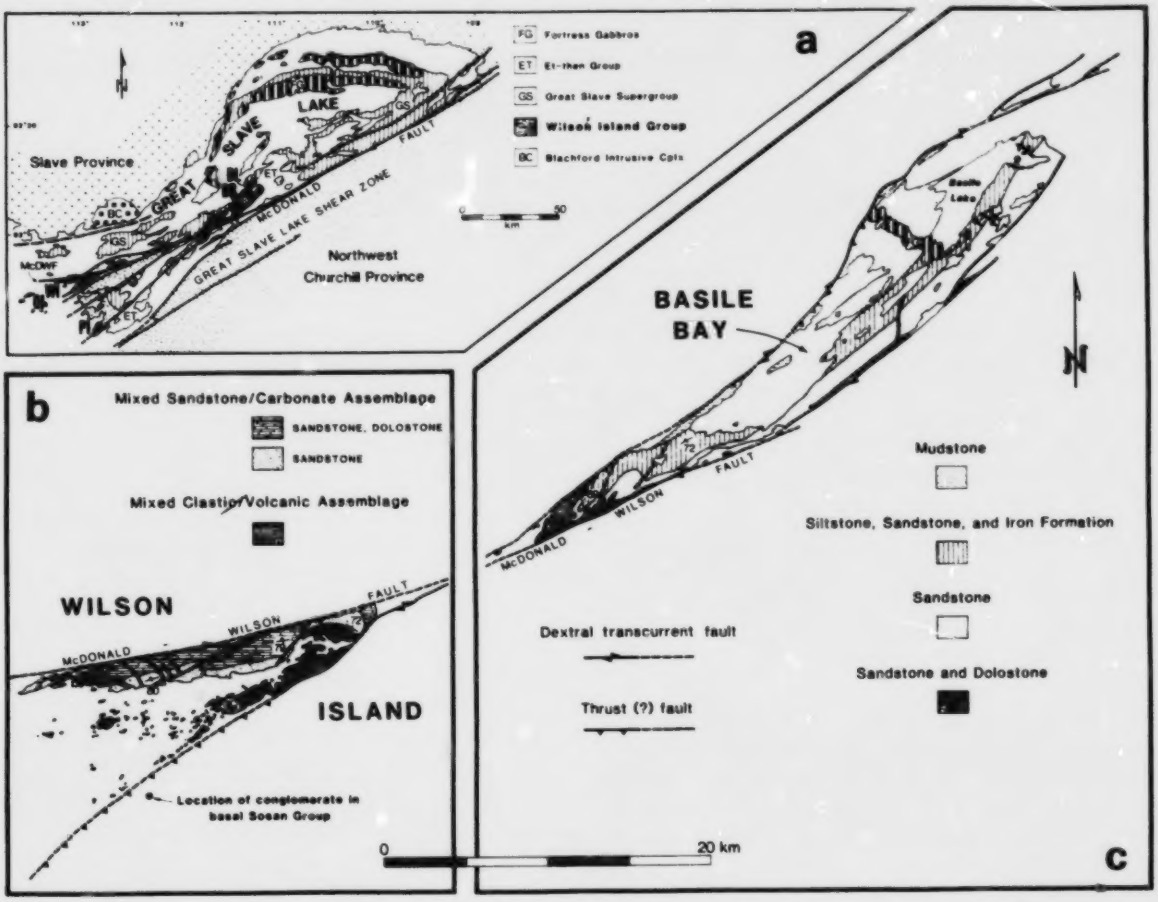

Figure 1: *Regional geology of the East Arm of Great Slave Lake (a), showing distribution of the Wilson Island Group. BB: Basile Bay; BL: Basile Lake; OI: Outpost Islands; PI: Petitot Islands; McDWF: McDonald-Wilson Fault. Adapted from Hoffman, 1985. Generalized geology of the Wilson Island area (b) and Basile Bay area (c), based on the present study. Following Hoffman (1985), some faults are labelled with both thrust and transcurrent fault symbols, to indicate that they probably have been loci of both types of movement.*

tary rocks forms the lower 1800 metres of exposed section, cropping out on Wilson Island and on adjacent islands (Fig. 1b). About half of this assemblage comprises volcanic and related hypabyssal intrusive rocks.

Thick felsic extrusive units, interpreted as subaerial domes, are linked to a network of porphyry feeder dikes. Phenocrysts of albitic plagioclase, present in all of the felsic units, commonly make up 20% of the rock. Some of these phenocrysts display zoning. Biotite, magnetite(?), chlorite, and epidote are common in some of the units. More siliceous units consist of alternate microcrystalline quartzo-feldspathic and sericitic layers, with phenocrysts of quartz and albite (or albitized potassium feldspar). Rocks of this more siliceous variety are probably true rhyolites, whereas the units in which mafic and calcic minerals abound may be closer to dacite in composition. Flow banding and abundant spherulites in many of the flows are indicative of rapidly cooled siliceous eruptions.

Amygdaloidal basalt flows are slightly less abundant than their felsic counterparts. They are composed of actinolite (typically in excess of 50% of the modal mineralogy), plagioclase, epidote, pyrite, magnetite(?), and small amounts of biotite and carbonate. Actinolite, biotite, and epidote also are abundant in plagioclase-phyric mafic dikes, which in many places are spatially associated with the felsic porphyries. Some felsic dikes contain abundant schistose biotite-rich inclusions, which may represent either xenoliths or quenched blobs of mafic magma. The latter of these two possibilities implies the coexistence of both mafic and felsic liquids.

Mixed pyroclastic-epiclastic units (Fig. 2a) occur both below and above one of the basalt flows. These consist of coarse quartz and feldspar sand grains, lapilli-sized fragments of biotite schist interpreted as pyroclasts (cf. Schmid, 1981), less common angular cobbles or blocks of basalt, and rare sedimentary rock fragments, in a fine-grained matrix of

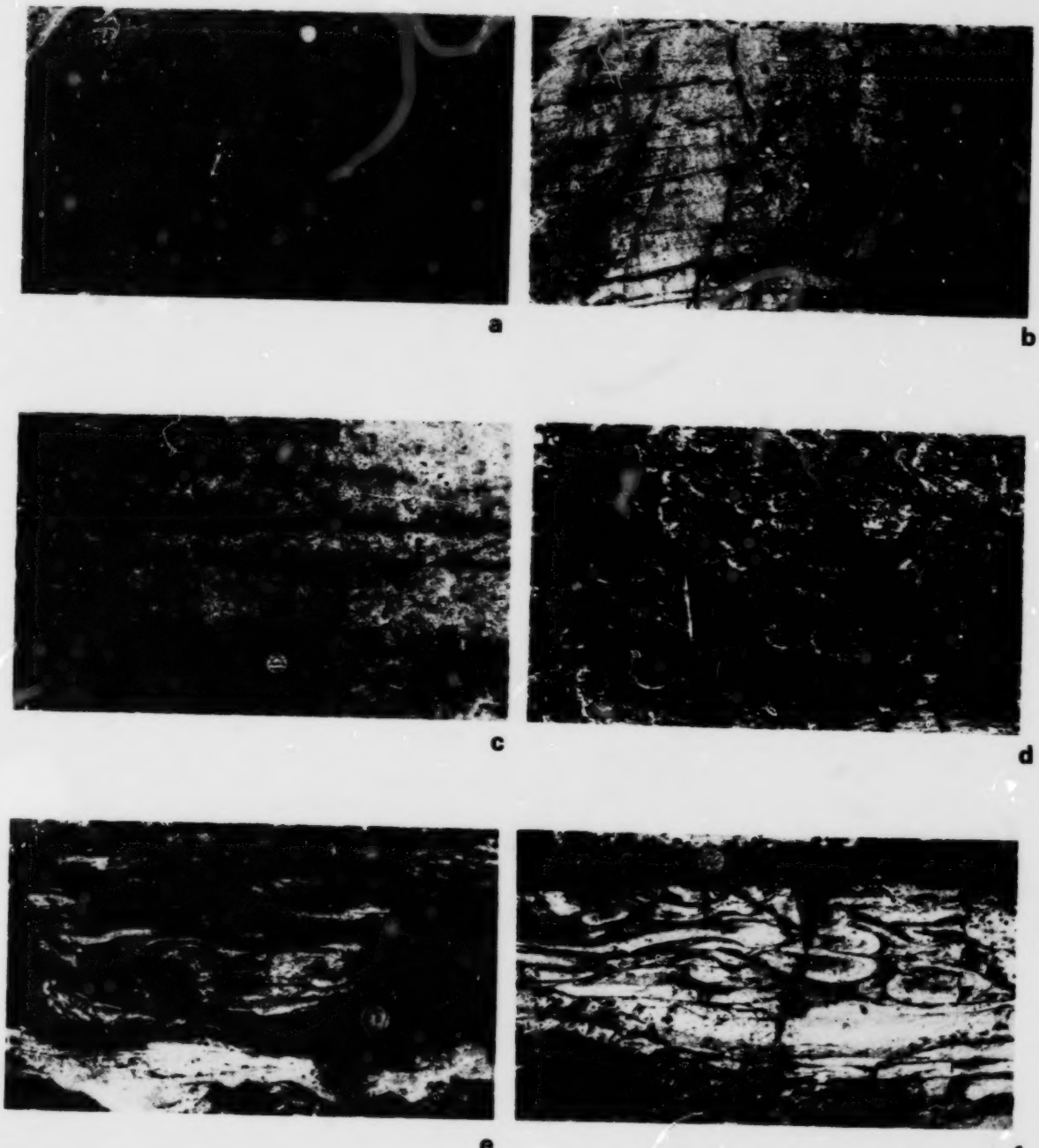

Figure 2: *a. Mixed pyroclastic-epiclastic debris flow unit, containing angular fragments of biotite schist (metamorphosed pyroclasts?), amygdaloidal basalt (large clast in lower centre), and light-coloured siltstone.*
b. Trough crossbeds and scoured channels with pebble lags in arkosic arenite of Mixed Clastic/Volcanic Assemblage. Top to right.
c. Trough crossbedded and current-rippled sandstone of Mixed Sandstone/Carbonate Assemblage. Ripple tops have been modified to form reactivation surfaces (dark laminae).
d. Slump-folded unit in dolostone near Basile Bay. The internal laminae define elliptical closures, a manifestation of smaller sheath folds within the compound folded unit (see text). Laminae near the lower right corner of photograph are truncated above a soft-sediment thrust fault (arrows).
e. Load-casted lenses in rippled and crossbedded sandstone.
f. Ball-and-pillow structures in sandstone (light colour) intercalated with argillaceous siltstone.

biotite, chlorite, and quartz inferred to be metamorphosed ash. They occur as massive, unstratified units up to 30 metres thick, and are interpreted as debris flows triggered by magmatic or phreatomagmatic eruptions.

Medium- to coarse-grained, immature to submature arkosic arenites and conglomeratic arkoses make up about half of the Mixed Clastic/Volcanic Assemblage. Pebbly and conglomeratic layers contain clasts of vein quartz, foliated and non-foliated granitoid rocks, mafic and intermediate volcanics, and metasedimentary rocks.

The arenites display extensive trough cross bedding, and fine-grained layers exhibit current ripple and parallel laminations. Scoured channels with pebble lags and small-scale fining-upward sequences are exposed in a few places (Fig. 2b). Typical cosets are less than 50 centimetres thick, and show marked lateral continuity. Such features collectively are characteristic of distal braided river and alluvial plain deposits (Rust, 1978). In many intervals, large-scale trough crossbedded units alternate with lenticular bedded or small ripple bedded units that commonly have been modified by reactivation. Although such features have been reported from fluvial successions (Collinson, 1970), tidal processes favour development of both lenticular bedding (Reineck and Singh, 1980) and reactivation surfaces (Klein, 1970). The arenites of the Mixed Clastic/Volcanic Assemblage thus may represent sedimentation in a combination of distal fluvial and marginal marine (tidal flat / deltaic ?) environments.

Conglomeratic arkoses in the upper part of the Mixed Clastic/Volcanic Assemblage contain abundant clasts (locally boulder sized) of felsic volcanic rocks derived from the underlying flows. Trough crossbeds and erosive-based fining-upward cycles in these units suggest that they in part are of fluvial origin. However, laterally continuous granulestones that mark the top of the Mixed Clastic/Volcanic Assemblage resemble gravel beach deposits.

Tectonic instability during deposition of the Mixed Clastic/Volcanic Assemblage is indicated by the presence of volcanic units and an abundance of soft-sediment deformation structures, and is supported by regionally extensive abrupt vertical changes from sand-dominated to gravel-dominated sedimentation (Johnson, 1985).

Mixed Sandstone/ Carbonate Assemblage

The remainder of the section at Wilson Island consists of some 2000 metres of intercalated sandstone (90%) and dolostone (10%), that gradationally overly the conglomeratic units of the Mixed Clastic/Volcanic Assemblage. The sandstones are medium- to coarse-grained arkosic to subarkosic arenites, are texturally more mature than arenites in the underlying Mixed Clastic/Volcanic Assemblage, and display abundant trough crossbedding. Paleocurrent patterns determined from these trough crossbeds are unimodal, suggesting braided fluvial deposition (Yeo, 1976a, 1976b). However, the dominance of ebb or flood tides can produce unimodal patterns in shallow marine sediments as well (e.g., Klein, 1970; Anderton, 1976), particularly when tidal processes are enhanced by storm surge (Anderton, 1976.).

The textural maturity of the sandstones, their tabular bedding style, and intimate association with carbonates are suggestive of shallow marine deposition, although a combination of distal fluvial and lacustrine sedimentation could also produce such an assemblage. Wavy bedded units are present in some intervals, along with rhythmically interbedded sandstone and mudstone resembling the "tidal bedding" described by Wunderlich (1970). Both of these bedding types are common in tidal sediments (Reineck and Singh, 1980). Reactivation surfaces in some of the cross bedded units (fig. 2c) provide additional evidence for tidal processes.

The sandstone components of this assemblage thus may represent marginal marine environments; the dolostones probably represent offshore (subtidal) carbonate environments. A westward decrease in the siliciclastic/carbonate ratio along Wilson Island, and the abundance of westerly directed crossbeds (restored on the basis of rotation of bedding, without correction for plunge of folds), are consistent with dominant ebb tide or storm-surge ebb, away from a terrigenous source to the east. Nevertheless, the possibility of a significant component of terrestrial deposition is not precluded.

Basile Bay: Sandstone and Dolostone

The oldest rocks at Basile Bay are medium- to coarse-grained arkoses that contain minor intercalated dolostone, similar to the youngest units on Wilson Island. These are overlain by siltstones which in turn are overlain by a succession of virtually uninterrupted dolostone about 300 metres thick. The latter typically weathers dark brown and forms resistant, high-standing outcrops.

The most common sedimentary structures in the dolostones are slump folds, which in many cases involve entire beds several metres thick. Internally, each slump folded unit is composed of smaller sheath folds, indicating that differential strain rates existed within each flowing mass (Fig. 2d). Soft-sediment thrust faults also are locally developed within the slump sheets. These thick carbonates most likely are of shallow-marine origin, and probably were deposited adjacent to a bathymetric inflection such as a reef margin or shelf edge, where frequent slumping could have occurred.

Sandstone

The dolostones are overlain by up to 1000 metres of pink, medium-grained quartzitic sandstone (Lower Quart-

zite, Fig. 3). The contact between these two units ranges from sharp and slightly erosional in the southwest to gradational in the northeast. The sandstones (predominantly submature arkosic arenites) display trough and planar cross bedding, graded bedding, and small-scale cross bedding. Yeo (1976a, 1976b) has suggested that these sandstones were deposited by braided rivers, because a unimodal southwesterly transport direction (restored by simple rotation of bedding) is indicated throughout most of the section by abundant trough and planar crossbeds. Although much of the succession probably is indeed of braided fluvial origin, bidirectional foresets in a few localities suggest that this unit is at least partly of shallow-marine origin (e.g., lower intertidal sand flats). The fluvial component of the depositional system may have consisted of numerous intertidal channels.

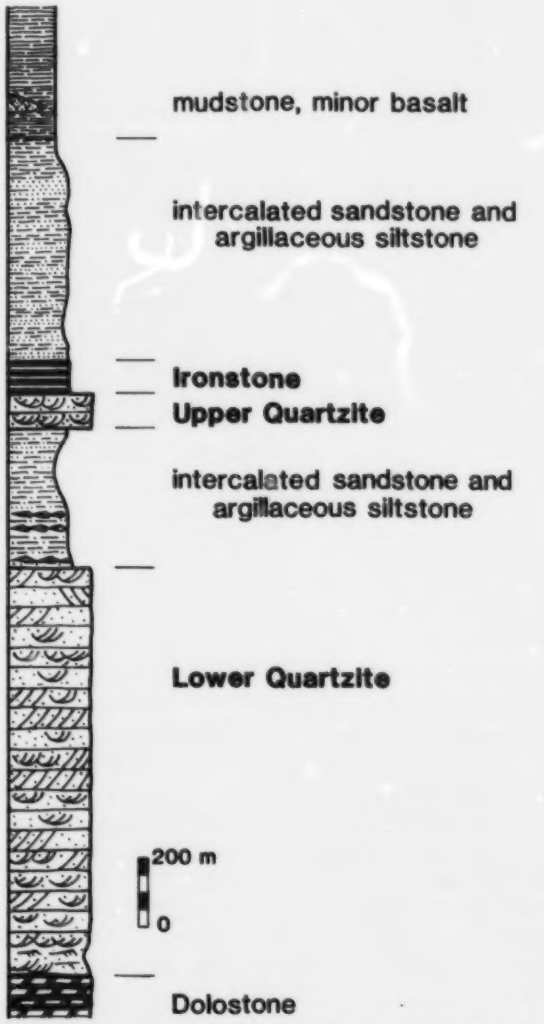

Figure 3: *Composite section of strata above dolostone unit, Basile Bay area. Scale approximate.*

Siltstone, Sandstone, and Iron Formation

The Lower Quartzite is overlain by argillaceous siltstones intercalated with grey, fine-grained sandstones. Wavy and lenticular bedding, load-casted sandstone lenses, and ball-and-pillow structure are common where the two rock types are thinly interbedded (Fig. 2e, f). This association may represent alternating bed load and suspended load sedimentation on intertidal flats. However, the environmental instability implied by the soft-sediment deformation structures may be an effect of rapid sedimentation by storms in a more distal (subtidal) environment. Graded bedding and planar lamination in many of the units are consistent with this hypothesis.

The 100-metre-thick Upper Quartzite (Fig. 3) is similar to the Lower Quartzite. It is extensively trough crossbedded, and may represent either braided rivers, tidal channels, or lower intertidal sand flats. The overlying Ironstone unit consists of gray fine-grained sandstone with abundant hematite banding. Planar lamination is the predominant sedimentary structure. The top of this unit is marked by a hematitic bed containing calcareous pisoliths. The pisoliths probably formed during temporary sub-aerial (vadose) exposure of the sediments, perhaps in a supratidal environment.

The Ironstone unit is overlain by several hundred metres of intercalated fine-grained grey sandstone and argillaceous siltstone, that form graded beds 5-100 metres thick. These rocks probably represent a gradual onlap from an intertidal to a subtidal environment, wherein the graded units were deposited by storm-generated turbidity currents.

Mudstone

Continued transgression or subsidence is recorded by gradation into an unknown thickness of green to dark gray, parallel-laminated phyllitic mudstone with minor intercalated porphyritic basalt. The top of the section is truncated by a fault which juxtaposes Wilson Island Group rocks against the younger Kahochella Group (Great Slave Supergroup).

Outpost Islands: Quartzite, Metagreywacke and Schist

Strata exposed on the main archipelago of the Outpost Islands consist of alternating quartzites, metagreywackes, and schist. Quartzites and micaceous quartzites in the lowermost unit (Fig. 4) are extensively trough crossbedded, and contain abundant quartz pebbles in the lower part of the exposed section. Subparallel to both bedding and schistosity in about the middle of the unit are zones rich in chalcopyrite and pyrite, that also contain gold, tungsten, and tin (Lord, 1951). Near the top of the unit, quartzite beds comprising crossbedded and current-rippled sets alternate with thin layers of biotite schist. The quartzites most closely resemble fluvial deposits, but by analogy with similar units on

Figure 4: *Geology of the main archipelago of the Outpost Islands. Rock units on southwesternmost island display an asymmetric S-shaped fold pattern, which is overprinted by a large Z-shaped kink fold. Location shown in inset. BI: Butte Island; OI: Outpost Islands; McDWF: McDonald-Wilson Fault; WI: Wilson Island.*

Wilson Island, may be of marine origin. The other quartzite units in this succession are more difficult to interpret, because sedimentary structures are only rarely exposed.

The metagreywacke units are schistose feldspathic quartzites which contain abundant metamorphic biotite and muscovite. Locally they contain beds (commonly boudinaged), pebbles, and boulders of white quartzite, and beds of pelitic schist. Sedimentary structures are absent or have been obscured by deformation. These units probably were in part deposited by sediment gravity flows (W.A. Padgham, pers. comm., 1985), either as alluvial or submarine fans.

The pelitic schists are typically rich in biotite, and contain porphyroblasts of staurolite and andalusite. Chlorite occurs as a retrograde product of biotite, and as sheaths around andalusite. The schist units contain beds of quartzite and metagreywacke.

The nature of the gold-tungsten-tin-sulfide mineralization is puzzling. Associated lenses and veins of quartz containing andalusite, sapphire, muscovite, and some gold (Lord, 1951) are suggestive of high-temperature fluids, but the timing of emplacement of these veins relative to mineralization is uncertain. The host rocks are richer in fine-grained white mica than the adjacent units, possibly as a result of sericitization (or simply as a function of composition of the original sediment). A magmatic heat source, possibly genetically related to a granitic pluton exposed on Butte Island (7 km east of the Outpost Islands), may have generated or aided in the mobilization of mineralizing hydrothermal fluids. Regional deformation may have controlled or modified the orientation of the mineralized zone with respect to strata; both are approximately parallel to the plane of flattening. However, Padgham (1984) has suggested that the unusual mineral association and stratabound nature of the zone favour a syngenetic origin for the mineralization. A detailed study of the ore mineral paragenesis must be undertaken before any hypothesis of origin can be substantiated.

Structure

The Wilson Island Group records a period of deformation and metamorphism which is inferred to have predated deposition of the Great Slave Supergroup. The main phase of deformation is expressed by open to nearly isoclinal folds, pervasive southeast-dipping foliation, and a steep down-dip stretching lineation on foliation surfaces. These structures collectively were produced in response to north-south compression, with a subvertical component of extension. The metamorphic grade is greenschist facies, except in the westernmost exposures (Outpost Islands), where rocks belonging to a deeper structural level are of amphibolite facies.

The stretching lineation typically is best developed where large-scale folds are prominent and where the rocks are strongly foliated; for example, in the core of a tight

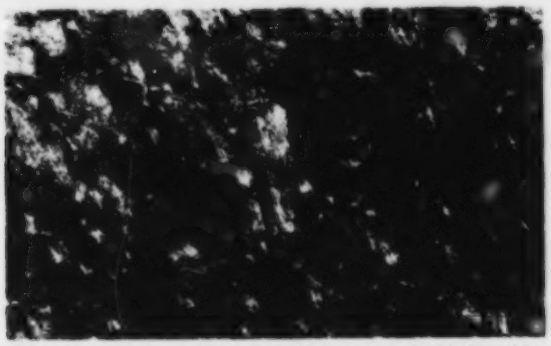

Figure 5: *Foliation surface of andalusite-muscovite-biotite schist, Outpost Islands. Elongate pressure shadows on andalusite porphyroblasts define the steep down-dip stretching lineation, a characteristic tectonic feature of rocks of the Wilson Island Group.*

syncline southwest of Basile Bay, deformed quartz granules in the Upper Quartzite unit have aspect ratios (X:Z) of at least 10:1. Pressure shadows on andalusite porphyroblasts define the stretching lineation in the Outpost Island schists (Fig. 5). Rotated inclusion trails in staurolite porphyroblasts, which occur in textural equilibrium with the andalusite, indicate that deformation was concomitant with metamorphism.

Bedding-cleavage intersections have yielded the regional pattern of fold axis orientations shown in Figure 6. Throughout most of the map area, especially along the main part of Wilson Island and in the region between Basile Bay and Basile Lake, bedding is essentially homoclinal and intersection lineations plunge moderately eastward. However, in the hinge areas of large folds, such as the aforementioned syncline southwest of Basile Bay (Fig. 1c), intersection lineations plunge steeply to the southeast, down the dip of the axial-plane cleavage and subparallel to the stretching lineation. Therefore, at the present level of erosion, these folds are reclined (cf. Hobbs *et al.*, 1976), in contrast to the predominant regional geometry of moderately plunging inclined structures. This incongruous pattern is inferred to be the result of progressive rotation of the hinges of the folds into the regional extension direction during deformation. Minor folds in some areas, such as south of Wilson Island, have southwest-plunging axes, suggesting that large scale folds are in part noncylindrical as well. Mechanisms for the formation of both incongruous and noncylindrical folds have been discussed by Ramsay and Sturt (1973).

An isolated remnant of possible Wilson Island Group rocks (Reinhardt, 1969) in the Petitot Islands (Fig. 1a) is mylonitized. Shear bands (Fig. 7) and a subhorizontal stretching lineation indicate dextral transcurrent shear at this locality. This style of deformation is characteristic of the youngest portions of the Great Slave Lake Shear Zone (Hanmer and Lucas, 1985), on the mainland east of the Petitot Islands (Fig. 1a).

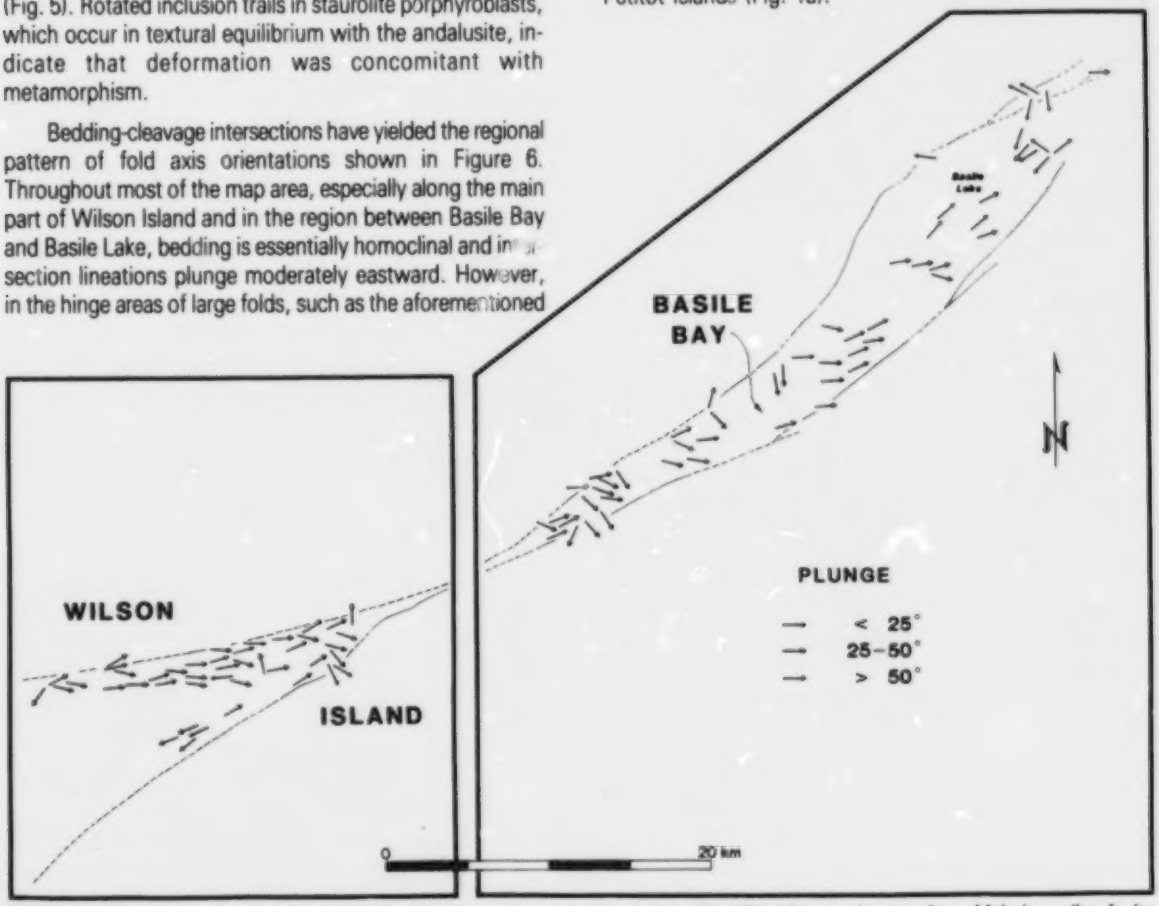

Figure 6: *Distribution of fold axis orientations based on measured and calculated bedding-cleavage intersections. Main bounding faults are shown to facilitate location with respect to Figure 1.*

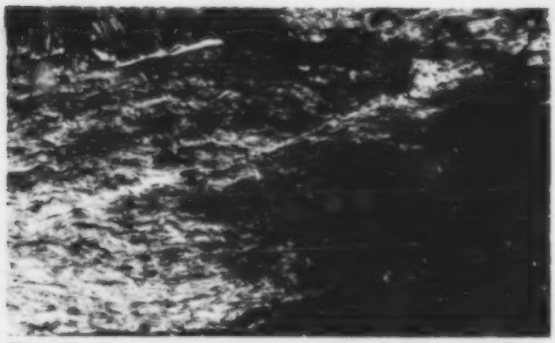

Figure 7: *Dextrally sheared mylonitic rocks, Petitot Islands. Shear bands extend from upper left to lower right.*

On the Outpost Islands, rock units displaying an asymmetric S-shaped fold geometry have been refolded by a steeply plunging Z-shaped kink fold, creating a flattened horseshoe-shaped interference pattern (Fig. 4). On the short limb of the kink, sulfide zones associated with intercalated thin beds of quartzite, metagreywacke, and schist, are deformed by abundant minor kink folds. Structures related to the main phase of deformation are regionally refolded by such kink folds on all scales. Similarly, the foliation in the hinge areas of main phase folds is deformed by crenulations, kinks, and (in the Outpost Islands) crenulation cleavage. The scale and intensity of kinking or crenulation is largely dependent on lithology. Whether these younger structures formed during a late stage of the main phase of deformation, or represent a separate event, has not been determined.

The folds have been truncated by thrust faults which now separate the Wilson Island Group from rocks of the Great Slave Supergroup (Hoffman, 1985), and subsequently have been dissected by numerous northeast-trending dextral transcurrent faults and northwest-trending normal faults of the McDonald fault system. The main bounding faults south of Wilson Island and north of the Basile Bay – Basile Lake area may be thrust faults which later served to localize transcurrent movement; these faults are labelled with both thrust and transcurrent fault symbols in Figure 1.

Discussion

Interpretation of the tectonic setting of the Wilson Island Group is complicated by its structural isolation with respect to other rock units. Previous workers have suggested that the depositional basin was a fault-bounded trough (Yeo, 1976a, 1976b) or rift (Hoffman *et al.*, 1977). The Great Slave Lake Shear Zone (Hanmer and Lucas, 1985), which delineates the northwestern margin of the Churchill Province (Fig. 1a), has recently been interpreted as a remnant of a magmatic arc that formed as a consequence of oblique east-dipping subduction at approximately 1.98-1.90 Ga (Hoffman *et al.*, 1986). This has raised the possibility that the Wilson Island Group is exotic to the Slave Craton, having been deposited in a forearc basin on the northwestern edge of the Churchill Province. The evidence presented in this paper is inconclusive with regards to this hypothesis; it appears possible, however, that the Wilson Island Group evolved as a forearc basin characterized by an early extensional phase and a later compressional phase.

Although no geochemical data are yet available, field and thin section evidence strongly suggest that the volcanic rocks are compositionally bimodal. With rare exceptions, bimodal volcanic assemblages are generated in areas underlain by either extending continental crust or thick oceanic crust (Hildreth, 1981). Granitoid pebbles and abundant potassium feldspar in the clastic rocks indicate that the Wilson Island Group was deposited on, or adjacent to, continental crust. Thus, an extensional tectonic regime probably was in effect during initial deposition.

Tidal and storm-induced sedimentation and formation of an overall fining-upward succession are in keeping with the gradual evolution of the rift basin into a subsiding open marine shelf or epicratonic platform. Subsequent folding, associated southeast dipping foliation, and down-dip stretching lineation are consistent with the structural style that could be expected to result from deformation of a northwest-facing forearc.

Acknowledgements

I extend thanks to the Geology Division of the Northern Affairs Program of DIAND for generous support of this project. Additional financial support has been provided through NSERC Operating Grant A5536 (to J.A. Donaldson). Field work was carried out in 1984 and 1985 with vital assistance from Rhonda Bell, Arnold Enge, Diane Gault, Sally Howson, Jennifer Wahlroth, and Anna Wong. Logistical support was provided (in the form of expediting service) by Martin Irving and Craig Robinson, and (in the form of wings) by Larry Zurloff of Latham Island Airways. Discussions in and out of the field with Larry Aspler, Al Donaldson, Simon Hanmer, Paul Hoffman, Bill Padgham, and Gary Yeo have given much-needed direction to the study.

References

Anderton, R. 1976: Tidal shelf sedimentation: An example from the Scottish Dalradian. Sedimentology, v. 23, p. 429-458.

Bowring, S.A., Van Schmus, R.W., and Hoffman, P.F. 1984: U-Pb zircon ages from Athapuscow Aulacogen, East Arm of Great Slave Lake, N.W.T., Canada. Can. J. Earth Sci.: v. 21, p. 1315-1324.

Collinson, J.D. 1970: Bedforms of the Tana River, Norway.Geografiska Annaler: v. 52-A, p. 31-56.

Hanmer, S., and Lucas, S.B. 1985: Anatomy of a ductile trans-current shear: the Great Slave Lake Shear Zone, District of Mackenzie, NWT (preliminary report); *in* Current Research, Part B. Geol. Surv. Can.: Pap. 85-1B, p. 7-22.

Hildreth, W. 1981: Gradients in silicic magma chambers: Implications for lithospheric magmatism. J. Geophys. Res.: v. 86, p. 10153-10192.

Hobbs, B.E., Means, W.D., and Williams, P.F. 1976: An outline of structural geology. John Wiley & Sons: New York, 571 pp.

Hoffman, P.F. 1980: Wopmay Orogen: A Wilson Cycle of Early Proterozoic age in the northwest of the Canadian Shield; *in* Strangway, D.F. (ed.), The continental crust and its mineral deposits. Geol. Assoc. Can.: Spec. Pap. 20, p. 523-549.

_____, P.F. 1981: Autopsy of Athapuscow Aulacogen: A failed arm affected by three collisions; *in* Campbell, F.H.A. (ed.), Proterozoic basins of Canada. Geol. Surv. Can.: Pap. 81-10, p. 97-102.

_____, P.F. 1985: Geology and tectonic maps of the Athapuscow Aulacogen (Proterozoic), East Arm of Great Slave Lake, N.W.T. Geol. Surv. Can.: Open File 1121.

Hoffman, P.F., Bell, I.R., Hildebrand, R.S., and Thorstad, L. 1977: Geology of the Athapuscow Aulacogen, East Arm of Great Slave Lake, District of Mackenzie; *in* Report of Activities, Part A. Geol. Surv. Can.: Pap. 77-1A, p. 117-129.

Hoffman, P.F., Culshaw, N.G., Hanmer, S.K., LeCheminant, A.N., McGrath, P.H., Tirrul, R., Van Breemen, O., Bowring, S.A., and Grotzinger, J.P. 1986: Is the Thelon Front (NWT) a suture?; *in* Program with Abstracts. v. 11, Geol. Assoc. Can.: p. 82.

Johnson, B.J. 1985: Preliminary report on the geology of the Wilson Island Group, Great Slave Lake, N.W.T. Contrib. Geol. Northwest Terr:, v. 2, p. 91-93. NWT Geol. Div., Yellowknife.

Klein, G. de V. 1970: Depositional and dispersal dynamics of intertidal sand bars. J. Sed. Pet.: v. 40, p. 1095-1127.

Lord, C.S. 1951: Mineral industry of District of Mackenzie, Northwest Territories. Geol. Surv. Can.: Mem. 261.

Padgham, W.A. 1984: Gold deposits of NWT classes, styles genesis, exploration methods and success probabilities. Contrib. Geol. Northwest Terr.: v. 1, p. 121-129. NWT Geol. Div., Yellowknife.

Ramsay, D.M., and Sturt, B.A. 1973: An analysis of noncylindrical and incongruous fold pattern from the Eo-Cambrian rocks of Soroy, northern Norway I. Noncylindrical, incongruous, and aberrant folding. Tectonophysics: v. 18, p. 81-107.

Reineck, H.E., and Singh, I.B. 1980: Depositional sedimentary environment with reference to terrigenous clastics; Springer-Verlag: Berlin, 549 pp.

Reinhardt, E.W. 1969: Wilson Island – Petitot Islands area, East Arm of Great Slave Lake (85 H/10, 11, 15 (south half)); *in* Report of Activities, Part A. Geol. Surv. Can.: Pap. 69-1, p. 177-181.

Rust, B.R. 1978: Depositional models for braided alluvium; *in* Miall, A. D. (ed.), Fluvial sedimentology. Can. Soc. Pet. Geol.: Mem. 5, p. 605-625.

Schmid, R. 1981: Descriptive nomenclature and classification of pyroclastic deposits and fragments: Recommendations of the IUGS Subcommission on the Systematics of Igneous Rocks. Geology: v. 9, p. 41-43.

Stockwell, C.H. 1933: Great Slave Lake – Coppermine River area, Northwest Territories; *in* Summary Report 1932, Part C. Geol. Surv. Can.: p. 37c-63c.

_____, C.H. 1936a: Eastern portion of Great Slave Lake (west half). Geol. Surv. Can.: Map 377A.

_____, C.H. 1936b: Eastern portion of Great Slave Lake (east half). Geol. Surv. Can.: Map 378A.

Wunderlich, F. 1970: Genesis and environment of the "Nellenkopf-chenschichten" (lower Emsian, Rheinian Devon) at locus typicus in comparison with modern coastal environment of the German Bay. J. Sed. Pet.: v. 40, p. 102-130.

Yeo, G.M. 1976a: Sedimentology and geochemistry of the Wilson Island Group, N.W.T. [abs.]; *in* Program with Abstracts, v. 1. Geol. Assoc. Can.: p. 83.

_____ 1976b: Sedimentology and geochemistry of the Wilson Island Group, N.W.T.; interim report. DIAND: Yellowknife.

Contribution to the Geology of the Northwest Territories, Volume 3, 1988, NWT Geology Division, INAC, Yellowknife.

The Formation of Gold Deposits with Particular Reference to Archean Greenstone Belts and Yellowknife

I Geological Boundary Conditions and Metal Inventory

R. Kerrich[1] and W.S. Fyfe[2]

Abstract

Gold, Ag-vein deposits in metamorphic rocks of ~2.7 Ga greenstone belts constitute the single largest source of lode gold production worldwide, second only to the Witwatersrand placers in cumulative yield. The origin of this class of lode deposit remains highly controversial.

At the scale of greenstone belts, most of the deposits are associated with major structures of transcrustal dimensions, or splays. The structures initiated as listric normal faults accommodating extensional displacement at the early stages of greenstone belt development, acting as the loci for ultramafic magmatism, and clastic and chemical sedimentation. At later stages, during transpressional deformation, the structures acted as conduits for alkaline rocks, signifying magma penetration from the subcontinental mantle, and for discharge of hydrothermal reservoirs involved in the gold deposits. In detail, the structures are sited at dilatant jogs, or on flexures of the major structures.

Archean lode gold deposits are characteristically enriched in a suite of rare elements including Au, Ag, B, W (± As, Sb, Se, Te, Bi, Pd) which are concentrated by 10^3 to 10^4 times background, whereas the abundant and soluble base metals, Cu, Pb, Zn, are present at only 10^{-1} to 10 times background. This separation may be accounted for if mineralizing fluids are generated under crust-dominated conditions of low water/rock, and low Cl, such that the absolute abundance of rare elements is not constrained by solubility, but base metal solute concentration is limited by availability of both H_2O and Cl. Sporadic development of Mo + graphite is a notable feature of some deposits. First order calculations of chemical mass balance reveal that a deposit with >100 t of Au, requires Au extraction from a crustal volume of 100-500 km³. The wide range of ambient Eh for gold deposition indicated by the coexistence of gold + hematite, to gold + pyrrhotite + graphite in different environments suggests that precipitation of gold is not simply mediated by redox and the availability of reduced S, as is the case for massive base metal sulphide deposits.

Gold-bearing vein systems formed during multiple episodes of hydrofracturing, from transient, pulsed hydrothermal discharge, under conditions where $P_{fluid} \geq \sigma_3 + T$, and P_{fluid} may have exceeded σ_1, the maximum principal stress. Pulsed discharge generated banded veins, and was probably induced by repeated breaching of a metamorphic fluid reservoir. This hydrodynamic regime for gold-bearing veins is in contrast to quasi-steady state convective circulation under hydrostatic conditions that generally applies to base metal massive sulphide ore-forming systems.

Au, Ag-vein deposits in the Mother lode, Cordillera of British Columbia (mesothermal deposits) and the Dahlonaga belt in Georgia, share some key features in common with their greenstone belt counterparts, including the pressence of clastic and chemical sediments, sporadic late alkaline magmatism, major crustal structures, variably abundant As, Sb, B, Se, Te, and Bi, low base metal contents, and gold deposition post-dating much of the deformation, magmatism and regional metamorphism.

Introduction: General Considerations and Boundary Conditions for Gold Deposits

Gold, silver-bearing veins in metamorphic rocks constitute a distinct class of ore deposit, both in terms of the magnitude of production, as well as in the characteristic metal inventory, mineral parageneses, and geological setting. Over the last decade, intensive efforts have been directed at understanding Au-Ag vein systems, particularly from the standpoint of geochemical and isotopic studies. In this paper, and a companion paper (Kerrich and Fyfe, 1987, Part II) we review recent geochemical data for this type of deposit, and discuss how such information bears on interpretation of their origin.

This paper attempts to convey a summary of the geochemical characteristics of Archean lode gold deposits of Canada, with special reference to Yellowknife. The survey is based on a synthesis of information presented in Kerrich (1983) and Fyfe and Kerrich (1984), along with additional data. The first section presents a synthesis of structural and geochemical data for the Yellowknife deposits, and ensuing sections report a compilation of results for the metal

1. Department of Geological Sciences, University of Saskatchewan, Saskatoon, Saskatchewan, Canada S7N 0W0
2. Department of Geology, University of Western Ontario, London, Ontario, Canada N6A 5B7

distribution of Archean deposits. In a companion paper (Kerrich and Fyfe, 1987) we discuss the source of the hydrothermal fluids and the geochemistry of alteration. The concluding section critically evaluates models for Archean gold deposits.

Geological Characteristics of Au-Ag Vein Deposits

Both the largest and most numerous Au-Ag vein systems occur in Archean greenstone belts (Anhaeusser, 1976; Bertoni, 1983; Woodhall, 1979; Groves and Phillips, 1987). These precious metal deposits of the North and South American, Australian, Southern African, Indian and Russian shield areas are second only to the Witwatersrand 'placers' in terms of cumulative production.

Most of the major mines are located in ~2.7 Ga greenstone belts, whereas the old 3.4 Ga supracrustal successions of Australia and Southern Africa do not possess a comparable scale of mineralization. The reasons for this disparity are not fully understood; however, based on the distribution and timing of mineralization, Groves and Batt (1984) have made the important empirical observation that the major deposits are generally confined to rift-style, rather than platform-style greenstone belts.

At the scale of individual greenstone belts it has been recognized from the early days of prospecting that the Au-Ag vein deposits are preferentially associated with major structures, also traditionally termed 'breaks' in the Canadian literature. Structurally, the breaks are characterized by megaboudinage, doubly plunging folds, complex anastamosing brittle-ductile shear zones, and generally steeply dipping lineations (Fryer et al. 1979; Kerrich, 1983, 1986a,b,c; Colvine et al. 1984). Two of the best-documented examples are the Destor-Porcupine, and Kirkland Lake-Cadillac-Bouzan fault systems in the Abitibi subprovince. The geometry of the structures and displacement vectors are poorly quantified.

Characteristically, these structures initiated as growth faults, and were sites for the episodic injection of magmas of ultramafic, trondhjemitic and alkaline composition. The structures appear to have juxtaposed volcanic-sedimentary terrain of contrasting character, such as the Kinojevis and Larder Lake groups at Kirkland Lake (Jensen, 1978; Kerrich, 1983; Hodgson, 1984; Jensen and Langford, 1985; Kerrich, 1986b, c; Ludden et al. 1986).

Younger equivalents to the Archean greenstone belt Au-Ag vein systems occur in volcanic terrain of Proterozoic and Phanerozoic age. These share many of the geological characteristics of the Archean deposits, although the scale of mineralization is greatly diminished. Examples include the gold belt of Northern Saskatchewan, in the Churchill Province, the Dahlonaga belt of Georgia, the Mother Lode of California, and Cordilleran mesothermal deposits in British Columbia. Auriferous quartz vein systems are also present in dominantly metasedimentary terrain of Proterozoic and Phanerozoic age. Included in this category are the Victoria goldfields in S. Australia, and the Meguma terrain of Nova Scotia.

The classification of ore deposits is fraught with difficulty, especially where genetic precepts are interwoven with observation. Notwithstanding these difficulties, Au-Ag vein deposits in metamorphic rocks appear, to a first approximation, to constitute a distinct style of mineralization, in terms of setting, metal inventory, paragenetic assemblage, and alteration characteristics. The association with metamorphic rocks is an empirical one, and does not necessarily imply a functional relationship between the two.

In deposits of the Superior Province, where time relations have been carefully evaluated, the major episode of gold mineralization overprints regional metamorphism, and is contemporaneous with the terminal plutonic-deformational event (Kerrich, 1983; 1986a; Colvine et al. 1984; Andrews et al. 1986). There is compelling evidence for introduction of gold with early as well as late structural episodes in the Barberton and Australian greenstone belts (Pearton 1984 personal communication; MacGeehan 1985). Some evidence, albeit ambiguous, has been presented for gold enrichments coeval with volcanism (Ridler, 1976; Fripp, 1976; Hutchinson, 1976; Barnett et al. 1982); but many of the so-called iron-formation deposits are clearly of replacement origin (Fyon et al., 1983a, b, 1984a, b; MacDonald, 1984; Barnett et al. 1982; Phillips et al. 1984; Phillips and Groves, 1983, 1984).

Gold, silver vein systems in metamorphic rocks are also referred to as mesothermal deposits, to serve as a distinction from the epithermal variety. Collectively, the former are characterized by a diagnostic element association consisting of sporadically enhanced concentrations of B, W, As, Sb, Se,Te, Bi and Mo, with systematically low abundances of Cu, Pb and Zn (Kerrich and Fryer, 1981); and a gangue mineralogy dominated by quartz, albite, carbonate, muscovite, pyrite and tourmaline. Mesothermal Au-Ag deposits are further characterized by Au/Ag averaging 5, $P_{fluid} \geq P_{lithostatic}$ (Kerrich and Allison, 1978), carbonate alteration, and ambient mineralization temperatures $\geq 300°C$. In contrast, their epithermal counterparts are distinguished by $Au/Ag \leq 5$, $P_{fluid} \simeq P_{hydrostatic}$, carbonates minor or absent, low density CO_2, presence of advanced argillic alteration, and temperatures generally $\leq 300°C$. Their respective characteristics endorse the implied depth discrimination of mesothermal and epithermal environments. Henley (1985) has reviewed the setting of epithermal precious metal deposits.

Polymetallic vein deposits exemplified by Finlandia, Peru (Kamilli and Ohmoto, 1977), and Sunnyside, Colorado (Casadevall and Ohmoto, 1977), may also be distinguished from the mesothermal and epithermal precious metal systems in terms of geological setting, metal inventory, and

paragenetic assemblages. Light stable isotope systematics of the three deposit classes, serve further to elucidate differences in their respective ambient conditions of formation and mode of origin, as discussed below.

General Considerations

Gold has fascinated man throughout his entire recorded history. The early fascination developed because it was rare, easy to form into various shapes and forms and resisted corrosion. It was a permanent material. Today the same uses continue but because of its good electrical conductivity, reflectance and resistance to corrosion and tarnish, new uses have been found in the electronics industry and many functions of space vehicles and advanced technology. Even medicinal uses of gold compounds have continued to develop.

With most natural materials, in a general way, their value is related to the versatility of their usefulness and their abundance. Gold is a rare element. Most common rocks in the earth's crust contain gold at the parts per billion level (1 ppb = 1 mg/t of rock, or 2.6 t of Au/km^3 of rock, 2.6×10^{15} g). In general most rocks contain gold at levels spanning 1-5 ppb and this range changes little in most common primary igneous rocks (Table 1). But in certain meteorites, particularly those with metallic phases, gold may attain 1000 *x* the crustal abundance, or 1 part per million. The reason for the low crustal abundance is that gold was concentrated in the earth's metallic core during the early differentiation of the planet; gold is very soluble in molten nickel-iron which dominates the chemistry of the core. This preference for metallic phases or siderophile character (Mason, 1982) is due to the fact that for most environments in the deep earth, which are reducing, gold is chemically inert and exists in a zero oxidation state, Au^0, not suitable for forming typical oxy-minerals such as silicates, oxides, carbonates and the like. Accordingly, gold was sequestered from liquid silicate, that now constitutes the mantle and crust, and partitioned into a liquid iron phase during meltdown of the planet and the ensuing separation of the core.

Today, economic gold deposits, i.e. those from which gold can be extracted at a reasonable profit (many are mined for political and other reasons where this is not true), contain gold at a level near 10 ppm (or 10 g/t). Thus in gold ores, some process has concentrated gold from common rocks with typical background abundances of Au by a factor of one thousand to ten thousand. The corresponding enrichment factors for elements such as zinc or copper are one hundred, and for iron or aluminum, only about five times - see below. Thus it is clear that very special processes are required to produce gold ores.

As modern plate tectonic processes demonstrate, the earth's crust is a highly dynamic system modified by deep convective forces. New crust is produced by igneous processes which move mantle materials (dominated by basalt and andesite) to the surface. Such processes occur mainly at the great ocean ridge systems, near subduction zones, and at hot spots like the Hawaiian Island chain. But crust formation is almost exactly balanced by return flow to the mantle at subduction zones initiated at ocean trenches. There is little evidence to show that the total mass of crust has changed drastically during earth history; it is continually recycled by convective processes (Uyeda, 1978). Thus in a sense, the primary step in forming gold deposits must start with some process which efficiently extracts gold from basaltic materials and concentrates it in a much smaller rock volume. Thus to form a large ore deposit such as at Yellowknife or in many other parts of the Archean shield areas of the earth, such as the Abitibi belt, where deposits with 100^+ t of Au occur at a grade of 10 ppm, requires that the gold in something like 100-500 km^3 of rock must be moved into a volume like 0.01 km^3 (at 10% extraction efficiency), a truly remarkable piece of natural chemical engineering.

The Extraction Process

Nature provides us with clues on how this extraction process may operate. First, most gold deposits occur in veins or rocks in which there has been addition of silica and perhaps the presence of quartz veins is the first clue to the possible mechanism of gold enrichment. We know from laboratory studies (e.g. the classic work of Kennedy, 1950) that quartz is soluble in water with a solubility that rises rapidly with fluid pressure and temperature. Thus at room temperature, quartz solubility is about 5 ppm, whereas at 800°C and 5000 bars pressure, it reaches about 4% or 40,000 ppm. When hot water ascends in the crust it will normally precipitate most of this silica in veins. Further (see below) the quartz crystals associated with quartz-gold veins, often contain fluid inclusions or samples of the fluid from which the quartz precipitated. These inclusions are generally dominated by liquid water with low salinity but sometimes contain appreciable amounts of carbon dioxide. The CO_2 content indicates that the original fluid source was very hot (500-600°C) for the CO_2 is buffered by reactions with common calcium silicate (e.g. $CaSiO_3 + CO_2 \rightarrow CaCO_3 + SiO_2$). Frequently, the quartz veins contain carbonate minerals and the rock near the veins is altered to carbonates. Thus in a general way, we know that the fluid which moves the gold is dominated by H_2O-CO_2 with small amounts of soluble chlorides.

Quartz-gold veins are associated with a wide range of other minerals which vary in quantity with different deposits. Typical are pyrite, arsenopyrite, carbonates, micas, feldspars, and tourmaline. Such minerals tell us that the fluids carry simple metal ions (Na^+, K^+), sulphur compounds, and elements like arsenic and boron in variable amounts.

Experimental studies (see Fyfe and Kerrich, 1984) show that gold can pass into solution under certain specific conditions. Such reactions (to our present knowledge) involve an oxidation step:

$$Au \rightarrow Au^{+} + e^{-} \qquad (1)$$

or

$$Au \rightarrow Au^{3+} + 3e^{-} \qquad (2)$$

When gold dissolves in aqua region, it is present in the form Au^{3+}. But normally, the gold ions also form a 'complex ion' which greatly stabilizes the oxidized state and promotes the solution process. This is familiar to us in the widely used extraction process which employs cyanide. In this process reactions occur such as:

$$Au + \tfrac{3}{4}\, O_2 + 3H^{+} \longrightarrow Au^{3+} + 1\tfrac{1}{2}\, H_2O \qquad (3)$$

and

$$Au^{3+} + 4CN^{-} \longrightarrow ([Au(CN)_4])^{-} \qquad (4)$$

Gold also forms a stable complex with chloride,

$$Au^{3+} + 4Cl^{-} \longrightarrow AuCl_4^{-} \qquad (5)$$

There are a host of molecules both inorganic and organic that form complexes with Au^{+} and Au^{3+}, including various complexes of S, As, Sb, and Te (see Boyle, 1979). It is now reasonably certain that in low temperature hydrothermal environments, that the dominant complexing reagent is $[Au(HS)_2]^{-}$ a complex of Au^{+} and HS^{-} (Seward, 1984). In very low temperature environments (e.g. soils) gold may be solubilized as chloride complexes or even with molecules such as thiosulphate which forms during the oxidation of pyrite at the surface. At very high temperatures, complexes with molecules like carbon monoxide present in equilibrium with CO_2, could be important. The fact is that we still have much to learn about the actual active species in various environments, but in general, oxidation plus a complexing molecule are necessary to mobilize gold. It is known that solubility tends to increase with temperature and always involves an aqueous fluid.

The formation of a gold deposit, or a gold enriched material, requires that an aqueous fluid with an appropriate complex forming species, attack a large volume of rock and then moves along a well focussed path into the site of precipitation (Fig. 1A). Thus the requirements are:

(a) a source rock which is permeable on a fine scale
(b) a large fluid volume of suitable chemistry
(c) an energy source to drive the flow
(d) a structure to focus the flow, and
(e) a precipitation mechanism, or mechanisms.

As our knowledge of gold enrichment processes advances we become increasingly aware that there are many geological situations where such conditions are met. Perhaps the rule of the game is that whenever large fluid volumes move through large rock volumes there is a chance of gold enrichment.

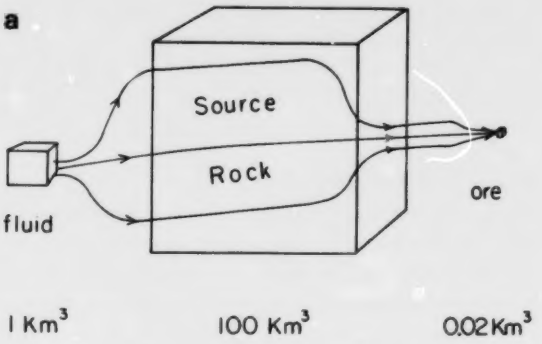

Figure 1a: *The gold extraction problem: a large fluid volume must pass through an even layer rock volume on a microscale and the output focussed into a small volume. In fact, it is even more efficient to generate the fluid in-situ by metamorphic processes (Fyfe and Kerrich, 1982).*

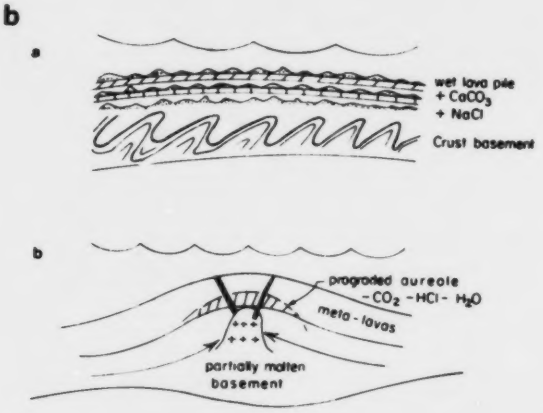

Figure 1b: *A typical Archean scenario. (a) Complex metamorphic basement is covered with lavas and sediments. (b) The loaded, depressed basement responds by partial melting and 'granitic' doming. Prograde metamorphism in the aureole of wet volcanics leads to gold leaching with focussed flow in hydraulic, or extensional fractures (Fyfe and Kerrich, 1984).*

One case for which there is direct observational data and excellent control via drilling, involves some modern geothermal fields such as at Broadlands, New Zealand (Seward, 1984). In this general area, large volumes of meteoric surface waters are involved in cooling hot, porous and fractured volcanics. The input into the system is diffuse occurring over a large area while the discharge is focussed in the hot spring systems. As descending oxygenated waters move to depth along their convective paths, sulphate is reduced to sulphide which complexes gold. On the discharge cycle, $[Au(HS)_2]^{-}$ is oxidized to form sulphate (a feeble Au complexer) and gold is precipitated near the surface. In this case, the energy source is deep, hot, igneous rock and the fluids are recirculated ground waters. The porous and fractured volcanics are moderately permeable. Focussing of discharge is probably associated with the

distribution of deep heat sources. It is possible that there are also hydrothermal fluids of metamorphic and (or) magmatic origin which carry gold and other metals in the Broadlands geothermal system.

Many of the great Archean gold-quartz lodes such as at Yellowknife and those of the Abitibi belt of Ontario-Quebec, almost certainly do not form by this type of mechanism. In these cases oxygen isotope systematics (see Part II) show that the fluids were predominantly derived by deep metamorphic processes, and structural evidence rules out simple convective circulation of hydrothermal fluids. Precipitation occurs at temperatures in the 300-400°C range or in the greenschist facies of metamorphism (Turner, 1980). The mineralization normally occurs in association with granitic plutons intruded into submarine basalt dominated volcanic piles, often 10km⁺ thick. The fluids are CO_2 rich, and highly reducing because of a moderate content of hydrogen which is typical of hot fluids in equilibrium with ferrous silicates (Fyfe *et al.* 1978). The same situation also applies to some Phanerozoic situations such as the famous Mother Lode system of California (Mesozoic) or gold in the greenschist terrains of Otago, New Zealand. In the Archean case, it is important to note that the gold-quartz mineralization often occurs in the vicinity of granitic plutons, or in the granitic plutons themselves, as at Lamaque, Quebec, although in the latter case the deposits are generally hosted by structures of regional extent, or their splays.

In Fig. 1B from Fyfe and Kerrich (Fig. 8, 1984) we show the type of environment which may promote the development of gold deposits. The sequence of events which may be envisioned are:

(1) a sialic basement is loaded with volcanic flows in a submarine environment. The volcanics cool by sea water convection as at modern ridges and become hydrated to greenschist facies conditions and contain abundant carbonate and sulphides.

(2) Because of thickening and heating the crustal basement begins to soften and melt, thus producing rhyolitic volcanism and granitic plutonism. Rhyolite dykes are injected into the cover and feed volcanics.

(3) Basaltic-komatiitic material coming from the mantle (Fig. 1B) underplates the softened crust (see Herzberg *et al.* 1983). Dense mafic rocks are assimilated and produce $H_2O - CO_2$ rich fluids at very high temperatures (1000°C⁺). Such fluids, rich in CO_2 and COS, may transport metals into the crust.

(4) As plutons and dykes cool, contraction produces permeable zones as does the deformation near the rising plutons.

(5) The thermal influences prograde the greenschist facies crust to amphibolite facies. Water rich metamorphic fluids are produced on a microscale through the lava pile and these low salinity fluids efficiently mobilize gold (Kerrich, 1983; Fyfe and Kerrich, 1984). The metamorphic fluids drain through the most permeable zones, dykes, shear zones and brittle-ductile faults. Some very rich metal-bearing fluids rich in CO_2 may be evolved near the Moho. If the gold is complexed by halogen or CO, as T falls precipitation will occur along with quartz, either in the most reduced wall rocks for chloride complexes, or oxidized zones for CO compelxes or both (e.g. AuCOCl).

Most regimes where hot fluids are generated on a large scale, such as deep fault zones, or overthrusts, may produce similar metamorphic events (Fyfe and Kerrich, 1985) as will deep sill injection.

The types of processes mentioned above frequently produce gold deposits in what can be considered as a single (complex) level. In this case the first stage of enrichment may not attain the desired level. In this case an enriched rock volume is produced which may be more easily reworked by a subsequent event. As Fig. 1 would suggest, if the source has 100 ppb Au rather than background levels of 1-5 ppb, then the second stage enrichment process requires smaller volumes of rock and fluids, and accordingly a lower energy input. Also, erosion and mechanical transport and enrichment of a more dispersed vein system may result in a sedimentary deposit. It now also becomes clear that in some deeply weathered terrain, gold may be enriched in surface soils as is commonly being found in lateritic terrains in Australia and Brazil. In a sense, gold behaves like uranium, being dissolved in oxidized acidic regimes (with Cl^- complex) and precipitated in more reduced regimes with higher pH. It is almost certain that this surface process produced the large gold nuggets.

Lode Gold Deposits in Shear Zones at Yellowknife

Geological Setting

The geology of the Yellowknife district has been described by Henderson and Brown (1966) and most recently by Padgham (1987a,b,c). Au-bearing vein deposits are located within major brittle-ductile shear zones at Yellowknife, in the Slave Province. The largest shear zones, the Con, Campbell and Giant, are 10-150 m wide, extending to known depths in excess of 1-2 km. Shear zones transect metabasic volcanic rocks and interflow metasediments at angles of 20-70 degrees in the vertical plane. In detail, the major structures consist of an anastomosing network of second-order shear zones which envelop lens-shaped domains of isotropic rock. The tectonic schistosity descibes a sigmoidal form between shear-zone boundaries, and contains a subvertically dipping lineation. These geometrical relations indicate that the shear zones conform to the simple shear model of Ramsay and Graham (1970).

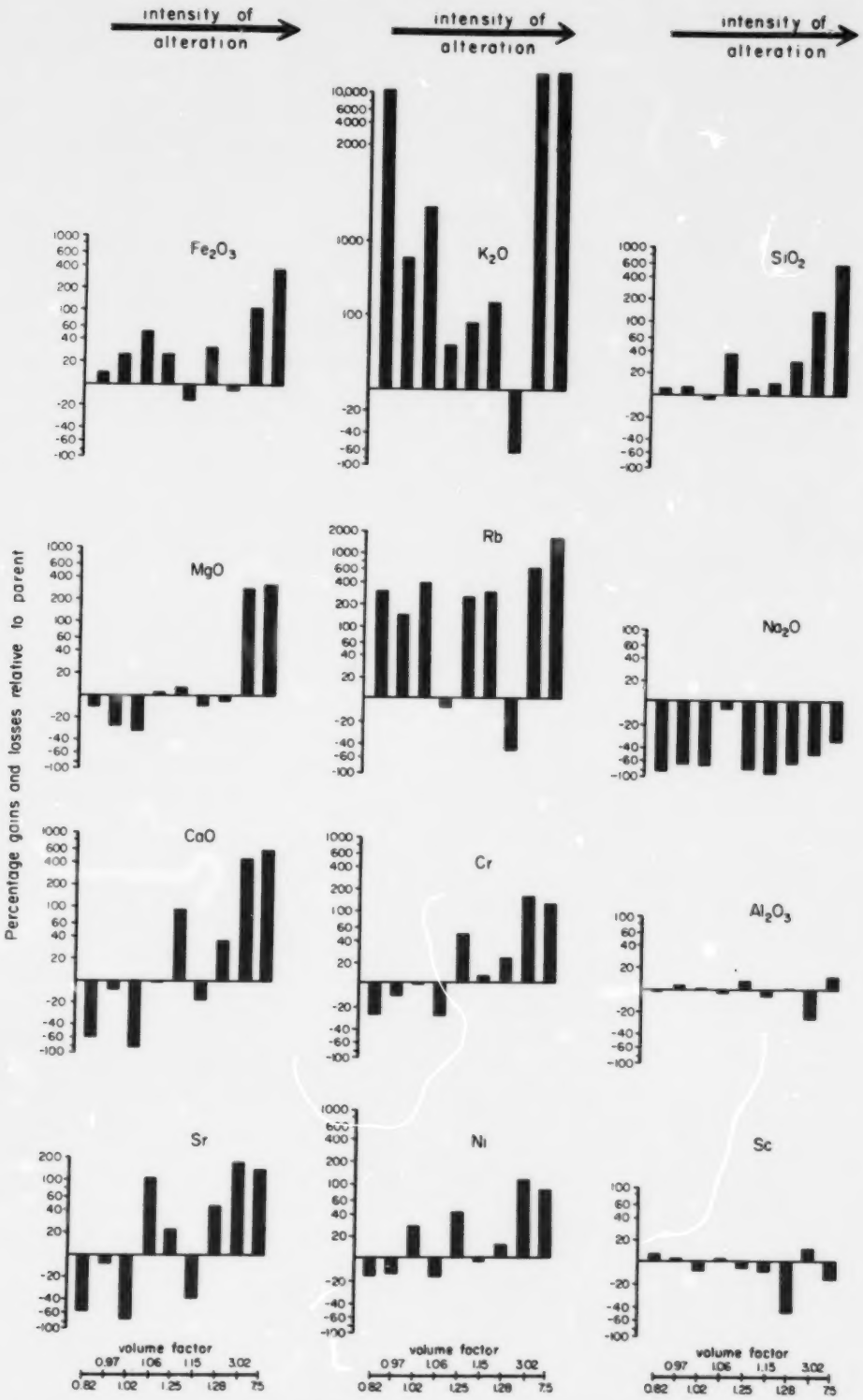

Figure 2a: *Gains or losses of major element oxides and selected trace elements in hydrothermally altered rocks of primary basaltic composition, Campbell and Con shear zones, Yellowknife. Gains and losses expressed as percentage changes relative to abundances in the unaltered parent rock, and ordered according to increasing volume factor (after Kerrich and Fyfe, 1981).*

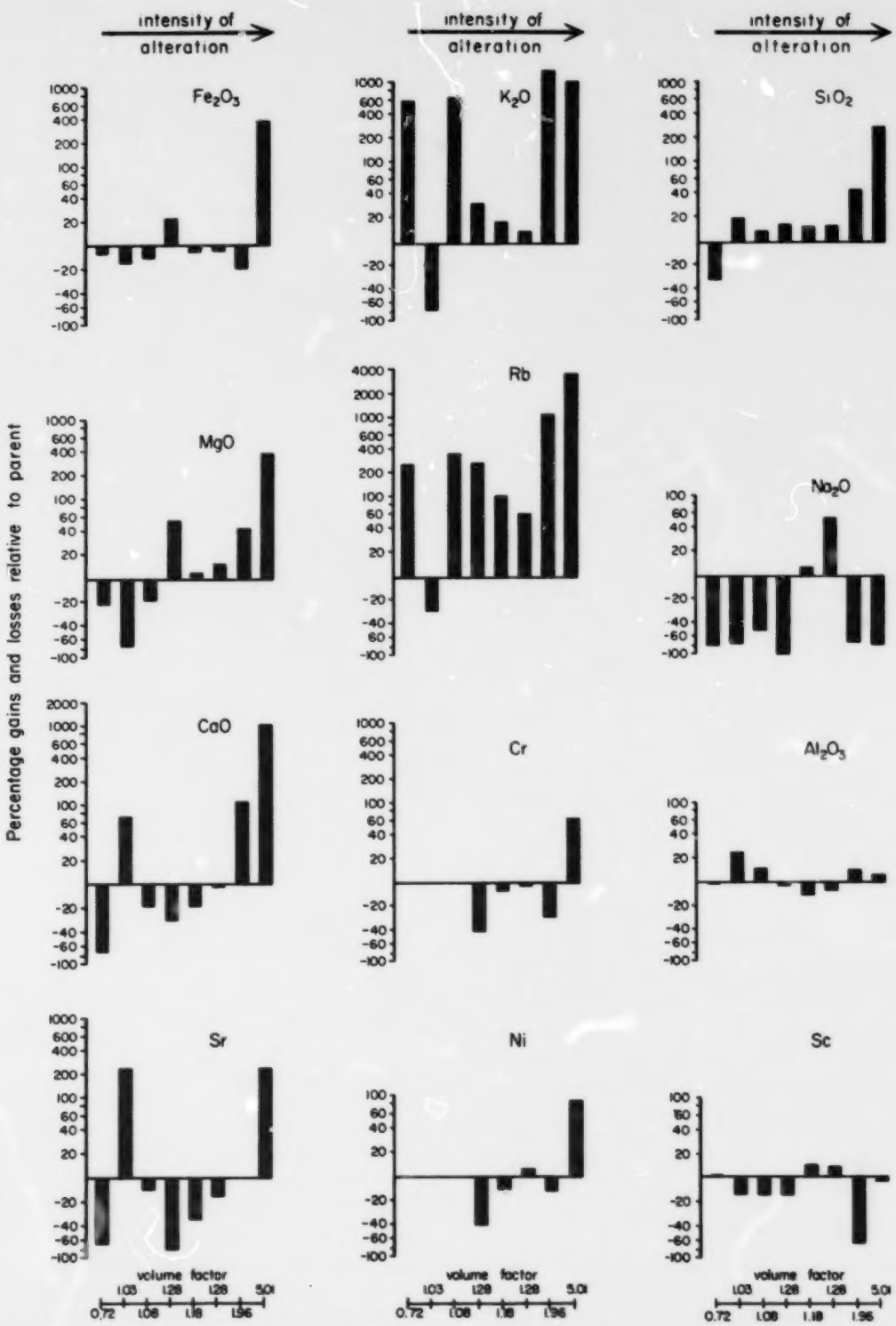

Figure 2b: *Gains or losses of major element oxides and selected trace elements in hydrothermally altered rocks of primary basaltic composition, Con shear zone, Yellowknife. Gains and losses expressed as percentage changes relative to abundances in the unaltered parent rock, and ordered according to increasing volume factor (after Kerrich and Fyfe, 1981).*

After initial development of the shear zones, these structures subsequently acted as permeable conduits for discharge of hydrothermal fluids which precipitated the Au-bearing quartz-carbonate veins. Such veins are typically located within the confluence of second-order shear zones, at the apices of the intervening domains of undeformed rock. The structures and orebodies contain in them have been described by Boyle (1961), Henderson and Brown (1966) and Breakey (1975). From considerations of the ambient stress regime for fluid flow along shear zones, Kerrich *et al.* (1977a) and Kerrich and Allison (1978) interpreted the gold-bearing vein deposits to have been formed from discharge of high-pressure hydrothermal fluids during successive episodes of hydraulic fracturing (see below).

Chemical Relations in the Shear Zones

Vein systems at Yellowknife traverse a relatively uniform series of metabasalts, but evaluation of alteration patterns is not a readily tractable problem due to a complex history of chemical alteration prior to vein emplacement. External to vein systems, basalt flows have erratic abundances of the alkali- and alkaline-earth metals, coupled with whole-rock $\delta\ ^{18}O$-values averaging 7 (compared to primary basaltic $\delta\ ^{18}O$-values of 5.7 ± 0.3 per mil). These data were interrupted by Kerrich and Fyfe (1981) to signify spilitization reactions in the presence of seawater at low temperatures, during and shortly after extrusion. Gold abundances of basalts remote from the shear zones are uniformly in the low ppb range, signifying that little or no gold enrichment occurred during this seawater-hydrothermal stage (spilitization).

A second stage of chemical transfer occurred during early propagation of the shear zones into which auriferous veins were later emplaced. Deformation of epidote-amphibolite-facies metabasalts to chlorite schists in the shear zone, initially by brittle transangular fracturing and subsequently by means of pressure solution and crystal plastic flow, involved loss of SiO_2 plus Na_2O with concomitant gains of H_2O + $C0_2$ (Kerrich *et al.* 1977b). Neither of these episodes of seawater-hydrothermal or deformation-induced alteration appears to have involved significant changes in abundance of the relatively immobile elements such as Al, Ti, Zr and Sc. Hence, deformed chlorite schists within unmineralized domains of the shear zones are probably the most reasonable parent rocks to select for comparison with mineralized counterparts.

Hydrothermal Alteration

Gains and losses of major-element oxides involved in hydrothermal alteration accompanying precipitation of the gold-bearing veins are tabulated by Kerrich and Fyfe (1981), and illustrated in Figs. 2a, b. Volume factors (fv), which monitor the departure from isovolumetric conditions (fv = 1), range from 0.8 at the periphery of alteration domains to 7 at vein margins where there is a significant admixture of gangue minerals in the form of vein arrays within the metabasic schists. The salient chemical mass transfers accompanying hydrothermal alteration are additions of SiO_2 and volatiles. the former is consistent with precipitation of quartz from cooling solutions, and the latter with hydration and fixation of CO_2 in carbonates. According to Boyle (1961), CO_2 increases from~1% in unmineralized basalts in the epidote amphibolite facies to~8% in sericite-carbonate schists adjacent to veins. CaO, MnO and MgO are depleted at volume factors of 1.3 or less reflecting the hydrolysis of chlorite + epidote to muscovite, but are added at $fv > 1.3$ where the bivalent metal cations are incorporated into ferroan dolomite. Na_2O is depleted and K_2O fixed over the entire range of volume factors, corresponding to the reaction of albite to muscovite. Small positive and negative variations of total Fe occur at $fv < 1.7$, with additions at $fv > 1.7$. Al_2O_3, Sc, and Zr are conserved at all states of hydrothermal alteration (Fig. 2a, b).

Precious metals, together with Cr, Ni, Cu, Zn, Pb, Rb, Cd and Ba, have been added from hydrothermal solutions to the veins and altered wall rocks, whereas V and Nb do not exhibit any large departures from background abundances. Rb and Sr behave sympathetically with K and Ca, respectively (Fig. 2a, b).

The simplest interpretation of these results is that the hydrothermal fluids contributed SiO_2, H_2O + CO_2, precious metals, and K_2O to the wall rocks, which is reflected in the presence of vein quartz, elevated precious-metal abundances, hydration and carbonation of wall rocks, together with pervasive development of muscovite. Such additions to the chlorite schist precursor require volume factors $\gg 1$.

It is suggested that some Ca, Mn and Mg (also possibly some Fe) are taken into solution in the peripheral alteration regions where $fv < 1$, and combine with CO_2 contributed to the hydrothermal fluids to yield carbonate minerals in regions of alteration where $fv > 1$, and in veins (Fig. 2a, b). Cr, Ni, Sr and sulphur may behave in the same manner to some extent, signifying some local redistribution, as well as absolute additions. It is difficult, however, to quantitatively assess the relative extent to which the wall rocks and hydrothermal fluids respectively contribute bivalent metal cations to the alteration carbonates. Inferred chemical changes are essentially the same for the Con, Campbell and Giant shear zones, at equivalent estimated volume factors, attesting to the overall coherence of alteration style.

REE patterns for unmineralized metabasalts are comparable to those of relatively fresh Archean tholeiitic basalts in general (Condie, 1981), excepting a slight monotonic decrease in abundance toward the heavy REE (Fig. 3). These results signify that the REE were largely unmodified by low-temperature seawater alteration, or possibly underwent only minor enrichments of the light REE. In deformed and

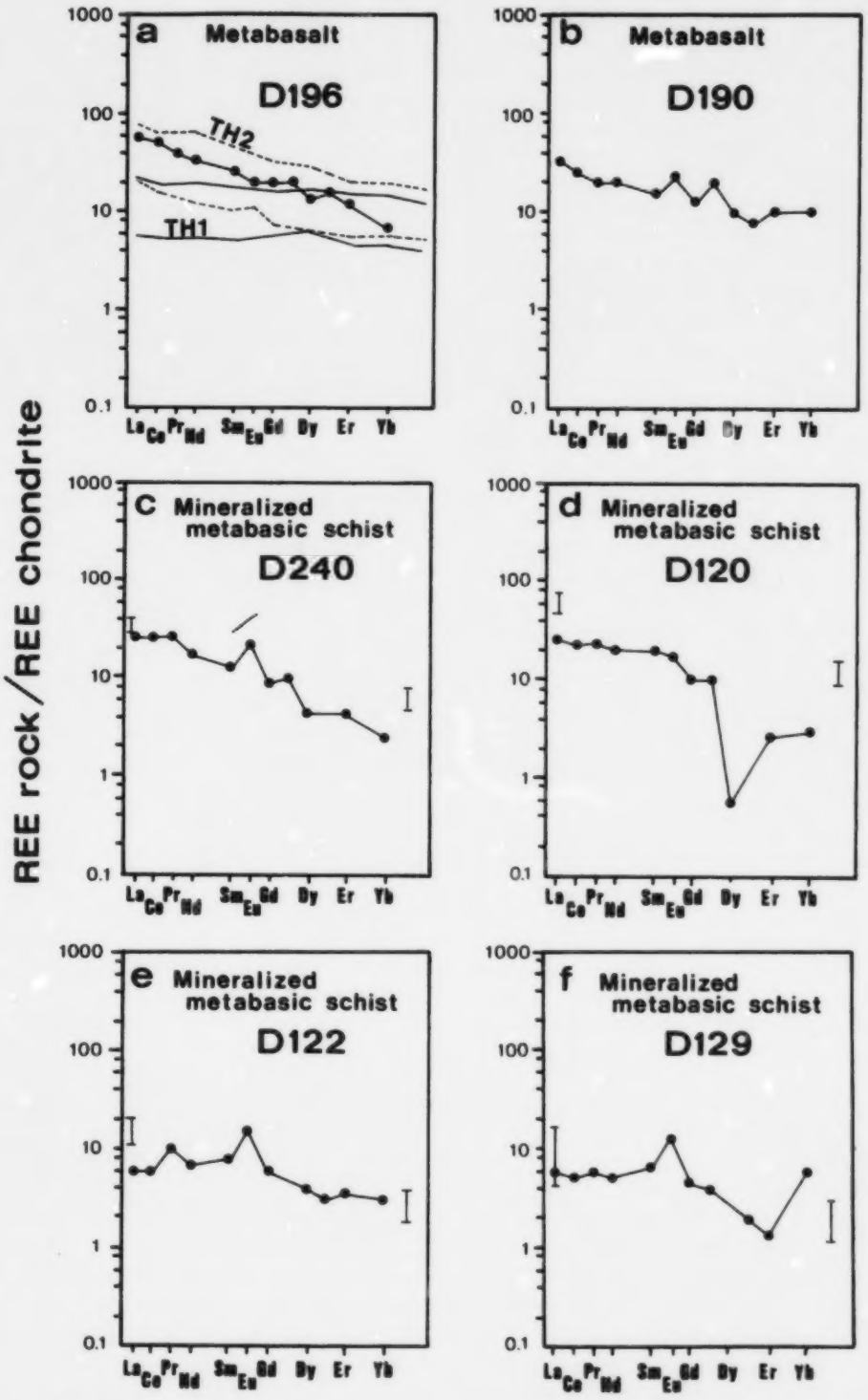

Figure 3: *REE distributions in unaltered (a, b) slightly mineralized (c, d) and intensely mineralized (e, f) basalts, Con Mine, Yellowknife. The vertical bars signify the extent to which La and Yb would be shifted by experiencing the same coherent dilution from the unalt state (a, b) as is evident for Al, Zr and Sc, due to additions of vein material relative to abundances in samples a and b (unaltered). Superimposed are the REE envelopes for enriched (TH2) and depleted (TH1) Archean tholeiites (after Condie, 1981).*

mineralized counterparts at progressively higher states of hydrothermal alteration (c, d intermediate; e, f intense veining, Fig. 3), the REE are shifted to lower absolute abundances with the original profiles essentially retained, except for higher scatter and a positive europium anomaly in some samples; the downward shift is attributable largely to dilution of the chlorite schist host by introduction of quartz veins possessing negligible REE contents. One sample (D120), however, which has undergone extensive hydrothermal leaching as evidenced by the apparent coherent increase in abundance of Al, Ti, Zr and Sc, also displays absolute depletions of the REE. These data confirm mobility of the REE during intense leaching as independently deduced from results obtained on hydrothermally leached samples of the Dome Mine (cf. Kerrich and Fryer, 1979).

In proximity to veins, the whole-rock $\delta^{18}O$ values and $Fe^{2+}/\Sigma Fe$ ratios exhibit a major perturbation from background values of +7 and 0.7 respectively (Au > 4 ppb), to +9 to +10 per mil and an average $Fe^{2+}/\Sigma Fe$ of 0.92 in carbonate-muscovite schists enveloping Au-bearing quartz veins (Au 1-40 ppm). The $\delta^{18}O$ of vein quartz at 12-13 is equal to that of quartz extracted from the carbonatized mafic schists, to within the limits of analytical precision, implying oxygen isotope equilibrium between hydrothermal fluids and altered wall rocks over a scale of a few metres (Kerrich and Fyfe, 1981). At greater distances from the veins, in mechanically isotropic metabasalts external to the shear zone boundaries, $\delta^{18}O$ quartz and the redox state diminish to background values.

Low redox states in mineralized wall rocks, indicated by the predominance of Fe^{2+}, is considered to result from the reduction of Fe^{3+} in silicates and metal oxides by hydrogen, during chemical exchange with a large flux of H_2-bearing aqueous solutions ascending along a T-P gradient through conduits in the shear zones, and precipitating gold, quartz, etc. (Fig. 4). Hydrogen is the most powerful reductant in natural systems, and its generation in hydrothermal reservoirs is discussed in a later section. Boyle (1977) has argued that the observed reduction in veins at Yellowknife is due to the "lateral diffusion" of components into the shear zones, including arsenic, which may act as a reducing agent. The hypothesis of lateral diffusion as an ore-forming process can probably be ruled out on the basis of several lines of chemical evidence, specifically oxygen isotopes (see Kerrich and Fyfe, 1987, Part II); and in addition it is important to note that wall rocks to auriferous veins are extensively reduced, even when the abundance of arsenic and sulphur is low.

The oxygen isotope composition of vein quartz falls in a narrow range of 11 to 13 per mil for the Con, Campbell and Giant vein systems, and quartz-muscovite and quartz-chlorite fractionations are relatively uniform at 3.8 to 3.4 per mil and 5.8 to 6.2 per mil respectively. From these data, the ambient temperature of mineralization can be estimated at 350-400°C, and the $\delta^{18}O$ of fluids from which the veins were precipitated was $+7.5 \pm 0.5$ – within the range of metamorphic fluids. Ferroan dolomite and calcite constituting the ubiquitous carbonate gangue has a uniform carbon isotope composition where $\delta^{13}C = -5$ to -2: however $\delta^{18}O$ values are scattered between 8 and 16. These results, which signify an isotopically uniform carbon reservoir, but O-isotopic disequilibrium between silicates and carbonates, are considered together with carbonate data for all deposits below.

Provisional results for primary liquid inclusions in vein quartz associated with precipitation of gold indicate fluids of low salinity (< 2 wt.% NaCl equivalent), with liquid CO_2 present. Halite daughter crystals are present in liquid inclusions of late-stage barren vein quartz.

Hydraulic Conditions During Vein Propagation

One of the fundamental questions pertaining to Archean lode gold deposits is the hydraulic regime of the ore-forming system. Are the geothermal fluids undergoing thermally driven convective circulation under approximately hydrostatic conditions and in equilibrium with surface waters, or alternatively do the extensive vein stockworks form by hydraulic fracturing in the presence of geopressurized aqueous reservoirs? This question has been addressed by Kerrich and Allison (1978) and Allison and Kerrich (1980) with reference to Yellowknife, and by Robert and Brown (1984) for the Sigma Mine, Val d'Or. At the Sigma Mine orientations of the principal stresses and ambient fluid pressures during vein propagation may be deduced given the well constrained geometry of shear zones and the vein arrays they host.

Three main stages of veining have been recognized in the shear zones at Yellowknife (Kerrich and Allison, 1978; Allison and Kerrich, 1980; Fig. 4) as follows:

1. The formation of the major shear zones, with concomitant development of the early en-echelon barren veins.
2. Development of the massive to banded gold-bearing quartz veins in the shear zones in an initial orientation which is approximately parallel to the schistosity.
3. Formation of late "ladder" vein systems, which are also locally auriferous, within the shear zones but at high angles to the schistosity.

This sequence is illustrated in Fig. 4b. The origin of each vein system will now be considered in turn.

The veins at Yellowknife formed by the infilling of tensile fractures. Close to the earth's surface tensile fractures may form, but at depth the increase of confining pressure (σ_3) induces propagation of shear fractures. However, under conditions of high fluid pressure (Pf) tensile failure by hydraulic fracturing may occur at depths in the crust, in excess of 30 km. The principles involved are discussed by Fyfe

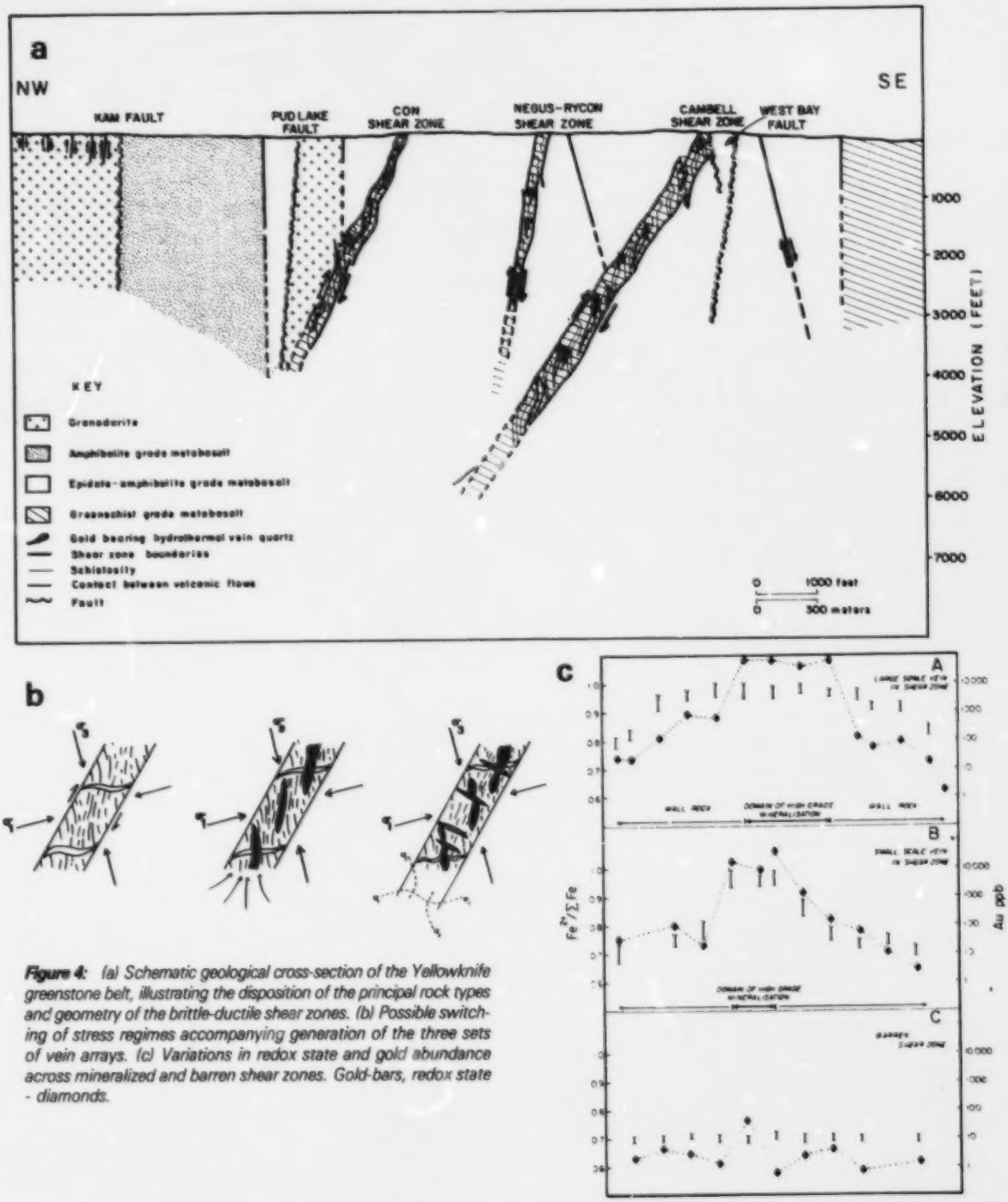

Figure 4: *(a) Schematic geological cross-section of the Yellowknife greenstone belt, illustrating the disposition of the principal rock types and geometry of the brittle-ductile shear zones. (b) Possible switching of stress regimes accompanying generation of the three sets of vein arrays. (c) Variations in redox state and gold abundance across mineralized and barren shear zones. Gold-bars, redox state - diamonds.*

et al. (1978). The stress conditions under which hydraulic fracturing can occur may be represented by

1. $\sigma_3 - Pf \leq T$ (6)
2. $\sigma_1 - \sigma_3 < -4T$ (7)

where σ_1 and σ_3 are the maximum and minimum principal stresses respectively, and T is the tensile strength of the rock. The first inequality represents the condition where the fluid pressure exceeds the confining stress by an amount equal to or greater than the tensile strength of the rock. The second inequality is the condition for suppression of the shear failure mode. These stress conditions may be portrayed on a Mohr diagram (Fig. 5).

The shear zones are characterized by an intense schistosity, the mechanical properties of which are highly anisotropic. In particular its tensile strength in a direction normal to the schistosity (T_i) will be low compared to that parallel to the schistosity (T_n). On a Mohr diagram the envelope for failure parallel to the schistosity will occur at lower stresses than the envelope for failure normal to the schistosity (Fig. 5b). However as the pore fluid pressure increases and the effective stresses are reduced until σ_3 intersects the Mohr envelope, failure will occur only if the schistosity is oriented normal to the direction of σ_3 (Fig. 5c). If the schistosity is oriented orthogonal to the σ_1 direction then failure along the schistosity will occur when the value of σ_1 intersects the Mohr envelope, as long as σ_3 is less than the tensile strength of the rock normal to the schistosity (Fig. 5d). It is thus possible to achieve hydraulic fracturing within the shear zone parallel to the schistosity with the same external stress regime that caused the initial development of the shear zones and the switch in orientation of stresses postulated by Kerrich and Allison (1978) and illustrated in Fig. 4b is plausible, but not necessary. The stress conditions which must be satisfied for these veins to develop are:

1. $\sigma_3 - Pf < T_n$ (8)
2. $\sigma_1 - \sigma_3 < -(T - T_n)$ (9)
3. $\sigma_1 - \sigma_3 < -4T_n$ (10)

The latest system of fractures occurs as an array of "ladder" veins oriented approximately normal to the schistosity and dipping at shallow angles towards the east. These veins cross-cut those of stage two which now have a pinch and swell structure as a result of progressive incremental deformation in the shear zones. The stress conditions for this late stage of hydraulic fracturing may be formulated as:

$\sigma_3 - Pf < T$ (11)
$\sigma_1 - \sigma_3 < -4T$ (12)
$\sigma_1 - \sigma_3 < -(T - T_n)$ (13)

and are portrayed on a Mohr diagram (Fig. 5e).

The geometry of the early veins and the schistosity within the shear zones accords well with the concept of shear zone development in rocks showing material behaviour transitional between brittle and ductile.

The geochemical evidence indicates local redistribution of material via migration in a fluid phase, and the absence of any significant gold mineralization during the initial development of the ductile shear zone structures. The second stage veins have a conspicuous banding and often contain slivers of schist oriented parallel to the vein margins. Later intracrystalline deformation has obliterated the original quartz microstructure. The banded nature of the veins, and the volumes of hydrothermal fluids involved collectively suggest that the veins were formed by repeated hydraulic fracturing and infilling by quartz precipitated from the hydrothermal fluids. One may envisage a repeated cycle of build up of a fluid reservoir accompanied by elevation of fluid pressure to a point sufficient to induce hydraulic fracture, leading to discharge of the geopressurized reservoir and a consequent reduction of fluid pressure in the source region. Repeated episodes of hydraulic fracturing under conditions of high Pf have cycled the effective confining stress (σ_3 - Pf) such that the rocks have in turn cycled through the brittle (σ_3 - Pf, low) to ductile (σ_3 - Pf, high) transition (Fig. 5f).

Mechanical anisotropy of schists within the shear zones will cause refraction of the stress, and hydraulic fracturing will tend therefore to form parallel or normal to the fabric as in the second and third stages of vein development (Figs. 4b, c, 5).

Development of the second stage veins requires fluid pressure to exceed the maximum principal stress by an amount equal to the tensile strength. This will occur if the fluid pressure has a value close to the geostatic pressure for a given depth rather than the hydrostatic condition. Hydraulic fracturing will permit upward movement of this fluid (Fig. 5). The hydraulic fractures will therefore propagate from depth towards the surface.

These structural considerations apply equally to many other of the vein gold deposits discussed below, which appear also to have formed under conditions of hydraulic fracturing induced by geopressurized hydrothermal reservoirs. This structural-hydraulic regime involving lithostatically pressurized hydrothermal reservoirs is in marked contrast to convective circulation of fluids under hydrostatic conditions, which is widely considered to apply to the formation of volcanic hosted base metal sulfide deposits.

Summary and Discussion

In summary, the gold vein deposits in the Yellowknife greenstone belt were emplaced into shear zones during episodes of hydrofracturing, from a hydrothermal reservoir at 400-450°C, at elevated pressure, characterized by moderate CO_2 content, low redox state and salinity, with $\delta^{18}O$ H_2O in the range of metamorphic fluids. Hydrothermal alteration of basaltic wall rocks was characterized by hydrolysis of Fe, Mg, Ca, Mn-silicates to Fe, Mg, Ca, Mn-carbonates, with the wall rocks donating the bivalent

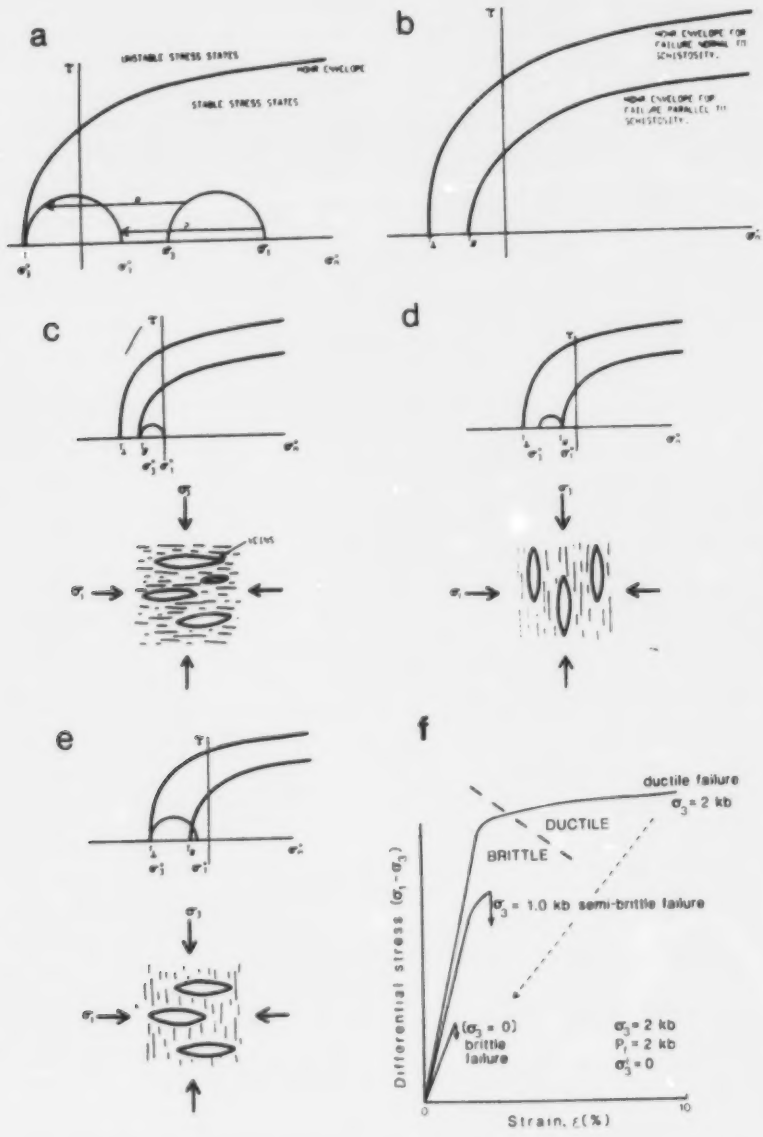

Figure 5a: *Mohr diagram illustrating the inferred stress conditions for formation by hydraulic fracturing of the enechelon veins of the first stage. Effective normal stresses, $\sigma_n = \sigma - P_f$, are plotted on abscissa and shear stresses, τ, an ordinate. Mohr's stress semicircle (1) represents the external stress condition. Semicircle (2) represents the external stresses, modified by a fluid pressure, Pf, at failure. The Mohr envelope is that of the Griffith criterion in the tensile regime and of the Navier-Coulumb criterion in the compressive region of the diagram. T is the tensile strength of the undeformed metabasalt. Note that all diagrams are symmetrical across the $\tau = 0$ line.*

b: *Mohr diagram illustrating the Mohr envelopes for failure parallel (II) to the schistosity and normal (1) to the schistosity. $T_\perp$ and T_{II} are the uniaxial tensile strengths of the schist in directions normal to the schistosity and parallel to the schistosity respectively.*

c: *Mohr diagram for the case of hydraulic fracturing parallel to the schistosity when it is oriented normal to the direction. This is one limiting case: the other is shown in Fig. 4.*

d: *Mohr diagram for the case of hydraulic fracturing across a plane perpendicular to the schistosity when the σ_1 direction is normal to this plane. This will occur only if $\sigma_1 - \sigma_3 \leq T_\perp - T_{II}$.*

e: *Mohr diagram illustrating the inferred stress conditions for the development of the late "ladder" veins. The differential stress exceeds the difference in strengths of the schist parallel and perpendicular to the schistosity (after Allison and Kerrich, 1980).*

f: *Generalized rheological behaviour of rock, illustrated in differential stress ($\sigma_1 - \sigma_3$) versus strain, coordinate space. Note the transition from brittle to ductile behaviour at elevated values of confining stress (σ_3). Switching from ductile to brittle behaviour can be induced by transient increases of fluid pressure which act to diminish the effective confining stress ($\sigma_3 - P_{fluid}$ [Kerrich, 1986b]).*

metal cations and fluids introducing CO_2. Hydrolysis of albite to muscovite accompanying alteration proceeded via massive additions of potassium from fluids to the wall rock, with concomitant loss of sodium to the fluid.

Important early studies of the geochemistry of altered rocks adajcent to Au-bearing veins at Yellowknife were conducted by Boyle (1961). Boyle suggested that Sb, As, Au, silica, transition metals and other elements were liberated during carbonate replacement alteration of rocks, and that this process is an important factor in the contribution of components to certain Au-bearing lodes. This premise is based on simple comparison of element abundances in carbonatized rocks and their precursors, taking into account changes of specific gravity (Boyle, 1961, Table 7 and p. 23), but not possible large changes of volume.

Under the conditions of large volume increase required

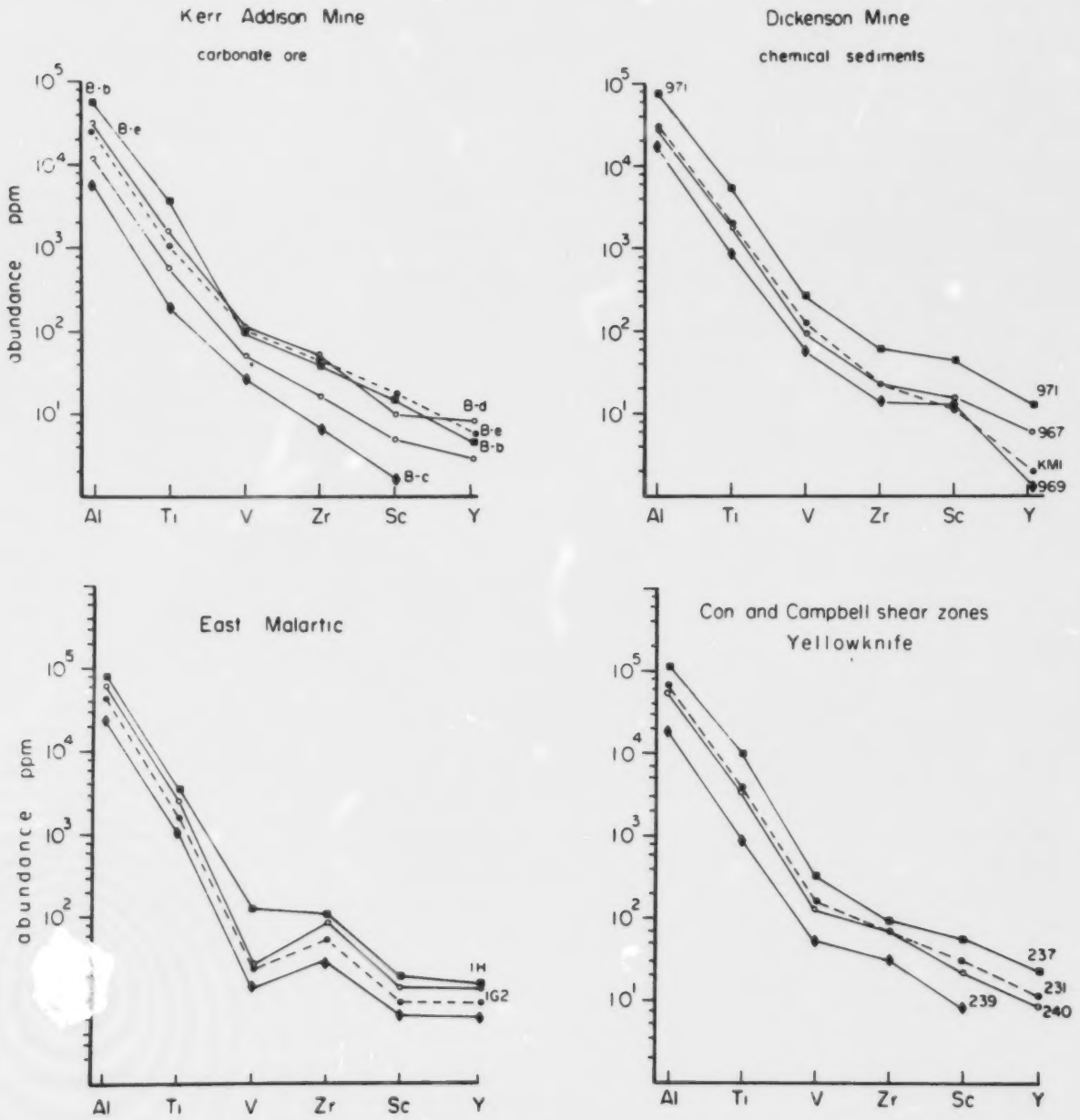

Figure 6: *Absolute abundances of Al, Ti, V, Zr, Sc, and Y, in gold deposits. The overall coherent dilution of these elements corresponds to increasing additions of a hydrothermal precipitant containing no Al, Ti, V, Zr, or Sc, to a wall-rock component to which these elements are exclusively indigenous (after Kerrich, 1983).*

for carbonatization and veining, involving additions of H_2O, CO_2 and SiO_2, together with decrease of specific gravity, all relatively immobile elements of the parent rocks will appear to undergo a similar proportional decrease in abundance by dilution - e.g., Al_2O_3, Sc, Zr (see Fig. 6). The analytically measured abundances of Cr, Ni and other elements may decrease from country rocks to carbonatized altered equivalents (cf. Boyle, 1961, pp. 61, 66; Boyle, 1976, Table 7), but if, as demonstrated above, volume factors accompanying carbonate alteration may exceed 7 then introduction of these elements into the system is required (Fig. 2a, b). However, the apparent decrease of Al_2O_3, Cr, Ni, etc., in carbonatized alteration zones to veins is treated as an absolute reduction in abundance by Boyle (1961; 1976, Table 7). Use of these inferred chemical gradients, without consideration of volume changes, to deduce the direction or magnitude of chemical fluxes from wall rocks into veins during mineralization is invalid.

The Metal Inventory of Lode Gold Deposits

Lode gold deposits are characterized by a distinctive metal inventory, or element association, raising the question as to why the rare element gold is preferentially enriched over the relatively abundant base and transition metals. Average abundances of Au, Ag, Pd, Fe_2O_3, MnO, S, CO_2, Be, B, As, Sb, V, Cr, Co, Ni, Cu, Zn, Mo, Sn, W, Hg, Pb, Cd, Ba and Th in 30 separate orebodies from 18 gold mines have been compiled by Kerrich and Fryer (1981), Kerrich and Hodder (1982), and Kerrich (1983). These results are graphically summarized in Figure 7, where examples of auriferous veins from a wide range of geological environments encompassing ultramafic, mafic and felsic volcanic rocks, along with detrital sediments are included. Metal distributions of deposits are portrayed in terms of enrichment factors, where enrichment is given by the average content of an element in a specified deposit, divided by its background abundance. A summary of the abundances of selected elements in various primary igneous rock types, and in Archean greywackes, is reported in Table 1, to facilitate comparisons of data from mines to background levels.

For the case of lode gold deposits, all enrichments are calculated relative to background levels in the most abundant host rock type present. Where many different rock types are present enrichments have been computed with reference to element contents of primary basalts, because mafic volcanic rocks are volumetrically predominant as contiguous rocks to the deposits (Hutchinson, 1976; Hodgson, 1983).

For purposes of comparison, enrichments of Au, Ag, Cu, Zn and Pb in base metal sulphide deposits are given in Figures 8 and 9. These are expressed relative to abundances in basalts and also relative to felsic volcanic rocks, inasmuch as the latter can frequently constitute the immediate footwall. However, the patterns of element enrichments in lode gold and base metal sulphide deposits, respectively, are distinctive and fundamentally unchanged, irrespective of whether enrichments are referenced to an assumed mafic or felsic background rock.

TABLE 1
Abundances of selected metals in primary igneous rocks and Archean greywackes.

	Ultramafic	Mafic	Felsic	Archean greywackes
Chromium	1600	170	22	74
Cobalt	150	48	7	25
Nickel	2000	130	15	48
Copper	10	87	30	61
Zinc	50	105	60	75
Lead	1	6	15	11
Gold	0.0008	0.0017	0.002	0.002
Silver	0.060	0.110	0.051	0.080
Palladium	0.009	0.016	0.002	
Platinum	0.011	0.009	0.008	
Arsenic		2		
Antimony		0.2		
Tungsten		0.4		
Selenium	0.05	0.05	0.05	
Tellurium			0.01 to 0.001	
Bismuth	0.001	0.01	0.01	

Abundances expressed in ppm.

Data compiled from Turekian and Wedepohl (1961), Kwong and Crocket (1976), Parthé and Crocket (1972), and Rösler and Lange (1972).

Data for Archean greywackes represents the mean of 20 analyses for the Kewagama and Cadillac groups.

Lode Gold Deposits

Concentration factors in the orebodies are 15,000 for Au, 80 for Ag and 20 for Pd relative to background abundances. Some of the mean Au enrichments given in Fig. 7 are greater than for the mines as a whole because predominantly high-grade ore was selected for determining metal distributions, with host rocks to the ore being collected and analyzed separately.

Several elements are typically present in association with Au, such as W, As, Sb and B, which have also undergone a high degree of concentration. Tungsten is a rare element with an average background abundance of 0.4 ppm in oceanic basalts (Helsen *et al.*, 1978), and has also been reported at anomalous concentrations in some chemical sedimentary rocks (Harmon *et al.*, 1975, 1978; Kerrich and Fryer, 1981, Table 1). Tungsten is present at 5 to 50 ppm in most gold-bearing veins, but lodes of scheelite are sporadically distributed in certain deposits, from some of which there has been past production, such as the Hollinger-

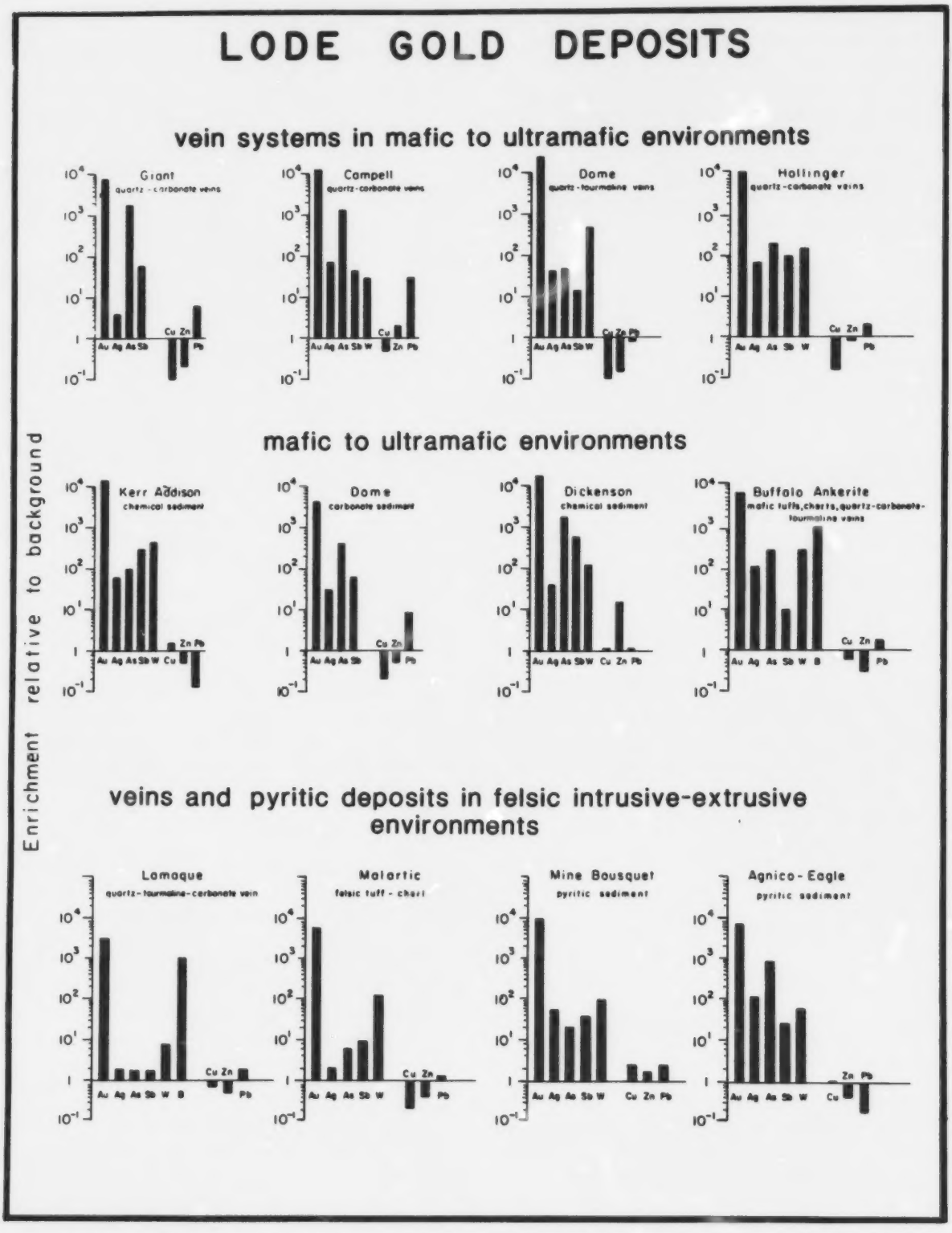

Figure 7: *Enrichments of selected elements in Archean lode gold deposits, referenced to background abundances in basalts. Note logarithmic coordinate (modified from Kerrich, 1983).*

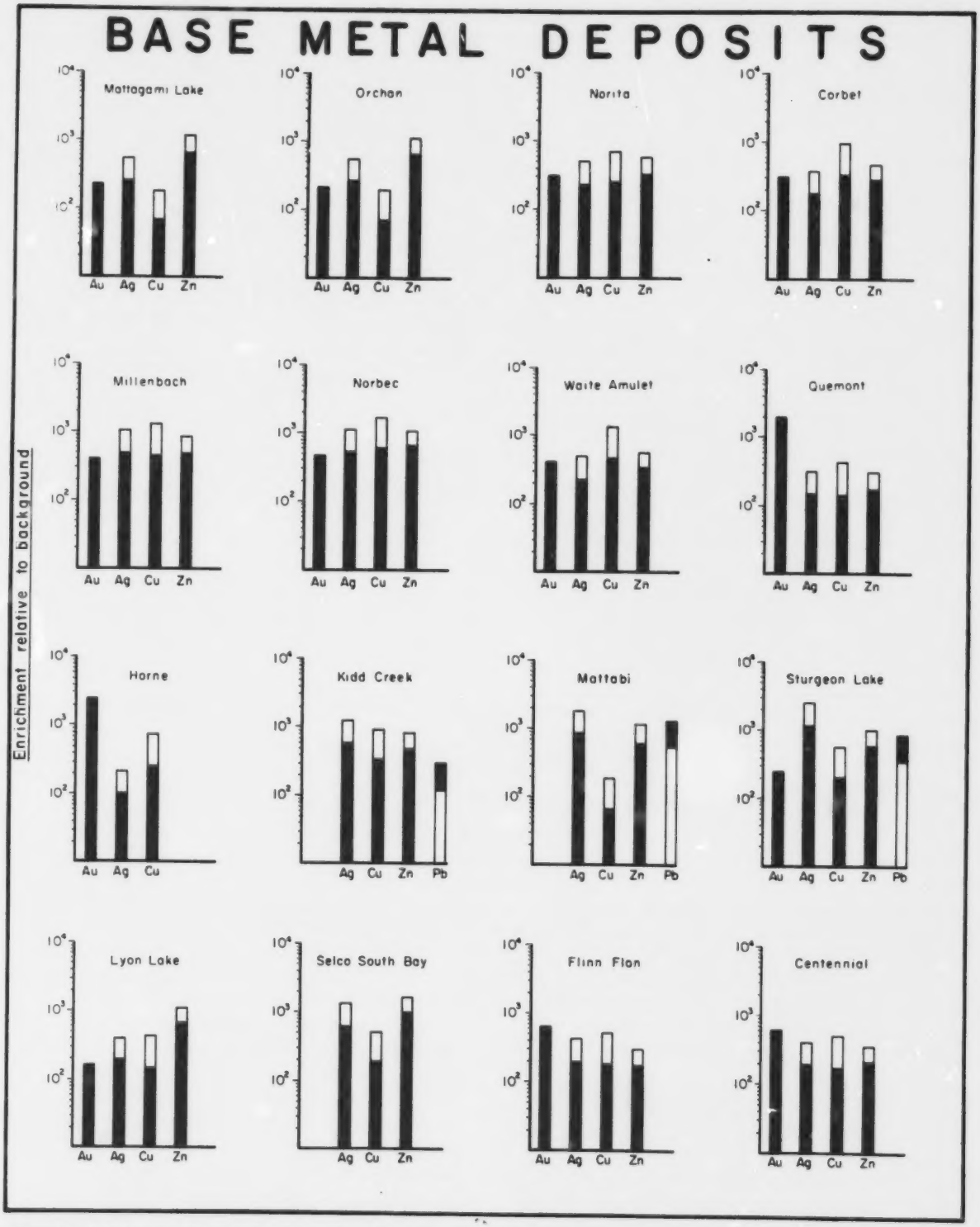

Figure 8: *Enrichments of Au, Ag, Cu, Zn and Pb where recovered in some Precambrian base metal massive sulphide deposits. Solid bars represent enrichments relative to background abundance in unaltered mafic volcanic rocks; open bars signify enrichments relative to abundances in primary felsic igneous rocks. Note logarithmic co-ordinate. Based on data in Worobec (1980), and additional sources (after Kerrich, 1983).*

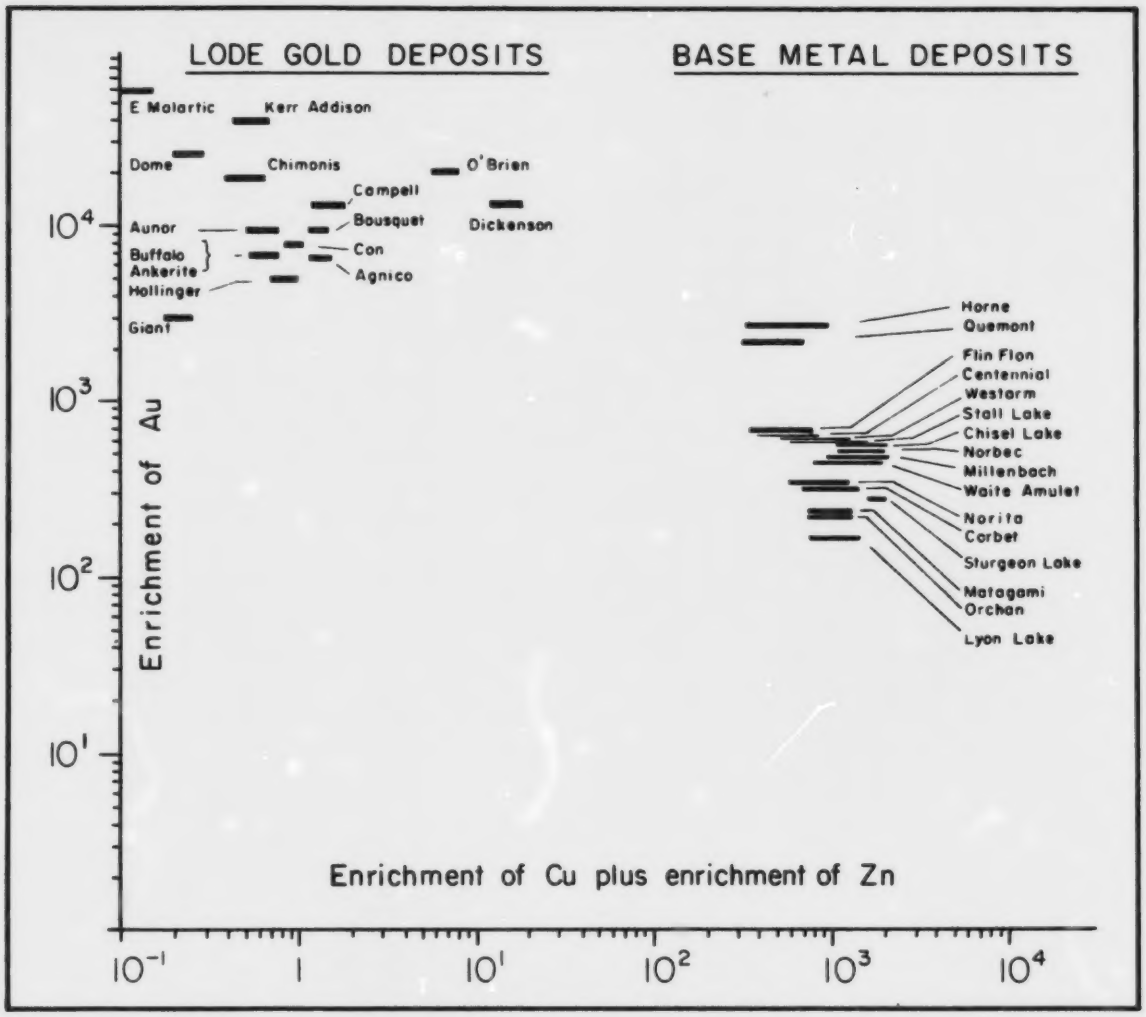

Figure 9: *Metal separation in lode gold vs. massive base metal sulphide deposits. Enrichment of Au versus the enrichment of Cu and the enrichment of Zn, for lode gold and base metal massive sulphide deposits. All enrichments calculated relative to background abundances in primary unaltered igneous rocks. The horizontal spread reflects enrichments computed utilizing background values for both mafic and felsic igneous rocks. Logarithmic coordinates (after Kerrich, 1983).*

MacIntyre mines, Timmins District; thus estimates of bulk W contents of gold ore are difficult to make.

Arsenic is another rare element, which is typically present at the 100- to 10,000-ppm level in gold lodes, being contained within the ubiquitous arsenopyrite and in pyrite. In laminated pyritic rocks of the Agnico Eagle Mine, Joutel, in the East South C Zone of the Dickenson mine, Red Lake district, and in quartz-carbonate veins of the Con mine, Yellowknife, the content of As is locally 0.2 to 2 per cent (Boyle, 1961; Kerrich *et al.*, 1981; Kerrich, 1983, Table 2), which therefore implies a concentration of 1000 to 10,000 times the background abundance of 2 ppm in basalts (Turekian and Wedepohl, 1961).

Boron is abundant in many gold-bearing veins and chemical sedimentary rocks, B being contained principally within tourmaline or axinite ((Ca, Mn, $Fe)_3Al_2BO_3[Si_4O_{12}]$ (OH)). Notable examples include the Dome and Buffalo Ankerite mines of the Timmins district, where tourmaline is present both in chemical sedimentary rocks and massive quartz-carbonate veins. Tourmaline is abundant in quartz veins near the No. 6 zone at Mine Bousquet, at Mine Doyon - Cadillac District, at the Lamaque, Sigma, Pascalis and Bras d'Or mines - Val d-Or district, and at Passagem de Mariana in Brazil. With a background content of 5 ppm in basalts and 20 ppm in shales (Turekian and Wedepohl, 1961), and levels exceeding 50 per cent in some ore deposits (Fleischer

and Routhier, 1973), the enrichment factor for B may be up to 100,000 depending on the nature of the source region.

Tellurides, selenides and bismuthides have a conspicuous association with lode gold deposits (Boyle, 1979): the Kirkland Lake gold district is among the prominent examples. Although the bulk Te, Se and Bi abundances of Archean lode gold deposits are not well known (Boyle, 1979, p. 151), the presence of Te-, Se- and Bi-bearing minerals signifies that these rare elements sporadically attain large degrees of enrichment in lode gold deposits, given their low background abundances of 0.01 to 0.001, 0.05 and 0.007 ppm respectively (Table 1; Turekian and Wedepohl, 1961; Rosler and Lange, 1972, p. 231).

In certain orebodies, Cr abundance is in excess of 2000 ppm, as in the quartz Cr-muscovite veins hosted in carbonate-altered ultramafic rocks ('green carbonate ore') at the Kerr Addison mine, Larder Lake district, in the quartz-muscovite veins of the Dome Mine, and No. 12 'vein' of the Hollinger mine open pit. In all of these examples the ore is enveloped by rocks of original ultramafic and Mg-tholeiitic composition. The mean Ni content in the East South C Zone sedimentary rocks, Dickenson mine, which are hosted by basalts, is 900 ppm. Hence, elevated abundances of Cr and Ni in gold orebodies typically appear to exist where ultramafic rocks are present, indicating that local rock composition mediates to a significant degree the abundance of these two transition metals in the orebodies. However, some hydrothermal transport of nickel and chromium may also occur along with the precious metals.

The average content of Pb, Zn and Cu in lode gold deposits is on average only 0.1 to 5 times their abundances in contiguous mafic volcanic rocks and in primary basalts worldwide, signifying a low degree of enrichment, or in some orebodies lower than background abundances of the base metals (Fig. 7). Minor erratic enrichments of Pb occurs in tandem with gold at the Con mine, Yellowknife, and in quartz-carbonate veins within quartz-feldspar 'porphyry' at the Dome mine; and zinc is sporadically enriched along with gold in the East South C zone, Dickenson mine. There is as yet no clear pattern to these minor anomalies of base metals in lode gold deposits, but they are quantitatively insignificant in terms of the low over-all base metal complement. Indeed, if base metal contents of lode gold deposits were significant, recovery of gold by conventional cyanidation alone would not be economically feasible, given the greater affinity of cyanide for Cu and Zn then for Au.

Molybdenum and graphite coated fractures are sporadically developed in some deposits: notable examples include those of the Kirkland Lake district, Taylor township near Timmins, and the Chadbourne Mine, Noranda. Molybdenite is a major component of the Hemlo orebodies, but its paragenetic relationship to gold is uncertain.

Figure 7 illustrates the magnitude by which the rare elements and the abundant transition metals are separated. In the Con Mine, Yellowknife, the enrichment factors for gold and copper are 10,000 and 0.1 respectively, signifying separation of these two elements by a factor of 100,000. The essential features of this distribution are repeated in the other orebodies, which encompass a wide variety of host rocks including chemical sedimentary rocks, and in diverse structural settings. There is thus an over-all coherence to the patterns of relative enrichment of elements in lode gold deposits.

Within the over-all characteristic enrichment pattern of gold and its associated elements (Ag, As, Sb, B, W, Se, Te, Bi) in Archean lode deposits, there is significant variability in the distribution of the gold-associated elements that does not appear to be a simple function of the immediate host rock type. For instance, arsenic is abundant in the pyritic gold deposit of Agnico Eagle, but not at the Thompson Bousquet or Dumagami deposits, all three of which are hosted by felsic fragmental rocks. Gold-bearing quartz-carbonate veins at Yellowknife, located within a sequence of metabasalts, possess As contents in the 10,000-ppm range coupled with low B, yet at the Dome Mine similar quartz veins also transecting basalts have As contents of only 100 ppm, but abundant tourmaline.

In summary, Archean lode gold deposits have extreme enrichments of certain rare elements, including B, As, Sb, W and Pd, with or without Te, Se and Bi, along with low enrichments of the abundant transition and base metals, relative to their enclosing rocks. The salient question that must be resolved is what is the fractionation process whereby rare elements, and metals such as Cr, Ni and W, conventionally considered to be immobile under conditions of low- to intermediate-grade metamorphism, are preferentially concentrated relative to the mobile and abundant base metals.

Base Metal Sulphide Deposits

Enrichment factors for Au, Ag, Cu, Zn and Pb, where present, are depicted for 20 essentially Zn-Cu massive base metal sulphide deposits in Figure 8. Most of the orebodies are disposed within Archean greenstone belts, but some examples of Proterozoic age are also included. Patterns of relative enrichment are remarkably uniform; Au, Ag, Cu and Zn are all concentrated by factors of 200 to 2000 times background, and there is thus no large separation of elements during their concentration from background rocks into the deposits. Data are for mines as a whole, notwithstanding the spatial separation of Cu and Zn within individual orebodies. These patterns of relative enrichment are reproduced in some massive sulphide deposits of younger age, for instance those in the Buchans camp and in the Iberian pyrite belt (Strauss *et al.*, 1977; Franklin *et al.*, 1981).

There is no comprehensive published information on the rare-element contents of more polymetallic massive sulphide deposits such as those of the Kuroko district, Japan. Mercer

(1976) reports abundances of Mo, Sb, As, Bi and Cd for Kuroko deposits, which correspond to approximate enrichment factors of 200, 1500, 10,000 and 3000 respectively.

Comparison of Lode Gold and Base Metal Deposits

Whereas there exists extreme separation of rare elements from the abundant and soluble base metals in lode gold deposits, massive base metal sulphide deposits do not possess any large separations of Au from Cu and Zn (Fig. 9). A continuum exists in gold content from Au-poor massive sulphide deposits such as at Flin Flon, Manitoba, through Au-enriched samples such as the Quemont and Horne mines of the Noranda district. However, the majority of Archean base metal massive sulphide deposits have a significantly lower absolute Au abundance than the lode gold deposits, and there are reasons to believe that the enhanced gold tenor of the Horne and Quemont mines, specifically is due to a later overprint by gold-bearing syenite dikes (Fig. 9). The salient feature is the over-all paucity of base metal content in lode gold deposits. Processes that have been advanced to account for the observed separation of rare elements from base metals in Archean lode gold deposits are critically examined in the following section.

A key feature of the element distribution in Archean lode gold deposits is the enrichment of a select group of lithophile elements (K, Rb, Ba, Cs) along with the rare elements as discussed above. Lithophile elements such as Be, Sn, REE, U and Th, with a general magmatophile association, do not appear to be characteristically enriched by the ore-forming hydrothermal system. A second observation to be emphasized is that the metal inventory is essentially independent of the composition of contiguous rocks hosting the deposits.

Separation of Base Metals from Rare Elements in Archean Lode Gold Deposits

Suggested mechanisms for the fractionation of base metals from rare elements in Archean lode gold deposits fall into four general categories: (1) those that appeal to special source rocks, (2) those involving selective precipitation of gold, and those that consider properties of the hydrothermal systems (3), and/or special ligands (4).

(1) Special Source Rocks

The question of possible genetic relationship of gold deposits to rocks of ultramafic composition is discussed below, but it is now clear that these 'primitive' magmas do not have an intrinsically elevated gold content overall, although they do possess slightly lower base metal abundances than mafic to felsic counterparts (Table 1). Hodgson and MacGeehan (1982, p. 225) have suggested that the preferred disposition of gold deposits at the contact of major volcanic and sedimentary sequences may be somehow related to the presence of sedimentary rocks into which gold has been preconcentrated. This conjecture is difficult to reconcile with the observation that major classes of base metal ore deposits are hosted by sedimentary sequences (Gustafson and Williams, 1981; Bjorlykke and Sangster, 1981), and that typical greenstone-belt turbidites in proximity to and remote from gold deposits have neither inherently elevated gold abundances nor low base metal contents relative to average crustal background values (Table 1). An alternative explanation for the observed spatial association of gold deposits with sedimentary rocks is that both are controlled by major transcrustal structures: the clastic sedimentary rocks developing along early rift faults, and subsequently in late transtensional basins along reactivated rift faults, and gold mineralization also being focussed by those structures.

(2) Selective Precipitation of Gold

It is possible that the auriferous mineralizing fluids do contain significant concentrations of base metals, but that formation of base metal sulphides is inhibited by low availability of reduced S and/or the absence of appropriate redox gradients, whereas gold precipitation is not. Such specialized conditions are difficult to reconcile with the fact that there are gold-bearing vein deposits with high contents of sulphur and reduced carbon, along with examples having low contents of these reduced species, as well as prominent examples where higher redox states are indicated by the presence of magnetite or hematite (cf. the Macassa mine - Kirkland Lake, Canadian Arrow mine, Matheson). Locally base metal sulphides are present, albeit in minor proportions, hence their formation is clearly not excluded by the ambient chemical environments of gold deposition, and an alternative explanation is required for their overall low content in the deposits.

Some Tertiary epithermal precious metal deposits of the western USA typically contain distinct base metal and gold-rich domains, in a given vein system, a notable example of which is the Sunnyside mine, Colorado. In this instance, separation of gold and the base metals via differing precipitation mechanisms seems likely (cf. Casadevall and Ohmoto, 1977; Barnes, 1979; White, 1981).

(3) Special Properties of the Hydrothermal System plus Special Ligands

Separation mechanisms which appeal to properties of hydrothermal fluids have centered on the possible role of differences in the water/rock ratio of marine convective vs metamorphic-derived mineralizing fluid reservoirs (Kerrich, 1979; Kerrich and Fryer, 1981; Kerrich, 1987; Kerrich and Hodder, 1982). An essential feature of metamorphic fluids, which are generated under conditions of a low water-to-rock ratio, is the potential to separate rare from abundant elements as a consequence of the restricted availability of

both solvent and ligands. In order to illustrate this process, consider 100 grams of metabasalt with 2 ppb Au and 100 ppm Cu + Pb + Zn. If 50 per cent of the metals are taken into solution as the rock evolves 5 weight percent volatiles at the greenschist-amphibolite transition (water/rock ≃0.05, Fyfe *et al.*, 1978), then the solute concentration of Au will be 20 ng/ml (20×10^{-9} g/ml) and 1 mg/ml base metals. Although the Au solute concentration is comparable to that reported for natural geothermal systems (Tilling *et al.*, 1973), the calculated figure for base metals is 100 times greater (Andrews and Fyfe, 1976) and implies that less than 1 per cent of the available base metals would be taken into solution. Therefore, in low water/rock systems the absolute abundance of rare elements in solution is not constrained by solubility, whereas base metal solute concentration is.

This mechanism provides some degree of separation of the rare elements from abundant base metals in solution, but the metamorphic fluid would still be saturated with respect to Cu, Pb and Zn, and it is necessary to postulate either a still lower intrinsic base metal content in the fluid and/or a process for selectively precipitating rare elements.

Consider further the partitioning of metals and potential ligands from rocks into the fluid phase during metamorphic dehydration reactions. Following the reasoning above, a metabasalt with an average content of 60 ppm Cl and 400 ppm F (Turekian and Wedepohl, 1961) would provide a maximum of 600 μg/ml Cl and 4,000 μg/ml F in solution, or much lower quantities if the halogens are strongly partitioned into metamorphic amphiboles and biotites, which is known to be the case. Inspection of alteration envelopes of auriferous veins (Bain, 1933; Kerrich and Fyfe, 1981) reveals that the most abundant cations added are typically K and Fe. These predominant metal cations in the hydrothermal fluid, in addition to the other cations present, such as Au, Ag, Cu, Pb and Zn, will compete for the restricted availability of water and halogens. If the rare elements compete more effectively for the limited halogens available for complexing, then this constraint may be a third factor suppressing base metal solute concentrations relative to the rare elements.

Conversely, in submarine hydrothermal convective systems which generate massive base metal sulphide deposits, water-rock ratios may be of the order of 10 to 100 (Wolery and Sleep, 1976; Spooner *et al.*, 1977) and thus 200 to 2,000 times greater than for lode gold deposits. Cl is present at 19,000 ppm in seawater, or 300 times the level calculated for metamorphic fluids. Here the solute abundances of base and precious metals are not constrained by solubility or availability of halogens for complexing, and probably broadly reflect background levels, with no large separations of elements in the hydrothermal solvent or deposit. For example, in typical Archean stratabound base metal massive sulphide deposits, such as Mattagami Lake Mines, and Millenbach or Corbet in the Noranda district, Zn and Cu are present in the low percentage range, silver at 10 to 50 and Au at 0.45 to 2 g/t (Worobec, 1980). This represents similar concentration factors for base metals (200-1,200), silver (200-1,100) and gold (250-1,000) relative to the background abundances (Fig. 9). Figures for the Zn, Cu, Ag and Au contents of base metal massive sulphide ore deposits in the Iberian pyrite belt are in the same range (Strauss *et al.*, 1977).

For lode gold deposits the ubiquitous presence of carbonate gangue requires hydrothermal solutions containing CO_2, and this raises the possibility that gold may be transported in solution as a carbonyl (CO), carbonyl chloride, COS or related ligand (Kerrich and Fyfe, 1981; Fyfe and Kerrich, 1984). Several authors (cf. Bain, 1933) have observed the close linkage of gold content in veins to wall-rock type and intensity of wall-rock alteration, raising the possibility that gold precipitation may be mediated by reactions between fluid and wall rock. During carbonate-forming reactions, CO_2 is scavenged from solution to form iron-magnesium-calcium carbonate minerals from Fe, Mg, Ca-silicate minerals in wall rocks (Boyle, 1961, 1970; Kerrich and Fyfe, 1981), and one effect of these reactions would be to break down a proportion of carbonate complexes in solution, lowering F_{CO_2}, and hence forcing precipitation of the complexed species. It has also been suggested recently that in certain hydrothermal tungsten deposits of the greisen type, W may be complexed with CO_3^{2-} in solution (Higgins, 1980).

The higher ambient temperatures of hydrothermal gold systems compared to submarine geothermal convection together with the possibility of ligands such as CO in the former, may promote aqueous transport of some relatively insoluble metals. Thus, the extent of enrichment of W and Pd documented above for lode gold deposits is much greater than is typical for massive base metal sulphide orebodies.

Several additional factors, including local perturbations of the chemical or physical environment, undoubtedly govern to some extent the separation of elements in ore deposits. Such factors may have controlled the recorded variations in abundance of B, As, Cr, Ni and Hg between individual orebodies as well as the sporadic occurrence of Mo plus graphite. Exceptions may represent anomalous concentrations in the source regions, mixing of different hydrothermal reservoirs, variations in the relative proportions of complexing agents, availability of reduced S or many other possible factors. There is, however, an over-all coherence to the patterns of enrichments in lode gold deposits, on the one hand, and of seafloor base metal massive sulphide deposits on the other hand (Fig. 9).

The observed distributions of elements could be accounted for in terms of two different hydrological regimes: a lower-temperature seawater system with a high water-rock

ratio and abundant halogens, in which base metals, silver and gold are concentrated to similar extents; and conversely, a high-temperature metamorphic system where the combination of a low water-rock ratio with a limited supply of halogens results in selective partitioning of certain rare elements into the fluid phase relative to abundant and mobile base metals. This interpretation is consistent with isotopic data for the temperature and fluid sources of the two systems and with geological relationships of the deposit types.

Irrespective of the metal complexing agents, a low water to rock ratio in the source region coupled with low chloride would serve to suppress uptake of abundant base metals into solution, resulting in a preferential concentration of certain rare elements into the hydrothermal reservoir.

(4) Special Ligands in Near-Neutral, Low-S Fluids

Lydon (1980) has proposed that in solutions of neutral to slightly alkaline pH, base metal and gold-thiocomplexes are the dominant solute species. If the total sulphur content of the solution is low (<10,000 ppm), then according to Lydon (1980) the extent of base metal thiocomplex formation is insignificant, whereas that of gold is still appreciable (e.g. base metals $\ll$ 1 ppm, Au 1-2 ppm in solutions of Cl = 3.0 m, pH = 6.5 log [S reduced/S oxidised] = 10.0, and at 200°C; Lydon, 1980, Fig. 21). Phillips and Groves (1983) suggest that $HAu(HS)_2$ complexes are the most likely candidates for hydrothermal transport of gold, and further that such ligands would selectively fractionate gold relative to base metals in solution.

Any such ligand-specific mechanisms for gold deposits must not only account for the separation of gold and base metals, but must also explain cosolution of the gold-associated elements such as Ag, As, Sb, B, W, Se, Te and Bi. Furthermore, the specified gold-transporting complex must be stable in neutral to slightly acidic fluids, as signified by the generally muscovite-dominated alteration assemblages (cf. Bain, 1933; Boyle, 1961; Kerrich and Fyfe, 1981; Rose and Burt, 1979).

It should be noted that under intermediate to high temperature-pressure conditions the concentrations of sulphur-bearing species in equilibrium with Fe^{2+}-bearing minerals is very low (cf. Carmichael *et al.*, 1974, p. 306; Kerrich *et al.*, 1977). However, given the low estimated gold solute concentrations (~20 ppb) in hydrothermal fluids (Kerrich and Fyfe, 1987, Part II), along with the absolute introduction of sulphur into vein deposits, molecules incorporating sulphur may provide a significant gold transporting ligand. Significant concentrations of S-compounds are known to exist in primary fluid inclusions within quartz, from the Archean lode deposits. Such sulphur compounds are 'scrubbed' from the gases released by decrepitating inclusions, prior to isotopic analysis of the fluid inclusion CO_2 (King *et al.* 1987).

Concluding Remarks

Gold is soluble under a wide range of geological conditions, and may be complexed in solution by a number of different ligands. However, the magnitude of the enrichment required to generate major gold deposits, combined with the systematic and highly selective fractionation of gold and other rare elements from the base metals, implies that special mineralizing processes operate.

Gold deposits formed in major structures of transcrustal extent, and from hydrothermal fluids at lithostatic pressure, as against the familiar hydrothermal convection models involving hydrostatic fluid circulation that are applied to base metal massive sulphide and other deposit types. Moreover, the largest and most numerous lode gold deposits appear to be confined to Archean greenstone belts of ~2.7 Ga.

Explanations for these and other special features of Archean lode gold deposits are examined in the companion paper, which deals with hydrothermal fluids, patterns of alteration, and genetic models of this deposit type (Kerrich and Fyfe, 1987, Part II).

Acknowledgements

The authors thank Bill Padgham for the invitation to write this contribution. Numerous mine geologists, especially D. Myers, D. Rogers, E. Van Hees, G. Nemcsok, S. Comline and P. Bedard kindly provided access to the gold mines from which much of the data for this manuscript is based. We are grateful to L.M. Willmore, B. Every, Y.C. Cheng, B. McKinnon and J. Forth for analytical assistance. A. Heppner is thanked for conducting the typing, and E. McLarty, L.M. Willmore and Mrs. R. Ringsman for drafting the diagrams and assisting with preparation of the manuscript. The Canadian Institute of Mining and Metallurgy is thanked for permission to reproduce some of the figures from Special Volume 27. This paper has benefited from an incisive review by R.W. Boyle, and editorial improvements by W. Padgham.

References

Allison, I., and Kerrich, R., 1980, History of deformation and fluid transport in shear zones at Yellowknife. In: Proceedings of Gold Workshop, Yellowknife, N.W.T., R.D. Morton (ed.), December, 1979.

Andrews, A.J., and Fyfe, W.S., 1976, The role of sea water in sub-seafloor metamorphism and massive sulphide generation on the ocean floor. Geosci. Can., v. 3, p. 83-94.

Andrews, A.J., Hugon, H., Durocher, M., Corfu, F. and Lavigne, M.J., 1986, The anatomy of gold-bearing greenstone belt: Red Lake, Northwestern Ontario. Canada. In: Gold '86. MacDonald, A.J. (ed.), Toronto, pp. 3-22.

Anhaeusseer, C.R., 1976, The nature and distribution of Archean gold mineralization in southern Africa. Mineral. Sci. Eng., v. 8, p. 46-84.

Bain, G.W., 1933, Wall rock mineralization along Ontario gold deposits. Econ. Geol., v. 28, p.705-745.

Barnes, H.D., 1979, Solubilities of ore minerals. In: Geochemistry of Hydrothermal Ore Deposits, II, Barnes, H.L. (ed.), Wiley, New York, p. 404-460.

Barnett, E.S., Hutchinson, R.W., Adamcik, A., and Barnett, R.L., 1982, Geology of the Agnico-Eagle gold deposit, Quebec. In: Precambrian sulphide deposits, H.S. Robinson Memorial Volume. Hutchinson, R.W., Spence, C.D., and Franklin, J.M. (eds.)., Geol. Assoc. Canada Special Paper.

Bertoni, C.H., (1983), Gold production in the Superior Province of the Canadian Shield. Bull. Can. Mineral. Metall., v. 76, p. 62-69.

Bjorlykke, A., and Sangster, D.F., 1981, An overview of sandstone lead deposits and their relationship to Red-Bed copper and carbonate hosted lead-zinc deposits. Econ. Geol., 75th Anniversary Vol., p. 179-213.

Boyle, R.W., 1961, The geology, geochemistry, and origin of the gold deposits of the Yellowknife district. Geol. Surv. Canada, Mem. 310.

Boyle, R.W., 1976, Mineralization processes in Archaean greenstone and sedimentary belts. Geol. Surv. Canada Paper 75-15.

Boyle, R.W., 1977, Discussion of: Iron reduction around gold-quartz veins, Yellowknife District, N.W.T., Canada. Econ. Geol., v. 70, p. 562-570.

Boyle, R.W., 1979, The geochemistry of gold and its deposits. Geol. Surv. Canada, Bull. 280, 584 p.

Breakey, A.R., 1975, A mineralogical study of the gold quartz lenses in the Campbell Shear, Con Mine, Yellowknife, N.W.T. Unpublished M.Sc. thesis, McGill University, Montreal, Que.

Carmichael, I.S.E., Turner, F.J., and Verhoogen, J., 1974, Igneous Petrology: McGraw Hill, New York, 739 p.

Casadevall, T., and Ohmoto, H., 1977, Sunnyside mine, Eureka mining district, San Juan county, Colorado. Geochemistry of gold and base metal ore deposition in a volcanic environment. Econ. Geol., v. 72, p. 1285-1320.

Colvine, A.C., Andrews, A.J., Cherry, M.E., Durocher, M.E., Fyon, A.J., Lavigne, M.J. Jr., MacDonald, A.J., Marmot, S., Poulson, K.H. and Troop, D.G., 1984, An integrated model for the origin of Archean gold deposits. Ontario Geol. Surv., Open File Rep. No. 5524, 98 p.

Condie, K.C., 1981, Archean Greenstone belts. Elsevier, Amsterdam, 434 pp.

Fleischer, R., and Routhier, P., 1973, The 'consanguineous' origin of a tourmaline-bearing gold deposit; Passagem de Mariana (Brazil). Econ. Geol., v. 68, p. 11-22.

Franklin, J.M., Sangster, D.M., and Lydon, J.W., 1981, Volcanic associated massive sulphide deposits. Econ. Geol. 75th Anniversary Volume, 485-627.

Fripp, R.E.P., 1976, Stratabound gold deposits in Archaean banded iron formations, Rhodesia. Econ. Geol., v. 71, p. 58-75.

Fryer, B.J., Kerrich, R., Hutchinson, R.W., Peirce, M.G., and Rogers, D.S., 1979, Archean precious metal hydrothermal systems, Dome Mine, Abitibi greenstone belt, I. Can. J. Earth Sci., v. 16, p. 421-439.

Fyfe, W.S., Price, N.J., and Thompson, A.B., 1978, Fluids in the Earth's Crust. Elsevier, Amsterdam, 383 pp.

Fyfe, W.S., and Kerrich, R., 1984, Gold: natural concentration processes. In: Gold '82: The Geology, Geochemistry and Genesis of Gold Deposits, ed. by R.P. Foster, A.A. Balkema, Rotterdam, p. 99-127.

Fyfe, W.S., and Kerrich, R., 1985, Fluids and thrusting. Chem. Geol., v. 49, p. 353-362.

Fyon, J.A., and Crocket, J.H., 1982a, Gold exploration in the Timmins District using field and lithogeochemical characteristics of carbonate alteration zones. In: Geology of Canadian Gold Deposits, Hodder, R.W. and Petruk, W. (eds.). Misc. Paper, Ontario Geol. Surv. 98, p. 90-107.

Fyon, J.A., Schwarcz, H.P., and Crocket, J.H., 1984a, Carbonatization and gold mineralization in the Timmins area. Abitibi greenstone belt: genetic links with Archean mantle CO_2-degassing and lower crust granulitization. Geol. Assoc. Canada Program with Abstr. 9, p. 65.

Fyon, J.A., Crocket, J.H., and Schwarcz, H.P., (1984b), The Carshaw and Malga iron-formation-hosted gold deposits of the Timmins area. In: The Geology of Gold in Ontario, Colvine, A.C. (ed.), Misc. Paper, Ontario Geol. Surv. 110, p. 98-110.

Groves, D.I., and Batt, W.D., 1984, Spatial and temporal variations of Archean metallogenic associations in terms of evolution of granitoid-greenstone terrains with particular emphasis on the Western Australian Shield. In: Archaean Geochemistry, Kroner, A., Hanson, G.N. and Goodwin, A.M. (eds.), Springer-Verlag Berlin, p. 73-98.

Groves, D.I., and Phillips, N., 1987, The genesis and tectonic control on Archean gold deposits of the Western Australia Shield - a metamorphic replacement model. Ore Deposits Reviews, v. 2, p. 287-322.

Gustafson, L.B., and Williams, N., 1981, Sediment-hosted stratiform deposits of copper, lead and zinc. Econ. Geol., 75th Anniversary Volume, p. 139-178.

Harmon, K.A., Crocket, J.H., and Shaw, D.M., 1975, Tungsten in iron formations. Geological Society of America, Abstracts with Programs, v. 7, p. 773.

Harmon, K.A., Shaw, D.M., and Crocket, J.H., 1978, Tungsten abundance in Precambrian iron-formations and other sedimentary rocks. Econ. Geol., v. 73, p. 1167-1170.

Helson, J.N., Shaw, D.M., and Crocket, J.H., 1978, Tungsten abundances in some volcanic rocks. Geochim. Cosmochim. Acta, v. 42, p. 1067-1070.

Henderson, J.F., and Brown, I.C., 1966, Geology and structure of the Yellowknife Greenstone Belt, District of Mackenzie. Geological Survey of Canada, Bull. 141, 87 p.

Herzberg, C.T., Fyfe, W.S., and Carr, M.J., 1983, Density constraints on the formation of the continental Moho and crust. Contrib. Mineral. Petrol., v. 84, p. 1-5.

Higgins, N., 1980, Fluid inclusion evidence for the transport of tungsten by carbonate complexes in hydrothermal solution. Can. Jour. Earth Sci., v. 17, p. 823-830.

Hodgson, C.J., 1983, The Structure and Geological Development of the Porcupine Camp - A Re-Evaluation. In: The Geology of Gold in Ontario. A.C. Colvine (ed.). Ontario Geological Survey Miscellaneous Paper 110, p. 211-225.

Hodgson, C.J., 1984, The structure and geological development of the Porcupine Camp - a re-evaluation. In: The Geology of Gold in Ontario, Colvine, A.C. (ed.), Misc. Paper Ontario Geol. Survey 110, p. 211-225.

Hodgson, C.J., and MacGeehan, P.J., 1982, A review of the geological characteristics of 'gold only' deposits in the Superior Province of the Canadian Shield. In: CIM Special Volume 24, Geology of Canadian Gold Deposits (R.W. Hodder and W. Petruk, (eds.), p. 211-229.

Hutchinson, R.W., 1976, Lode gold deposits; the case for volcanogenic derivation. In: Proceedings Volume, Pacific Northwest Mining and Metals Conference, Portland, Oregon, 1975, Oregon Dept. Geol. and Mineral Ind., p. 64-105.

Jensen, L.S., 1978, Larder Lake synoptic mapping project, Districts of Cochrane and Timiskaming. Ontario Geol. Surv. Misc. Paper 94, p. 64-69.

Jensen, L.S., and Langford, F.F., 1985, Geology and petrogenesis of the Archean Abitibi Belt in the Kirkland Lake Area, Ontario. Ontario Geol. Surv., Misc. Paper 123, p. 130.

Kamilli, R.J., and Ohmoto, H., 1977, Paragenesis, zoning, fluid inclusion and isotope studies of the Finlandia Vein, Colqui District, Central Peru. Econ. Geol., v. 72, p. 950-982.

Kennedy, G.C., 1950, A portion of the system silica-water. Econ. Geol., v. 45, p. 629-653.

Kerrich, R., 1979, Lode gold deposits in greenstone belts, chemical and hydrodynamic constraints. In: Gold: Exploration and Outlook. T. Anderson, P. Chamois and D. Desnoyers (eds.), Proceedings, Adams Club 8th Annual Special Symposium, February 1979, McGill University, Montreal, p. 13-34.

Kerrich, R., 1980, Archean lode gold deposits: a synthesis of data on metal distribution, fluid inclusions and stable isotopes, with special reference to Yellowknife. Proceedings, Gold Workshop, Yellowknife, December 1979.

Kerrich, R., 1983, Geochemistry of gold deposits in the Abitibi greenstone belt. CIM Special Paper 27, 75 p.

Kerrich, R., 1986a, Archean lode gold deposits of Canada: Parts I and II, a synthesis of geochemical data from selected mining camps, with emphasis on patterns of alteration. Information Circular, Econ. Geol. Res. Unit, Univ. Witwatersrand, Johannesburg 192, 34 p.

Kerrich, R., 1986b, Fluid infiltration into fault zones: chemical, isotopic and mechanical effects. J. Pure Applied Geophys., v. 124, p. 225-268.

Kerrich, R., 1986c, Fluid transport in lineaments. Phil. Trans. Royal Soc. London, Ser. A317, p. 219-251.

Kerrich, R., 1987, The stable isotope geochemistry of Au-Ag vein deposits in metamorphic rocks. In: T.K. Kyser (ed.) Stable Isotope Geochemistry of Low Temperature Fluids. MAC Short Course v. 13, p. 287-336.

Kerrich, R., and Allison, I., 1978, Vein geometry and hydrostatics during Yellowknife mineralization. Can. Jour. Earth Sci., v. 15, p. 1653-1660.

Kerrich, R., and Fryer, B.J., 1979, Archean precious metal hydrothermal systems; Dome Mine, Abitibi greenstone belt; II REE and oxygen isotope relations. Can. Jour. Earth Sci., v. 16, p. 440-458.

Kerrich, R., and Fryer, B.J., 1981, The separation of rare elements from abundant base metals in Archean lode gold deposits: implications of low water/rock source regions. Econ. Geol. (in press).

Kerrich, R., Fryer, B.J., Milner, K., and Peirce, M.G., 1981, The geochemistry of gold-bearing chemical sediments: Dickenson Mine, Red Lake, Ontario: a reconnaissance study. Can. Jour. Earth Sci., v. 18, p. 624-637.

Kerrich, R., and Fyfe, W.S., 1981, The gold-carbonate association: source of CO_2 and CO_2-fixation reactions in Archean lode deposits. Chemical Geology, v. 33, p. 265-294.

Kerrich, R., Fyfe, W.S., and Allison, I., 1977a, Iron reduction around gold-quartz veins, Yellowknife district, Northwest Territories, Canada. Econ. Geol., v. 72, p. 657-663.

Kerrich, R., Fyfe, W.S., Gorman, B.E., and Allison, I., 1977b, Local modification of rock chemistry by deformation. Contrib. Mineral. Petrol., v. 65, p. 183-190.

Kerrich, R., and Hodder, R.W., 1982, Archean lode gold and base metal deposits: chemical evidence for metal separation into independent hydrothermal systems. In: CIM Special Volume 24, Geology of Canadian Gold Deposits (R.W. Hodder and W. Petruk, eds.), p. 144-160.

King, R.W. and Kerrich, R., and McLarty, E., 1987, Systematics in $\delta^{13}C$ distribution of hydrothermal carbonates and fluid inclusion CO_2 from Au vein deposits of the Abitibi Subprovince. GAC-MAC Abstracts with Program, v. 12, p. 61.

Ludden, J., Hubert, C., and Gariepy, C., 1986, The tectonic evolution of the Abitibi greenstone belt of Canada. Geol. Magazine, v. 123, p. 153-166.

Lydon, J.W., 1980, The behaviour of metals in hydrothermal systems with emphasis on gold. Workshop on Epithermal Deposits, Geoscience Forum, Whitehorse, Yukon.

MacDonald, A.J., 1984, The iron formation-gold association. Evidence from Geraldton area. In: The Geology of Gold in Ontario, Colvine, A.C. (ed.). Ontario Geol. Surv. Misc. Paper 110, p. 75-83.

MacGeehan, P.J., 1985, The metamorphism and deformation of Archean gold deposits: the importance of structural documentation in the evaluation of gold mineralization. Geol. Soc. Amer., Abstr. with Programs, v. 17, p. 150.

Mason, B., 1982, Principles of Geochemistry, 4th ed., John Wiley & Sons Inc., 344 pp.

Mercer, W., 1976, Minor elements in metal deposits in sedimentary rocks - a review of the recent literature. In: Handbook of Stratabound and Stratiform Ore Deposits, Wolf, K.H. (ed.), Elsevier, Amsterdam, p. 1-27.

Padgham, W.A., 1987a, Yellowknife volcanic belt: setting and stratigraphy. In: Yellowknife Guidebook. W.A. Padgham (ed.) Yellowknife GeoWorkshop Committee, p. 11-20.

Padgham, W.A., 1987b, Access to anorthosite and sheeted dykes in the Chan Formation. In: Yellowknife Guide Book. W.A. Padgham (ed.). Yellowknife GeoWorkshop Committee, p. 41-42.

Padgham, W.A., 1987c, Guide to parts of the Crestaurum, Townsite, and Yellowknife Bay Formations and the Banting Group. In: Yellowknife Guide Book. W.A. Padgham (ed.). Yellowknife Geoworkshop Committee, p. 55-80.

Phillips, G.N. and Groves, D.I., 1983, The nature of Archaean gold-bearing fluids as deduced from gold deposits of Western Australia. Journal of the Geological Society of Australia, v. 30, pp. 25-39.

Phillips, G.N., Groves, D.I., and Martyn, J.E., 1984, An epigenetic origin for Archean banded iron-formation-hosted gold deposits. Econ. Geol., v. 79, p. 162-171.

Ramsay, J.G., and Graham, R.H., 1970, Strain variation in shear belts. Canadian Jour. Earth Science, v. 7, p. 786-813.

Ridler, R.H., 1976, Stratigraphic keys to the gold metallogeny of the Abitibi belt. Can. Mining J., v. 97, p. 81-88.

Robert, F. and Brown, A.C., 1984, Chemical exchanges between gold-mineralizing fluids and wallrocks at the Sigma Mine, Abitibi region, Quebec. GAC-MAC Joint Annual Meeting, Program with Abstracts, v. 9, p. 100.

Rose, A.W., and Burt, D.M., 1979, Hydrothermal Alteration. In: The Geochemistry of Hydrothermal Ore Deposits. H.L. Barnes (ed.). Wiley, New York, p. 173-235.

Rosler, H.J. and Lange, H., 1972, Geochemical Tables. Elsevier, Amsterdam, 468 p.

Seward, T.M., 1984, The transport and deposition of gold in hydrothermal systems. In: Gold '82, Foster, R.P. (ed.), Balkema, Rotterdam, p. 341-344.

Spooner, E.T.C., Chapman, J.H., and Smewing, J.D., 1977, Strontium isotope contamination and oxidation of the ophiolitic rocks of the Troodos Massif, Cyprus. Geochim. Cosmochim. Acta, v. 41, p. 873-890.

Strauss, G.K., Madel, T.J., and Alonso, F.F., 1977, Exploration practice for strata-bound volcanogenic sulphide deposits in the Spanish-Portuguese Pyrite Belt: geology, geophysics and geochemistry. In: Time and Stratabound Ore Deposits, Klemm, D.D., and Scheider, H.-J. (eds.), Springer Verlag, Berlin, p. 53-93.

Tilling, R.I., Gottfried, D., and Rowe, J.J., 1973, Gold abundance in igneous rocks: bearing on gold mineralization. Econ. Geol., v. 68, p. 168-186.

Turekian, K.K., and Wedepohl, K.H., 1961, Distribution of the elements in some major units of the earth's crust. Geol. Soc. America Bull., v. 7, p. 175-192.

Turner, F.J., 1981, Metamorphic Petrology: Mineralogical, Field, and Tectonic Aspects. McGraw-Hill, New York, 327 p.

Uyeda, S., 1978, The new view of the earth. W.H. Freeman & Co., 217 pp.

White, D.E., 1981, Active Geothermal Systems and Hydrothermal Ore Deposits. Econ. Geol., 75th Anniv. Vol., p. 397-423.

Wolery, T.J., and Sleep, N.H., 1976, Hydrothermal circulation and geochemical flux at mid-ocean ridges. Jour. Geology, v. 84, p. 249-275.

Woodall, R., 1979, Gold - Australia and the world. In: Gold Mineralization, Glover, J.E. and Groves, D.I. (eds.), Univ. Western Australia, Geol. Dept. and Extension Serv., Publication 3, p. 1-34.

Worobec, A., 1980, Canadian Mines Handbook. Northern Miner Press, Toronto, 368 pages.

Contribution to the Geology of the Northwest Territories, Volume 3, 1988, NWT Geology Division, INAC, Yellowknife.

The Formation of Gold Deposits with Particular Reference to Archean Greenstone Belts and Yellowknife

II Source of hydrothermal fluids, alteration patterns and genetic models

R. Kerrich[1] and W.S. Fyfe[2]

Abstract

Hydrothermal reservoirs involved in the generation of Archean lode gold deposits are characterized by distinctive isotopic and geochemical properties. Hydrothermal solutions transporting gold were isotopically characterized by $\delta^{18}O = 6$ to 9 per mil and $\delta D = -80$ to -40 per mil, consistent with a metamorphic fluid reservoir. These fluids were at temperatures of 270 to 400°C, possessed low salinities of < 2 wt.% NaCl equivalent, near neutral pH, $Na/K \simeq 0.1$, and contained significant quantities of CO_2, along with the reduced gas species CH_4, CO, H_2, and ultrafine particulate hydrocarbons. The CO_2 may have been derived from mixtures of various possible crustal carbon reservoirs, including marine and igneous carbonate, decarbonated marine carbonate or decarboxylation of organic hydrocarbons, with a component of mantle CO_2.

The hydrothermal fluid characteristics are all consistent with a metamorphic or magmatic fluid reservoir; whereas none of these geochemical features are typical of marine-water-derived ore-forming fluids. Hydrothermal fluids carried more radiogenic Sr and Pb than contemporaneous mantle, komatiites or tholeiites, and thus carried a contribution from older sialic basement. Mineralized faults possess enrichments of LIL elements including K, Rb, Li, Cs, B, and CO_2, as well as rare elements such as Au, Ag, As, Sb, Se, Te, Bi, and W.

The ubiquitous gangue carbonate minerals formed via hydrolysis of Fe, Mg, Ca, Mn-silicates to Fe, Mg, Ca, Mn-carbonates in which wall rocks donate the bivalent metal cations and CO_2 is indigenous to the hydrothermal fluids. Ultramafic rocks and oxide facies iron formation are effective CO_2 sinks, given their inherently elevated complement of bivalent metal cations. In general, wall rocks to veins are intensely reduced ($Fe^{2+}/\Sigma Fe$ 0.9) relative to background ($Fe^{2+}/\sigma Fe$ 0.7), and this is also reflected in sporadic positive anomalies of Eu^{2+}. The reductant involved was probably H_2, a product of the dissociation of H_2O under high T and P conditions in the source rocks.

Of the various models proposed for greenstone-belt lode gold deposits, most are incommensurate with the geological and goechemical boundary conditions. Derivation of gold from quartz-feldspar porphyry bodies spatially associated with many deposits is incompatible with known differences in isotopic, redox, REE and alteration patterns of stocks and deposits or with relative times of emplacement; and given their small volume, with considerations of material balance for the gold source. Lateral secretion of gold and gold-associated chemical components into dilatant openings from enclosing wall rocks is not consistent with the known range of grain boundary diffusion distances over geological time spans. There is no evidence that greenstone-belt rock types contain more abundant gold than their Proterozoic and Phanerozoic counterparts, except possibly for the volumetrically minor Algoman BIF. Primary ultramafic rocks possess lower gold contents than mafic or felsic igneous rocks. Hence, there is no basis for proposed genetic links between various source rocks conjectured to have inherently elevated gold abundances and deposits. Gold deposits are spatially associated with a wide variety of igneous rock types, but the K, Rb, Ba interelement relationships are not consistent with the involvement of magmatic fluids in the gold forming system.

Archean greenstone-belt Au and Ag vein deposits appear to form during the discharge of low-Cl, CO_2-rich aqueous fluids likely of metamorphic origin, at depth in a compressive, crustal regime. This discharge represents the return flow of a cycle in which H_2O and CO_2 from the hydrosphere are initially transferred to rocks as hydrates, carbonates and hydrocarbons, during cooling of volcanic flows at the ocean floor. These components are subsequently returned to the hydrosphere via outgassing of the volatile-laden volcanic sequence under conditions of burial accompanied by crustal heating. Outgassing occurs during thrusting, and in the envelopes of rising batholiths. A wide array of major structures are present in greenstone belts, but the gold deposits are preferentially associated with those that have associated clastic and chemical sediments, and alkaline magmas. It is suggested that rift environments, with high heat fluxes, are appropriate for efficient gold concentration. Here, listric normal faults initially control extension along with ultramafic volcanism, provide pathways for mafic and felsic magmas, and are responsible for scarp-dominated sedimentary rocks. At later stages of greenstone-belt development, reverse motion on the faults accommodates crustal compression, and structures act to focus hydrothermal discharge generating the gold deposits, as well as conduits for trondhjemitic and alkalic magmas. The geometry of listric faults may be particularly efficient for tapping large volumes of crust.

[1]Department of Geological Sciences, University of Saskatchewan, Saskatoon, Saskatchewan, Canada S7N 0W0
[2]Department of Geology, University of Western Ontario, London, Ontario, Canada N6A 5B7

Contribution to the Geology of the Northwest Territories, Volume 3, 1998, NWT Geology Division, INAC, Yellowknife.

The Formation of Gold Deposits with Particular Reference to Archean Greenstone Belts and Yellowknife

II Source of hydrothermal fluids, alteration patterns and genetic models

R. Kerrich[1] and W.S. Fyfe[2]

Abstract

Hydrothermal reservoirs involved in the generation of Archean lode gold deposits are characterized by distinctive isotopic and geochemical properties. Hydrothermal solutions transporting gold were isotopically characterized by $\delta^{18}0 = 6$ to 9 per mil and $\delta D = -80$ to -40 per mil, consistent with a metamorphic fluid reservoir. These fluids were at temperatures of 270 to 400°C, possessed low salinities of < 2 wt.% NaCl equivalent, near neutral pH, $Na/K \simeq 0.1$, and contained significant quantities of CO_2, along with the reduced gas species CH_4, CO, H_2, and ultrafine particulate hydrocarbons. The CO_2 may have been derived from mixtures of various possible crustal carbon reservoirs, including marine and igneous carbonate, decarbonated marine carbonate or decarboxylation of organic hydrocarbons, with a component of mantle CO_2.

The hydrothermal fluid characteristics are all consistent with a metamorphic or magmatic fluid reservoir; whereas none of these geochemical features are typical of marine-water-derived ore-forming fluids. Hydrothermal fluids carried more radiogenic Sr and Pb than contemporaneous mantle, komatiites or tholeiites, and thus carried a contribution from older sialic basement. Mineralized faults possess enrichments of LIL elements including K, Rb, Li, Cs, B, and CO_2, as well as rare elements such as Au, Ag, As, Sb, Se, Te, Bi, and W.

The ubiquitous gangue carbonate minerals formed via hydrolysis of Fe, Mg, Ca, Mn-silicates to Fe, Mg, Ca, Mn-carbonates in which wall rocks donate the bivalent metal cations and CO_2 is indigenous to the hydrothermal fluids. Ultramafic rocks and oxide facies iron formation are effective CO_2 sinks, given their inherently elevated complement of bivalent metal cations. In general, wall rocks to veins are intensely reduced (Fe^{2+}/Σ Fe 0.9) relative to background (Fe^{2+}/σ Fe 0.7), and this is also reflected in sporadic positive anomalies of Eu^{2+}. The reductant involved was probably H_2, a product of the dissociation of H_2O under high T and P conditions in the source rocks.

Of the various models proposed for greenstone-belt lode gold deposits, most are incommensurate with the geological and goechemical boundary conditions. Derivation of gold from quartz-feldspar porphyry bodies spatially associated with many deposits is incompatible with known differences in isotopic, redox, REE and alteration patterns of stocks and deposits or with relative times of emplacement; and given their small volume, with considerations of material balance for the gold source. Lateral secretion of gold and gold-associated chemical components into dilatant openings from enclosing wall rocks is not consistent with the known range of grain boundary diffusion distances over geological time spans. There is no evidence that greenstone-belt rock types contain more abundant gold than their Proterozoic and Phanerozoic counterparts, except possibly for the volumetrically minor Algoman BIF. Primary ultramafic rocks possess lower gold contents than mafic or felsic igneous rocks. Hence, there is no basis for proposed genetic links between various source rocks conjectured to have inherently elevated gold abundances and deposits. Gold deposits are spatially associated with a wide variety of igneous rock types, but the K, Rb, Ba interelement relationships are not consistent with the involvement of magmatic fluids in the gold forming system.

Archean greenstone-belt Au and Ag vein deposits appear to form during the discharge of low-Cl, CO_2-rich aqueous fluids likely of metamorphic origin, at depth in a compressive, crustal regime. This discharge represents the return flow of a cycle in which H_2O and CO_2 from the hydrosphere are initially transferred to rocks as hydrates, carbonates and hydrocarbons, during cooling of volcanic flows at the ocean floor. These components are subsequently returned to the hydrosphere via outgassing of the volatile-laden volcanic sequence under conditions of burial accompanied by crustal heating. Outgassing occurs during thrusting, and in the envelopes of rising batholiths. A wide array of major structures are present in greenstone belts, but the gold deposits are preferentially associated with those that have associated clastic and chemical sediments, and alkaline magmas. It is suggested that rift environments, with high heat fluxes, are appropriate for efficient gold concentration. Here, listric normal faults initially control extension along with ultramafic volcanism, provide pathways for mafic and felsic magmas, and are responsible for scarp-dominated sedimentary rocks. At later stages of greenstone-belt development, reverse motion on the faults accommodates crustal compression, and structures act to focus hydrothermal discharge generating the gold deposits, as well as conduits for trondhjemitic and alkalic magmas. The geometry of listric faults may be particularly efficient for tapping large volumes of crust.

[1]Department of Geological Sciences, University of Saskatchewan, Saskatoon, Saskatchewan, Canada S7N 0W0
[2]Department of Geology, University of Western Ontario, London, Ontario, Canada N6A 5B7

Introduction and Scope of Study

Archean greenstone belts of 2.7 Ga, exemplified by the Superior and Slave Provinces, host the richest and most numerous lode gold deposits. However, the source of gold and associted chemical components has remained one of the least tractable and resolved problems in ore deposits geology. In this companion paper to Part I (Kerrich and Fyfe, this vol.), we address questions of the source and properties of hydrothermal reservoirs involved in Archean lode gold deposits using various isotopic and geochemical tracers, and in addition consider the source of the hydrothermal solutes, such as K, CO_2, Si, Pb, Sr, and gold itself. The following sections describe the characteristic geochemical patterns of alteration which develop and the functional relationships between alteration and chemical mass transport. Specific questions that are considered in terms of the hydrothermal ore-forming systems are as follows:

1. Sources of volatile components such as H_2O, CO_2, and H_2S.
2. The nature of rock reservoirs donating lithophile and other elements that are locally enriched in the orebodies.
3. Ambient temperature-pressure and hydraulic conditions.
4. The history of incremental displacements along gold-bearing structures.
5. The presence of highly sodic and/or alkaline magmas along structures hosting the deposits.

Any viable genetic scheme for Archean lode deposits must satisfy the sum of geological and geochemical boundary conditions. Accordingly, in the final section we critically examine the various models that have been proposed for this deposit type, in the light of quantitative data reported in the preceding sections.

Source of Volatile Components

The source, temperature, and magnitude of aqueous fluid reservoirs participating in the lode gold deposits may be evaluated from oxygen and hydrogen isotope data. Five distinct terrestrial fluid reservoirs have been identified based on their oxygen and hydrogen isotope compositional ranges. These are marine, meteoric, magmatic and metamorphic fluids, together with formation brines that generally contain a large component of isotopically 'evolved' meteoric waters (Taylor, 1974, Fig. 1). Oxygen isotope data on mineral separates also permit estimates of ambient fluid temperatures during precipitation of hydrothermal minerals, given that the fractionation of oxygen isotopes between coexisting silicates or metal oxides is a function of temperature alone (Javoy, 1977; Friedman and O'Neil, 1977). Problems of identifying fluid flow through rocks are particularly amenable to evaluation by oxygen isotope analyses, since isotopic exchange between rocks and an aqueous reservoir is reflected in shifts

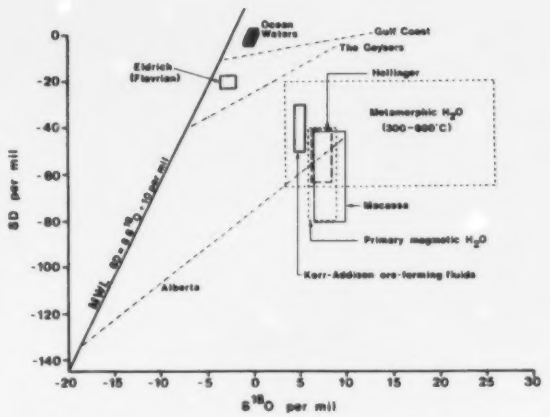

Figure 1: *Isotopic composition of natural terrestrial fluid reservoirs in δD, $\delta^{18}O$ coordinate space, modified after Taylor (1974). MWL = Meteoric Water Line. Also shown are trends for Alberta and Gulf Coast formation brines, and the Gysers hot springs. Calculated fields for Macassa, Kerr Addison and Hollinger ore forming fluids (after Kerrich, 1986a,b,c) and gold mineralization at the Eldrich mine in the Flavrian pluton, Noranda, after Kennedy and Kerrich (1982).*

of $\delta^{18}O$ rock or mineral from an initial value by a magnitude that depends on the $\delta^{18}O$ fluid, ambient temperature, and the fluid to rock ratio (Taylor, 1974, 1979). Similarly, carbon and sulphur isotope data may provide tracers of the reservoirs contributing C and S to the ore forming fluids, and place constraints on the redox state during Au precipitation.

Characteristics of the Hydrothermal Fluids

A compilation of oxygen isotope data for hydrothermal silicates from Au-Ag vein deposits in the Superior and Slave Provinces is given in Figures 2 and 3, and calculated fluid isotopic compositions and temperatures are summarized in Figure 4.

A prominent feature of Au-Ag vein deposits in the Abitibi subprovince is the uniformity in isotopic composition of quartz: the majority of measured ^{18}O values are in the restricted interval between 12.5 and 15.0 per mil. This uniform population of data embraces deposits distributed over 400 km, and variously hosted by ultramafic, mafic or felsic volcanic rocks, granitoids, and sedimentary rocks. In all of the examples studied, quartz in mineralized selvages of the bounding wall rock is isotopically similar to its vein counterpart, whereas quartz in contiguous rocks, external to the volume influenced by mineralization, constitutes distinct isotopic populations. These relationships imply a fluid dominated system along the hydrothermal conduit, a topic discussed further below.

Variations in the $\delta^{18}O$ values of hydrothermally precipitated quartz may occur in response to a number of independent parameters. Quantitatively the most important of these are the $\delta^{18}O$ value of the fluid and ambient

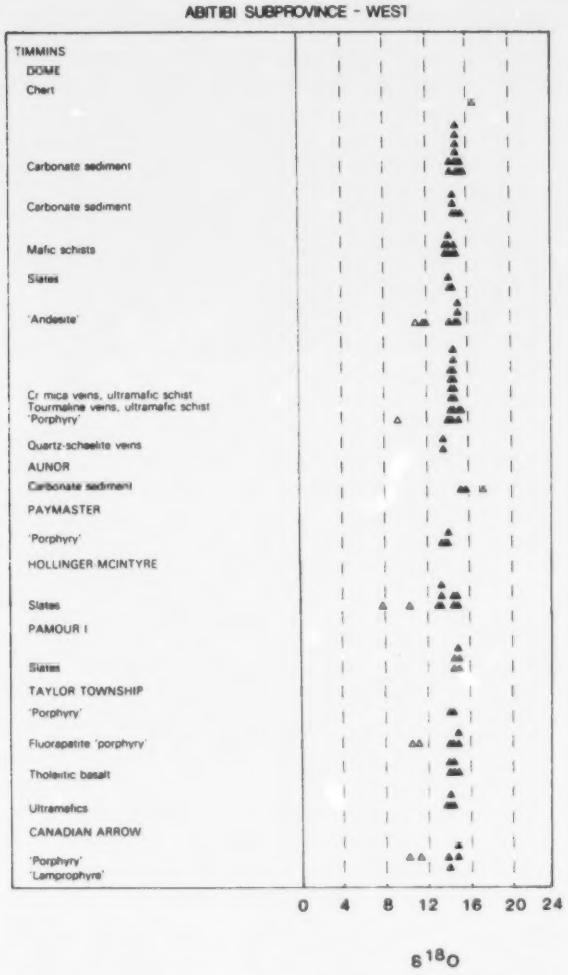

Figure 2: *Compilation of oxygen isotope data for hydrothermal quartz from Au-Ag vein deposits of the Timmins camp and neighbouring areas, western Abitibi subprovince (circa 2,680 Ma). Quartz $\delta^{18}O$ values in solid triangles. Also shown are data for quartz in cherts, and whole rock $\delta^{18}O$ values for various specified host lithologies (open triangles). Sources of data, Dome Mine, Kerrich and Fryer (1979); Taylor Township, King and Kerrich (1987); Canadian Arrow, McNeil and Kerrich (in press); Aquarius, Burlington (1984); data for remaining deposits from Kerrich (1983, 1986a,b).*

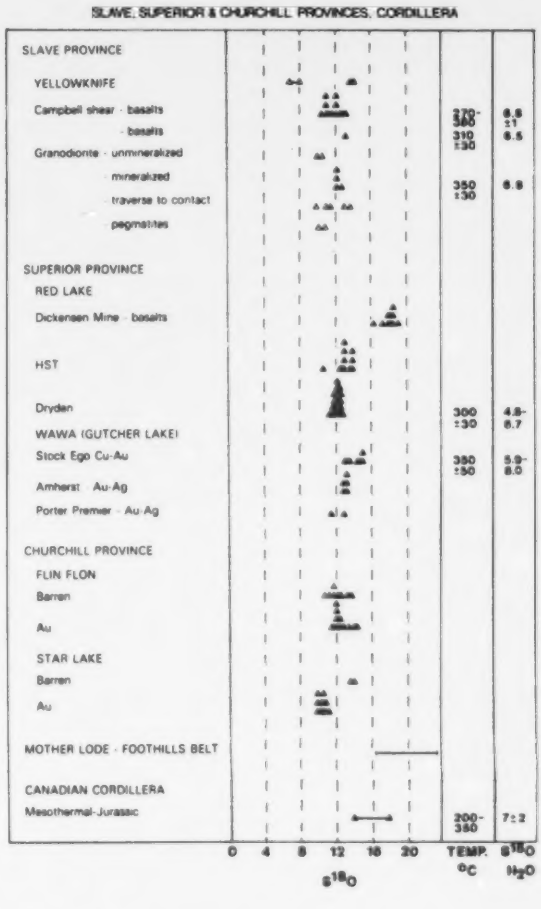

Figure 3: *Compilation of oxygen isotope data for hydrothermal quartz from specified Au-Ag vein deposits. Host lithologies in open triangles. Sources of data; Slave Province, Kerrich, 1980; 1981; Kerrich and Fyfe (1981), Kerrich et al. (1984); Red Lake, Kerrich et al. (1981); HST, Bradbrook (1982); Dryden, Kerrich (unpublished data); Wawa, Studemeister (1982); Churchill Province (Kyser et al. (1986); Canadian Cordillera mesothermal deposits, Nesbitt et al. (1986). The two right hand columns give estimates of temperature and ^{18}O fluid respectively.*

temperature of mineralization. In source regions, $\delta^{18}O_{H_2O}$ is govered by the original isotopic composition of the fluid reservoir, the $\delta^{18}O$ values of the rock reservoir at source, the water/rock ratio, and exchange temperature. At the site of mineralization the $\delta^{18}O$ of hydrothermal fluids may be modified by 1) exchange reactions with wall rocks, 2) precipitation or solution of an oxygen bearing phase either depleted or enriched in ^{18}O with respect to the fluid, and in a closed system, 3) immiscible separation of CO_2, or 4) mixing with an isotopically distinct fluid reservoir. In many examples variables 1) and 2) can be ruled out based on arguments presented above for high fluid/rock ratios in the hydrothermal conduits. Moreover, the solubility of most hydrothermal minerals in the deposits is sufficiently low that their precipitation is accompanied by negligible isotopic shifts in the fluid phase. Fluid mixing can probably be eliminated as a first order effect, from the observation that ore-forming solutions were at lithostatic or greater pressures during hydraulic fracture-vein events, and from the consistency of paragenetic assemblages in successive vein stages. However, some mixing of magmatic and metamorphic fluids is possible.

Taking these considerations into account, the uniformity in $\delta^{18}O$ values of quartz in the Au-Ag vein deposits, implies a corresponding homogeneity to both the $\delta^{18}O$ values of hydrothermal fluids, as well as the ambient temperature

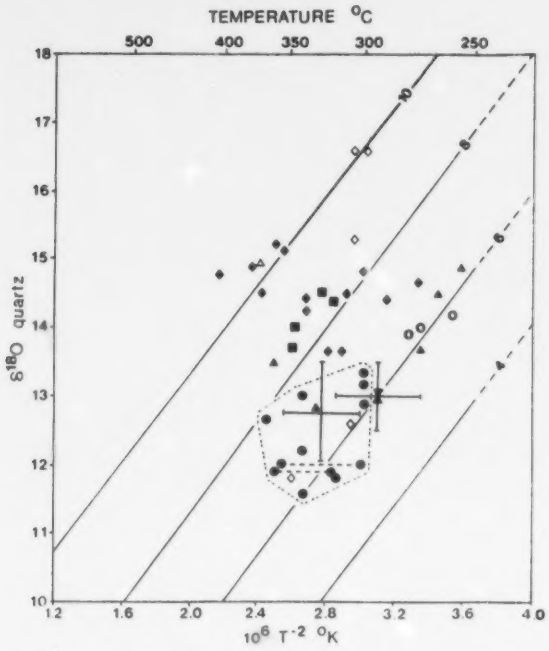

Figure 4: *The $\delta^{18}O$ of quartz from specified Archean Au-Ag vein deposits of Canada, together with ambient temperatures of mineralization calculated from mineral pair fractionations or estimated from fluid inclusion data. Solid circles, Yellowknife; open circles, unmineralized mafic schists. Diamonds, Dome mine; closed top, quartz-muscovite pairs; closed bottom, quartz-muscovite pairs in scheelite lode. Open triangle, Paymaster; closed triangle, McIntyre; semiclosed triangle, Hollinger; solid squares, Canadian Arrow; open diamond, Macassa. Cross with bowtie, Kerr Addison; cross, Chadbourne. Most temperatures calculated from quartz-chlorite fractionations.*

of mineralization. The only alternative is that some combination of variables covaried in a manner such as fortuitously to produce an isotopically uniform population.

Calculated isotopic temperatures for 16 deposits are plotted in Figure 3, which also depicts the $\delta^{18}O$ values of quartz and waters. The majority of results are in the range of 270 to 340°C, with only sporadic values as high as 400°C. Temperature estimates from coexisting quartz-muscovite-chlorite are generally in agreement to within 40°C, but there are few examples of triple isotopic concordance. Given textural evidence for their coprecipitation in each case, it is not clear as to whether this lack of equilibrium represents selective retrograde exchange of chlorite, or alternatively is due to errors inherent in the mineral-water calibrations. Fluid inclusion filling temperatures are in general consistent with isotopic temperatures, but the former are systematically low by 20 to 60°C, due to uncertainties in the appropriate pressure correction. The magnitude of fluid pressure during vein growth remains one of the most intractable problems in understanding the environment of formation of these deposits. Estimates vary from 2 to 3 kb corresponding to depths of 8 to 12 km (Kerrich, 1983) to as high as 7 kb; the ubiquitous presence of high density CO_2 eliminates shallow environments (Colvine *et al.*, 1984).

Calculated hydrogen and oxygen isotopic compositions of the hydrothermal fluids involved in four of the largest gold deposits of the Superior Province, namely the Hollinger, Dome, Macassa and Kerr Addison mines, are portrayed in Figure 1. These are based on analyses of actinolite, muscovite and chlorite. Results of δD measurements on fluid inclusions are also indicated.

Fluid compositions estimated from the mineral data are mutually consistent for all of the four deposits, collectively forming a data array which overlaps both the magmatic and metamorphic fields. Hydrogen isotopic compositions of water in fluid inclusions extend from −50 to +5 per mil. Fyon *et al.* (1983a) argue that the magnitude of dispersion in δD_{H_2O} values cannot be attributed to mixing of light ($\delta D \sim -50$) and heavier ($\delta D \sim 0$) fluid reservoirs. Any such mixing would be reflected in shifts of both δD and $\delta^{18}O$ fluid, but the uniformity of quartz $\delta^{18}O$ values eliminates this possibility. Rather, the observed range in δD_{H_2O} may be due to the presence of H_2 and/or CH_4 in the aqueous fluid, coupled with immiscibility of the reduced gas species (Fyon *et al.*, 1982a, b; see also Taylor, 1974; Ohmoto, 1986). Wood *et al.* (1986) have published data in compliance with the aforementioned work.

Based on hydrogen and oxygen data alone, it is not possible to discriminate between fluids of magmatic or metamorphic origin as the prime hydrothermal reservoir involved in the Au-Ag vein deposits, a point emphasized by Kerrich and Watson (1984). Some formation brines, and geothermal systems, with a significant component of meteoric water, may undergo extensive oxygen and limited hydrogen isotope exchange with sedimentary rocks, thereby evolving into the magmatic and metamorphic fields (Figure 4). For instance, Alberta basin formation brines extend from $\delta^{18}O = -15$, $\delta D = -130$ up to $\delta^{18}O = +9$, $\delta D = -50$. Further complexities may arise if such evolved formation brines become involved in a hydrothermal system where low water/rock ratios prevail. Field and Fifarek (1985) have shown that under these conditions fluids will evolve along j-shaped trajectories. However, such evolved waters are invariably hypersaline, whereas fluids involved in the Au-Ag veins are characteristically dilute solutions ($\leq$2 wt% NaCl equivalent, Kerrich 1983; Roedder 1984a,b). Accordingly evolved formation brines can be discounted as the predominant reservoir contributing to the hydrothermal ore-forming solutions, and new discriminants will be required to select between the magmatic versus metamorphic alternatives.

Implications of the Isotopic Data

Two important constraints on the nature of Archean gold-forming hydrothermal systems are provided by the isotopic data. First, the disparity in $\delta^{18}O$ between veins and unmineralized wall rock contraindicates suggestions that the isotopic data record an overprint of a late putative metamorphism, and for this reason yield a 'metamorphic' signature. Rather, field and petrographic relations demonstrate that most Archean gold deposits postdate any early marine water induced 'spilitic' alteration, or regional metamorphism of the volcanic sequences, and this observation has been known from the time of the classic work of Knopf (1929), Bain (1933) and Boyle (1961, 1979). In addition, the preservation of a distinct meteoric water isotopic signature, as well as that of marine water related alteration and the main gold-forming hydrothermal event (Fig. 1), rules out any pervasive isotopic overprinting.

Second, the restricted range of measured $\delta^{18}O$ quartz, and calculated temperature, $\delta^{18}O_{H_2O}$ and δD_{H_2O}, implies a uniform hydrothermal reservoir or reservoirs, isotopically buffered by a large source volume. This reservoir cannot have mixed with isotopically distinct fluid sources and at the same time maintained uniform $\delta^{18}O$ values, and was thus hydraulogically isolated from surface fluid reservoirs, as independently deduced from the high fluid pressures implied by hydrofracturing. Such relations are in contrast to the isotopic characteristics of base metal massive sulphide or copper porphyry deposits where the incursion of an external marine or meteoric water source to the main ore reservoir, induces large dispersions in the isotopic composition of minerals (cf. Taylor, 1974, 1979).

Isotope Systematics of Carbonates

The ubiquitous presence of hydrothermal carbonate minerals in Au-Ag vein deposits provides compelling evidence that the fluid reservoir contained oxidized carbon compounds. Liquid CO_2 has been reported in primary fluid inclusions from several deposits (Guha *et al.*, 1982; Kerrich, 1983; Colvine *et al.*, 1984; Smith and Kesler, 1985), and these observations collectively raise questions as to the source of the carbon. Ferroan dolomite is the predominant variety of carbonate mineral, but calcite, magnesite or siderite are sporadically abundant where Ca, Mg or Fe respectively constitutes the principal bivalent metal cation in the host rock.

Vesicle-filling calcites in spilitized volcanic rocks, from Timmins specifically, as well as the Slave and Superior Provinces in general, encompass significant intervals of both $\delta^{13}C$ (−4 to +1.5) and $\delta^{18}O$ (+10 to +21) values. In general, the range of $\delta^{13}C$ values is comparable to those determined for calcite in Phanerozoic ocean floor spilites. However, $\delta^{18}O$ values are systematically lower, consistent with the oxygen isotope relations in Archean marbles and cherts and with their inferred higher temperature of formation (Schidlowski *et al.*, 1975; Knauth and Lowe, 1978).

The total range of $\delta^{13}C$ values for Fe-dolomites in Au-Ag vein deposits of the Timmins camp is from −5.9 to +0.4 per mil, although individual deposits are typically characterized by a more restricted set of values. Fyon *et al.* (1983a, b; 1984a, b) have noted that within the population of data as a whole, dolomites from deposits proximal to graphitic sediments are 1 to 2 per mil enriched in ^{13}C relative to their distal counterparts.

Average values, with standard deviations, for populations of carbon and oxygen isotope data from a large array of Au-Ag vein deposits in the Abitibi subprovince are plotted in Figure 5. This represents a compilation of more than 1,600 analyses of ferroan dolomites and/or calcites from 20 Au-mines, and rocks in unmineralized structures, as reported by Kerrich *et al.* (1987), exclusive of data for the Timmins camp.

The total range of $\delta^{13}C$ values is −10.0 to +0.5 per mil, and $\delta^{18}O$ values span 6.9 to 17.8 per mil. The range of average values for ore deposits are −8.5 to −2.7, and 9.1 to 15.4 per mil respectively. Despite the large overall range, carbon isotope compositions are, on the whole tightly clustered within individual mining camps. For instance $\delta^{13}C$ values span −0.5 to −3.5 per mil in the Timmins area, −2.0 to −4.5 per mil at Kirkland Lake, −6.0 to −8.5 per mil at East Malartic, and −4.5 to −6.5 per mil at Lamaque; indicative of provinciality to the distribution of carbon isotope signatures.

$\delta^{13}C$ values of vein carbonates are dependent upon the temperature, Eh, and pH during precipitation, as well as the carbon isotopic composition of carbon-bearing species in solution (Ohmoto and Rye, 1979). Oxidized carbon species in hydrothermal fluids may originate from a magmatic source, from oxidation or hydrolysis of reduced carbon in sedimentary and metamorphic rocks, or from the decarbonation or leaching of carbonate minerals. Each of these sources may contribute carbon of differing isotopic composition to hydrothermal solutions (Ohmoto and Rye, 1979). According to Ohmoto and Rye (1979) the average $\delta^{13}C$ of igneous, sedimentary and metamorphic rocks is approximately −5.5 per mil, whereas Hoefs (1978) quotes a value of −7.0 per mil (Figure 5).

Given the redox dependence for $\delta^{13}C$ values of hydrothermal carbonates relative to the total carbon isotopic composition of the fluids it is important to constrain the ambient fluid oxidation potential. Based on diagnostic mineral assemblages most authors consider conditions of f_{O_2} to have been generally close to QFM, and above CO_2-CH_4, at the ambient conditions (Kerrich, 1983; Fyon *et al.*, 1983a, b; 1984; Kishida and Kerrich, 1987). Methane is only locally an important gas phase in fluid inclusions and it is generally confined to veins within carbonaceous rocks. If this is correct, and taking into account deposition temperatures of 270 to 350°C, then $\delta^{13}C_{Ca,Mg(CO_3)}$, $\delta^{13}C_{H_2CO_3}$ apparent $\delta^{13}C$ fluid.

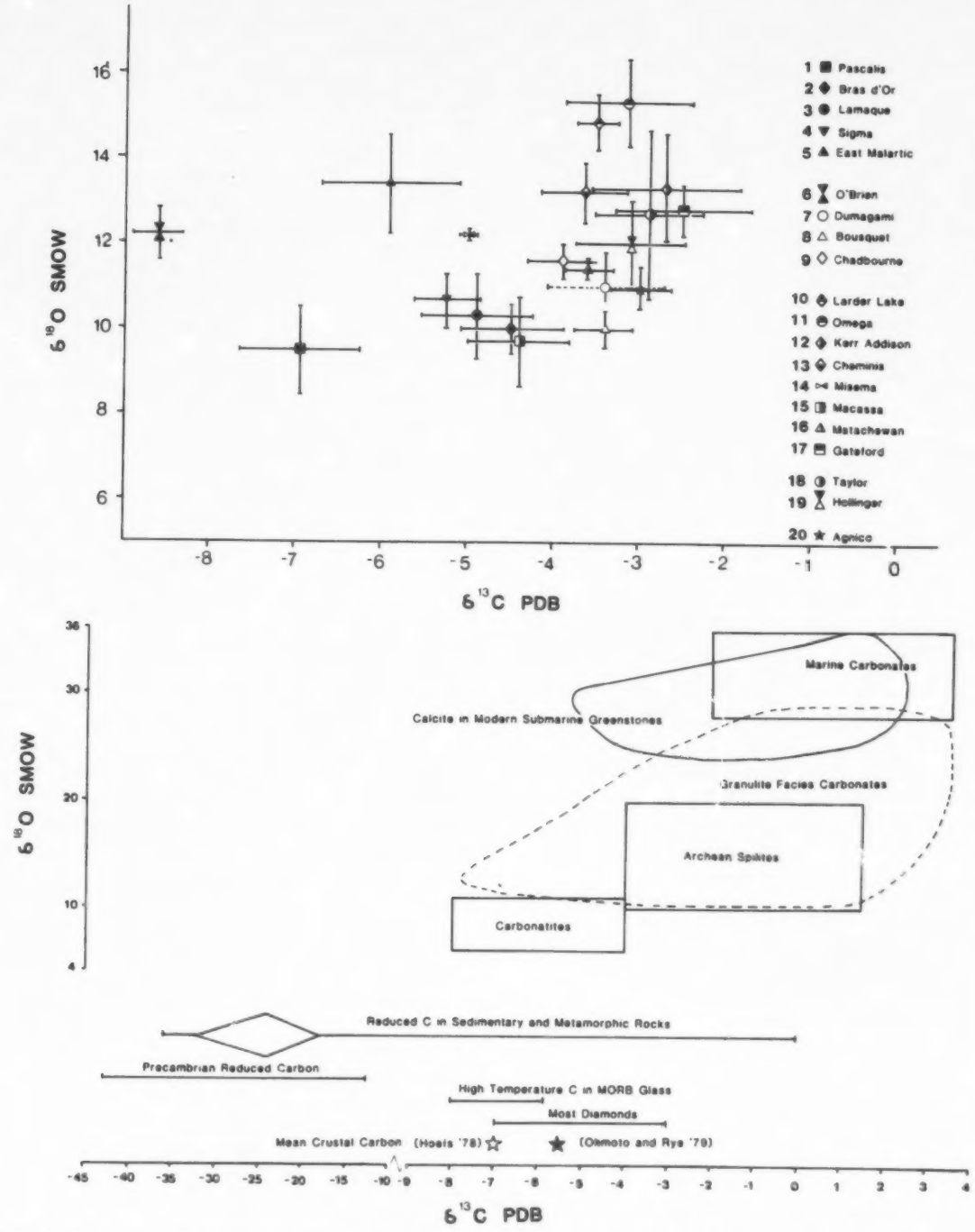

Figure 5: *(upper) Average carbon and oxygen isotopic compositions of hydrothermal Fe-dolomites or calcites from specified Au-Ag vein deposits of the Abitibi subprovince. Bars represent one standard deviation of the mean. Source of data, Kerrich (1986a,b,c), Kerrich et al. (1987). Results for Joutel from Wyman et al. (1986); Gateford and Omega, Foy (1985) and Kerrich (unpublished data); Taylor Township from King and Kerrich (1987).*

(lower) The oxygen and/or carbon isotopic composition of specified carbon reservoirs. Carbonatite field and granulite facies carbonates after Valley (1986); reduced carbon in Superior Province rocks from Schoell and Wellmer (1981); vesicle-filling calcite in Slave and Superior Provinces after Kerrich (1986c); high temperature C in MORB glass from Kyser (1986); and carbonate in modern submarine greenstones from Muehlenbachs and Clayton (1972a,b). Fields for marine carbonate, most diamonds, and reduced C in metamorphic and sedimentary rocks after Ohmoto and Rye (1979). Estimates of average crustal carbon from Hoefs (1978) and Ohmoto and Rye (1979).

The carbon isotope data for hydrothermal ferroan dolomites has been interpreted in a number of ways, both in terms of processes responsible for observed variability, as well as in the source of carbon itself. Based on the clustering of $\delta^{13}C$ values at -3.2 ± 0.7 in the Timmins area, Fyon *et al.* (1984a) and Colvine *et al.* (1984) concluded that one possible source of $\delta^{13}C$ was mantle degassing. It was argued that magmatic CO_2 of circa -5 per mil could be shifted to -3 per mil if small quantities of methane (δ 10 mol.%) were generated in the C-O-H fluid, by an excursion of the ambient thermal or Eh conditions. For example, the CO_2-CH_4 fractionation is ~25 per mil at 300°C. Such a shift could account for the bulk of measured $\delta^{13}C$ values of ~ -4 per mil to -2 per mil.

Following the model of Newton *et al.* (1980) these authors considered mantle CO_2-streaming processes as responsible for granulitization of the lower crust, with the attendent depletion of LIL-elements. However, Lambe and Valley (1984) have shown that the ambient conditions of Eh in most granulites is such that CO_2 introduced from the mantle would be reduced to graphite. Since most granulites do not contain extensive graphite, the mantle CO_2 mechanism cannot readily account for the formation of most granulites: accordingly, the proposed link between CO_2, granulitization and LILE depletion on the one hand, and Au-Ag deposits characterized by enrichments of LILE and carbonate, on the other hand, remains open to question. Moreover, Schoell and Wellmer (1981) have determined that the $\delta^{13}C$ of graphite in high grade metamorphic rocks in the Superior Province is -20 to -46 per mil, and that the carbon is biogenic in origin (Fig. 5). In contrast, graphite precipitated by the reduction of mantle CO_2 ($\delta^{13}C = 05$) at 600 to 800°C would have an isotopic composition of -10 to -12 per mil (cf. Bottinga 1969; see also Weiss *et al.*, 1981).

The distribution of $\delta^{13}C$ values in deposits of the Superior Province, and Golden Mile, Kalgoorlie, has also been accounted for in terms of a mixture of isotopically heavier crustal carbon with lighter carbon from a mantle or 'juvenile' reservoir (Kerrich, 1983; 1985, 1986a,b,c; Golding and Wilson, 1983). Specifically, data at the lower end of the distribution (-10 to -8 per mil) have been interpreted as reflecting a contribution of ^{13}C-depleted carbon of biogenic origin in source regions to these deposits (Kerrich, 1986b,c; Kerrich *et al.*, 1987).

Based on a comparison of the 'magmatic' Mink Lake Mo, showing with Au-Ag vein systems at Hollinger (average $\delta^{13}C$ carbonate -3.0 ± 1.5 (n = 14) and -3.3 ± 0.4 (n = 13) per mil respectively), Burrows *et al.*, (1986a,b) conjectured that the latter was also magmatic in origin. The speculation of Burrows *et al.* (1986a, b) that $\delta^{13}C$ values of about 3 per mil are uniquely diagnostic of a magmatic carbon reservoir, and at the same time rule out CO_2 derived from metamorphic or mantle-granulitization environments, can be dismissed. The tacit assumption that correspondence of carbonate $\delta^{13}C$ values to the magmatic range also implies a genetic equivalence is an unwarranted and hazardous generalization, especially when applied to hydrothermal environments. Ohmoto and Rye (1979) also caution that $\delta^{13}C$ values of -5 ± 2 per mil are difficult to interpret with regard to the carbon source, precisely because magmatic, sedimentary and metamorphic rocks are all characterized by average $\delta^{13}C$ values in this range. Moreover, there is no uniquely diagnostic $\delta^{13}C$ values of magmatic CO_2, because such values change during the degassing of magmas (Javoy *et al.*, 1986).

Carbon in greenstone belt supracrustal sequences is present as carbonate, chiefly filling vesicles and in chemical sediments; and as reduced carbon compounds in black shales and interflow units. Carbonate in modern submarine basalts encompasses a range of $\delta^{13}C$ values from -6 to -2 per mil, rather than being restricted to the uniform reservoir of marine bicarbonate. This is also the case for calcite in Archean spilites which brackets -4 to $+1$ per mil. Granulite facies carbonates extend to values as low as -8 per mil (Figure 5). There is little information on the carbon isotopic composition of reduced C-compounds in supracrustal lithologies; but Schoell and Wellmer (1981) have shown that graphite in high grade metamorphic rocks from the Superior Province spans -20 to -46 per mil.

The notion that $\delta^{13}C$ values of -3.0 ± 1.5 per mil at Hollinger rule out granulitization processes (Burrows *et al.*, 1986a,b) can similarly be discounted because it fails to take into account possible fractionations between fluid and carbonate arising from redox shifts at the site of deposition.

As discussed above, $\delta^{13}C$ values of hydrothermal Fe-dolomites may shift by ± 3 per mil where fluids encounter graphite-bearing rocks (Fyon *et al.*, 1983a, b; 1984a; Kerrich, 1986a,b,c). Consequently, fluids with total carbon isotopic compositions within the magmatic or 'mantle' range of -5 ± 2 per mil may precipitate carbonates with $\delta^{13}C$ values in the characteristic magmatic range may be derived from fluids where $\delta^{13}C_c$ is either greater or less than -5 ± 2 per mil.

In summary, the total spread of $\delta^{13}C$ values from -10 to $+0.5$ per mil can be resolved into variations at two scales. Within individual mining camps such as Timmins there is a relatively tight clustering of $\delta^{13}C$ values, implying a correspondingly uniform total carbon isotopic composition to the ore-forming fluids. Superimposed on this are small positive or negative shifts that are evident at a low scale. The former arise from excursions in the fluid redox state to low Eh, buffered by reaction with reduced carbon in wall rocks, whereas the latter are the product of oxidation of isotopically light C, and/or Rayleigh fractionation accompanying immiscible separation of CO_2. At the provincial scale, systematic differences in the average $\delta^{13}C$ values of hydrothermal carbonates between camps may reflect variations intrinsic to the carbon of the source rock. It is clear that the source or sources of carbon cannot as yet be

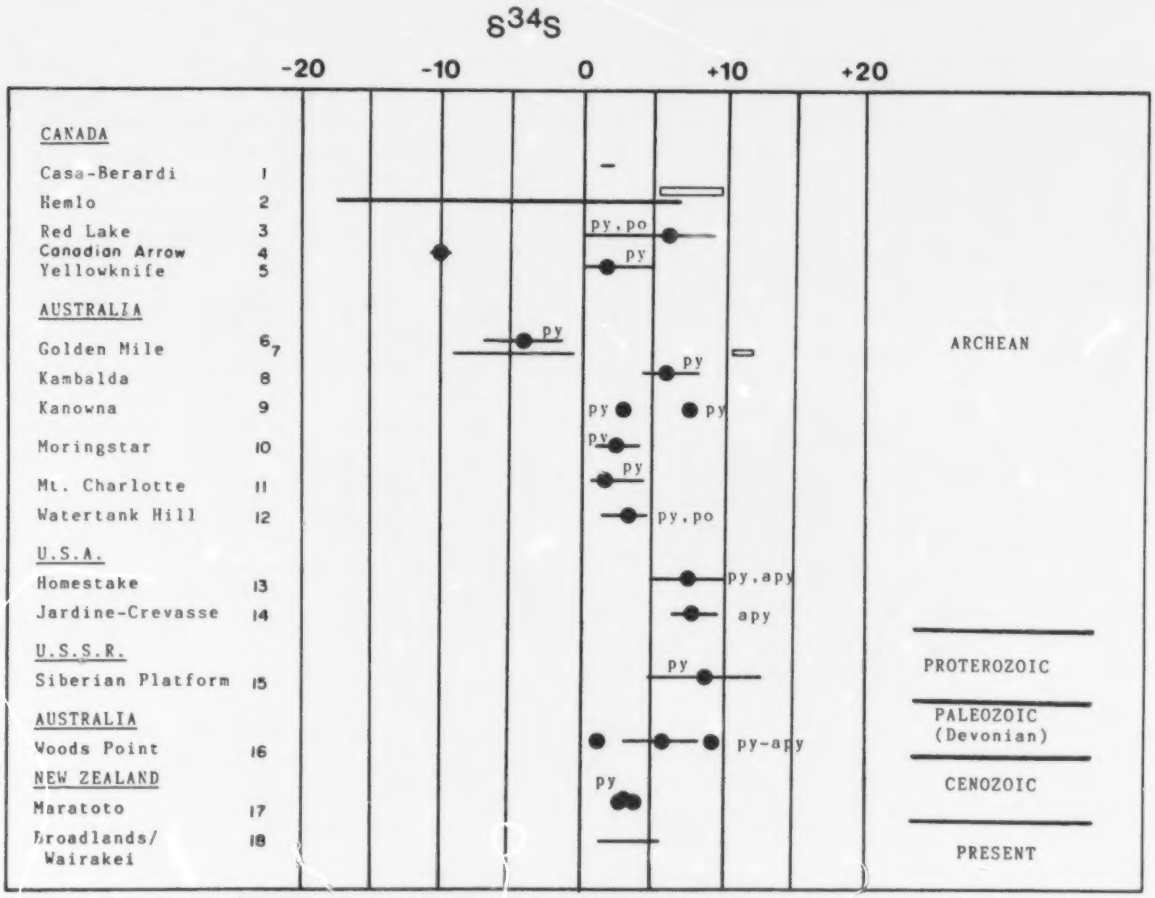

Figure 6: *Compilation of $\delta^{34}S$ analyses of sulphides minerals associated with gold mineralization from specified locations. Sources of data: 1, Pattison et al. (1986) reporting Cameron, GSC, personal communication, 1985; 2. Cameron and Hattori (1985); 3, Lavigne and Crocket (1982); 4, Schwarcz and Rees (1984); 5, Wanless et al. (1960); 6, 8-10 Lambert et al. (1984a,b); 7, Phillips et al. (1986); 11, Rye and Rye (1974); 12, Brookins and Brown (1966); 13, Zairi et al. (1978); 14, Green et al. (1982); 15, Robinson and Christie (1980); 16, Robinson and Christie (1980), Kusakabe (1974). Sulphate (barite) at Hemlo, open rectangle. Golden Mile anhydrite (open rectangle), from Hattori and Cameron (1986).*

resolved with certainty; even the most depleted values measured ($\delta^{13}C$ circa – 10 per mil) could arise either from oxidation of depleted carbon, or its assimilation into a magma.

A compilation of sulphur isotope measurements from Archean lode gold deposits is given in Figure 6. The data form a fairly consistent grouping, with the bulk of the $\delta^{34}S$ values concentrated in the interval +1 to +6 per mil. However the Hemlo and Canadian Arrow deposits in Canada, and the Golden Mile deposit, Kalgoorlie, are systematically depleted relative to the main population of data.

Sulphur isotopic compositions of hydrothermal S-bearing minerals are controlled by the total S isotopic composition of the fluids, and by the temperature, Eh, and pH at the site of mineralization (Rye and Ohmoto, 1974; Ohmoto and Rye, 1979; Ohmoto, 1986). The first parameter can be regarded as a source characteristic, whereas the latter three related to the environment of deposition. Accordingly, interpretation of the distribution of $\delta^{34}S$ values relies on a knowledge of the mineral parageneses that constrain the ambient temperature, Eh and pH. If the oxidation state of the fluid is below the SO_2/H_2S boundary, then the $\delta^{34}S$ of pyrite will be insensitive to redox shifts.

Given the geological setting of Archean Au-Ag vein systems, quantitively the most important reservoir that could contribute S to the deposits is igneous rocks. Sulphur may have been derived by 1) direct input from magmatic fluids, 2) leaching or desulphidation of primary or secondary minerals in igneous rocks and 3) leaching or desulphidation of sulphide minerals from hydrothermal sediments or clastic sedimentary rocks. Sedimentary sulphates are not abundant in Archean supracrustal sequences, but anhydrite is an underrated component of vesicle fillings; and in the Hemlo

area barite is present as vesicle fillings, and as a component of what are arguably primary sediments. The $\delta^{34}S$ values of sulphides in Archean igneous rocks is for the most part tightly grouped around 0 per mil (see Colvine *et al.*, 1984 and citations therein). There is little information on the isotopic composition of sulphide minerals from clastic sedimentary rocks: $\delta^{34}S$ values of hydrothermal sulphates cluster at 10 to 14 per mil (Kerrich and Fyfe, 1983).

In the light of these considerations, the relatively tight clustering of $\delta^{34}S$ values in the interval of 0 to +9 per mil can be interpreted to indicate that the fluid redox state was below the SO_2/H_2S boundary, and that the sulphur source was isotopically uniform, and bracketed by −1 to 8 per mil. Sulphur of this composition could be derived either directly from magmas, or indirectly by dissolution and/or desulphidation of primary magmatic sulphide minerals. A similar conclusion was arrived at by Lambert *et al.* (1983, 1984) for the Archean deposits of Australia.

Negative $\delta^{34}S$ values obtained for the Golden Mile deposits were attributed by Lambert *et al.* (1984) and Phillips *et al.* (1986) to significant oxidation of the fluids during extensive reaction with rocks at the site of deposition. Schwarcz and Rees (1984) have shown that pyrite from the Canadian Arrow deposit is depelted in ^{34}S ($\delta^{34}S = -11.2 \pm 1.0$ per mil, n = 18) relative to counterparts from gold deposits of the Timmins camp ($\delta^{34}S = 2.7 \pm 1.9$ per mil). They suggested a well mixed sulphur reservoir to account for the tight clustering of isotopic compositions, coupled with stable, relatively oxdizing conditions to yield $\delta^{34}S$ values depleted by a consistent magnitude. The presence of hematite in K-feldspar alteration selvages, corroborates the hydrothermal Eh as being oxidizing (McNeil and Kerrich, 1986). Similarly, Cameron and Hattori (1985) have argued that the trend of $\delta^{34}S$ depletion at Hemlo from +2 to −16 per mil reflects progressive oxidation of the hydrothermal fluids.

Data from Fluid Inclusions: CO_2/H_2O, Salinity, CH_4 and Na/K

The dissolved solid content of ore-forming fluids may be estimated by measuring the melting point of aqueous liquid inclusions that have been frozen, and such 'salinities' are generally expressed as weight per cent NaCl equivalent (Roedder, 1979). CO_2 also acts to depress the melting point of frozen aqueous inclusions, and hence the true fluid salinity will in general be less than the measured value for CO_2-bearing inclusions, which are ubiquitous in Archean vein gold deposits. In H_2O-CO_2 inclusions, a clathrate phase, $CO_2 \cdot 5.75H_2O$, forms during cooling, which, when pure, melts at about +10°C (Collins, 1979). Solutes present in hydrothermal fluids also act to depress the clathrate melting temperature, providing an independent means of determining hydrothermal fluid salinities for the case of CO_2-rich fluids. However, methane and solutes exert opposed effects on the clathrate melting behaviour: hence, melting-point data from liquid inclusions are not easy to interpret without knowledge of the gas species present.

In a review of fluid inclusion data on gold deposits, Roedder (1982, 1984a,b) concluded that the hydrothermal fluids are generally characterized by low salinities and high CO_2 contents. Inclusions in Archean lode gold deposits also indicate rather dilute solutions of 0.5 to 2.6 wt.% NaCl equivalent, well below the value of 3.6% for modern seawater (Guha *et al.*, 1982, Mine Doyon; Kerrich, 1983; see also Graves and Zentilli, 1982; and Roedder, 1972) for veins in metamorphic rocks.

In a detailed fluid inclusion study of the Hollinger Mine, Timmins, Smith and Kesler (1985) have shown that fluids associated with gold mineralization were CO_2-H_2 mixtures, where $CO_2 \simeq 12$ mole %. Zoning peripheral to the domains of economic mineralization is characterized by diminishing grades, in conjunction with lower proportions of CO_2 in the fluids (1−2 mole %) and ankerite in alteration envelopes.

It is important to note that when marine water is trapped in pore spaces during the accumulation of rock sequences, the pore fluids will initially have a salinity close to that of seawater (~3.5% salinity, 19,000 ppm Cl). Pore fluids will tend to increase in salinity during progressive burial at low temperatures, as some of the water is consumed by participating in hydration reactions of anhydrous minerals in the rock, leaving the remaining pore fluid as a relatively more concentrated salt solution. Once such saline fluids have been expelled during burial and compaction, any further evolution of fluids from the rocks will proceed by dehydration reactions at higher temperatures. Such metamorphic fluids, in contrast to seawater or expelled pore water, will tend to have a relatively low chlorine content, because of the low chlorine abundance of rocks at 60 ppm (Turekian and Wedepohl, 1961) coupled with the stability of chlorine in metamorphic amphibole and biotite. Evidence for some saline fluids is indicated by the presence of halite crystals in liquid inclusions from late-stage, post-Au quartz veins at the Con and O'Brien Mines (Boyle, 1961; Krupka *et al.*, 1977, respectively). These veins with saline fluid inclusions could arise from incursion of lower-pressure hypersaline formation brines into a fracture array induced by discharge of a high-pressure, low-salinity auriferous metamorphic fluid reservoir, after decay in the hydraulic pressure of the latter. Alternatively, such saline fluids could be generated during condensation of a supercritical fluid, where the solutes are preferentially partitioned into the liquid phase, leaving a CO_2-rich vapour phase possessing low solute concentrations.

In addition to ubiquitous CO_2, methane is a well-known product of fluid inclusion decrepitation in the Con Mine, Yellowknife, and several other major Archean deposits. Smith and Kesler (1985) have identified CH_4 in fluid inclusions in vein quartz at the Hollinger Mine where such veins intersect graphitic and/or carbonaceous units. Guha *et al.* (1982) have identified several generations of liquid inclusions

at Mine Doyon (formerly Silverstack), Quebec, of over-all low salinity, containing 16 to 95% CO_2 and methane. Immiscibility of CO_2, identified from highly variable CO_2/H_2O ratios, appears to have accompanied gold precipitation in some instances (Kerrich, 1983; Colvine *et al.*, 1984; see also Higgins and Kerrich, 1982).

Modern seawater has Na/K of about 28. Analysis of liquid inclusions from vein stockworks beneath base metal massive sulphide deposits, which are generally thought to have formed from modified seawater, reveals that Na K in accord with the proposed dominant seawater origin of mineralizing fluids (Franklin *et al.*, 1981). Data for Archean gold-bearing vein deposits are available only for the O'Brien Mine, Quebec, where Krupka *et al.* (1977) report Na/K 1 for liquid inclusions in quartz associated with the main stage of mineralization. A more plausible value is 10, based on independent considerations (see below). In general, data from liquid inclusions indicate that high-temperature fluids have much smaller Na/K than seawater (Roedder, 1972).

A summary fluid inclusion data for Archean lode gold deposits is given by Colvine *et al.* (1984, Table 6). In general, the fluids were characterized by high density CO_2 (0.8 g/cm³), filling temperatures of 200-400°C, and variable CO_2/H_2O mixtures. According to Colvine *et al.* (1984) the variable CO_2/H_2O ratios may be accounted for by several mechanisms including mixing of CO_2 and H_2O-rich fluids, or immiscible separation of CO_2 from an CO_2-H_2O mixture.

Mineralogical Constraints on Fluid Chemistry

Hydrothermal mineral assemblages in Au-Ag vein deposits vary considerably, but in general the characteristic species are quartz plus carbonate, along with subordinate muscovite, albite, chlorite, talc, tourmaline, scheelite, and various sulphides and/or arsenides. The relative proportions of minerals and their composition depend critically on the lithology that mineralized faults intersect. For instance, where structures traverse granitic rocks the dominant carbonate is generally calcite, whereas in tholeiitic basalts and ultramafic rocks ferroan dolomite and magnesite predominate respectively. A summary of diagnostic alteration mineral assemblages in lode gold deposits of Canada is reported by Colvine *et al.* (1984, Tables 1, 2, 4) and Kishida and Kerrich (1987), classified according to area, lithology, and hydrothermal-metamorphic grade.

Progressive mineralogical reactions of these types, involved in hydrothermal alteration of Fe-theoliites and ultramafic rocks along the Kirkland Lake fault zone, have been studied in detail by Kishida (1984). Such reactions can be evaluated in terms of T, X_{CO_2}, a_{K^+/H^+}, and a_{Na^+/H^+}, according to equilibria given by Montoya and Hemley (1975). Two reactions are illustrated here, namely chlorite + calcite + CO_2 ⇌ ankerite + muscovite and quartz; and chlorite

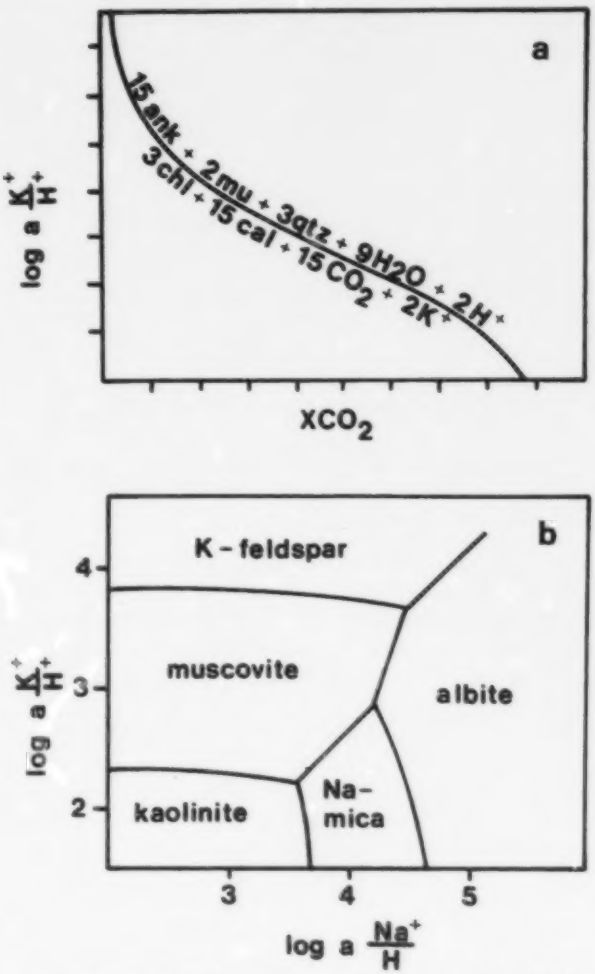

Figure 7: ***a, b*** *Equilibria relations for specified reactions applicable to hydrothermal alteration at the Kerr Addison mine (after Montoya and Hemley, 1975; Kishida and Kerrich, 1987).*

⇌muscovite + albite (Fig. 7A, B). Reaction 1 depends on small changes of X_{CO_2} and a_{K^+/H^+}, whereas reaction 2 is mediated by a_{K^+/H^+} but is independent of X_{CO_2}. Assuming a temperature of 300°C coupled with isothermal conditions an $a_{(Na^+/K^+)}$ of ≥ 10:1 can be deduced for carbonate + albite + muscovite alteration (cf. Montoya and Hemley, 1975). From the above considerations it can be deduced that fluids responsible for the specified hydrothermal mineral assemblages along the Kirkland Lake fault were characterized by $X_{CO_2} \simeq 0.1$, a neutral to slightly acidic pH, and aqueous Na^+/K^+ of 10:1.

Similar results for altered rocks associated with gold mineralization have been obtained for hydrothermal fluids involved in the 2.8 ± 0.1 Ga granitoid-greenstone terrains of Australia. Phillips and Groves (1983) have determined that the mineralizing solutions were H_2O + CO_2 mixtures, of slightly alkaline pH, low Eh and salinity, at temperatures of approximately 400°C.

In summary, fluids implicated in Archean lode gold deposits possess low salinity, high CO_2 contents, reduced gas species such as methane, variable contents of nitrogen gases (King *et al.*, 1987), relatively high $K/Na \simeq 0.1$, and in some instances exhibit evidence of transient CO_2 immiscibility accompanying precipitation of gold. The presence of nitrogen gases in the ore-forming fluids may result from the breakdown of NH_4-bearing biotite in the same region.

Patterns of Oxidation-Reduction Reactions

Reduction of iron in rocks adjacent to auriferous veins was noted by Bain (1933). Inasmuch as rocks are generally resistant to changes of oxidation state during metamorphism, the observed dominance of Fe^{2+} requires the introduction of large volumes of reductant in the auriferous hydrothermal solutions, implying high fluid fluxes through fracture conduits. It is probable that the reductant involved is H_2, which is a product of the dissociation of water in equilibrium with the QFM buffer system (cf. basalts) at elevated temperatures (Eugster, 1959; Eugster and Wones, 1962; Eugster and Skippen, 1967).

The extreme reduction observed in many wall rocks implies extensive interaction with fluids originating under high-temperature reducing conditions. Note that for aqueous fluids at high temperatures, the equilibrium $P_{H_2} \gg P_{O_2}$ on account of reactions of the type Fe^{2+}-silicate + $H_2O \rightarrow$ Fe_3O_4 + silicate + H_2. Hydrogen fixation in wall rocks takes place in response to the difference in equilibrium H_2 pressure at decreasing temperature-pressure states, as the mineralizing solutions ascend through the crust. Estimates of minimum fluid/rock ratios obtained from shifts in the oxidation state are >3:1 (see Kerrich *et al.*, 1977a). REE distributions in veins and wall rocks to veins sporadically exhibit marked positive Eu^{2+} anomalies, which, along with the presence of methane and hydrocarbons, provide independent evidence for chemical exchange with fluids of low redox potential (see Kerrich, 1983; Kerrich and Fryer, 1979).

Locally, where vein systems intersect carbonaceous sediments, such as in stope 15-26-16 of the Schumacher Mine at the Pearl Lake Porphyry, or in Carlin-type deposits (Radke and Scheiner, 1970), reduced carbon may act as an additional reductant or precipitant, as well as generating methane. In such environments, the $\delta^{13}C$ of hydrothermal carbonates shifts to more enriched values as discussed above.

Several important exceptions to the generally reduced character of Archean lode gold deposits are known. At the Macassa Mine - Kirkland Lake, and Canadian Arrow deposit - Matheson, trivalent iron is present in magnetite, and/or hematite signifying relatively more oxidizing conditions during precipitation (depending on the ratio of oxidized to reduced sulphur species in solution). Lambert *et al.* (1983) and Schwarz and Rees (1984) have noted that where more oxidizing conditions of mineralization occurred, the $\delta^{34}S$ of pyrite is depleted relative to pyrite in the majority of other deposits (see above).

According to Lambert *et al.* (1983) oxidation of fluids may be in response to reactions such as:

$$Fe_3O_4 + 3CO_2 \rightarrow 3FeCO_3 + \tfrac{1}{2}O_2$$

and

$$2O_2 + H_2S \rightarrow SO_4^{2-} + 2H^+$$

The $\delta^{18}O$ of vein quartz at Macassa and Canadian Arrow is within the range of the Abitibi lode gold deposits collectively, implying that in terms of oxygen isotopic composition and temperature, hydrothermal fluids at these two deposits did not differ significantly from gold deposits in general, although the inferred redox state was higher.

Fluid Volumes — Solute Concentrations

Total production of gold from the Porcupine District up to 1976 was 1.7×10^9 g (Pyke, 1976). If it is assumed that this mass of gold was derived by 25% efficient leaching of metabasalts with an average Au abundance of 2 ppb (Tilling *et al.*, 1973; Kwong and Crocket, 1978), then the source volume would be of the order of 1,200 km^3 (1 km^3 of rock contains 5.6×10^6 g Au at 2 ppb). If hydrothermal fluids are derived from the freezing of magmas, then similar volumes of magmatic rock would be required. Based on the premise that Si, Au, Ag, Pd, W, Ni and Cr together with other elements present in veins, were leached and transported during metamorphic outgassing at the greenschist-amphibolite , or high grade metamorphic transitions, when approximately 5 wt.% structural water is released from a hydrated rock of basaltic composition, then the hydrothermal solvent volume would be of the order of 180 km^3.

An independent estimate of the hydrothermal fluid volume may be derived as follows, using gold-bearing quartz veins, which are essentially pure quartz, as examples. In cooling from 550°C to 300°C, 1 kg of quartz-saturated water will precipitate 2.6 g of quartz, assuming a thermal gradient of 100°C/km, and an hydraulic gradient equal to the lithostatic gradient (Holland, 1967). Gold is present in the veins at an average level of 5 ppm, and therefore if Au and quartz were coprecipitated from a solution cooling along a geothermobar then 1 kg of solvent would precipitate 2.6×10^{-5}g Au, and the average decrease in concentration of gold in the hydrothermal solution would be 12 mg/ml. The total carrier fluid volume for 1.7×10^9 g Au is then 130×10^{12} kg, or 65 km^3, based on the generalized assumption that gold is dominantly precipitated over the stated temperature interval, a figure in accord with the independently derived

estimate, as above. Estimates of fluid volume are slightly increased if a lower thermal gradient is assumed or if CO_2 consumption from the hydrothermal fluid acts to decrease the rate of change of silica solubility during cooling.

Further, consider 100 g of metabasalt containing Au at 2 ppb. If 25% of the gold is taken into solution as the metabasalt evolves 5 wt.% water at the greenschist-amphibolite transition, then the solute concentration will be 10 ng/ml Au (10 ppb), which is comparable to the figure estimated above and the value of 50 ng/ml reported by Tilling *et al.* (1973) for gold in natural thermal waters. These calculations are intended to demonstrate the magnitude of source and fluid volumes, and provide estimates of Au solute concentrations. Independent estimates for gold transport in solution are given by Helgeson and Garrels (1968) and Fyfe and Henley (1973).

Seward (1979) reports deposition of ore-grade gold material, along with Ag, Sb, Hg and Tl, from dilute fluids with 1000 ppm chloride, 0.04 ppb Au and 0.7 ppb Ag, in the Wairiki geothermal system, New Zealand. For fluids carrying 0.04 ppb Au, 800 km^3 of hydrothermal solution would contain a million ounces of gold. Although these solute concentrations for gold in a modern system are about one hundred times lower than the maximum values calculated above for the higher temperature Archean vein deposits, and the values determined by Tilling *et al.* (1973), they serve to illustrate that high metal concentrations in hydrothermal fluids are not necessary to form ore-grade deposits, but rather that large fluid volumes are required.

Gold Carbonate-Potassium Association

A ubiquitous feature of gold-bearing vein deposits in Archean greenstone belts is the present of abundant carbonate minerals co-existing with K-aluminosilicate phase. The latter is typically muscovite, but K-feldspar or biotite are sporadically predominant. Quartz and carbonates are the dominant gangue in hydrothermal veins, and are typically present in the extensive domains of alteration which envelop veins. This gold-carbonate-potassium association has attracted intense interest from the standpoint of timing in the volcanic-sedimentary sequences, implications for gold precipitation, potential as an exploration criterion, and significance in terms of the nature of the ore-forming system and source of the CO_2 and K.

The nature of wall-rock alteration in proximity to Au-bearing veins has been comprehensively documented by Bain (1933) from studies of lode deposits in Ontario. Bain identified carbonate, chlorite and sericite as the dominant alteration minerals. Extensive development of carbonate minerals in the Bendigo and Mother Lode systems was reported by Lindgren (1905) and Knopf (1929) respectively. The subject of carbonate alteration occurring in conjunction with gold vein deposits has been discussed by several workers, including Boyle (1961, 1976, 1979), Meyer and Hemley (1967), Rose and Burt (1979), Kerrich and Fyfe (1981), Kerrich (1983) and Colvine *et al.* (1984). In general, there is a consensus that reactions between CO_2 and K-bearing hydrothermal fluids and Ca–, Fe–, Mg–, Mn-bearing silicates in the wall rocks are implicated in the formation of the carbonate and K-aluminosilicate minerals.

The solubility relations of carbonate minerals are more complex than for quartz (Holland and Malinin, 1979). In general, calcite solubility decreases as function of increasing temperature (T) at constant P_{CO_2}, or diminishes with decreasing P_{CO_2}, at constant T. The negative temperature coefficient of solubility dominates the positive effect of pressure, such that carbonates become less soluble with respect to increasing temperature, and carbonate precipitation is not anticipated from cooling fluids under typical crustal P-T cooling paths. Specialized conditions such as immiscible separation of CO_2 from an aqueous fluid are required for carbonate disposition from cooling solutions. Thus, the abundance of carbonate and its coprecipitation with quartz in Au-bearing vein deposits requires explanation.

In contrast, the distribution of quartz and carbonate minerals in convective hydrothermal systems is as predicted for simple temperature-solubility relations. Carbonate veins are present in the peripheral recharge areas where surface fluids heat during penetration into the crust, whereas quartz is the dominant gangue mineral in vein stockworks which represent the loci of hydrothermal discharge of fluids cooling during return flow to the surface (Andrews and Fyfe, 1976; Spooner *et al.*, 1977; Fyfe and Lonsdale, 1981; Meyer and Hemley, 1967). Examples of such hydrothermal systems include seawater circulation through hot basalts at mid-ocean ridges and convection of meteoric fluids in proximity to Cu-porphyry deposits (Lowell and Guilbert, 1970; Sheppard *et al.*, 1971; Wolery and Sleep, 1976; Fyfe and Lonsdale, 1981).

Several explanations have been advanced to account for the precipitation of carbonate minerals from cooling fluids, as discussed by Holland (1967): additional processes are discussed in the section on the source of CO_2. An important factor is believed to be boiling of solutions, which will take place during fluid ascent at the point when the confining pressure becomes less than the vapour pressure of the solution. This condition will be met in proximity to the terrestrial surface (<2 km), and boiling of hydrothermal solutions has been identified during stages of calcite deposition at the shallow-level Providencia Mine, Mexico (Sawkins, 1964).

The ambient hydraulic pressure or crustal depth at which gold-bearing veins formed are poorly constrained. However, based on the premise that fluids were derived by outgassing reactions under conditions at the greenschist-amphibolite transition, and assuming a geothermal gradient

of 50°C/km with $P_{fluid} > P_{lithostatic}$, fluid pressures and depths of 8 km, 2 kbar (200 MPa) to 10 km, 2.5 kbar (250 MPa) are indicated. These conditions are well above the vapour curve for H_2O-CO_2 solutions of 6 wt.% equivalent NaCl (Takenouchi and Kennedy, 1965). Furthermore, inspection of primary fluid inclusions in vein quartz from the Con Mine, Yellowknife, has not revealed evidence for boiling of the hydrothermal fluids (Kerrich and Fyfe, 1981).

Observations of Au-bearing vein deposits in Archean greenstone belts, together with examination of the literature on this subject, reveal a broad empirical relationship between carbonate composition and the nature of the wall rock which the vein transects. In general, the predominant carbonate minerals are ankerite and ferroan dolomite in mafic rocks, magnesite and Fe-dolomite in ultramafic rocks, calcite in felsic rocks, and siderite and rhodochrosite in iron formation. Transitions in wall rock over the length of individual veins are reflected by corresponding changes in carbonate gangue composition (Bain, 1933). These observations support the deductions from chemical mass balance (see above) that the wall rock dominates the supply of the bivalent metal cations, and CO_2 is introduced by the hydrothermal fluids.

Significantly, carbonates in gold-bearing veins are distinct in texture, chemistry and carbon isotopic composition (see above) from pre-existing carbonates associated with early spilitization. Pearton (1982) has emphasized the fact that hydrothermal carbonates from the Sb-Au ores of Muchison possess different compositions from marine carbonates.

Source of CO_2

During normal prograde regional or burial metamorphism, fluid pressures are in the same order of magnitude as lithostatic pressures (Fyfe *et al.*, 1978). Except in environments where partial melting occurs, total fluid pressure is close to the sum of partial pressures of H_2O and CO_2, the dominant volatiles. If the mixtures are considered ideal, the partial pressures are directly related to the mole fractions. As the average crustal content of carbon is around 200 ppm and the water content is close to 20,000 ppm, it is clear that water is the dominant volatile species in metamorphism (Fyfe *et al.*, 1978).

For given lithostatic pressures and temperatures, studies of the chemistry of fluids (Ellis and Mahon, 1977) and experimental studies of carbonate and hydrate equilibria (Winkler, 1976; Fyfe *et al.*, 1978) clearly show that for most temperatures up to the amphibolite facies P_{H_2O} is much greater than P_{CO_2}. Only under extreme conditions, as for the granulite facies (Janardhan *et al.*, 1979), does CO_2 become a major or even dominant volatile species. This observation is in accord with the great thermal stability of relatively pure carbonate rocks. Most work on metamorphic rocks shows that given the very low porosity and permeability of rocks at depth, massive degassing proceeds only where the geothermal gradient intersects the equilibrium vapour pressure curves when the later approach the lithostatic pressure. Thus, for pure dolomite or siliceous marbles temperatures in excess of 800°C (migmatite temperatures) are required to achieve conditions of $P_{CO_2} \simeq P_{lithostatic}$.

In the general case of regional metamorphism and dewatering of a pile of complex lithology including marine sediments and spilitic rocks, the primary carbonate content is likely to be significantly greater than 200 ppm. In Archean sections where altered submarine volcanic rocks are dominant, again the CO_2 content is likely to be large via fixation of marine carbonate into cooling basalts. Jolly (1974) indicates that calcite is ubiquitous in the low-grade metavolcanics of the Archean Abitibi belt in Ontario. Aumento *et al.* (1976) indicate that CO_2 may reach 3% in heavily altered sea-floor basalts, and Hallberg *et al.* (1976) report CO_2 contents of 0.1-0.3 wt.% even for relatively unaltered Archean basalts.

In such environments, given thermal gradients in the order of 30°C/km, P_{H_2O} will rise 280 bar/km. At 300°C (10 km), P_{fluid} will be in the order of 2800 bar and P_{CO_2} will be no more than 100 bar. At 500°C (17 km), P_{fluid} will approach 5000 bar with P_{CO_2} in the 1000-bar range. At Yellowknife, the presence of sphene in epidote-amphibolite-facies metabasalts, formed via the reaction:

$$CaTiSiO_5 + CO_2 \longrightarrow CaCO_2 + TiO_2 + SiO_2$$

sets the CO_2 of metamorphic fluids to < 0.5 at 500°C and 2 kbar (Hunt and Kerrick, 1977).

It is clear that if this metamorphic fluid moves upward and remains in equilibrium with Ca-Fe-Mg-silicates, it will precipitate carbonates by wall-rock alteration until virtually all CO_2 is removed. Inspection of carbonate equilibria (Winkler, 1976; Fyfe *et al.*, 1978; Turner, 1981) indicates that maximum, carbonate formation will occur in the greenschist-facies region if the source-rocks have moderate CO_2 contents. In summary, Au and quartz precipitation is related to the above-equilibrium CO_2 pressures relative to wall-rock alteration equilibria (a similar situation to reduction reactions related to excess H_2 pressures discussed above under redox reactions). Additional reactions producing CO_2, together with reduced gas species such as CO and CH_4, in metamorphic fluids may include the oxidation and hydrolysis of reduced carbon or hydrocarbon compounds present in many interflow sediments. For instance, the reduction of hematite or magnetite linked to the oxidation of carbon yields CO_2; and the hydrolysis of carbon may produce $CO_2 + CH_4$.

Potassium Metasomatism

Potassium metasomatism is a characteristic feature of many magmatic- related ore deposits, and of the alteration domains in Archean Au, Ag-vein deposits. During the evolution of magmas by crystal fractionation, K, Rb and Ba follow

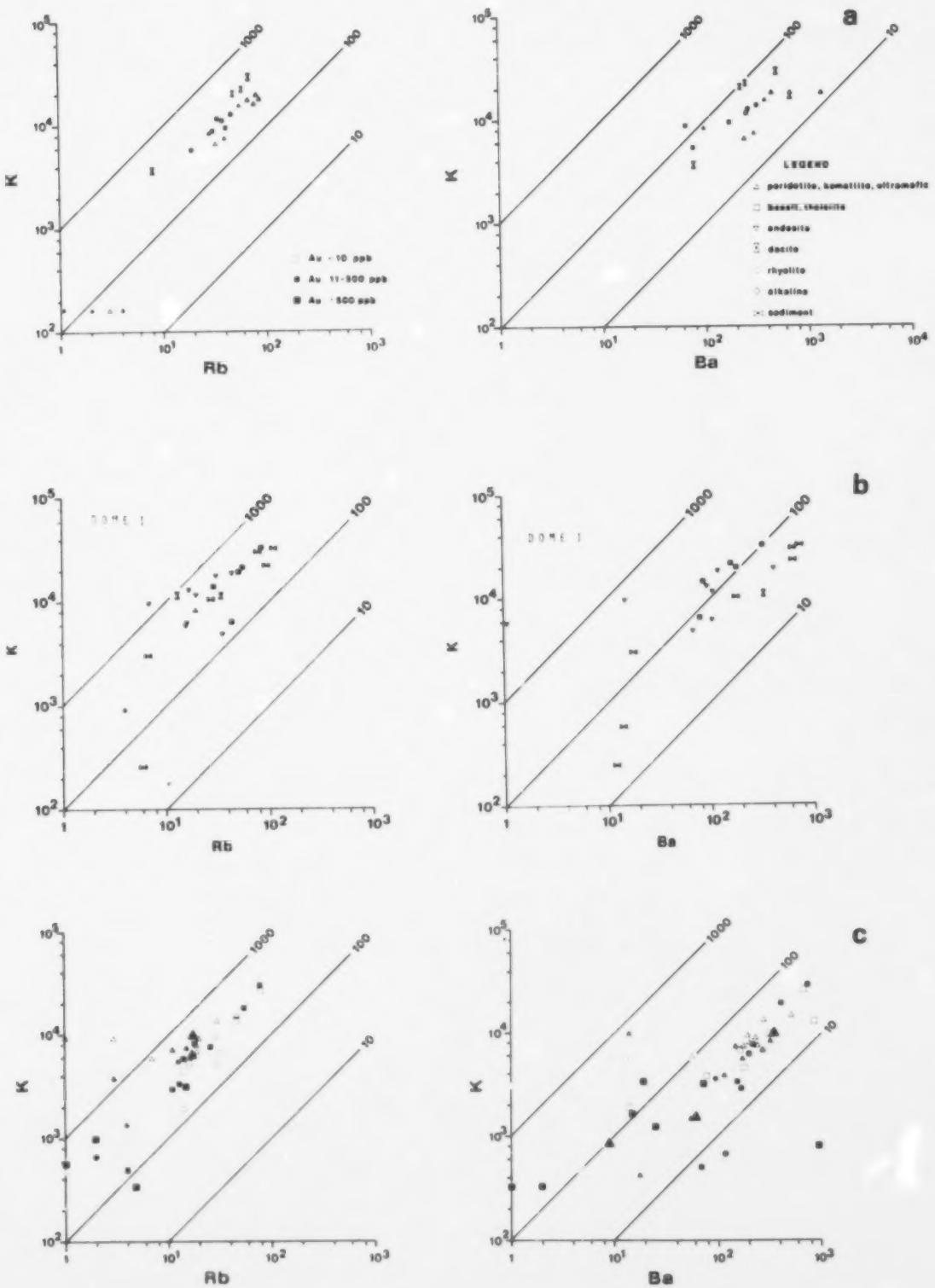

Figure 6: *K-Rb and K-Ba relationships in the alteration domains and contiguous rocks of specified lode gold deposits of the Abitibi greenstone belt.* **a** *- Hollinger Mine, Timmins;* **b** *- Dome Mine, Timmins;* **c** *- Kerr Addison mine, Virginiatown.*

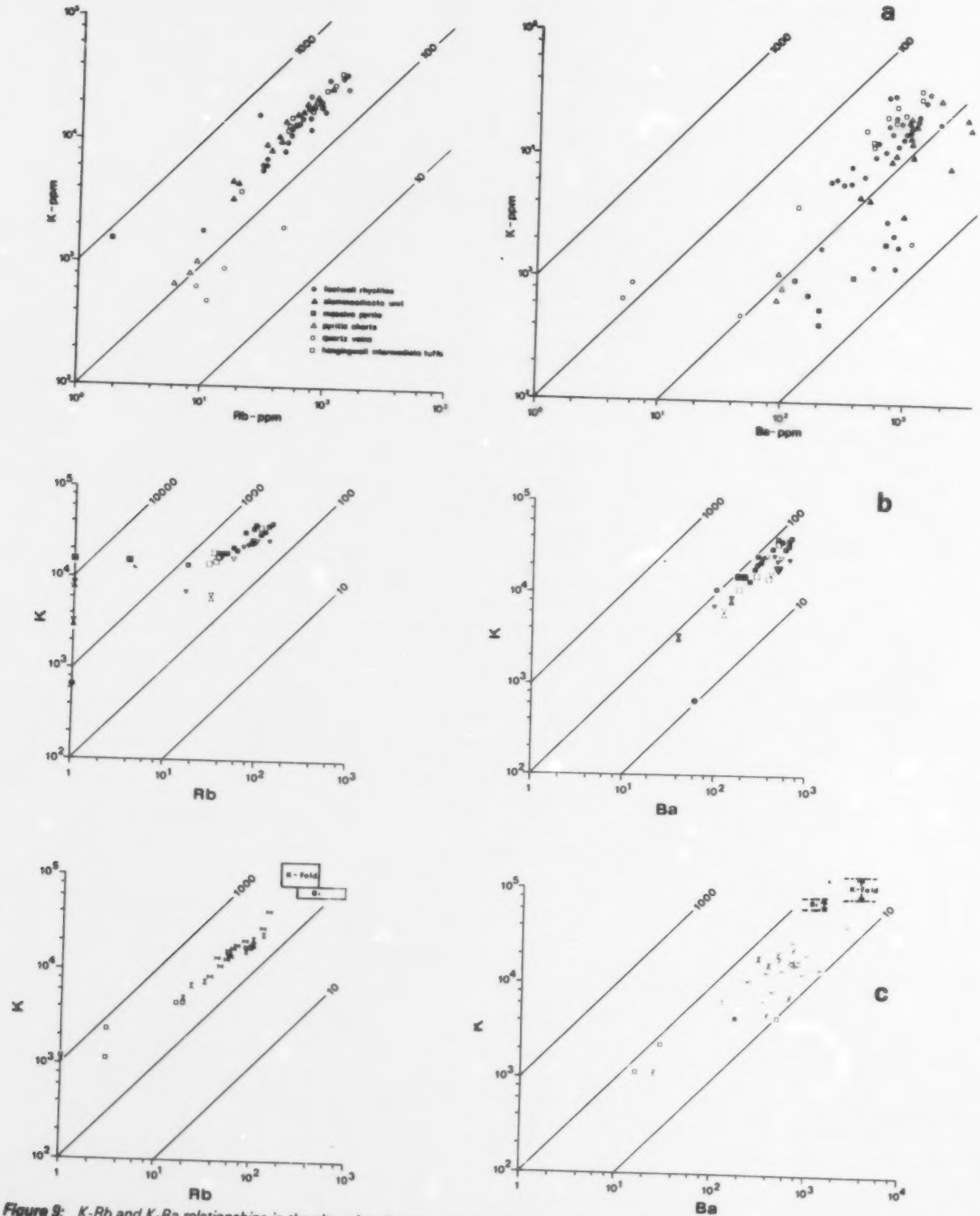

Figure 9: *K-Rb and K-Ba relationships in the alteration domains and contiguous rocks of specified lode gold deposits.* **a** *- Dumagami, and* **b** *- Thompson Bousquet mines, Bousquet township, Quebec.* **c** *- Cadillac, Kewagama and Blake River Groups, unmineralized, Bousquet township.*

systematic interelement trends that are governed by their respective partition coefficients between crystals, silicate melt, and aqueous phases (Shaw, 1968, and references therein; Fairbridge, 1972). Such trends are distinct from K, Rb, Ba interelement relationships in non-magmatic hydrothermal systems (Armbrust and Gannicott, 1980; Munha *et al.*, 1980; Kerrich and Fryer, 1987).

Data for K, Rb and Ba concentrations in the potassic alteration domains of the four Au, Ag-vein deposits are plotted in Figures 8 and 9. K and Rb are highly correlated in mineralized and altered rocks from each of the deposits: the correlation coefficient, r, ranges from 0.74 to 0.89. The covariant relationship holds where mineralization is developed variously in rocks of ultramafic, mafic or felsic composition, and accordingly is independent of the host rock lithology. Coherent behaviour of K and Rb is also present over almost three orders of magnitude in K content, from 100 ppm to in excess of 80,000 ppm K. This relationship is particularly clear where gold mineralization has overprinted rocks of primary ultramafic composition, such as in the Hollinger and Kerr Addison Mines (Fig. 8). Ultramafic rocks possess intrinsically low primary abundances of the lithophile elements (Nesbitt and Sun, 1976), and consequently the enhanced measured levels of K, Rb and Ba must result exclusively from their co-enrichment by the hydrothermal ore-forming system.

Average K/Rb ratios of the four deposits cluster tightly, with a total range of 220 to 280: there is no statistical difference between the population of K/Rb ratios of the individual deposits at a 95% confidence level (Fig. 8). The data tend to scatter at low abundances, which is interpreted to result from diminished analytical precision where levels of Rb are 5 ppm, and K 600 ppm.

Potassium and Ba in the same rocks are also generally well correlated, though to a lesser degree than is observed for K and Rb. The K-Ba correlation holds over about 2½ orders of magnitude in absolute abundance (Figs. 8 & 9). The correlation coefficient, r, varies from 0.61 at Dome to 0.90 at Thompson Bousquet. As is the case for K-Rb plots, a greater degree of scatter is evident at low concentrations of K and Ba as a result of diminished analytical precision at low absolute abundances. Average K/Ba ratios of the deposits are relatively uniform, with a total range of 40 (Hollinger) to 60 (Kerr Addison). K-Ba covariation, and the magnitude of the K/Ba ratio, do not appear to be influenced by lithological type. An exception to the generally coherent behaviour of K and Ba is evident in one mineralized zone at the Dumagami Mine, which possesses enhanced Ba abundances and correspondingly diminished K/Ba ratios. This trend is reflected in Ba-rich muscovite, where the oelacherite component may attain 20% (R.L. Barnett, personal communication, 1984).

For the population of mineralized rocks under consideration, K, Rb and Ba reside predominantly in the K-silicate phase of the hydrothermal paragenetic assemblage, rather than being partitioned between K-silicate, and co-existing phases such as chlorite, ferroan dolomite, and tourmaline. This inference has been confirmed by determinations of K, Rb and Ba concentrations in a limited number of mineral separates of K-feldspar, muscovite, and biotite from mineralized rocks. Further indirect corroboration of the siting of K, Rb and Ba in K-silicates comes from analyses of coexisting gangue minerals such as chlorite, ferroan dolomite, and tourmaline which contain negligibly low contents of K, Rb, Ba, Li or Cs (King and Kerrich, 1986). Neither barite nor witherite have been identified to date in those deposits.

In a landmark paper, Shaw (1968) identified three populations of rocks characterized by distinct K/Rb ratios, from a review of K-Rb covariation in suites of igneous rocks. These were: (1) a main trend (MT), where K/Rb averages 230, (2) oceanic tholeiites (OT) for which K contents are 0.1 wt.%, and K/Rb ratios may approach 3,000, and (3) the pegmatite hydrothermal (PH) trend where K abundances are greater than about 4 wt.%, and K/Rb ratios may approach values of 50.

Many classes of ore deposits that are widely regarded as having a key magmatic contribution to the ore-forming system display interelement trends between K, Rb, Ba and Sr that are in keeping with the characteristic partitioning trends of late-stage magmatic systems as discussed above. Examples include Cu-, and Mo-porphyry deposits, Sn-W greisens, and certain pegmatites.

Studies of the distribution of K and Rb in several of the porphyry copper deposits in Chile have shown positive Rb anomalies, in conjunction with low K/Rb ratios, relative to all background rocks (Armbrust *et al.* 1971, 1977; Oyarzun, 1974). These anomalies are present irrespective of mineral paragenesis and have been interpreted to result from hydrothermal alteration by a Rb enriched aqueous phase that separated from a magma.

The distribution of K, Rb, Ba and Sr in altered rocks associated with porphyry copper deposits of the Highland Valley, British Columbia is more complex. Olade and Fletcher (1975, 1976) documented increases of K/Ba, Rb/Sr and Ba/Sr ratios, but also local departures from those 'late-stage' trends. In porphyry systems, the high temperature magmatic stage alteration, was overprinted during a subsequent stage of low temperature meteoric water infiltration, such that complexities to the distribution patterns of K, Rb, Ba and Sr are anticipated.

From a compilation of geochemical data for 'magmatic' Sn-W deposits and greisens Govett (1985) has shown that decreased K/Rb and K/Li ratios, in conjunction with elevated Rb/Sr and K/Ba ratios, are pronounced in mineralized rocks relative to the host granitoids. These trends are particularly clear for those units of the Ackley granite, Newfoundland,

which contain Mo, and Sn-W, mineralization (Tuach *et al.* 1986).

Volcanic hosted base metal sulphide deposits formed in the submarine environment are characterized by quite distinct K-Rb-Ba interelement systematics compared to the magmatic-related counterparts. Marine water has much larger K/Rb (~3,300) and K/Ba (~19,900) ratios than average continental crust, where K/Rb 286 and K/Ba 37 (Holland, 1978; Taylor and McLennan, 1985, p. 67). This is due to the selective absorption of Rb and Ba onto marine clays, relative to K. As a consequence, the alteration of volcanic rocks by seawater at low temperature acts to shift K/Rb and K/Ba ratios from typical igneous values towards higher ratios.

Munha *et al.* (1980) have shown that spilitized rhyolites in the Iberian Pyrite Belt have average K/Rb (330) and K/Ba (160) ratios well in excess of primary values. The various types of alteration zone in the footwall of the Seneca Zn-Cu-Pb-Ag massive sulphide deposit, in British Columbia, have average K/Rb ratios (503 peripheral alteration, 464 sericitic, 485 chloritic) which are all significantly in excess of unaltered dacites, where K/Rb averages 386. Armbrust and Gannicott (1980) interpret the results in terms of seawater interaction with the footwall rocks. Altered volcanic host rocks at the Mattagami Lake Zn-Cu massive sulphide deposit, Quebec, are also characterized by K/Rb and K/Ba ratios that are an average systematically lower than values typical of unaltered equivalents (Costa *et al.*, 1983; Thurston and Fryer, 1983).

It is clear from the foregoing discussion that the coherent behaviour of K, Rb and Ba in the Au, Ag-vein deposits is unlike the trends observed in magmatic-related, or massive base metal sulphide deposits. Accordingly, a different origin for the gold deposits is likely, involving neither dominantly magmatic nor heated marine hydrothermal fluids. This conclusion has been independently borne out by light stable isotope studies of the gold deposits (Kerrich and Fryer, 1979; Kerrich, 1987), which indicate that fluids of metamorphic origin, focussed along structures of regional extent, are the most likely candidate for the ore-forming hydrothermal reservoirs involved in genesis of Au, Ag vein systems.

Fyon *et al.* (1984) and Colvine *et al.* (1984) have suggested that the greenstone belt lode gold deposits form in response to granulitization of the lower crust, which in turn is promoted by streaming of mantle-derived CO_2 (see Newton *et al.* 1980). The lower continental crust is depleted overall in most of the lithophile elements including K, Rb, Ba Th and U, relative to the continental crust as a whole, or the upper crust as represented by Phanerozoic greywackes (Taylor and McLennan, 1985, pp. 67, 09, 126). At first sight then, K, Rb, Ba enrichment in gold deposits is an attractive compensator for the hypothetical depletion of lithophile elements in the lower crust. The extent of depletion of an element in the lower crust depends on the degree of incompatibility. K/Rb (534) and K/Cs (28,300) ratios are higher, but K/Ba (19), Rb/Sr (0.023) and Ba/Sr (0.652) ratios are lower than in the continental crust as a whole, owing to the selective depletion of Rb and Cs relative to K, of K relative to Ba, and of Rb and Ba relative to Sr (Taylor and McLennan, 1985, p. 67).

There is at present no concensus as to the mechanism(s) which generate granulites and the attendant lithophile element depletions. A number of hypotheses have been advanced including (1) melt extraction (Fyfe, 1973), (2) depletion during dehydration of protoliths, or mantle volatile streaming, and (3) generation of some granulites with intrinsically low primary abundances of the lithophile elements (see Tarney, 1975). It should be noted however, that if lithophile element enrichments in the gold deposits were linked exclusively to depletions accompanying granulitization, then in the deposits, Rb and Cs should be enhanced relative to K, K enhanced relative to Ba and Th and U display absolute enrichments: the data are not in compliance with such hypothetical trends.

An alternative hypothesis suggested here, is that the ore-forming hydrothermal reservoirs are generated by dehydration of serpentinites and mafic igneous rocks, in the root zones of structures along which different greenstone terrains have been juxtaposed. Such lithologies are characterized by intrinsically low, but finite abundances, of the lithophile elements, and in particular one depleted in Cs. During the dehydration of serpentine K, Rb/Ba will be excluded in a volatile phase, in approximately the same proportions as they occurred in the original rock because there are no available sites for lithophile elements in metamorphic olivine and pyroxene. This process could account for their proportional co-enrichment in the deposits.

The Source Rock Question

In many instances, genetic theories of gold deposits have been formulated on the tacit assumption that the physical association of deposits with a specific rock type also implies a genetic link. Pyke (1975, 1976) has noted a relationship of Au mineralization and ultramafic volcanic rocks in the Porcupine camp, Ontario, claiming that ultramafic rocks are favourable 'source beds' because of their intrinsically elevated Au abundance. Analysis of Au by sensitive modern techniques reveals that unaltered ultramafic rocks have abundances of 0.5-2 ppb Au, in the same range as other primary igneous rocks (Tilling *et al.*, 1973; Anhauesser *et al.*, 1975; Kwong and Crocket, 1978): these data contraindicate the 'source-bed' concept.

There are two further aspects to the source-bed problem; namely the regional geological association and local casual factors. Although prominent gold deposits are physically related to ultramafic rocks, a case can be made for gold associations with a multitude of 'special' rock types.

In the Porcupine and Malartic camps, at Mine Bousquet and Mine Doyon - Cadillac District, and at Agnico Eagle, Quebec, gold deposits are associated with Na-enriched felsic intrusive-extrusive igneous rocks. At the Kirkland Lake, Larder Lake and Matachewan camps, Ontario, gold is locally hosted by alkali gabbros, syenites and trachytes. Similarly, the presence of Au in granodiorites is notable at Val d'Or, Quebec, and Red Lake and Dryden, Ontario. Rather, a feature common to many greenstone belt lode gold deposits is the presence of a complex lithological ensemble. However, as Hutchinson (1976) and Hodgson (1983) have pointed out, the overwhelming preponderance of Au produced from Archean lode deposits is from mines located within mafic igneous rocks. There is thus no geological basis for claiming a special relationship of Au with ultramafic rocks.

At the local scale, ultramafic rocks may provide favourable chemical environments for gold precipitation. In a typical granite, basalt and ultramafic rock, the sum of cations (Fe, Mn, Mg and Ca) which may combine with CO_2 to form carbonates is 4, 21 and 32 wt.% respectively. From this it is clear that ultramafic rocks have the greatest capacity to undergo intense carbonate-replacement alteration, and thus to exert the greatest integrated chemical effect on fluids exchanging with the rocks via scavenging of CO_2. If wall-rock reactions may locally mediate precipitation of Au [for which there is abundant empirical evidence, cf. Bain (1933)] in addition to temperature (Fyfe and Henley, 1973), then it is possible that some of the Au may be transported as a carbonyl (CO), COS or related complex, with carbonate-forming reactions mediating Au precipitation by diminution of P_{CO_2} and (or) decrease of acidity (see Part I). It is well known (Ephraim, 1948, pp. 776-810) that many metals capable of forming carbonyl and carbonyl-chloride complexes are also enriched in lode Au deposits. The presence of Au-bearing quartz veins in greenstone belts may also partly reflect the high capacity of mafic and ultramafic rocks to store volatiles during early sea-floor spilitization reactions, the volatiles being released subsequently during crustal heating, as discussed above.

A brief summary of the various rock types which have been proposed as 'sources' for the chemical components concentrated in gold deposits is given in Table 1 in Part 1, (page 50).

Source of the Hydrothermal Solutes

The origin of fluid reservoirs which were involved in Archean gold systems has been considered above on the basis of light stable isotope evidence. However, the source rock reservoir for hydrothermally transported solutes, such as Si, CO_2, K, Rb, Li, Cs, Sr and rare metals including Au, Ag, As, Sb, B, Se, Te, Pb, Bi, W (etc.) is a more subtle problem. Here, the question is explored by means of radioisotope tracers, namely $^{87}Sr/^{86}Sr$ and $^{207}Pb/^{204}Pb$, $^{208}Pb/^{204}Pb$, which may be diagnostic of the specific rock reservoir from which the solutes were derived.

Contemporaneous $^{87}Sr/^{86}Sr$ ratios of the ore-forming hydrothermal fluids have been estimated from analyses of tourmaline, scheelite and piemontite, all of which possess $^{87}Sr/^{86}Sr$ 0.004, and therefore have negligibly small radiogenic strontium evolution over the elapsed time since formation. Moreover, these minerals, unlike ferrodolomites present in the fault zones, appear to have behaved as isotopically closed systems. Strontium isotope data for selected deposits are compiled in Figure 10.

If the estimated range of 0.7010 to 0.7041 for the source rock reservoir of hydrothermal solutes has validity, then this reservoir was more radiogenic than the upper mantle at 2,690 Ma (0.700 ± 0.001), the Matachewan diabase dyke swarm (0.701 ± 0.001), or contemporaneous Abitibi belt volcanics of mafic to ultramafic composition (0.7000 to 0.7012) (Fig. 10; Faure, 1977; Gates and Hurley, 1973; Hart and Brooks, 1974). An inferrred radiogenic character for the source may implicate contributions from sialic basement to the greenstone belt, and/or felsic volcanic rocks of the Lower Supergroup, in addition to volatiles released from the mafic to ultramafic volcanic sequence (Fig. 10).

Franklin *et al.* (1983) have shown on the basis of lead isotopic work that in general, fault-hosted gold mineralization in the Abitibi greenstone belt also possesses a characteristically more radiogenic signature and higher than contemporaneous mafic volcanic rocks (Fig. 10b).

Thus the deduced Sr and measured Pb-isotopic character of the fault mineralization are more evolved than their contiguous mafic volcanic bounding media, collectively implicating a deeper level, more radiogenic source for these components. This source is likely the same one as that donating Si, CO_2, K, Rb, Li, Cs, Au, Ag, As, Sb, B (etc.). Long range communication to a deep crustal source is corroborated by the presence of the major structures themselves, as well as independent estimates of transport distances based on enrichments of rare elements in the structures (see above; Kerrich and Fryer, 1979; Kerrich, 1983).

Sodic and Alkaline Igneous Rocks

Magmas of sodic or alkaline composition are characteristically associated with the major gold districts, and both are spatially linked to major structures of regional extent. Prominent examples include trondjhemites of the Malartic and Timmins areas, and alkaline rocks at Kirkland Lake and Matachewan. In the Yellowknife district, the Pud Lake Stock and lamprophyric dyke, both close to the gold hosting structure, represent trondhjemitic and alkalic magmas respectively.

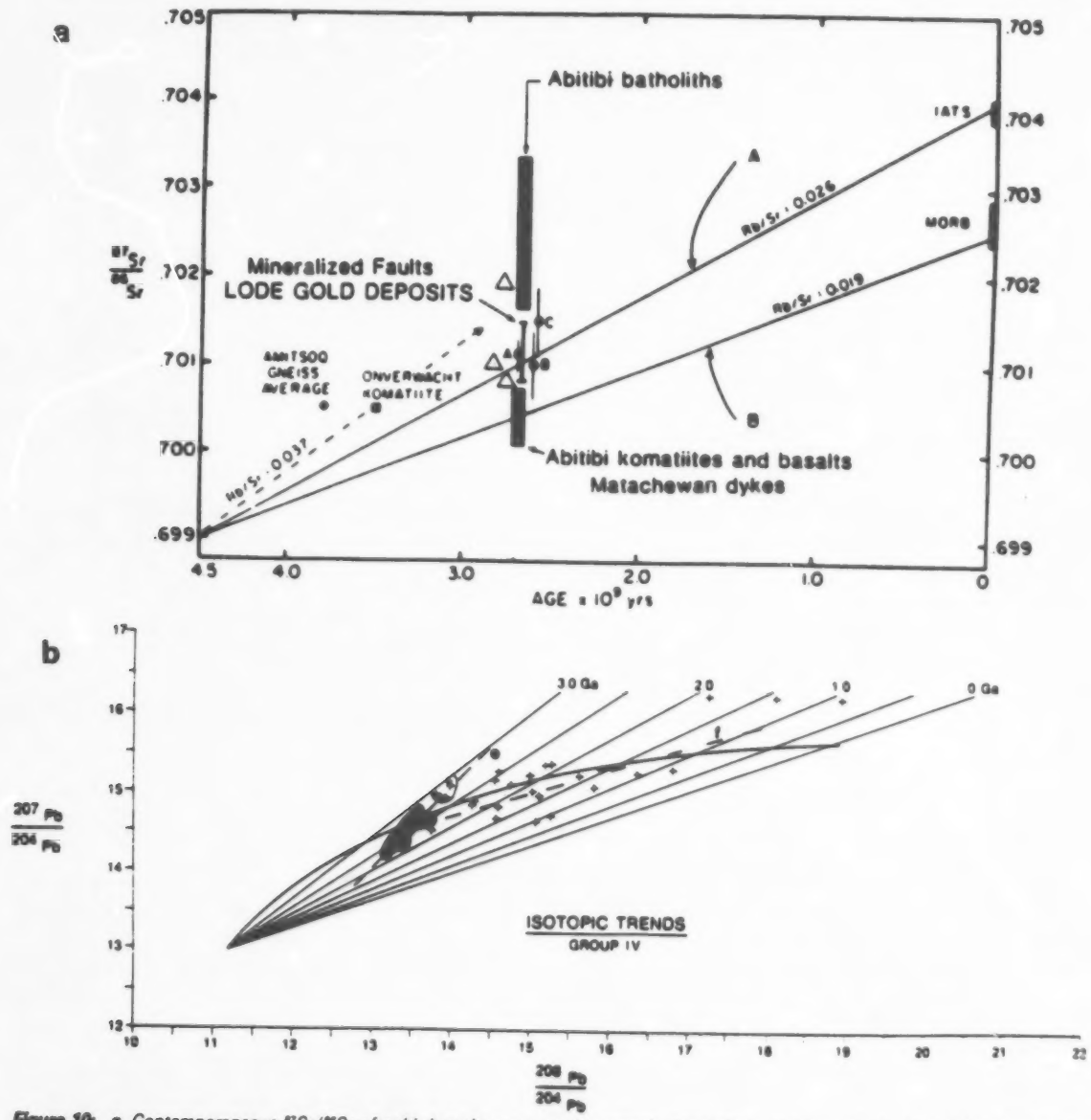

Figure 10: *a. Contemporaneous $^{87}Sr/^{86}Sr$ of gold deposits, compared to mantle, komatiites, and granodiorite batholiths, for the Abitibi greenstone belt at 2.7 Ga. b. Lead isotopic composition of massive sulphides (solid) and mineralized structures (crosses), after Franklin et al., 1981.*

The sodic rocks conform in most respects to the definition of a trondhjemite based on major element oxides, according to Barker *et al.* (1979), namely SiO_2 68% usually 75%, Al_2O_3 typically 15% at 70% SiO_2 and 14% at 75% SiO_2, and Na_2O 4.50-5.5% (etc.). Most such trondhjemites have elevated primary Na_2O contents, but this is incremented during pervasive spilitic alteration in the presence of marine water, under conditions of low temperature, as evidenced by reversed quartz-feldspar fractionations, (Fryer *et al.*, 1979; Kerrich and Fryer, 1979; Kerrich, 1983). A general concensus exists that sodic magmas of this type form by partial melting of mafic granulites at the base of the greenstone belt sequence (Collerson and Fryer, 1978; Barker *et al.*, 1979).

Groups of alkaline igneous intrusions and tuffs at Kirkland Lake are characterized by SiO_2 in the range of 48-56%, and K_2O 5.5 to 9.8%. Relative abundant ilmenite, hornblende and/or augite is reflected in elevated TiO_2, Fe_2O_3, MnO, CaO and MgO contents, along with high concentrations of mafic-affiliated elements such as V, Cr, Co, Ni and Sc. Formerly termed syenites these rocks are in fact alkali

gabbros, potassic basalts and trachytes. Rare earth element distributions for unaltered species of the alkaline rocks are remarkably diagnostic (Fig. 11), defining a coherent array with La_{cn} 1000 to 2000, and the HREE 10 times chondritic abundances.

A general consensus exists that alkalic mafic rocks are the products of low degrees of partial melting of upper mantle, or 'enriched' upper mantle, possibly mixed with rocks from the base of the crust, and such fusion products have a preferred spatial association with linear fracture zones, such as rifts. Along with the alkaline magmas, are lamprophyric dykes and domains of fenitization, highly enriched in large ion lithophile elements. Representative chondrite normalized diagrams are depicted in Fig. 11.

The spatial association of trondhjemites and alkaline magmas with major linear structures is interpreted in terms of translithospheric fractures, which tap magmas of sodic composition generated at the base of the crust, and deep mantle partial melts of alkaline compositions. Such magmatic activity is broadly coeval with venting of hydrothermal fluids, probably from a mid-crustal reservoir. Thus the 'exotic' magmas, and gold deposits, are both functionally related to a specific tectonic environment, but a genetic link between deposits and magmas remains open to question.

Models for Generation of Lode Gold Deposits

Boundary Conditions

Any hypothesis which encompasses geological and chemical characteristics of lode gold deposits in greenstone belts must satisfy the following constraints:

1. Concentration of gold in major transcrustal fracture systems, independent of lithology or stratigraphic position.
2. Precipitation of gold over a significant range of ambient redox conditions, from sulphate-hematite to pyrrhotite-graphite-methane.
3. Separation of base metals from rare elements at all stages of gold enrichment.
4. Au concentration factors in the order of 10,000 and therefore source rock volumes of hundreds of km^3.
5. Source of abundant carbon dioxide.
6. Relatively high, uniform fluid temperatures of about 270° to 400°C.
7. Hydrothermal solutions with $\delta^{18}O$ 5 to 8 per mil, δD −80 to −40 per mil, high K/Na, high CO_2, low salinity, and the presence of reduced gas species such as H_2, CO and CH_4.
8. Hydraulic pressure ≥ lithostatic pressure in veins.
9. Water/rock ratios sufficient to cause complete oxygen isotope exchange of host rocks with the aqueous reservoir along flow conduits, and to extensively modify primary host-rock chemistry.
10. Mineralizing hydrothermal solutions originating under highly reduced conditions, leading to extensive reduction of Fe^{3+} silicates in wall rocks along hydrothermal conduits.
11. A mechanism which is intrinsically efficient under Archean crustal conditions, speicfically 2.7 Ga ± 1 Ga greenstone belts.

Models for Lode Gold Deposits

A number of hypotheses have been advanced to account for the source of Au and generation of lode gold deposits in greenstone belts. In summary, these are:

(1) Derivation of Au from stocks of quartz-feldspar porphyry considered to be of subvolcanic origin (Carter, 1948; Ferguson *et al.*, 1968; Griffis, 1968; Boyle, 1976).

(2) Lateral secretion of vein material from the enclosing rocks (Hurst, 1935; Boyle, 1961, 1976, 1979).

(3) Derivation of Au from granitic batholiths of Kenoran age (George, 1967; Jones, 1948).

(4) Mobilization of Au from ultramafic rocks (Pyke, 1975, 1976) or sediments (Hodgson and MacGeehan, 1982) postulated to have a high primary abundance of gold.

(5) Multistage origin (a): primary syngenetic enrichment of Au into gold-bearing chemical sediments generated from circulation of marine water, or from 'volcanic exhalations', during periods of volcanic quiescence. Precious metals and gangue constituents are considered to be remobilized into fractures from the primary chemical sediments during subsequent deformation and metamorphism (Hutchinson, 1976; Fripp, 1976; Ridler, 1976; Karvinen, 1978, 1980). Alternatively, gold-bearing veins are presumed to be discharge sites of a marine-water geothermal system (MacGeehan and Hodgson, 1982; Hodgson and MacGeehan, 1982; MacGeehan *et al.*, 1982; Fyon and Crocket, 1981, 1982).

(6) Multistage origin (b): solution and transport of gold by fluids generated during crustal dehydration, with a possible initial concentration in the near seafloor environment, and main phase concentration into hydrofractures.

(7) Deposition of gold in veins from fluids containing a significant compound of low-Cl, low-^{18}O meteoric water in some felsic batholiths that emerged above sea level (Kennedy and Kerrich, 1982). Such

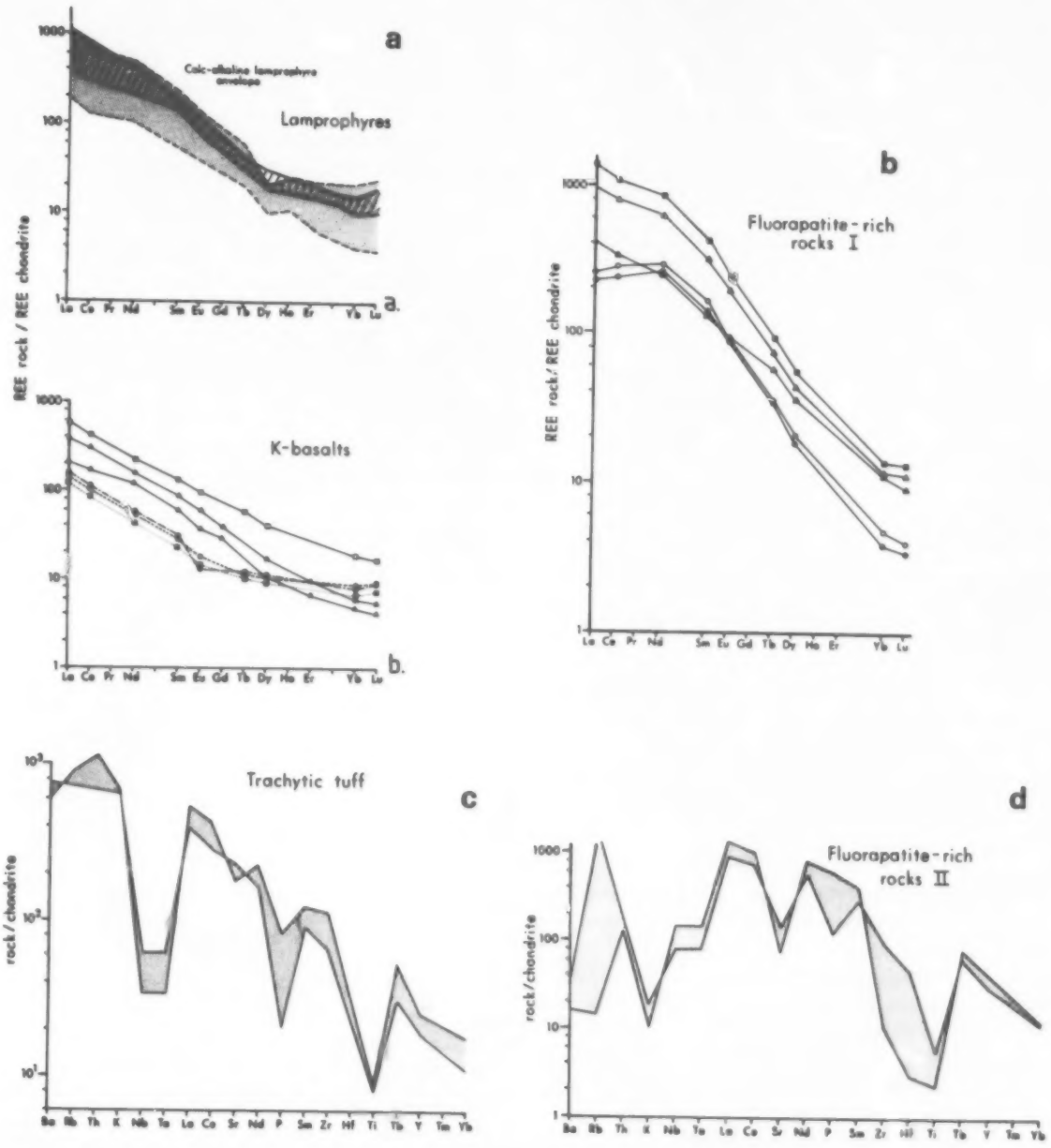

Figure 11: *Chondrite normalized element distributions for specified suites of alkaline magmas.* **a.** *REE diagrams for a) lamprophyres from the Canadian Arrow deposit, b) alkali gabbros and basalts from Kirkland Lake.* **b.** *REE diagrams for fluorapatite rich rocks (from King and Kerrich, 1986).* **c.** *Extended chondrite normalized diagram for alkali-trachytic tuffs from Kirkland Lake.* **d.** *Extended chondrite normalized diagram for fluorapatite rich rocks on the Destor-Porcupine fault (after King and Kerrich, 1986).*

deposits are neither abundant nor large producers, and are not commented upon further here.

These models and their variants are critically discussed below.

(1) Derivation of Gold from quartz feldspar porphyries (QFP'S).

A number of earlier workers referenced above, and Hodgson (1983), have pointed out the apparently anomalous abundance of felsic intrusive rocks with lode gold deposits of the Superior Province. Various possible explanations that have been proposed for this spatial association are:

1. magmas were a source for metalliferous hydrothermal solutions
2. the intrusions provided heat, or
3. acted as conduits for the mineralization process.

Fryer *et al.* (1979) and Kerrich and Fryer (1979) suggested that the preferred siting of veins at margins of felsic intrusions at the Dome Mine, is a result of a structurally disharmic style generated by folding of a volcanic sequence containing an irregular intrusive body. The various possible genetic factors have been re-evaluated by Marmont (1983).

Calculations of mass balance based on the volumes and measured precious metal abundances of relatively unaltered porphyry (Fryer *et al.*, 1979) do not support the hypothesis that these igneous bodies contributed a significant fraction of gold to the orebodies. In addition, Davies (1977), Roberts (1980) and Gorman *et al.* (1981) point out that many of the major auriferous quartz veins post-date emplacement and spilitization of the porphyries.

Karvinen (1978, 1980) has convincingly demonstrated that many of the porphyries in the Porcupine Camp were extruded at a horizon contiguous with some of the auriferous sediments, and coevally with the precipitation, although the timing of gold introduction to the sediments is equivocal. Given their 'spilitic' character, the QFP's almost certainly provided energy to drive seawater convection, as discussed for East Malartic (Kerrich *et al.*, 1982; Munha *et al.*, 1981; Kerrich and Hodder, 1982); but this geothermal regime was probably not the one responsible for gold enrichment, based on the reducing character, low salinity, high $\delta^{18}O$, high CO_2 and low Na/K of fluids in the auriferous system.

Hodgson and MacGeehan (1981) have conjectured that 'magmatic' hydrothermal fluids play an essential role in transporting heat and at least some dissolved constituents from deep magma sources to near-surface hydrothermal systems. However, the most abundant mafic magmas in greenstone belts, namely basalts, and the most pronounced gold-associated felsic magmas, the QFP's of trondhjemitic composition, are notably anhydrous in contradistinction to the 'granitic' magmas associated with copper and molybdenum porphyries which may have relatively high volatile contents.

It should be emphasized that the intrusives encompass a wide range of compositions, from diorite through granodiorite to high K-granites, as well as syenites, alkali gabbros and trondhjemites (Kerrich, 1983; Kerrich and Watson, 1984; Colvine *et al.*, 1984). Moreover, the association of 'felsic' intrusives with gold deposits is not so apparent in the Southern Africa and Australian greenstone belts (cf. Groves and Batt, 1984). If Archean lode gold deposits, worldwide, formed via a similar mechanism, as indicated by uniformity of $\delta^{18}O$ quartz $\delta^{13}C$ carbonate (etc.), then the role of felsic intrusions as a structural focus seems more likely than as a metal donor.

A magmatic origin for the Hollinger Mine, Timmins, as recently proposed by Burrows *et al.* (1986a,b) and Wood *et al.* (1986) on the basis of carbon isotope data, is open to question, given that the measure $\delta^{13}C$ values of -3 per mil, are not uniquely diagnostic of a magmatic source. Moreover, the K, Rb, Ba systematics at Hollinger and elsewhere are unlike magmatic trends.

(2) Lateral Secretion

The possibility of lateral secretion of material into veins from their enclosing volcanic rocks (Hurst, 1935; Boyle, 1961, 1976) may be evaluated with reference to the rate equations which describe possible independent mechanisms of chemical transport. Chemical transport through the crust may occur by means of (1) solid-state diffusion through crystalline structures; (2) grain-boundary diffusion; and (3) hydrothermal transport in solution.

An approximation of the characteristics transport distance (X) in a diffusive process is given by: $X = (2Dt)^{0.5}$, where D is the coefficient of diffusion at a specified temperature and t is time in seconds. The coefficients of solid-state diffusion, and grain-boundary diffusion through an inter-granular fluid, at temperatures of 500°C are of the order of 10^{-20} cm^2s^{-1} and 10^{-6} cm^2s^{-1}, yielding characteristic transport distances of 800 m and 80m respectively over a time interval of 10^6 years (Fletcher and Hofmann, 1974; Fisher and Elliott, 1974; Ildefonse and Gabis, 1976). This distance of grain-boundary diffusion is too small by a factor of 100 in view of the calculations on gold transport given by Helgeson and Garrels (1968), Fyfe and Henley (1973), and Kerrich and Fryer (1979). The driving force for lateral diffusion is presumed to be gradients of chemical potential from wall rocks into dilatant zones of lower pressure and chemical potential. However, as discussed in a previous section, it can be deduced from structural relations that many auriferous vein systems underwent incremental opening under conditions of anomalously high fluid pressure, where $P_{fluid} > P_{wallrock}$. If the inferred hydraulic pressure relations are correct, then the very basis of lateral secretion is invalidated for the case of auriferous veins. Anomalously high fluid pressures in veins, with limited penetration into wall rocks, is entirely consistent with the gradients in element

abundances, redox state and $\delta\ ^{18}O$ in a direction orthogonal to the vein boundaries.

The 'lateral diffusion' or 'lateral secretion' mechanism has been supported by Wanless *et al.* (1960), and independently advanced by Roslyakova and Roslyakov (1975) to account for a large number of Russian lode gold deposits. However, Ames (1964) and Ridge (1968) argue that none of the data reported by Boyle (1961) in support of 'lateral diffusion' are incompatible with a hydrothermal origin for the deposits.

In addition, the hypothesis of lateral diffusion is difficult to reconcile with the following observations: (a) Adjacent to vein margins the profiles of gold and silica abundances, representing the putative chemical potential gradients to drive diffusion, are opposed according to the diagrams of Boyle (1961, 1979), and yet these two components are both interpreted to have diffused into the veins in response to potential gradients. (b) The inferred depletion of Al_2O_3 in dilatant zones would require diffusion of this low-mobility component out of the system coupled with diffusion of silica in. (c) Lateral diffusion is not consistent with the oxygen isotope data, which indicate isotopic equilibrium of veins and immediate wall rocks, but disequilibrium of these with country rocks at distances of >20m from veins. (d) This proposed diffusion mechanism accounts neither for the highly reduced state of wall rocks, (e) nor for the observed separation of base metals from rare elements, nor (f) for the predominance of lode gold deposits in greenstone belts vs. Phanerozoic and Proterozoic metamorphic terrain.

Finally, if lateral diffusion operated, a relationship might be anticipated between the distinctive trace-element suites of various rock types and their abundances in veins, but this is not the case (Kerrich, 1983, Tables 1 and 2). For instance, lead does not exhibit preferential enrichment in veins traversing felsic igneous rocks, nor is copper more abundant in mafic-hosted veins.

(3) Kenoran Batholiths as a Source

Derivation of gold from granitic batholiths of Kenoran age is difficult to evaluate in the absence of adequate geochemical tracers. However, field relationships demonstrate that the gold deposits are preferentially located in major structures which cross-cut diverse lithological types, rather than one specific type of granitoid.

(4) Au Donation from 'Special' Source Rock Types

The source of gold in lode deposits has been a long-standing question. Such deposits display field associations with both mafic-ultramafic volcanic rocks and/or sediments or the lower stratigraphic levels of greenstone belts (Viljoen *et al.*, 1970; Anhauesser, 1976; Hutchinson, 1976; Pyke, 1975, 1976); and with felsic intrusive rocks emplaced later in the overall development of the volcanic complexes (Goodwin, 1965; Ridler, 1970; Goodwin and Ridler, 1977; Hodgson, 1983).

A direct genetic link between ultramafic rocks and lode-gold deposits has been proposed by Viljoen *et al.* (1970) and Pyke (1975, 1976), based on the assumption of source rocks have an enhanced primary Au content. The elevated gold abundances quoted to substantiate this were obtained by fire assay, which is now known to yield anomalously high values at low abundance levels. Studies of precious-metal contents in igneous rocks determined by more reliable analytical techniques have conclusively demonstrated that ultramafic rocks have lower Au (0.75 ppb) and Ag (40 ppb) compared to primary basalts, which contain an average 2 ppb Au and 100 ppb Ag (Table 1; Tilling *et al.*, 1973; Frueh and Vincent, 1974; Anhauesser *et al.*, 1975; Kwong and Crocket, 1978). The studies of Kwong and Crocket (1978) on gold abundances in rocks of an Archean greenstone belt show that all unaltered igneous and sedimentary rocks have <2 ppb Au, and carbonated ultramafic rocks are only weakly anomalous (4 ppb). For the Timmins district, Fyon and Crocket (1982) report that the mean Au abundance of Mg-tholeiitic basalts of 2.4 ppb is greater than that of ultramafic rocks (mean 1.9 ppb); and Saager *et al.* (1982) did not detect a differentiation trend of Au from ultramafic to mafic rocks in greenstone belts of Southern Africa.

The conclusion that emerges from these studies is that the spatial association between lode gold deposits and specific rock types does not provide unequivocal evidence for a genetic link between host rock and lode. On the contrary, the magnitude of transport distances, as derived in a previous section, contradicts close spatial relationships being correlated with genetic factors. Given that ultramafic rocks do not represent an intrinsically gold-enriched source rock, then the observed local association of gold deposits with rocks of ultramafic affinity had been attributed to several factors, including: (i) preferential gold release during carbonatization (Boyle, 1961, 1979; Fyon *et al.*, 1982a,b); (ii) ultramafic rocks signal the onset of new volcanic cycles, with quiescent episodes favouring seawater circulation and attendent chemical sedimentation (Fyon *et al.*, 1982a,b); (iii) ultramafic rocks provide efficient sinks for gold from hydrothermal solutions (Kerrich and Fyfe, 1981); and (iv) ultramafic rocks represent the base of a submarine rift environment, of high heat flow, in which mafic and ultramafic rocks initially store hydrates, carbonates and hydrocarbons during reaction with seawater, and subsequently undergo continuous dehydration and decarbonation during progressive burial (Kerrich, 1983; Groves and Batt, 1984).

Hodgson and MacGeehan (1982, p. 225) have proposed, as one of several possible alternatives, that the spatial association of gold deposits in greenstone belts with detrital sedimentary rocks may be due to preconcentration of gold and/or the gold-mobilizing constituents into the sediments. The putative gold enrichments in detrital sedimentary rocks can be discounted for Abitibi belt gold deposits from the available data on gold abundances in this rock type (Kwong and Crocket, 1978; Table 1), although it is not possible to

comment on the unspecified 'gold-mobilizing constituents' of Hodgson and MacGeehan (1982). However, Saager *et al.* (1982) report that sedimentary rocks (mean Au 130 ppb) are significantly enriched in gold over volcanic rocks (mean Au 10.8 ppb) in Southern African greenstone belts. Thus, several authors have concluded that the bulk of rocks in Archean greenstone belts are not better gold source beds than equivalent rock types of the Proterozoic or Phanerozoic eras, except for the volumetrically small iron formations (Kwong and Crocket, 1978; Fryer *et al.*, 1979a; Kerrich and Fryer, 1979; Kerrich, 1980; Fyon *et al.*, 1982a,b; Saager *et al.*, 1982).

The preferred spatial association of lode gold deposits with the boundary between volcanic and sedimentary domains in greenstone belts is attributed here to the controls of structure and permeability on discharge of hydrothermal reservoirs.

(5) Multistage Origin (a): Seawater Transport of Au, With or Without Remobilization

There exists a large body of field, sedimentological, textural, isotopic and REE evidence for some enrichment of gold into chemical sediments (Hutchinson, 1976; Fripp, 1976; Ridler, 1976; Karvinen, 1978, 1980; Fryer *et al.*, 1979; Fyon *et al.*, 1980, 1981). Saager *et al.* (1982) report that ferruginous chemical sediments in greenstone belts of Southern Africa are distinctly more auriferous (mean Au 172 ppb) than Superior iron formations. However, it is not known with certainty if the origin of the auriferous chemical sediments was primary, secondary replacement, or a combination of the two processes.

Several authors have tacitly presumed that convecting seawater hydrothermal fluids form syngenetic sedimentary gold enrichment (Fripp, 1976; Fyon and Crocket, 1981; Fyon *et al.*, 1982; Hodgson and MacGeehan, 1982; MacGeehan and Hodgson, 1980, 1982; MacGeehan *et al.*, 1982), although no direct evidence is presented for seawater involvement. However, the balance of available evidence suggests that the auriferous fluids implicated in gold deposits were different from sea-water geothermal systems generating base metal deposits, in terms of temperature, ^{18}O, fluid pressure, Na/K, CO_2/H_2O, salinity, Mg/Fe, redox, relative metal solute concentrations and reduced gas species. These differences in fluid properties are reflected in divergent metal distributions and patterns of alteration of the two deposit types. Furthermore, any model that involves seawater cannot readily account for the predominance of lode gold deposits in Archean greenstone belts coupled with their relative paucity in Proterozoic and Phanerozoic marine environment. Base-metal deposits which are generally considered to have been formed from seawater-hydrothermal fluids exist in sequences of most age from the Archean to the present. However, Archean-type lode gold deposits are not prominent in Phanerozoic mid-ocean-ridge, island arc or ocean island environments. Extensive carbonate alteration, LIL element enrichments, massive quartz veins and lode gold deposits are known neither from observations of the modern ocean-floor basalts subjected to seawater alteration nor to obducted fragments of ocean crust.

It has been suggested that gold may locally be mobilized out of chemical sedimentary rocks with a postulated primary Au enrichment during crustal deformation (Hutchinson, 1976; Fripp, 1976; Ridler, 1976; Karvinen, 1978, 1980; Fyon *et al.*, 1980, 1981), leading to vein deposits in the vicinity. However, most vein deposits do not appear to have acquired their precious-metal complement from local remobilization of gold in the sediments. The putative remobilization does not account for separation of rare from abundant elements in the veins, for K_2O enrichments coupled to Na_2O depletions around veins, or for the pronounced differences in REE distributions, carbonate mineral chemistry, $\delta^{18}O$, and redox between sediments and veins.

Hodgson and MacGeehan (1982) have likened Archean gold deposits in proximity to epizonal intrusions to precious metal deposits associated with Tertiary epizonal stocks of the western USA. However, the latter typically possess base metal and precious metal domains, unlike the Archean examples (cf. Sunnyside Mine, Casadevall and Ohmoto, 1977). The only feature in common with the precious metal zones of the two ages of epizonal deposits is a low-chloride hydrothermal reservoir: low-Cl, high-^{18}O (metamorphic) fluids in a submarine environment for the Archean; and low-Cl, low-^{18}O (meteoric) fluids in a continental environment for the Tertiary.

Macdonald (1983), and Phillips *et al.* (1984) and Pearton (personal communication, 1985) have provided cogent field and mineralogical evidence for an epigenetic origin of iron-formation hosted gold deposits.

(6) Multistage Metamorphic Fluid Systems

The remaining hypothesis presented to account for the origin of lode gold deposits involves focussed discharge of metamorphic fluids. Single-stage models for veins have been proposed by Fyfe and Henley (1973) and Henley *et al.* (1976), and multistage models by Kerrich and Fryer (1979), Kerrich and Fyfe (1981), Kerrich and Hodder (1982), and Kerrich (1979, 1980,1981, 1983). During burial of hydrated greenstone-belt assemblages, devapourization reactions generate significant fluid volumes (Fyfe, 1973, 1974; Fyfe *et al.*, 1978). Fluids are continuously released within the greenschist facies; and at the greenschist-amphibolite transition, which takes place at 450-500°C, about 5 wt.% structural water and volatiles including CO_2 are released from a hydrated rock of mafic composition. Large fluid volumes are also generated higher grades of metamorphism.

The volume relations of dehydration reactions are such that metamorphic fluids are evolved under conditions where $P_{fluid} \geq P_{lithostatic}$. A second factor contributing to elevated

hydraulic pressures is differentiated thermal expansion of pore fluids (Norris and Henley, 1976; Knapp and Knight, 1977) and possibly immiscible separation of CO_2 (cf. Kerrich 1983; Higgins and Kerrich, 1982). This effect is enhanced under conditions of steep geothermal gradients. Hence, a metamorphic fluid reservoir satisfies the observed temperatures, $\delta^{18}O$ and δD of the mineralizing solutions, together with the low salinity, and elevated CO_2/H_2O and K/Na ratios. In addition, a metamorphic reservoir accounts for the requirement of fluids generated under high temperature reducing conditions, at elevated hydraulic pressures and inferred low water/rock ratios. As stated above a magmatic hydrothermal fluid, or mixtures of magmatic and metamorphic are also possible based on present data. Immiscible separation of CO_2 would act to promote oxidation of the residual fluid, since reduced gas species such as H_2S and CH_4 partition into the gaseous phase. This mechanism may account for some of the relatively oxidized ore deposits, such as Macassa and Canadian Arrow, in addition to the redox reactions discussed by Lambert *et al.* (1984).

A common argument raised against the involvement of metamorphic fluids in Archean lode gold deposits is that hydrothermal alteration associated with the gold deposits overprints regional metamorphic assemblages, and accordingly, mineralization must postdate metamorphism. We suggest that during thrusting associated with closure of rifts or terrain accretion, fluids generated by dehydration in the lower plate will discharge through the upper plate, and overprint its metamorphic assemblage.

The residence and accumulation of metamorphic fluids in the crust is determined by the balance between the rates of fluid generation and fluid expulsion. In the Archean crust where thermal gradients are generally accepted to have been high, particularly in provinces of continuous volcanic activity, the rate of fluid generation of metamorphic dehydration reactions must have been faster and occurrerd over narrower vertical crustal intervals, leading to an increased probability of generating and ponding extensive metamorphic fluid reservoirs. When the hydraulic pressure exceeds the sum of the crustal horizontal stress plus the tensile strength of the rock, subvertical hydraulic fracturing must ensue, providing focussed discharge for the ponded reservoir, and high fluid/rock ratios in the conduit. High boron and CO_2 concentrations in many gold-bearing veins and chemical sediments may be a consequence of ponding hydrothermal reservoirs beneath impermeable sediments in source regions; inasmuch as sediments have greater abundance of B than igneous rocks and typically contain hydrocarbons which may oxidize to CO_2 (Turekian and Wedepohl, 1961). Haack *et al.* (1984) have demonstrated the loss of many trace metals, especially the LIL elements - Tl, Ba, Pb, Bi, Hg, Zn and Cd, from pelites during regional metamorphism, and most granulites are known to be depleted in LIL elements (cf. Barbey and Cuney, 1982).

Subsequent generations of vein deposits may form in response to additional burial and heating of rocks arising from superimposesd thrust sheets. The ubiquitous conjunction of brittle fracturing and ductile deformation in lode gold deposits attests to cycling through the brittle-ductile transition at depths of 8-12 km in response to fluctuations of fluid pressure (see Kerrich and Fyfe, this volume).

It is suggested that rift environments, with high heat fluxes, are appropriate for efficient gold concentration (Kerrich, 1983; Groves and Batt, 1984). Here, listric normal faults initially control extension along with ultramafic volcanism, provide pathways for mafic and felsic magmas, are responsible for scarp-dominated sedimentary rocks, and act as conduits for hydrothermal discharge. At late stages of greenstone belt development, reverse motion on the fault accommodates crustal compression, along with continued hydrothermal discharge.

The structural setting of Archean lode gold deposits has been emphasized by many workers from the earliest times, such as Knopf (1929), Bain (1933) and authors of 'The Structural Geology of Canadian Ore Deposits' (1948). Gunning and Ambrose (1940) have emphasized the association of gold deposits with 'breaks', where this term carries the connotation of linear domains including gradients of deformation intensity in conjunction with the juxtaposition of diverse rock types, typically volcanic and sedimentary. Boyle (1961, 1979) and Henderson and Brown (1966) have emphasized the importance of structural control on the ore deposits at Yellowknife.

Structural control of Archean lode gold deposits in general, and the genetic role of structure in generating large plumbing systems has subsequently been endorsed by Fyfe and Henley (1973), Fryer *et al.* (1979), Kerrich and Allison (1978), Kerrich and Fryer (1979), Kerrich (1983), this paper and recently by Colvine *et al.* (1984). Thus structure is of paramount importance for both chemical sedimentary and vein-type lode gold deposits.

Acknowledgements

The authors thank Bill Padgham for the invitation of write this contribution. Numerous mine geologists, especially D. Myers, D. Rogers, E. Van Hees, G. Nemcsok, S. Comline and P. Bedard kindly provided access to the gold mines on which this manuscript is based. We are grateful to L.M. Willmore, B. Every, Y.C. Cheng, B. McKinnon and J. Forth for analytical assistance. A. Heppner is thanked for conducting the typing, and E. McLarty, L.M. Willmore and Mrs. R. Ringsman for drafting the diagrams and assistiing with preparation of the manuscript. The Canadian Institute of Mining and Metallurgy are thanked for permission to reproduce some of the figures from Special Volume 27. This paper has benefited from an incisive review by R.W. Boyle, and editorial improvements by W. Padgham.

References

Ames, R.L., 1964, The origin of the gold quartz deposits, Yellowknife, N.W.T. Econ. Geol., v. 57, p. 1137-1140.

Andrews, A.J. and Fyfe, W.S., 1976, The role of seawaterin sub-seafloor metamorphism and massive sulphide generation on the ocean floor. Geosci. Can., v. 3, p. 83-94.

Anhauesser, C.R., 1976, The nature and distribution of Archean gold mineralization in southern Africa. Minerals Science Engineering, v. 8, p. 46-84.

Anhauesser, C.R., Fritz, K., Fyfe, W.S., and Gill, R.C.O., 1975, Gold in 'primitive' Archean volcanics. Chemical Geology, v. 16, p. 129-135.

Armbrust, G.A., and Gannicott, R.A., 1980, K/Rb ratios as a source indicaters for hydrothermal fluids of the Seneca volcanogenic massive sulfide deposit,.British Columbia. Economic Geology, v. 75, 466-477.

Armbrust, G.A., Oyarzun, J. and Arias, J., 1977, Rubidium as a guide to ore in Chilean porphyry copper deposits. Economic Geology, v. 72, 1086-1100.

Armbrust, G.A., Oyarzun, J., and Arias, J., 1971, Rubidium as a guide to ore at El Teniente (Broden) Chile [abs.]. Economic Geology, v. 66, 977.

Aumento, F., Mitchell, W.S., and Fratta, M., 1976, Interaction between sea water and oceanic layer two as a function of depth and time. I. Field evidence. Canadian Mineralogist, v. 14, p. 269-290.

Bain, G.W., 1933, Wall rock mineralization along Ontario gold deposits. Econ. Geol., v. 28, p.705-745.

Barbey, P. and Cuney, M., 1982, K, Rb, Sr, Ba, U and Th geochemistry of the Lapland granulites (Fennoscandia). LILE fractionation controlling factors. Contrib. Mineral. Petrol., v. 81, pp. 304-316.

Barker, F., Arth, J.C., and Millard, H.T., 1979, Archean trondjemites of the Southwestern Big Horn Mountains, Wyoming: a preliminary report. Chapter 12, In: F. Barker (ed.), Trondjemites, dacites and related rocks. Developments in Petrology 6, Elsevier, Amsterdam, 401-414.

Bottinga, Y., 1969, Calculated fractionation factors for carbon and hydrogen isotope exchange in the system calcite-carbon dioxide-grarphite-methane-hydrogen-water vapor. Geochim. Cosmochim. Acta, v. 33, p. 49-64.

Boyle, R.W., 1961, The geology, geochemistry, and origin of the gold deposits of the Yellowknife district. Geol. Surv. Canada, Mem. 310.

_____, 1963, Diffusion in vein genesis; Symp. Problems of Post-magmatic Ore Deposition, Prague, Czech., v. 1, p. 377-383.

_____, 1976, Mineralization processes in Archean greenstone and sedimentary belts. Geological Survey of Canada, Paper 75-15.

_____, 1979, The geochemistry of gold and its deposits. Geol. Surv. Canada, Bull. 280, 584 p.

Bradbrook, C.J., 1982, The nature and origin of the auriferous Hill-Sloan-Tivey quartz horizon, Uchi Lake, N.W. Ontario, M.Sc. thesis, Univ. Western Ontario, London, Canada, p. 237.

Brookins, D.G. and Brown, L.E., 1966, Sulphur isotopic analyses from Park County, Montana. Econ. Geol., v. 61, p. 613-617.

Burlington, J.L. 1985, The geology and geochemistry of the Aquarius deposit, Timmins, Ontario, Canada. Unpublished M.Sc. thesis, University of Western Ontario, London, Canada, 231 p.

Burrows, D.R., Wood, P.C. and Spooner, E.T.C., 1986a, Carbon isotope evidence for a magmatic origin for Archean gold-quartz vein ore deposits. Nature, v. 321, p. 851-854.

Burrows, D.R., Wood, P.C., Thomas, A.V. and Spooner, E.T.C., 1986b, A magmatic origin for Archean gold-quartz vein mineralization in the Mink Lake granodiorite stock, NW Ontario, and from the Hollinger Au deposit, Timmins, N Ontario. Geocongress '86, Johannesburg, Extended Abstr., p. 283-286.

Cameron, E.M. and Hattori, K., 1985, The Hemlo gold deposits, Ontario: a geochemical and isotope study. Geochim Cosmochim. Acta, v. 49, p. 2041-2050.

Carter, O.F., 1948, Coniarum Mine. In: Structural Geology of Canadian Ore Deposits, v. 2. CIM Spec. Vol., Montreal, p. 497-507.

Collerson, K.D. and Fryer, B.J., 1978, The role of fluids in the formation and subsequent development of early continental crust. Contributions to Mineralogy and Petrology, v. 67, pp. 151-167.

Collins, P.L.F., 1979, Gas hydrates in CO_2-bearing fluid inclusions and the use of freezing data for estimation of salinity. Econ. Geol., v..74, p. 1435-1444.

Colvine, A.C. et al., 1984, An integrated model for the origin of Archean Gold Deposits. Ontario Geological Survey Open File Report 5524, 98 p.

Costa, U.R., Barnett, R.L., and Kerrich, R., 1983, The Mattagami Lake Mine Archean Zn-Cu sulphide deposit, Quebec: Hydrothermal coprecipitation of talc and sulphides in a sea-floor brine pool-evidence from geochemistry, $^{18}O/^{16}O$ and mineral chemistry. Economic Geology, v. 78, 364-372.

Davies, J.F., 1977, Structural interpretation of the Timmins mining area, Ontario. Canadian Jour. Earth Sciences, v. 14, p. 1046-1053.

Ellis, A.J., and Mahon, W.A.J., 1977, Chemistry and Geothermal Systems. Academic Press, New York, 392 pp.

Ephraim, F., 1948, Inorganic Chemistry. Gurney and Jackson, London.

Eugster, H.P., 1959, Reduction and oxidation in metamorphism. In: Researches in Geochemistry, v. 1, P.H. Abelson, (ed.), John Wiley and Sons Inc., New York, pp. 492-520.

Eugster, H.P., and Skippen, G.B., 1967, Igneous and metamorphic reactions involving gas equilibria. In: Researches in Geochemistry, v. 2, P.H. Abelson, (ed.), John Wiley and Sons Inc., New York, pp. 492-520.

Eugster, H.P., and Wones, D.R., 1962, Stability relations of the ferruginous biotite, annite. Jour. Petrology, v. 3, p. 82-115.

Fairbridge, R.W., 1972, The Encyclopedia of geochemistry and environmental sciences. Dowden, Hutchinson and Ross, Inc., Stroudsburg, Pennsylvania, 1321 pp.

Faure, G., 1977, Principles of Isotope Geology. John Wiley and Sons, Toronto, 464 p.

Ferguson, S.A., Burram, B.S.W., Carter, O.F., Griffis, A.T., Holmes, T.C., Hurst, M.E., Jones, W.A., Lone, H.C., and Langley, C.S., 1968, Geology and ore deposits of Tisdale township, District of Catrane. Ontario Department of Mines, GR 58, 177 p.

Field, C.W., and Fifarek, R.H., 1985. Light stable-isotope systematics in the epithermal environment, in Berger, B.R. and Bethke, P.M. (eds), Geology and Geochemistry of Epithermal Systems, Soc. Econ. Geol. Reviews in Econ. Geol., Vol. 2, p. 99-128.

Fisher, G.W., and Elliott, D., 1974, Criteria for quasi-steady diffusion and local equilibrium in metamorphism. In: Geochemical Transport and Kinetics, A.W. Hofmann et al., (eds.), Carnegie Inst. of Washington, Publication 634, pp. 231-241.

Fletcher, R.C., and Hofmann, A.W., 1974, Simple models of diffusion and diffusion-infiltration metasomatism. In: Geochemical Transport and Kinetics, A.W. Hofmann et al., (eds.), Carnegie Inst. of Washington, Publication 634, pp. 243-259.

Foy, R., 1985, Geochemistry of the Kirkland Lake Larder Lake Fault. B.Sc. thesis, Univ. of Western Ontario, London, 46 pp.

Franklin, J.M., Sangster, D.M., and Lydon, J.W., 1981, Volcanic associated massive sulphide deposits. Econ. Geol. 75th Anniversary Volume, 485-627.

Franklin, J.M., Roscoe, S.M., Loveridge, W.D., and Sangster, D.F., 1983, Lead isotope studies in Superior and Southern provinces. Geol. Surv. of Canada, Bull. 351, 60 p.

Friedman, I., and O'Neill, J.R., 1977, Compilation of stable isotope fractionation factors of geochemical interest, Chapter KK. Data of Geochemistry, U.S. Geol. Surv., Prof. Paper 440-KK.

Fripp, R.E.P., 1976, Stratabound gold deposits in Archean banded iron formation, Rhodesia. Econ. Geol., v. 71, p. 58-75.

Fryer, B.J., Kerrich, R., Hutchinson, R.W., Peirce, M.G. and Rogers, D.S., 1979. Archean precious metal hydrothermal systems, Dome Mine, Abitibi greenstone belt, I. Canadian Jour. Earth Sci., v. 16, 421-439.

Frueh, A.J., and Vincent, E.A., 1974, Silver: Abundance in common igneous rock types. In: Wedepohl, K.H. (ed.), Handbook of Geochemistry, II/2, Springer Verlag, New York, p. 47E1-47E4.

Fyfe, W.S., 1973, Dehydration reactions. American Assoc. Petroleum Geol. Bull., v. 57, p. 190-197.

_____ 1974, Low-grade metamorphism: some thoughts on the present situation. Canadian Mineralogist, v. 12, p. 439-444.

Fyon, J.A., Crocket, J.H., Schwarcz, H.P., Kabir, A., and Knyf, M., 1981, Trace element and stable isotope geochemistry of auriferous iron formations in the Timmins area. In: E.G. Pye, (ed.), Geological Research Grant Program, Ontario Geol. Surv. Misc. Paper 98, p. 90-107.

_____, Schwarcz, H.P., and Crocket, J.H. 1982a, Oxygen, carbon and hydrogen isotopes: tracers for gold mineralization? Abstract, Ontario Geological Survey Geoscience Research Seminar, Toronto, December 1981.

_____, 1982b, Timmins gold deposit types: regional and detailed exploration criteria.

_____, 1983a, Application of stable isotope studies to gold metallogeny in the Timmins-Porcupine camp. Ontario Geol. Surv., Open File Rep. 5464, pp. 182.

_____, 1983b, The Carshaw and Malga iron-formation-hosted gold deposits of the Timmins area. In: The Geology of Gold in Ontario, A.C. Colvine (ed.). Ontario Geol. Surv. Misc. Paper 110, pp.98-110.

_____, Schwarcz, H.P., and Crocket, J.H., 1984, Carbonatization and gold mineralization in the Timmins area, Abitibi greenstone belt: genetic links with Archean mantle CO_2-degassing and lower crust granulitization. Geol. Assoc. Canada Prog. with Abstracts, v. 9, p. 65.

Gates, T.M. and Hurley, P.M., 1973, Evalutaion of Rb-Sr dating methods applied to the Matachewan, Abitibi, Mackenzie, and Sudbury dike swarms in Canada. Can. J. of Earth Science, v. 10, p. 900-919.

George, P.T., 1967, The Timmins District. In: CIM Centennial Field Excursion, Northwestern Quebec and Northern Ontario, pp. 103-107.

Golding, S.D. and Wilson, A.F., 1983, Geochemical and stable isotope studies of the No. 4 lode, Kalgoorlie, Western Australia. Econ. Geol., v. 78, p. 438-450.

Goodwin, A.M., 1965, Volcanism and gold deposition in the Birch Uchi Lakes area. Canadian Institute of Mining and Metallurgy Transactions, 68, pp. 91-104.

Goodwin, A.M., and Ridler, R.H., 1977, The Abitibi orogenic belt. In: The Archean. G.J.H. McCall (ed.). Dowden, Hutchinson and Ross Inc., Stroudsburg, Pennsylvania, pp. 138-165.

Gorman, B.E., Kerrich, R., and Fyfe, W.S., 1981, Geochemistry and field relations of lode gold deposits in felsic igneous intrusions - porphyries of the Timmins District. Ontario Geological Survey Miscellaneous paper 98, p. 108-124.

Govett, G.J.S., 1985, "Rock geochemistry in mineral exploration". *Handbook of Exploration Geochemistry*, vol. 3, Elsevier, Amsterdam, 462 pp.

Graves, M. C., and Zentilli, M., 1982, A review of the geology of gold in Nova Scotia. CIM Special Volume 24, Geology of Canadian Gold Deposits, R.W. Hodder and W. Petruk, (eds.), p. 233-241.

Green, A.H., Donnelly, T.H., Jahnke, F.M. and Keays, R.R., 1982, Evolution of gold-bearing veins in dykes of the Woods Point Dyke Swarm, Victoria. Mineral. Deposits, v. 17, p. 175-192.

Griffis, A.T., 1968, McIntyre Porcupine Mines Limited. In: Geology and Ore Deposits of Tisdale Township, Ontario. Dept. of Mines, Geol. Report 58, p. 122-130.

Groves, D.I., and Batt, W.D., 1984, Spatial and temporal variations of Archean metallogenic associations in terms of evolution of granitoid-greenstone terrains with particular emphasis on the Western Australian Shield. In: Archean Geochemistry, A. Kroner, G.N. Hanson and A.M. Goodwin (ed.) SpringerVerlag, New York, p. 73-98.

Guha, J., Gauthier, A., Vallee, M., Descarreaux, J., and Lange-Brard, F., 1982, Gold mineralization at the Doyon Mine (Silverstack), Bousquet, Quebec. CIM Special Volume 24.

Gunning, H.C., and Ambrose, J.W., 1940, Malartic Area, Quebec. Geol. Surv. Canada Memoir 222, Publ. 2454. Geology of Canadian Gold Deposits, R.W. Hodder and W. Petruk, (eds.), p. 50-66.

Haack, U., Heinrichs, H., Boneb, M., and Schneider, A., 1984, Loss of metals from pelites during regional metamorphism. Contrib. Mineral. Petrol., v. 85, pp. 116-132.

Hallberg, J.A., Johnston, C., and Bye, S.M., 1976, The Archean Marda igneous complex, Western Australia. Precambrian Res., v. 3, p. 111-136.

Hart, S.R. and Brooks, C., 1974, Clinopyroxene-matrix partitioning of K, Rb, Cs, Sr, and Ba. Geochim. Cosmochim. Acta, v. 38, p. 1799.

Hattori, K., and Cameron, E.M., 1986, Archean magmatic sulphate. Nature, v. 319, p. 45-47.

Helgeson, H.C., and Garrels, R.M., 1968, Hydrothermal transport and deposition of gold. Econ. Geol., v. 63, p. 622-635.

Henderson, J.F., and Brown, I.C., 1966, Geology and structure of the Yellowknife Greenstone Belt, District of Mackenzie. Geological Survey of Canada, Bull. 141, 87 p.

Henley, R.W., Norris, R.J. and Peterson, C.J., 1976, Multistage ore genesis in the New Zealand Geosyncline, a history of postmetamorphic lode emplacement. Mineralium Deposits, v. 11, 180-196.

Higgins, N., and Kerrich, R., 1982, Progressive ^{18}O depletion during CO_2 separation from a carbon dioxide rich hydrothermal fluid: evidence from the Grey River tungsten deposit. Can. Jour. Earth Sci. (in press).

Hodgson, C.J., 1983, The Structure and Geological Development of the Porcupine Camp - A Re-Evaluation. In: The Geology of Gold in Ontario. A.C. Colvine (ed.). Ontario Geological Survey Miscellaneous Paper 110, p. 211-225.

Hodgson, C.J., and MacGeehan, P.J., 1981, Gold ore formation at the Campbell and Dickenson mines, Red Lake area. Ont. Geol. Survey Misc. Paper 98, p. 132-143.

Hodgson, C.J., and MacGeehan, P.J., 1982, A review of the geological characteristics of 'gold only' deposits in the Superior Province of the Canadian Shield. CIM Special Volume 24, Geology of Canadian Gold Deposits, R.W. Hodder and W. Petruk, (eds.), p. 211-229.

Hoefs, J., 1978, Some pecularities in the carbon isotopic composition of 'juvenile' carbons. Dept. Sci. Industrial Res. Bull. 220, p. 181-184.

Holland, H.D., 1967, Gangue minerals in hydrothermal ore deposits. In: Geochemistry of Hydrothermal Ore Deposits, H.L. Barnes, (ed.), Holt, Rinehart and Winston, New York, p. 382-486.

Holland, H.D., 1978, The chemistry of the atmosphere and oceans. Wiley Interscience, New York, 351 pp.

Holland, H.D., and Malinin, S.D., 1979, The solubility and occurrence of non-ore minerals. In: Geochemistry of Hydrothermal Ore Deposits, H.L. Barnes, (ed.), Wiley, New York, N.Y., p. 461-508.

Hunt, J.A., and Kerrick, D.M., 1977, The stability of sphene; experimental redetermination and geologic implications. Geochimica et Cosmochimica Acta, v. 41, p. 279-288.

Hurst, M.E., 1935, Vein formation at Porcupine, Ontario. Econ. Geol., v. 30, p. 103-127.

Hutchinson, R.W., 1976, Lode gold deposits; the case for volcanogenic derivation. In: Proceedings Volume, Pacific Northwest Mining and Metals Conference, Portland, Oregon, 1975, Oregon Dept. Geol. and Mineral Ind., p. 64-105.

Ildefonse, J.P., and Gabis, V., 1976, Experimental study of silica diffusion during metasomatic reactions in the presence of water at 550° and 1000 bars. Geochimica et Cosmochimica Acta, v. 40, p. 297-303.

Janardhan, A.S., Newton, R.C., and Smith, J.V., 1979, Ancient crustal metamorphism at low P_{H_2O}: charnokite formation at Kabbaldurga, South India. Nature (London), v. 278, p. 511-514.

Javoy, M., 1977, Stable isotopes and geothermometry. Journal of the Geological Society of London, v. 133, pp. 609-636.

Javoy, M., Pineau, F. and Delorme, H., 1986, Carbon and nitrogen isotopes in the mantle. Chem. Geol., v. 57, p. 41-62.

Jolly, W.T., 1974, Regional metamorphic zonation as an aid in study of Archean terrains: Abitibi region, Ontario. Canadian Mineralogist, v. 12, p. 499-508.

Jones, W.A., 1948, Hollinger Mine. In: Structural Geology of Canadian Ore Deposits, vol. 2, Canadian Institute of Mining and Metallurgy, Mercury Press, Montreal, p. 464-481.

Karvinen, W.O., 1978, The Porcupine Camp - a model for gold exploration in the Archean. Can. Min. Jour., Sept. 1978, p. 49-53.

Karvinen, W.O., 1980, Geology and evolution of gold deposits, Timmins area, Ontario. In: G.C. Roberts, (ed.), Genesis of Archean, Volcanic-Hosted Gold Deposits, Symposium, Waterloo, 1980; Ont. Geol. Surv. Open File Report 5293, p. 1-43.

Kennedy, L.P., and Kerrich, R., 1982, Transition from marine to meteoric water hydrothermal regimes in an emerging Archean intrusive complex: ^{18}O evidence from the Morran pluton. American Geophys. Union Abstracts, San Francisco, December 1982.

Kerrich, R., and Allison, I., 1978, Vein geometry and hydrostatics during Yellowknife mineralization. Canadian Jour. Earth Sci., v. 15, 1653-1660.

Kerrich, R., 1979, Lode gold deposits in greenstone belts, chemical and hydrodynamic constraints. In: Gold: Exploration and Outlook, T. Anderson, P. Chamois and D. Desnoyers (eds.), Proceedings, Adams Club 8th Annual Special Symposium, February 1979, McGill University, Montreal, p. 13-34.

Kerrich, R., 1980, Archean gold-bearing chemical sediments and veins: a synthesis of stable isotope and geochemical relations. In: R.G. Roberts, (ed.), Genesis of Archean, Volcanic-Hosted Gold Deposits, Symposium, Waterloo, 1980; Ontario Geol. Surv. Open File Report 5293, p. 137-211.

Kerrich, R., 1981, Archean lode gold deposits: a synthesis of data on metal distribution, fluid inclusions and stable isotopes, with special reference to Yellowknife. Proceedings, Gold Workshop, Yellowknife, December 1979.

Kerrich, R., 1983, Geochemistry of gold deposits in the Abitibi greenstone belt. CIM Special Paper 27.

Kerrich, R., 1985, Archean lode gold deposits: the solute source problem. Geol. Soc. Amer., Abstr. with Programs 17, p. 627.

Kerrich, R., 1986a, Archean lode gold deposits of Canada: Parts I and II, a synthesis of geochemical data from selected mining camps, with emphais on patterns of alteration. Information Circular, Econ. Geol. Res. Unit, Univ. Witwatersrand, Johannesburg 192, 34 pp.

Kerrich, R., 1986b, Fluid infiltration into fault zones: chemical, isotopic and mechanical effects. J. Pure Applied Geophys., v. 124, p. 225-268.

Kerrich, R., 1986c, Fluid transport in lineaments. Phil. Trans. Royal Soc. London, Ser. A317, p. 219-251.

Kerrich, R., 1987, The stable isotope geochemistry of Au-Ag vein deposits in metamorphic rocks. In: T.K. Kyser (ed.). Mineralogical Association of Canada, Short Course, v. 13, p. 287-336.

Kerrich, R., and Fryer, B.J., 1979, Archean precious metal hydrothermal systems; Dome Mine, Abitibi greenstone belt; II REE and oxygen isotope relations. Can. Jour. Earth Sci., v. 16, p. 440-458.

Kerrich, R.W., and Fryer, B.J., 1987, Lithophile element systematics of Archean vein Au deposits: monitor of source processes. Geol. Assoc. Canada, Program with Abstracts, v. 12, p. 61.

Kerrich, R., Fryer, B.J., King, R.W., Willmore, L.M., Van Hees, E. and Daddar, R., 1987, Crustal outgassing and LILE enrichment in major lithosphere structures, Archean Abitibi greenstone belt: evidence on the source reservoir from Sr and C isotope tracers. Contrib. Mineral. Petrol. (in press).

Kerrich, R., Fryer, B.J., Milner, K., and Peirce, M.G., 1981, The geochemistry of gold-bearing chemical sediments; Dirkenson mine, Red Lake, Ontario: a reconaissance study. Canadian Jour. Earth Sci., v. 18, 624-637.

Kerrich, R. and Fyfe, W.S., 1983, The ^{18}O, temperature and ^{34}S of Archean Ocean Bottom Water (2.8 Ga). Abstract, G.S.C. A37.

Kerrich, R., and Fyfe, W.S., 1981, The gold-carbonate association: source of CO_2 and CO_2-fixation reactions in Archean lode deposits. Chemical Geology, v. 33, p. 265-294.

Kerrich, R., Fyfe, W.S., and Allison, I., 1977a, Iron reduction around gold-quartz veins, Yellowknife district, Northwest Territories, Canada. Econ. Geol., v. 72, p. 657-663.

Kerrich, R., and Hodder, R.W., 1982, Archean lode gold and base metal deposits: chemical evidence for metal separation into independent hydrothermal systems. In: CIM Special Volume 24, Geology of Canadian Gold Deposits, R.W. Hodder and W. Petruk, (eds.), p. 144-160.

Kerrich, R., LaTour, T.E., and Willmore, L.M. 1984, Fluid participation in deep fault zones: geological and $^{18}O/^{16}O$ evidence. Jour. Geophys. Res., v. 89, 4331-4343.

Kerrich, R., and Watson, G.P., 1984, The Macassa Mine Archean lode gold deposit, Kirkland Lake, Ontario: Geology, patterns of alteration, and hydrothermal regimes. Econ. Geol., v. 79, pp. 1104-1130.

King, R.W., Kerrich, R., 1987; (in press), Fluorapatite fenitization and gold enrichment in sheeted trondhjemites, with the Destor-Porcupine fault zone, Taylor Township, Ontario: Can. J. Earth Sci.

King, R.W. and Kerrich, R., 1987, Fluorpatite fenitization and gold enrichment in sheeted trandhjemites within the Destor – Porcupine fault zone, Taylor Township, Ontario. Canadian Jour. of Earth Sci., v. 24, 479-502.

King, R.W., Kerrich, R., and Hofmann, E., 1986, Tourmaline geochemistry in Archean lode gold deposits. Proceedings, Gold '86, Toronto.

Kishida, A., 1984, Hydrothermal alteration zoning and gold concentration at the Kerr-Addison Mine, Ontario, Canada. Ph.D. thesis, University of Western Ontario, London, Canada, 231 p.

Kishida, A. and Kerrich, R., 1987, Hydrothermal alteration zoning and gold concentration at the Kerr-Addison Archean lode gold deposit, Kirkland Lake, Ontario. Econ. Geol. (in press).

Knapp, R.B., and Knight, J.E., 1977, Differential thermal expansion of pore fluids: fracture textured peridotites and magnesian and low magnesian tholeiites. Earth and Planet. Sci. Lett., v. 31, p. 433-453.

Knauth, P., and Lowe, D.R., 1978, Oxygen isotope geochemistry of cherts from the Onverwacht Group (3.4 billion years), Transvaal, South Africa, with implications for secular variations in the isotopic composition of cherts. Earth Planet. Sci. Lett., v. 41, p. 209-222.

Knopf, A., 1929, The Mother Lode system of California. U.S. Geological Survey, Prof. Paper 157.

Krupka, K.M., Ohmoto, H., and Wickman, F.E., 1977, A new technique in neutron activation analysis of Na/K ratios of fluid inclusions and its application to the gold-quartz veins at the O'Brien mine, Quebec, Canada. Can. Jour. Earth Sci., v. 14, p. 2760-2770.

Kusakabe, M., 1974, Sulphur isotope variations in nature: 10. Oxygen and sulphur isotope study of Wairakei geothermal well discharges. New Zealand J. Sci., v. 1, p. 183-191.

Kwong, Y.T.J., and Crocket, J.H., 1978, Background and anomalous gold in rocks of an Archean greenstone assemblage, Kakiqi Lake Area, Northwestern Ontario. Econ. Geol., v. 73, p. 50-63.

Kyser, T.K., Janser, B.W., Wilson, M.R. and Hattie, I., 1986, Stable isotope geochemistry related to gold mineralization and exploration in the Western Shield. In: Gold in the Western Shield, L.A. Clark, (ed.). CIM Special Vol. 38, p. 470-498.

Kyser, T.K., (1986), Stable Isotope Variations in the Mantle. In: Valley, J.W., Taylor, H.P., Jr., and O'Neil, J.R. (eds.). Stable Isotopes in High Temperature Geological Processes. Min. Soc. America, Revs. in Mineralogy, v. 16, 141-164.

Lambe, W., and Valley, J.W. (1984), Metamorphism of reduced granulites in low CO_2 vapour-free environment. Nature. v. 312, 56-58.

Lambert, I.B., Donelly, T.H., Phillips, G.N., and Groves, D.I., 1983, S-isotope compositions and genesis of Archaean Au mineralization, Western Australia. CSIRO Review, pp. 96-97.

Lambert, I.B., Phillips, G.N. and Groves,D.I., 1984, Sulphur isotope compositions and genesis of Archean gold mineralization, Australia and Zimbabwe. In: Proceedings Symposium Gold '82, Geol. Soc. Zimbabwe, Spec. Publication 1, A.A. Bulkema, (ed.), Rotterdam, The Netherlands.

Lavigne, M.J. and Crocket, J.H., 1982, A comparative study of sulphur isotope distribution of sulphide facies banded iron formations and the East South C ore zone, Dickenson gold mine, Red Lake District: a preliminary report. Current Research Part A, Geol. Surv. of Canada, Paper 82-1A, p. 265-274.

Lindgren, W., 1905, Metasomatic processes in the gold deposits of Western Australia. Econ. Geol., v. 1, p. 530-544.

Lowell, J.D., and Guilbert, J.M., 1970, Lateral and vertical alteration mineralization zoning in porphyry ore deposits. Econ. Geol., v. 65, p. 373-408.

Lydon, J.W., 1980, The behaviour of metals in hydrothermal systems with emphasis on gold. Workshop on Epithermal Deposits, Geoscience Forum, Whitehorse, Yukon.

Macdonald, A.J., 1983, The iron formation - gold association: evidence from Geraldton area. In: The Geology of Gold in Ontario, A.C. Colvine, (ed.). Ontario Geol. Surv. Misc. Paper 110, p. 75-83.

MacGeehan, P.J., and Hodgson, C.J., 1980, Relationship of gold mineralization to volcanic and metamorphic features in the area of Campbell, Red Lake, and Dickenson Mines, Red Lake Area, Ontario. In: Pyye, E.G., and Roberts, R.G. (eds.) Genesis of Archean volcanic-hosted gold deposits. Ontario Geol. Surv. Misc. Pap. 97, 94-110.

———, 1982, Environments of gold mineralization in the Campbell, Red Lake and Dickenson Mines, Red Lake District, Ontario. In: Hodder, R.W. and Petruk, W., (eds.) Geology of Canadian Gold Deposits. CIM Special Volume 24, 184-207.

MacGeehan, P.J., Sanders, T., and Hodgson, C.J., 1982, Meter-wide veins and a kilometer-wide anomaly: wall-rock alteration at the Campbell, Red Lake and Dickenson mines, Red Lake District, Ontario. CIM Bulletin, v. 75, no. 841, p. 90-102.

Marmont, S., 1983, The role of felsic intrusions in gold mineralization. In: The Geology of Gold in Ontario, A.C. Colvine, (ed.). Ontario Geol. Surv. Misc. Paper 110, p. 38-47.

McNeil, A.M. and Kerrich, R., (in press), Archean lamprophyric dykes and gold mineralization, Matheson, Ontario: the conjunction of LIL-enriched mafic magmas, deep crustal structures and Au concentration.

Meyer, C., and Hemley, J.J., 1967, Wall rock alteration. In: Geochemistry of Hydrothermal Ore Deposits, H.L. Barnes, (ed.), Holt, Rinehart and Winston, New York, p. 166-235.

Montoya, J.W. and Hemley, J.J., 1975, Activity relations and stabilities in alkali feldspar and mica alteration reactions. Econ. Geol., v. 70, pp. 577-594.

Muehlenbachs, K., and Clayton, R.N., 1972a, Oxygen isotope studies of the fresh and weathered submarine basalts. Can. Jour. Earth Sci., v. 9, p. 172-184.

Muehlenbachs, K., and Clayton, R.N., 1972b, Oxygen isotope geochemistry of submarine greenstones. Can. Jour. Earth Sci., v. 9, p. 471-478.

Munha, J., Fyfe, W.S., and Kerrich, R., 1980, Adularia, the characteristic mineral of felsic spilites. Contributions to Mineralogy and Petrology, v. 75, p. 15-19.

Nesbitt, R.W. and Sun, S.S., 1976, Geochemistry of Archean spinifex textured peridotites and magnesian, and low magnesian tholeiites. Earth Planet. Sci. Lett., v. 31, 433-453.

Nesbitt, B.E., Murowchick, J.B. and Muehlenbachs, K., 1986, Dual origin of lode deposits in the Canadian Cordillera. Geology, v. 14, p. 506-509.

Newton, R.C., Smith, J.V., and Windley, B.F. 1980, Carbonic metamorphism, granulites and crustal growth. nature, v. 288, 45-50.

Norris, R.J., and Henley, R.W., 1976, Dewatering of a metamorphic pile. Geology, v. 4, p. 333-336.

Ohmoto, H., 1986, Stable isotope geochemistry of ore deposits. In: Stable Isotopes in High Temperature Geological Processes, J.W. Valley, H.P. Taylor Jr., and J.R. O'Neil, (eds.). Reviews in Mineral., v. 16, p. 491-560.

Ohmoto, H., and Rye, R.O., 1979, Isotopes of sulphur and carbon. In: Geochemistry of Hydrothermal Ore Deposits, 2nd edition, H.L. Barnes, (ed.), John Wiley and Sons, New York, pp. 509-562.

Olade, M.A. and Fletcher, W.K., 1975, Primary dispersion of rubidium and strontium around porphyry copper deposits, Highland Valley, British Columbia. Econ. Geol., v. 70, p. 15-21.

Olade, M.A. and Fletcher, W.K., 1976, Trace element geochemistry of the Highland Valley and Guichon Creek Batholith in relation to porphyry copper mineralization. Econ. Geol., v. 71, p. 733-748.

Oyarzun, J., 1974, Rubidium and strontium as a guide to copper mineralization emplaced in some Chilean andesitic rocks [abs.]. International Geochem. Explor. Symp., 5th Vancouver, p. 48.

Pattison, E.F., Sauerbrei, J.A., Hannila, J.J. and Church, J.F., 1986, Gold mineralization in the Casa Berardi Area, Quebec, Canada. In: Proceedings Gold '86, A.J. MacDonald, (ed.), p. 170-183.

Pearton, T.N., 1982, Gold and antimony mineralization in altered komatiites of the Murchison greenstone belt, South Africa. In: Komatiites, N.T. Arndt and E.G. Nisbet, (eds.). George Allen and Unwin, London, p. 459-475.

Phillips, G.N. and Groves, D.I., 1983, The nature of Archaean gold-bearing fluids as deduced from gold deposits of Western Australia. Journal of the Geological Society of Australia, v. 30, pp. 25-39.

Phillips, G.N., Groves, D.I., and Martyn, J.E., 1984, An epigenetic origin for Archean banded iron-formation-hosted gold deposits. Econ. Geol., v. 79, pp. 162-171.

Phillips, G.N., Groves, D.I., Neall, F.B., Donnelly, T.H. and Lambert, I.B., 1986, Anomalous sulphur isotopic compositions in the Golden Mile, Kalgoorlie. Econ. Geol., v. 81, p. 2008-2015.

Pyke, D.R., 1975, On the relationship of gold mineralization and ultramafic volcanic rocks in the Timmins area. Ontario Div. Mines, Misc. Paper 12, 23 p.

Pyke, D.R., 1976, On the relationship of gold mineralization and ultramafic volcanic rocks in the Timmins area, Northeastern Ontario. CIM Bulletin, v. 69, no. 773, p. 79-87.

Radke, A.S., and Scheiner, B.J., 1970, Studies of hydrothermal gold deposition (I). Carlin deposit, Nevada: the role of carbonaceous material in gold deposition. Econ. Geol., v. 65, p. 87-102.

Ridge, J.D., 1968, Changes and developments in concepts of ore genesis - 1933-1967. In: J.D. Ridge (ed.), Ore Deposits of the United States, 1933-1967, p. 1713-1834.

Ridler, R.H., 1970, Relationship of mineralization to volcanic stratigraphy in the Kirkland Larder Lakes area, Ontario. Proceedings of the Geological Association of Canada, 21, pp. 33-42.

Ridler, R.H., 1976, Stratigraphic keys to the gold metallogeny of the Abitibi Belt. Can. Mining Jour., v. 97, p. 81-88.

Roberts, R.G., 1980, The volcanic-tectonic setting of gold deposits in the Timmins area. In: Genesis of Archean, Volcanic-Hosted Gold Deposits, R.G. Roberts, (ed.), Ont. Geol. Surv., Open File Rept. 5293, p. 359-387.

Robinson, B.W., and Christie, A.b., 1980, Epithermal silver-gold mineralization, Maratoto Mine, New Zealand: stable isotopes and fluid inclusions. Proc. 5th Quadrennial IAGOD Symp., Stuttgart, Germany, p. 719-730.

Roedder, E., 1972, Composition of fluid inclusions, Chapter JJ: U.S. Geol. Surv., Prof. Pap. 440-JJ. 164 p.

_____, 1979, Fluid inclusions as samples of ore fluids. In: Barnes, H.L. (ed.) Geochemistry of hydrothermal ore deposits. Wiley Intersci.

_____, 1984a, The fluids in salt: 1929 Am. Mineral (in press).

_____, 1984b, Fluid inclusion evidence bearing on the environments of gold deposition: in Proceedings of Symposium: Gold 82, Geol. Soc. Zimbabwe Spec. Pub. 1; R.P. Foster and A.A. Balkema, eds., Rotterdam, pp. 129-163.

Rose, A.W. and Burt, D.M., 1979, Hyrdothermal Alteration. In: Barnes H.L. (ed.) Geochemistry of hydrothermal ore deposits. Wiley, New York, 173-235.

Roslyakova, N.V. and Roslyakov, N.A., 1975, Gold deposit endogenic halos. Geol. Surv. Canada Translation 896. Akad. nauk SSSR Sibirskoe otdelenie, 182, Novasilivisk, USSR.

Rye, R.O., and Ohmoto, H., 1974, Sulfur and carbon isotopes and ore genesis: a review. Econ. Geol., v. 69, p. 826-842.

Rye, D.M., and Rye, R.O., 1974, Homestake gold mine, South Dakota: I. Stable isotope studies. Econ. Geol., v. 69, p. 293-317.

Saager, R., Meyer, M., and Muff, R., 1982, Gold distribution in supracrustal rocks from Archean greenstone belts of Southern Africa and from Palaeozoic ultramafic complexes of the European Alps: metallogenic and geochemical implications. Econ. Geol., v. 77, p. 1-24.

Sawkins, F.J., 1964, Lead-zinc ore deposition in the light of fluid inclusion studies, Providencia Mine, Zacatecas, Mexico. Econ. Geol., v. 59, 883-919.

Schidlowski, M., Eichmann, R. and Tunge, C.E., 1975, Precambrian sedimentary carbonates: carbon and oxygen isotope geochemistry and implications for the terrestrial oxygen budget. Precambrian Research, v. 2, p. 1-19.

Schoell, M. and Wellmer, F.W., 1981, Anomalous ^{13}C depletion in early Precambrian graphites from Superior Province, Canada. Nature, v. 290, p. 696-699.

Schwarcz, H.P. and Rees, C.E., 1984, S-34 in pyrite from gold deposits. In: Geoscience Research Seminar and Open House '84, Abstracts. Ont. Geol. Surv., p. 1.

Seward, T.M., 1979, Modern hydrothermal systems in New Zealand and their relation to gold mineralizing processes. Publs. Geol. Dep. and Extension Service, Univ. West Australia, 3.

Shaw, D.M., 1968, A review of K-Rb fractionation trends by covariance analysis. Geochimica Cosmochimica Acta, v. 32, p. 573-601.

Sheppard, S.M.F., Nielsen, R.L., and Taylor, H.P., 1971, Hydrogen and oxygen isotope ratios in minerals from porphyry copper deposits. Econ. Geol., v. 66, p. 515-542.

Smith, I.J. and Kesler, S.E., 1985, Relation of fluid inclusion geochemistry to wallrock alteration and lithogeochemical zonation at the Hollinger- McIntyre gold deposit, Timmins, Ontario, Canada. CIM Bulletin, v. 78, no. 876, pp. 35-46.

Spooner, E.T.C., Chapman, J.H., and Smewing, J.D., 1977, Strontium isotope contamination and oxidation of the ophiolitic rocks of the Troodos Massif, Cyprus. Geochim. Cosmochim. Acta, v. 41, p. 873-890.

Takenouchi, S., and Kennedy, A.C., 1965, The solubility of carbon dioxide in CaCl solutions at high temperatures and pressures. Amer. Jour. Sci., v. 263, p. 445-454.

Tarney, J., 1975, Geochemistry of Archean high-grade gneisses, with implications as to the origin of the Precambrian Crust. In: The Early History of the Earth. B.J. Windley (ed.). John Wiley, London, p. 405-417.

Taylor, H.P., 1974, The application of oxygen and hydrogen isotope studies to problems of hydrothermal alteration and ore deposition. Econ. Geol., v. 69, p. 843-883.

Taylor, H.P., 1979, Oxygen and hydrogen isotope relations in hydrothermal mineral deposits. In: Geochemistry of Hydrothermal Ore Deposits. H.L. Barnes, (ed.), Wiley, New York, pp. 236-277.

Taylor, S.R., and McLennan, S.M., 1985, The Continental Crust: its Composition and Evolution. Blackwell Scientific, Oxford, 312 pp.

Thurston, P.C., and Fryer, B.J., 1983, The Geochemistry of repetitive cyclical volcanism from basalt through rhyolite in the Uchi-Confederation greenstone belt, Canada. Contributions to Mineralogy and Petrology, v. 83, p. 204-226.

Tilling, R.I., Gottfried, D., and Rowe, J.J., 1973, Gold abundance in igneous rocks: bearing on gold mineralization. Econ. Geol., v. 68, p. 168-186.

Turekian, K.K., and Wedepohl, K.H., 1961, Distribution of the elements in some major units of the earth's crust. Geol. Soc. America Bull., v. 7, p. 175-192.

Turner, F.J., 1981, Metamorphic Petrology. McGraw-Hill, New York, 524 pp.

Valley, J.W. (1986), Stable Isotope Geochemistry of Metamorphic Rocks. In: Valley, J.W., Taylor, H.P., Jr., and O'Neil, J.R. (eds.). Stable Isotopes in High temperature Geological Processes. Min. Soc. America, Reviews in Mineralogy, v. 16, 445-490.

Viljoen, R.P., Saeger, R., and Viljoen, M.P., 1970, Some thoughts on the origin and processes responsible for the concentration of gold in the early Precambrian of Southern Africa. Mineralium Deposita, v. 5, p. 164-180.

Wanless, R.K., Boyle, R.W., and Lowden, J.A., 1960, Sulphur isotope investigation of the gold-quartz deposits of the Yellowknife district. Econ. Geol., v. 55, p. 1591-1621.

Weiss, P.L., Friedman, I. and Gleason, J.P., (1981), The origin of epigenetic graphite: evidence from isotopes. Geochim. Cosmochim. Acta, v. 45, p. 2325-2332.

Winkler, H.G.F., 1976, Petrogenesis of Metamorphic Rocks. Springer Verlag, New York, 334 p.

Wolery, T.J., and Sleep, N.H., 1976, Hydrothermal circulation and geochemical flux at mid-ocean ridges. Jour. Geol., v. 84, p. 249-275.

Wood, P.C., Burrows, D.R., Thomas, A.V. and Spooner, E.T.C., 1986, The Hollinger-McIntyre Au-quartz vein system, Timmins, Ontario, Canada; geologic characteristics, fluid properties and light stable isotope geochemistry. Proc. Gold '86, A.J. MacDonald, (ed.), Toronto, p. 56-80.

Wyman, D.A., Kerrich, R., and Fryer, B.J., 1986, Gold mineralization overprinting iron formation at Agnico-Eagle Deposit, Quebec, Canada: mineralogical, microstructural and geochemical evidence. In: Proc. Gold '86, A.J. MacDonald, (ed.), Toronto, 1986, p. 108-123.

Zairi, N.M., Sher, S.D., Strizhev, V.P., Batrak, V.N. and Pankratyeva, L.D., 1978, Isotopic composition of sulphur from the zone of a gold-bearing sulphide impregnation. Inter. Geol. Revue, v. 20, p. 935-941.

Contribution to the Geology of the Northwest Territories, Volume 3, 1988, NWT Geology Division, INAC, Yellowknife.

Thrusting Between the Cameron River Greenstone Belt and the Sleeply Dragon Metamorphic Complex, Slave Province, District of Mackenzie

Timothy M. Kusky

Department of Earth and Planetary Sciences,
The Johns Hopkins University, Baltimore, Maryland, 21218, U.S.A.

Introduction

The Archean Slave Province is a granite – greenstone terrane in the northwestern portion of the Canadian shield. Unconformities between greenstone belt lithologies and older gneissic rocks have been reported from the Cameron River volcanic belt, approximately 100 km northeast of Yellowknife, and from the Point Lake area farther to the north (Baragar and McGlynn, 1976; Henderson, 1981, 1985). Most workers report that the unconformities have been modified by "later" faulting (e.g., Davidson, 1972; Baragar and McGlynn, 1976; Lambert, 1977; Henderson, 1981, 1985; Padgham, 1985) and the significance of this deformation needs to be assessed. As a start of such a reassessment the Cameron River Greenstone Belt and the Sleepy Dragon Metamorphic Complex were mapped in the vicinity of Webb Lake (85 I/14) and Sleepy Dragon Lake (85 I/15) (Figure 1) during the summer of 1985, extending the work of Davidson (1972) and Lambert (1974; 1977; 1982). Complimentary studies by W.K. Fyson and R. Cullen were underway in 1985 and 1986 to the north of this area.

Lithologies

The Cameron River Greenstone Belt consists predominantly of mafic to intermediate pillowed and massive

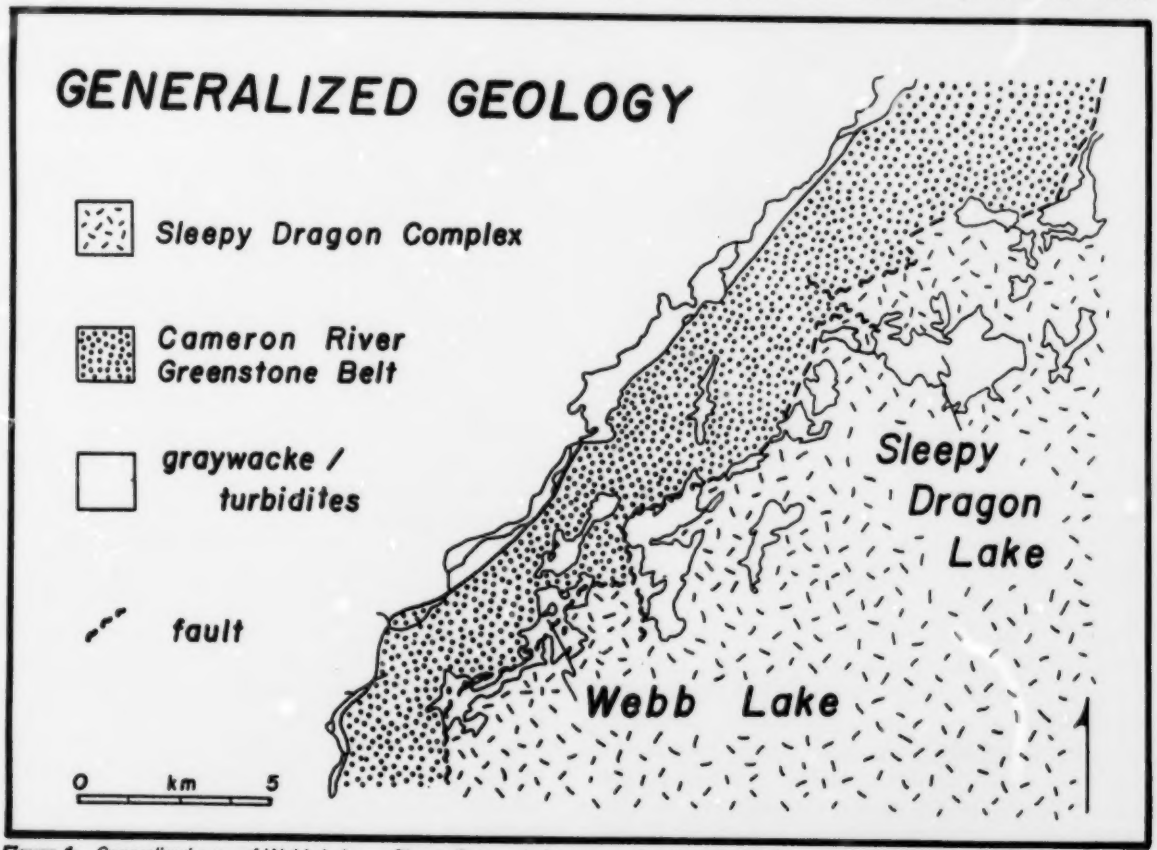

Figure 1: *Generalized map of Webb Lake – Sleepy Dragon Lake area, approximately 100 km northeast of Yellowknife. Modified from Henderson (1976).*

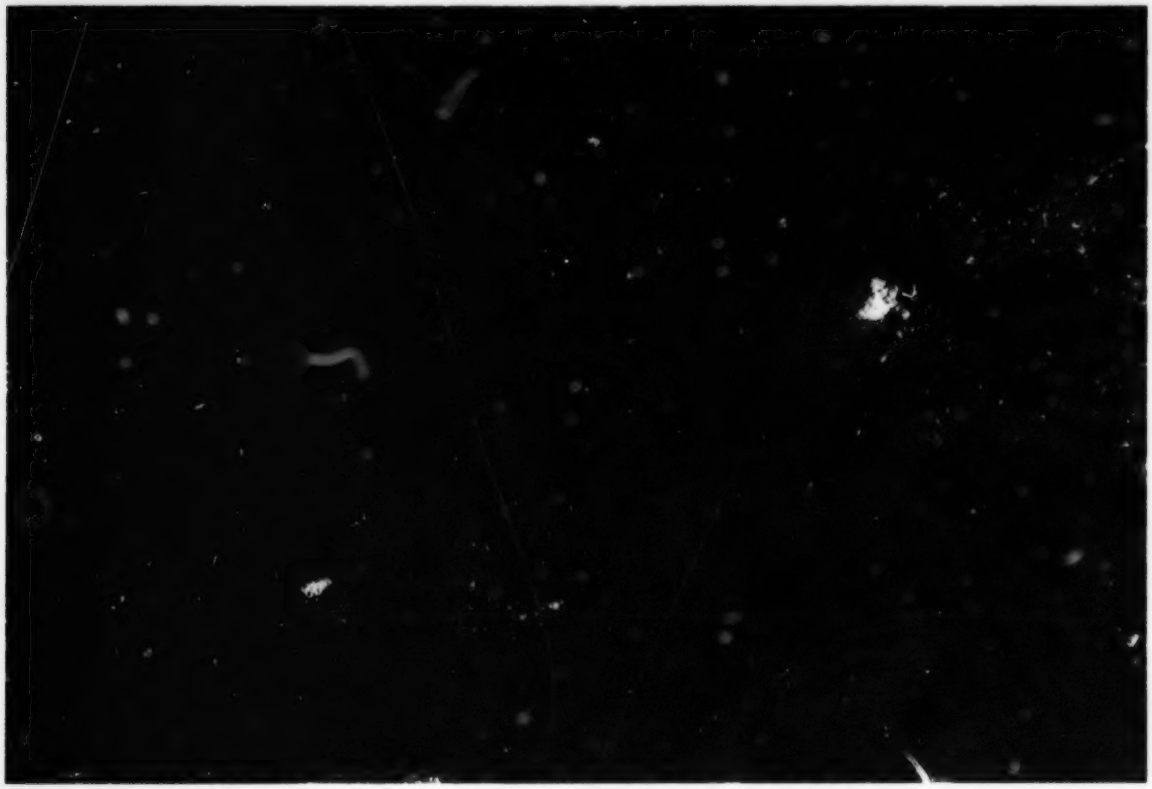

Figure 2: *Fiamme-like lenses in a tuff bed from the Cameron River Greenstone Belt west of Webb Lake.*

flows, and numerous dike and sill complexes (Lambert, 1977). The pillows typically have well-developed selveges and in some places exhibit amygdules. Empty (through leaching) and calcite filled feeder tubes are locally present and serve as a useful way-up indicator. Thick sills are difficult to distinguish from massive flows because of their common gradational nature and also because of the metamorphic overprinting of primary textures. Near the preserved base of the greenstone belt gabbroic dikes locally exhibit a sheeted aspect and display one-way chilling. In many cases the dikes have altered chlorite and epidote-rich centers, suggesting some interaction of hydrothermal fluids (sea water?) with the volcanic 'hypabyssal section (eg. Hoffman, 1985). Several pyroclastic units have also been recognized, including a spectacular tuff with clasts which have been flattened both parallel to bedding and parallel to cleavage (Figure 2). Although most of the larger quartz grains in this unit are clearly volcanic in origin (doubly terminated prismatic habit), the rounded character of some grains suggests that the tuff has been resedimented or deposited in a subaqueous environment. Euhedral to rounded blue quartz grains in the tuff have asymmetric pressure shadows developed around them, defining a vertical lineation and providing reliable sense of shear indicators. Although present, volcanic breccias are scarce in the Cameron River Belt, in comparison with the Yellowknife Greenstone Belt (eg. Padgham, 1981).

Rocks of the Sleepy Dragon Metamorphic Complex are highly variable, and include orthogneisses, paragneisses, augen-gneisses, biotite and muscovite schists, and several foliated granitoid plutons (Davidson, 1972). Quartz ribbons are ubiquitous in the gneissic rocks and close inspection reveals rootless isoclinal fold hooks in the foliation plane. Numerous mylonite zones cut the Sleepy Dragon Complex both obliquely and parallel to the local gneissic foliation. The mylonites show S-C banding, rotated porphyroclasts, and asymmetric pressure shadows; sense of shear determinations aimed at understanding their origin and significance are in progress. Older gneisses and mylonites are intruded by several younger phases of mafic to silicic plutonic rocks which show different states of deformation (Figure 3). Using these cross-cutting relationships together with isotopic dates it is anticipated that a structural chronology will be established for the Sleepy Dragon Complex.

Mafic dikes are abundant near the contact with the Cameron River Greenstone Belt (Lambert, 1982). Both the texture and xenolith content of these dikes appear to be generally different from those in the greenstone belt. Different suites of deformational and metamorphic fabrics in the dikes of the Sleepy Dragon Metamorphic Complex indicate that they belong to at least two, and probably three generations. Work is currently under way to determine which, if

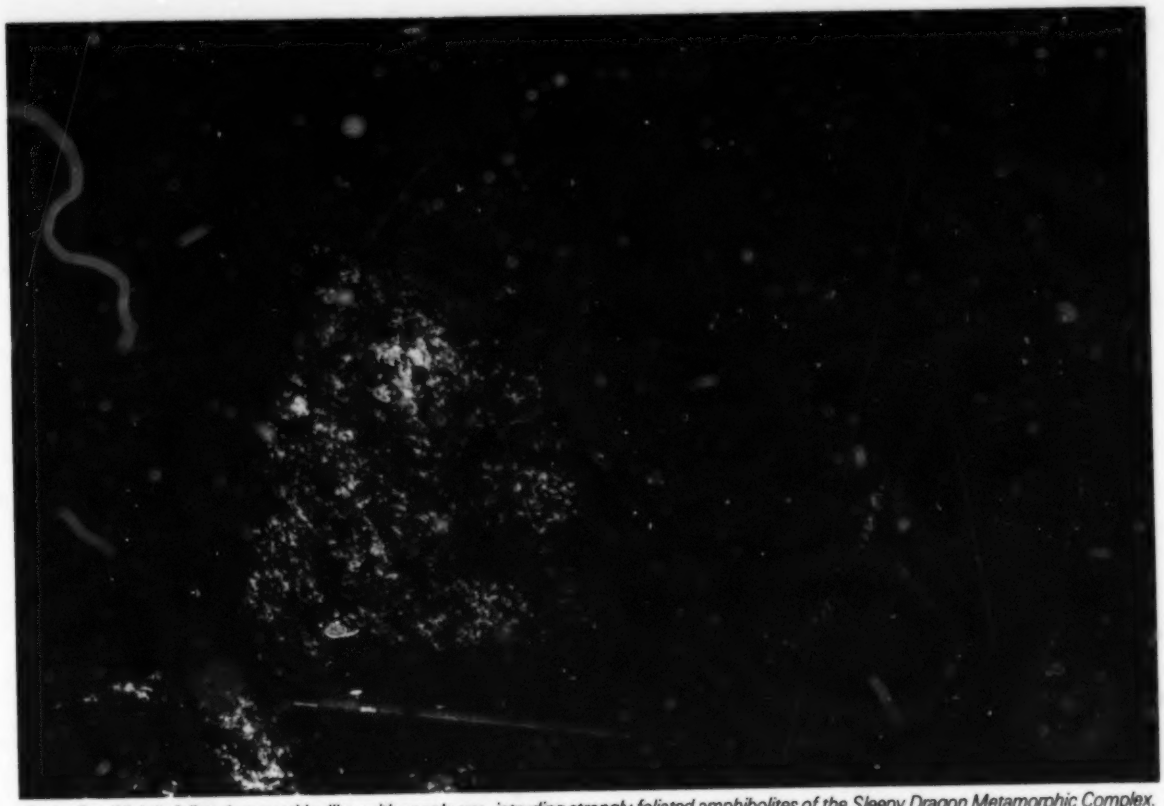

Figure 3: *Slightly foliated pegmatitic dike, with apophyses, intruding strongly foliated amphibolites of the Sleepy Dragon Metamorphic Complex.*

any, of the Sleepy Dragon dikes were contemporaneous with intrusions in the Cameron River Belt (cf. Lambert, 1982).

Basement-Cover Relationships

The contact between the Cameron River Greenstone Belt and the Sleepy Dragon metamorphic Complex was found to be a half-kilometer wide zone of very complex structure. All rocks within this high strain zone have a strong steeply plunging stretching lineation, although rocks from throughout the area also have a less intense vertical lineation. Transposed layering and intensely folded or boudinaged quartz segregations are present (Figures 4 and 5); their style of deformation is dependent on what their initial, undeformed orientation was. Sheath folds with vertically plunging hinges are common in some localities, indicating very high shear strains. Macroscopic sense of shear indicators are not abundant but generally suggest that the Cameron River Belt was thrust over the Sleepy Dragon Complex. Supporting microscopic work is currently underway. In one area north of Webb Lake some thin slivers of gneissic basement are intercalated with phyllonites of the major high-strain zone (Figure 6); kinematic indicators from this locality show that the volcanic belt has been thrust up against the Sleepy Dragon Complex, and imbricate faults sliced off pieces of the gneiss in the process. No other examples of Archean basement-involved thrusting of greenstone belt lithologies are yet known from the Slave Province (J. Brophy, pers. comm., 1985).

Pillow lavas of the Cameron River Belt immediately adjacent to the basal high-strain zone typically have aspect ratios exceeding 3:1:1/3. In a less strained area to the northwest of Sleepy Dragon Lake these lavas are overturned in an anticline as shown by locally consistent facing directions. The axial trace of this fold is parallel to the basal high strain zone, and its geometry is consistent with formation as a hanging wall anticline during thrusting of the Cameron River Belt over the Sleepy Dragon Complex. Mapping in the greenstone belt has revealed the presence of a few other subparallel shear zones containing structures similar to those just described; a common origin is tentatively inferred pending more detailed mapping. Thin mylonite zones were found as far as half way up from the base of the volcanic belt.

Interpreting the structures within the Sleepy Dragon Metamorphic Complex is difficult because of the complex deformation history of this terrane. The only structure which, at this point, can unambiguously be related to movement along the contact with the Cameron River Belt is a foliation which trends parallel to and increases in intensity towards the contact zone. The foliation cuts earlier structures including folded gneissic and mylonitic foliations. The fact that this foliation is cut by some plutonic bodies, and only partly

Figure 4: *Rootless folds and boudins of quartz in schist from the high strain zone at the base of the Cameron River Greenstone Belt.*

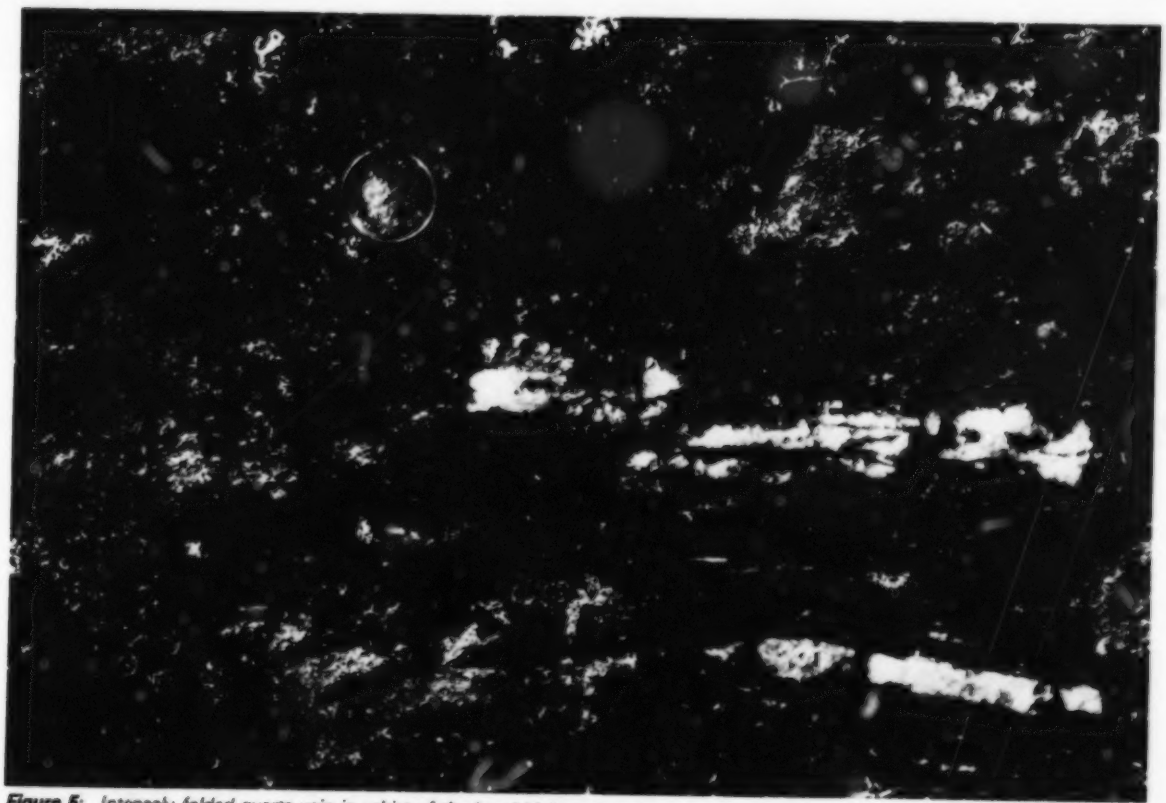

Figure 5: *Intensely folded quartz vein in schist of the basal high strain zone.*

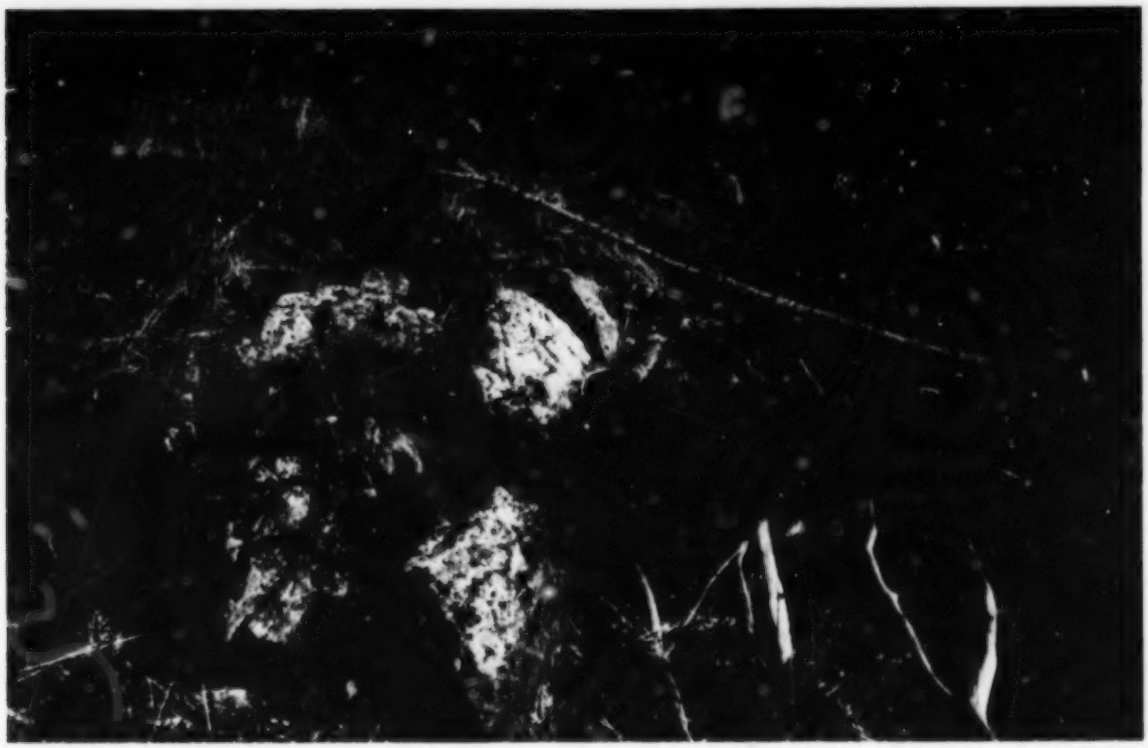

Figure 6: *Sliver of gneiss of the Sleepy Dragon Complex (light colored) incorporated in phyllonites from the high strain zone at the base of the Cameron River Greenstone Belt.*

developed in others, suggests that by using isotopic methods the age of deformation along the contact may be determined.

Conclusions

Preliminary mapping of the Cameron River Greenstone Belt and the Sleepy Dragon Metamorphic Complex in the vicinity of Webb Lake and Sleepy Dragon Lake has resulted in the discovery of a major high strain zone between the two distinct terranes. Sparse sense of shear indicators suggest that deformation along the contact is related to thrusting of the greenstone belt over the gneissic basement rocks. Imbrication and folding of the greenstone belt, as well as incorporation of slices of the basement into the basal shear zone, resulted from large displacements along this zone. Further mapping will be aimed at characterizing the style and geometry of this thrust zone, and will determine if relationships observed in the Webb Lake – Sleepy Dragon Lake area are valid elsewhere in the Cameron River Greenstone Belt. Whether this deformation is the result of the modification of an original unconformable relationship between genisses and greenstones, or whether it is a consequence of the juxtaposition of two once widely separated terranes is a question that will be studied in future field studies.

Acknowledgements

This work could not have progressed if it were not for the helpful discussions and logistical support of Bill Kidd, Bill Padgham, John Brophy, John Henderson, Maurice Lambert, Tony Davidson, Kris Saboda, Martin Irving, Bill Fyson, Declan DePaor, and Dwight Bradley. Funding was provided by the Geological Society of America and by The Johns Hopkins University.

References

Baragar, W.R., and McGlynn, J.C., 1976, Early Archean basement in the Canadian Shield: A review of the evidence; Geological Survey of Canada: Paper 76-14.

Davidson, A., 1972, Granite studies in the Slave Province; *in*: Report of Activities, Part A. Geological Survey of Canada: Pap. 72-la, pp. 109-115.

Henderson, J.B., 1976, Yellowknife (85J) and Hearne Lake (85I) map-areas. Geological Survey of Canada: Open File 353.

Henderson, J.B., 1981, Archean basin evolution in the Slave Province; *in*: Precambrian Plate Tectonics. A. Kroner (ed.), pp. 213-235.

Henderson, J.B., 1985, Geology of the Yellowknife-Hearne Lake Area, District of Mackenzie: A segment across an Archean basin. Geological Survey of Canada: Memoir 414, 135 pp.

Hoffman, S., 1985, The 3.5 B.Y. old Onverwacht Group: A *remnant of ancient oceanic crust; in*: Burke, K., (ed.), Workshop on the Early Earth. The interval from accretion to the older Archean, Lunar and Planetary Institute Technical Report 85-01: pp. 31-33.

Lambert, M.B., 1974, Archean volcanic studies in the Slave Bear Province; *in*: Report of Activities, April to October, 1973. Geological Survey of Canada: Pap. 74-1, Pt. A, pp. 177-179.

Lambert, M.B., 1977, Anatomy of a greenstone belt – Slave Province, N.W.T. Geological Association of Canada: Special Paper no. 16, pp. 331-340.

Lambert, M.B., 1982, Synvolcanic intrusions in the Cameron River Volcanic Belt, District of Mackenzie. Geological Survey of Canada: Paper 82-1A, pp. 165-167.

Padgham, W.A., 1981, Geology of the Yellowknife Volcanic Belt; *in*: Morton, R.D., (ed.), Proceedings of the Gold Workshop, Yellowknife, 1979. Yellowknife Gold Workshop Committee: pp. 288-322.

Padgham, W.A. 1985. Observations and speculations on supracrustal successions in the Slave Structural Province; *in*: Evolution of Archean supracrustal sequences, Ayres, L.D., Thurston, P.C., Card, K.D., and Weber, W., (eds.). Geological Association of Canada: Special Paper 28, pp. 133-151.

Contribution to the Geology of the Northwest Territories, Volume 3, 1988, NWT Geology Division, INAC, Yellowknife.

The Petrotectonic Environment of Basalts of Point and Redrock Lakes, Slave Province NWT.

Karen St.Seymour, Paul Budkewitsch and Stephen Kumarapeli

Concordia University, Montreal
Montreal, Quebec, H4B 1R6

Introduction

The petrotectonic environment represented by greenstone belts has remained a puzzle for workers investigating Archean terrains. The problems that Archean rock sequences present, stem from their fragmental preservation combined with tectonic complexity; the metamorphic imprint on their chemistry; uncertainties pertaining to the geochemical evolution and physical conditions of melting of the Archean mantle. Unfortunately, the probable characteristics of the Archean mantle and the presence of rocks such as ultramafic komatiites restricted to the Archean, have overshadowed the essential similarity between Archean and more recent volcanic rock assemblages. Due to this essential similarity, we think that the use of distribution patterns of High Field Strength (HFS) elements such as Ti, Zr, Y, considered to be immobile during metamorphism provides a useful tool for defining the volcanic environment. The interpretations from such data can be supported with the evidence provided by the major element and REE characteristics of the volcanic lithologies and the sedimentary characteristics of the depositional basin. The Point Lake and Redrock Lake Archean greenstone belts in the Slave Province were selected for research because of the following:

(1) Geochemical work on the volcanic lithologies was minimal for the Point Lake belt (Bostock, 1980; Easton, 1985) and non existent for the Redrock Lake belt therefore our study would establish a geochemical data base for these greenstone belts.
(2) There is excellent documentation of the stratigraphy, sedimentological character, basement-cover relationships, metamorphism and deformational regime for the Point Lake area to provide the background essential for the interpretation of the volcanic lithogeochemistry of this greenstone belt: Stockwell (1933); Henderson (1975, 1981); Henderson and Easton (1977); Easton (1985); Bostock (1980); Jackson (1983).

Field and Analytical Procedures

Three weeks of field work (July 1985) by a two person team provided 50 rock samples that were devoid of visible weathering or alteration other than the low grade regional metamorphic assemblage typical of these rocks. These have been analyzed for major and trace elements by XRF methods, thin-sectioned and studied. Five representative samples, petrographically screened for alteration have been analyzed for rare earths by Neutron Activation techniques.

Point Lake Greenstone Belt

General Geology

The southern half of the Point Lake area comprises three geological domains (Easton, 1985): 1) The westernmost terrain consists of para- and orthogneisses and migmatites. This terrain comprises a chloritized monzogranite to granodiorite with an age of 3.15 Ga, thought to be the infrastructure of the Yellowknife Supergroup. Rocks belonging to the Yellowknife Supergroup are found in 2) a central, north-south trending greenstone belt, and 3) a metasedimentary belt to the east, comprised of the Keskarrah (conglomerate) and Contwoyto (turbidite) Formations.

The volcanic stratigraphy of the Point Lake area has been described by Henderson and Easton (1977), Bostock (1980), and Jackson (1983) as a volcanic sequence starting with 100 to 500 m of mafic metatuff to the west, succeeded by massive and pillowed mafic to intermediate flows overlain by isolated centres of rhyolite and rhyodacite of predominantly pyroclastic character. The felsic volcanics are in a predominantly sedimentary succession at the eastern margin of the north-south trending greenstone belt. Three phases of deformation have been documented in the gneiss terrain, two of which have been traced in the supracrustal rocks in which the deformation complexity decreases basinwards (i.e. eastwards) from the gneiss (Jackson, 1983). The area of this study lies within the domain where overprinting of D_1 by D_2 structures defines the north-south trending structural grain, and in the vicinity of the southern arm of Point Lake (Fig. 1a).

Volcanic Petrology

The mafic volcanic rocks at Point Lake represent pillowed as well as massive flows the former being more voluminous, with beds of volcanic agglomerate, mafic tuff and rusty weathering intraflow sediments. They are basalts, and higher in the sequence are basaltic andesites and andesites. Conglomerate and sandstone of the Keskarrah Formation are locally stratigraphically interlayered with the flows. The colour of the mafic volcanics is determined by

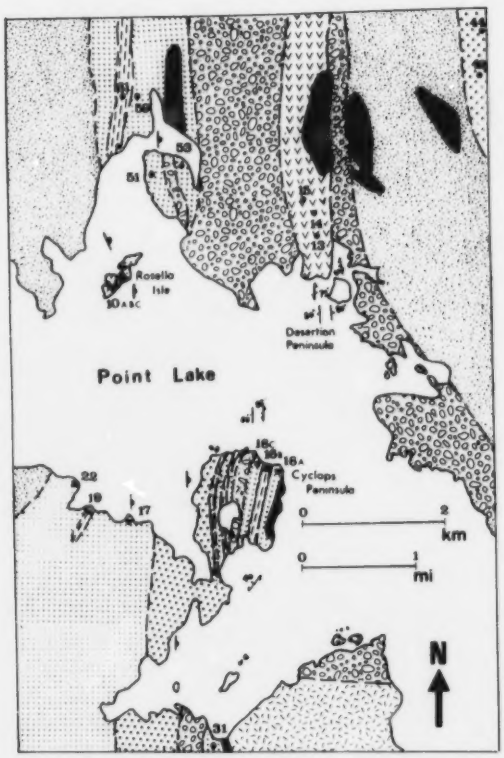

PROTEROZOIC

diabase

ARCHEAN

turbidite
conglomerate
sandstone
'mugearite'
pillow basalt
massive basalt
felsic volcaniclastics
granidiorite

Figure 1a: *Map of part of Point Lake showing sites sampled.*

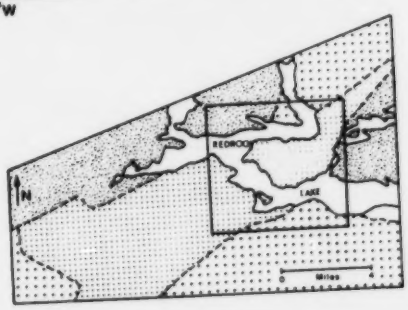

PROTEROZOIC

undivided

ARCHEAN

greenstone
granite

Figure 1b: *Index map of Point and Redrock Lake areas above and sites sampled at Redrock Lake below.*

PROTEROZOIC

undivided

ARCHEAN

pillow basalt
sheared pillow basalt
massive basalt
Carousel Massive Granite
Redrock Lake Granite

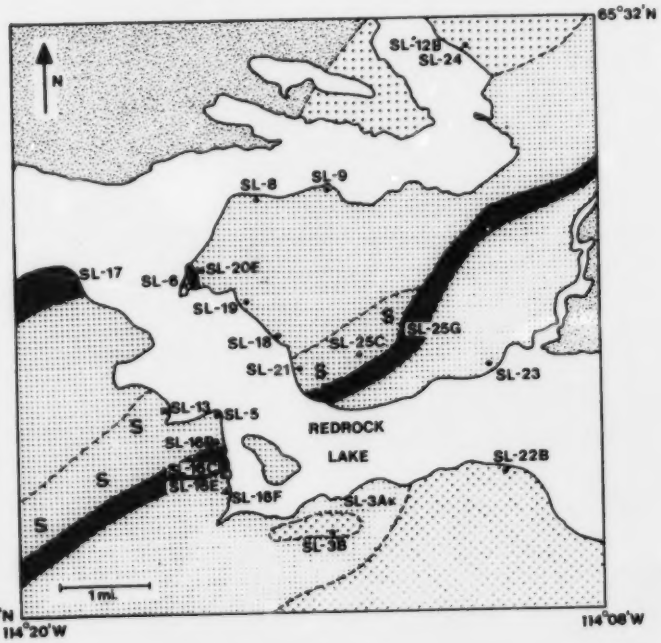

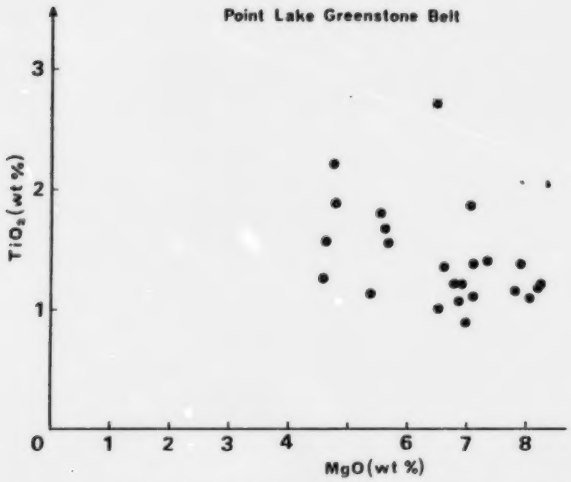

Figure 2: *TiO_2 vs MgO % diagram for Point Lake mafic volcanic rocks.*

their composition and metamorphic grade (Beaudry and St. Seymour, 1986) which increases in the Point Lake area towards the east (Bostock, 1980). The basaltic andesites are grey-greenish and the basalts range from light green in the greenschist facies to dark green in the amphibolite facies to the east. Flow sequence profiles commonly display a massive flow at the bottom succeeded by lava tubes and pillow sacs and finally pillow breccia at the top. The pillowed portion is usually volumetrically more prominent with the pillowed zones commonly twice the thickness of the pillow breccia zones (average 6 vs 3 m). The pillows are invariably folded and foliated. Their dimensions range from 20 to 60 cm x 70 to 200 cm, with an average maximum diameter of 100 cm. The basaltic andesite pillows are similarly deformed with average dimensions of 20 x 70 cm. Chilled pillow margins range from 3 to 5 mm thickness in the basaltic andesites to 10 mm in the basalts. In the former, 0.5 to 3 mm roundish vesicules are concentrated in the outer 3 cm of the pillows while in the basalts the vesicules are larger (5 to 10 mm), flattened and commonly amygdaloidal. The pillow interstices in the basalts are occupied by rusty hyaloclastite, carbonate and quartz. In the andesites, however, the pillow interstices, as well as the matrix to pillow breccia is occasionally composed of magnetite or jasper. Pillow budding is more common in the basaltic andesites which may reflect basin-bottom topography. The massive flows are fine to medium-fine grained, commonly plagioclase-phyric (3 mm laths), with an ophitic to subophitic texture. They range in thickness from 2 to 6 m with an average of 2 m, and have well developed brecciated lava tops that usually occupy one third of the flow thickness. The massive flows may display columnar jointing due to cooling which transgresses the full thicknesses of cooling units but which is better developed in their upper portions. The flows may show ropy lava zones and lensoid instead of tabular forms. They are intercalated with pillowed flows, conglomerate, volcanic agglomerate with ellipsoid felsic volcanic clasts and mafic fragments showing plastic deformation (bombs? Bostock, 1980), rusty weathering carbonate and quartz-rich intraflow sediments and occasionally mafic tuff beds.

Geochemistry

The Point Lake mafic volcanics are mostly basalts with basaltic andesites and andesites represented amongst the normalized volatile-free XRF analyses (Tables 1 and 2). A cursory examination of the twenty-eight analyzed Point Lake samples reveals three groups of basalts. Representative analyses from each of these groups are shown in Table 1. The "High-Al" group includes the massive and pillowed basalts of the Rosella Isle (RI basalts). The basaltic andesites and andesites of the Desertion Peninsula (DP) are also high in alumina (Table 2). In the second group belong the "High Fe-Ti" basalts of the Cyclops Peninsula (CP basalts). The third group includes the rest of the Point Lake basalts which are neither high in Fe nor in Al. On a TiO_2 vs MgO diagram, the Point Lake volcanics cluster into two groups. The high TiO_2 group comprises mainly the high Fe (CP) basalts (Fig. 2).

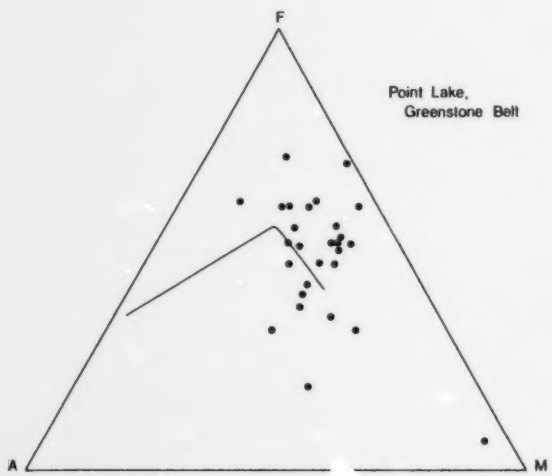

Figure 3: *AFM plot of Point Lake mafic volcanics.*

The basalts are predominantly olivine normative tholeiites. On an AFM diagram (Fig. 3) however, a few of the mafic volcanics (RI basalts and DP andesites) straddle into the calc-alkaline field. Fe contents range from 7.2-18.0 wt%, FeO.MgO from 3.2 wt% (in the more Fe-rich sample) up to 8.2 wt%. Ti varies sympathetically with Fe and ranges from 1.0-4.5 wt% TiO_2. No extensive alkali mobility is indicated in combined alkalies vs SiO_2 space where the Point Lake mafic rocks, with the exception of the DP andesite (i.e. "mugearite" of Bostock, 1980) which shows transitional alkali character, are restricted to the subalkaline field (Fig. 4).

TABLE 1

Representative Compositions of Point and Redrock Lake Basalts [a] Compared to Basalts from Various Petrotectonic Regimes [b]

	(1)	(2)	(3)	(4)	(5)	(6)	(7)	(8)	(9)	(10)	(11)	(12)	(13)	(14)	(15)	(16)
SiO_2	51.25	51.93	51.70	50.21	51.48	49.61	51.14	51.59	50.49	49.77	51.42	49.28	50.29	50.36	49.48	48.00
TiO_2	1.40	1.91	1.41	1.09	1.55	1.43	2.74	1.52	1.02	0.53	1.50	0.90	0.96	0.66	0.66	2.27
Al_2O_3	17.29	13.85	14.97	14.91	15.81	16.01	13.09	17.00	16.79	15.47	15.08	17.03	15.09	15.84	12.95	13.30
FeO	14.82	16.59	10.02	12.69	12.16	11.49	13.66	10.76	8.47	3.09	15.47	10.31	12.66	11.05	11.90	20.10
MgO	8.05	4.86	7.19	6.94	7.09	7.84	5.47	4.60	9.26	10.22	5.02	6.58	7.80	8.65	13.26	5.19
CaO	3.99	6.46	10.58	12.98	8.21	11.32	10.50	10.27	11.23	13.15	8.66	13.53	10.58	11.44	9.93	8.86
Na_2O	3.05	3.78	2.13	1.03	2.81	2.76	2.42	3.30	2.43	1.53	2.63	2.22	2.23	1.68	1.32	1.91
K_2O	0.03	0.45	1.93	0.05	0.72	0.22	0.66	0.78	0.21	0.17	0.21	0.15	0.31	0.26	0.51	0.23
P_2O_5	0.12	0.18	0.12	0.10	0.18	0.14	0.32	0.23	0.10	0.06	–	–	0.08	0.06	0.06	0.16

[a] Recalculated volatile free to 100%. All Fe as FeO. Analyses done by XRF on fused beads. Detection limit 0.01%.
[b] Sample 5 from Condie (1981); samples 6-12 from Basaltic Volcanism Study Project (1980).

1. Rosella Island "High Al" Basalt, Point Lake; (PL-10E, RI Basalt, Group I)
2. Cyclops Peninsula "High Fe-Ti" Basalt, Point Lake; (PL-16A, CP Basalt, Group III)
3. Point Lake, "High-K" tholeiite (PL-59)
4. Point Lake "Low-K" tholeiite (PL-17)
5. Archean LREE enriched tholeiite (Average TH2, Condie 1981)
6. Average Ocean Floor Basalt
7. Average of 44 Lower Deccan Traps
8. Keweenawan "transitional" or "High Fe-Ti" Basalt
9. New Britain Island Arc Reference Suite – "High Al" Basalt
10. New Britain Island Arc Reference Suite – Tholeiite
11. Iron rich Archean basalt, Lawlers, W. Australia
12. Al-rich Basalt, Abitibi, Canada
13. Massive Basalt, Redrock Lake (SL-16C)
14. Pillowed Basalt, Redrock Lake (SL-19)
15. "High Mg" Basalt, Redrock Lake (SL-21)
16. "High Fe-Ti" Basalt, Redrock Lake (SL-17)

TABLE 2

Point and Redrock Lake "Andesite" Compositions* Compared to "Andesites" from Various Tectonic Domains

	(1)	(2)	(3)	(4)	(5)	(6)	(7)	(8)	(9)
SiO_2	57.59	61.62	52.48	60.23	60.12	55.04	58.59	61.10	58.12
TiO_2	1.39	1.28	1.40	0.58	0.69	0.52	0.95	0.67	1.00
Al_2O_3	18.96	17.55	20.15	15.95	17.16	17.32	15.56	16.08	16.77
FeO	6.82	7.33	6.37	8.09	6.05	8.87	9.37	6.07	8.07
MgO	6.14	4.62	5.52	4.09	3.31	5.40	5.58	4.67	4.54
CaO	5.34	2.56	4.30	8.18	7.22	9.41	6.82	5.29	6.22
Na_2O	3.32	3.49	6.34	2.05	3.91	2.80	3.51	4.15	4.11
K_2O	0.31	1.42	3.31	0.73	1.30	0.46	0.69	1.97	1.16
P_2O_5	0.13	0.42	0.11	0.10	0.20	0.17	–	–	–
Cr	300	–	420	34	39	76	125	88	105
Ni	140	–	130	23	9	34	70	60	55
Ti	8340	7680	8400	3480	4140	3120	–	–	–
Zr	60	20	–	34	114	38	150	190	104
Y	10	10	–	12	18	16	25	35	40
Nb	20	10	–	1	1	–	–	–	–
Sr	80	30	–	384	490	380	278	580	210

*All values for major elements recalculated volatile-free to 100%. Total Fe as FeO. Trace elements in ppm. Rocks 1, 2, 4, 5, 7, 8, 9 not strictly andesites according to definition given by Gill (1981)

1. Point Lake Andesite
2. Redrock Lake Andesite
3. Point Lake "Mugearite" (Bostock 1980)
4. Calc-alkaline "Low K" Andesite (Gill 1981)
5. Calc-alkaline "Medium K" Andesite (Gill 1981)
6. Calc-alkaline "Low K" Basaltic Andesite (Gill 1981)
7. Type I Archean Andesite (Condie 1981)
8. Type II Archean Andesite (Condie 1981)
9. Type III Archean Andesite (Condie 1981)

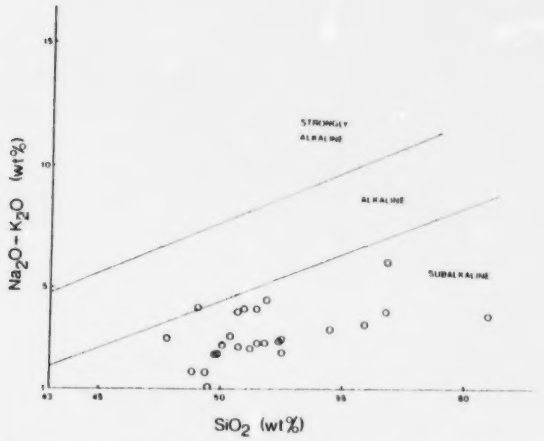

Figure 4: *Total alkalies vs SiO_2 weight % diagram. Point Lake basalts and andesites.*

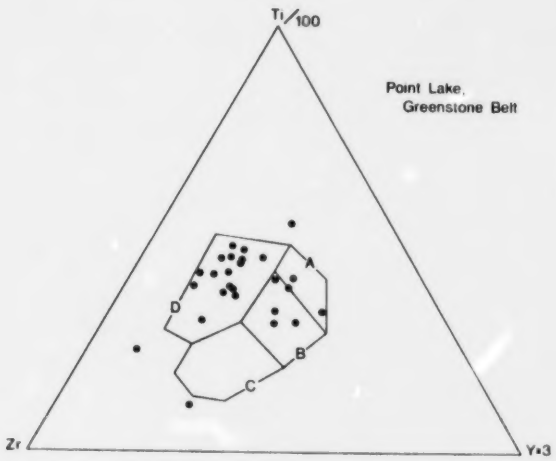

Figure 5: *Ti-Zr-Y diagram. Point Lake mafic volcanic rocks.*

The Y/Nb ratios of the Point Lake mafic rocks (Table 3) range from tholeiitic to transitional "within plate" basalts (Pearce and Cann 1973), while two out of three andesite samples are near and within the range of calc-alkaline arc volcanics. Their HFS compositional ranges and average values are similar to those of back arc and arc basalts except for Nb, which is similar to the Nb contents of continental basalts (Fig. 13).

On a Ti-Zr-Y diagram (Fig. 5) the majority of Point Lake basalts plot in the "D" domain (within-plate oceanic or continental). The RI basalts and DP basaltic andesites and andesites plot within areas "A" and "B" showing geochemical affinities to arc, back arc, and MOR tholeiites and calc-alkaline basalts (Pearce and Cann 1973). Since the CP basalts of the "within-plate" group, stratigraphically interfinger with very coarse continentally derived clastic sedimentary rocks they are presumed to have been emplaced proximal to or on a continent.

The REE profiles of the Point Lake mafic rocks (Fig. 6) do not show the same degree of LREE enrichment usually observed in post-Archean continental basalts but show very

TABLE 3

3a. Sr, Y, Ar, Nb (ppm) Contents of the Point Lake Mafic Volcanic Rocks*

	PL-10A	PI-10B	PL-10C	PL-10D	PL-10E	PL-13	PL-14	PL-15	PL-16A	PL-16C	PL-16-6	PL-17	PL-19
Sr	70	110	100	120	50	80	90	100	100	160	60	110	20
Y	10	30	20	10	20	10	30	30	10	20	20	10	50
Zr	60	70	50	60	60	60	90	100	100	160	60	110	180
Nb	20	20	20	30	10	20	10	20	10	30	10	10	30
	PL-22	**PL-31**	**PL-51**	**PL-53**	**PL-55**	**PL-59**	**PL-60**	**PL-61**	**PL-64A**	**PL-67**	**PL-68A**	**PL-70**	
Sr	160	140	110	90	100	310	110	130	480	1500	70	80	
Y	10	20	20	10	20	10	10	20	30	10	10	50	
Zr	20	130	60	70	100	70	50	110	260	200	50	150	
Nb	20	10	10	10	30	30	20	20	30	30	30	30	

*All analyses done by XRF on pressed powder pellets. Detection limit: 5 ppm

3b. Sr, Y, Zr, Nb (ppm) Contents of the Redrock Lake Mafic Volcanic Rocks

	SL-3A	SL-5	SL-6	SL-8	SL-9	SL-16B	SL-16C	SL-16E	SL-16F	SL-17	SL-18	SL-19	SL-20
Sr	100	70	40	30	140	70	100	100	100	80	10	100	130
Y	10	20	30	10	10	10	30	10	10	30	10	10	20
Zr	40	20	70	20	40	60	40	20	30	80	10	30	40
Nb	20	20	10	10	20	20	10	30	10	10	20	10	40
	SL-21	**SL-23**	**SL-25C**	**SL-25G**									
Sr	50	90	100	20									
Y	10	20	10	10									
Zr	30	20	30	30									
Nb	20	10	10	30									

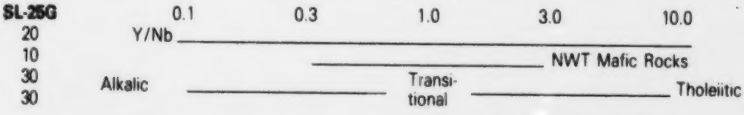

(Pearce & Cann 1973)

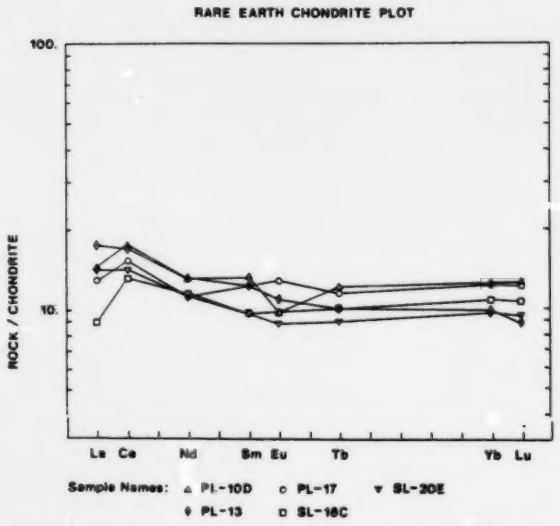

Figure 6: *Rare earth profiles of Point and Redrock Lakes basalts and andesite.*

similar profiles to island arc tholeiites (Basaltic Volcanism Study Project 1981). However, the Triassic flood basalts from New Jersey (Kay and Hubbard 1978), as well as some of the less evolved Tertiary plateau basalts from Iceland (Basaltic Volcanism Project 1981), do show similar profiles to the Point Lake basalts and andesite.

The LIL abundances and ratios in the Point Lake mafic volcanics (Table 3) show ranges partly overlapping with those of continental and island arc basalts, except for a much lower limit of K in the NWT basalts. However, caution should be exercised in LIL element interpretation since all these elements are very mobile.

Summarizing, the presented geochemical evidence for the Point Lake basalts favours their deposition within a continent where subduction and local rifting were active.

Redrock Lake Greenstone Belt

General Geology

The Redrock Lake volcanic belt occurs directly south (structurally below) the "basal decollement" between Proterozoic rocks of the Wopmay Orogen and Archean rocks of the Slave Province (Fig. 1b). The Carousel Massif biotite granite is in intrusive contact with the volcanic belt. Eastwards the belt is in contact with more Archean granite whilst southwards it is limited by the Redrock Lake fault, one of a set of NE striking dextral transcurrent faults which cut across both Proterozoic and Archean rocks (St-Onge *et al.*, 1983). The volcanic belt comprises predominantly pillowed basalts, massive flows, minor intraflow sediments, and a feeder system of synvolcanic dykes and sills. Proterozoic diabase dykes cut the belt at high angles.

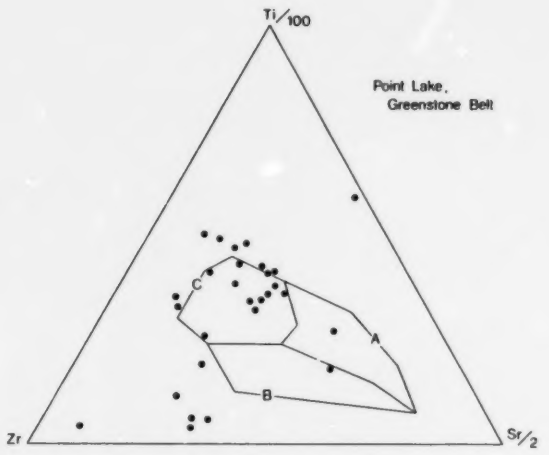

Figure 7: *Ti/100-Zr-Sr/2 diagram of Point Lake mafic volcanic rocks.*

Structure

At least two phases of deformation affected the Archean mafic volcanics of the Redrock Lake area. The two events may be correlative to those found by Jackson (1983) deforming the supracrustal rocks of the Point Lake area. The D_1 event produced a strong bedding-parallel foliation (S_1) which trends northeast and dips steeply to the southeast (Fig. 8). S_1 is axial planar to early F_1 folds that are typically tight to isoclinal and whose fold axes plunge steeply to the south-southwest. The intersection of north-south trending foliation (S_1) with subparallel bedding produces subvertically to moderately plunging intersection lineations of the same trend.

The later D_2 folding phase results in the rotation of the earlier D_1 structures where the fold axis of the second event nearly coincides with the F_1 fold axis direction. F_2 folds are open to tight with axial planes trending NNW, and dipping steeply to the east-northeast. No evidence of good, penetrative S_2 foliation was observed. From Fig. 8 (F_2) fold axes pitch moderately to steeply either to the south or north within F_2 axial planes. Type 3 interference patterns of Ramsay (1967) were observed in the field. This style of superimposed folding is normally predicted from the orientations of the D_1 and D_2 structural elements described.

Volcanic Petrology

The Archean mafic volcanic succession at Redrock Lake comprises pillow and massive basalt with minor intraflow sediments. Pillows range from small and bulbous (20 x 30 cm), to larger (50 x 200 cm) flat sacs, displaying lava septa (now white quartz fillers). Inflated (300 x 100 cm) lava tubes often display "budding" with up to 3 daughter pillows inside the main tube. The small, bulbous pillows display 1 cm thick chilled margins, and 25 to 30 vol%

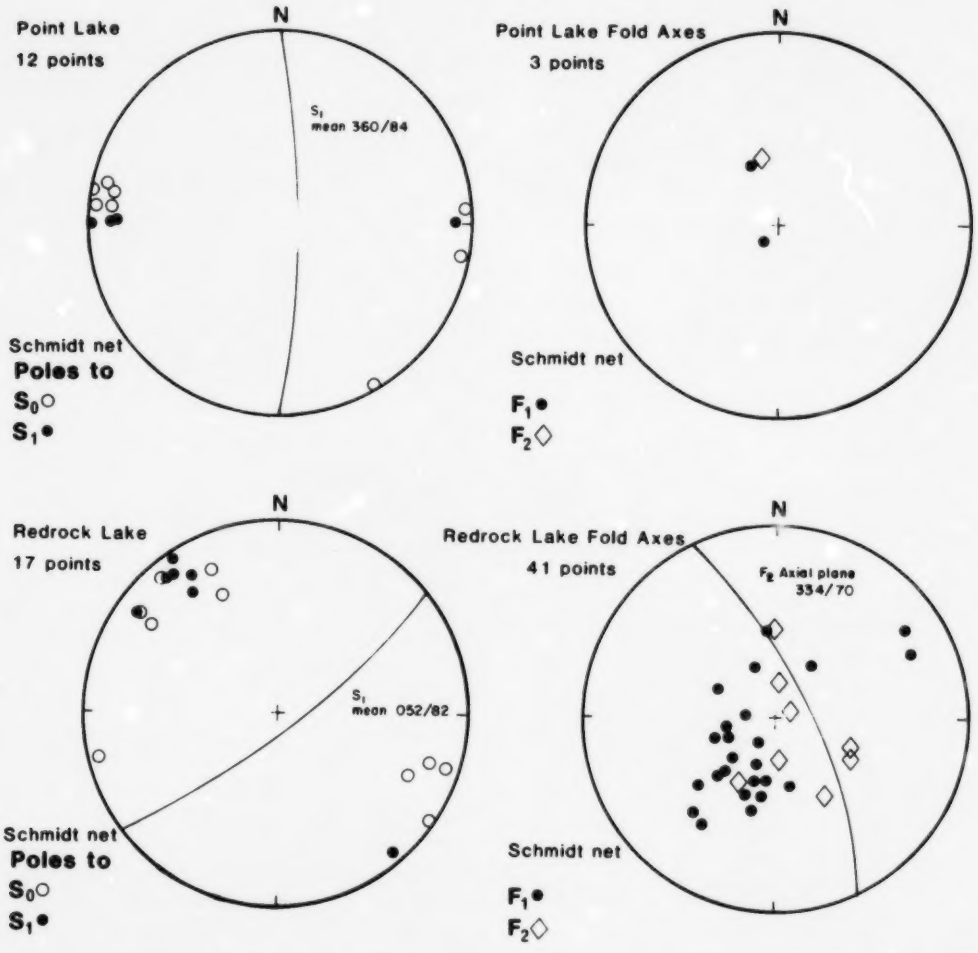

Figure 8: *Schmidt diagrams of a) Poles to So, S_1 b) F_1, F_2 fold axes (Redrock Lake greenstone belt).*

vesicules (0.5 to 1 mm) in a concentric zone 1 cm inwards from the margin. Some display quartz-filled amygdules. These pillowed basalts are commonly plagioclase-phyric with swallow-tail, hopper plagioclase; occasionally they are variolitic. The varioles are lighter coloured than the basaltic matrix and variable in size, averaging 2 mm in diameter. Triangular pillow interstices are filled with carbonate, quartz or magnetite or jasper.

The Redrock Lake basalts are fine grained and composed of mineral assemblages typical of greenschist to lower amphibolite metamorphic facies. These include at low grades, predominantly (65 to 85%) actinolitic amphibole in sheafs pseudomorphing a relic spherulitic primary texture with subordinate euhedral to subhedral epidote and interspersed chlorite. This matrix is intersected by anastomosing 0.5 mm veinlets filled with an assemblage of subhedral epidote and calcite or calcite or epidote. Pseudomorphs of plagioclase are occasionally retained. At higher grade, actinolite is replaced by hornblende.

The massive basaltic flows are commonly lensoidal in form and range from 1 to 5 m at their thickest portions but are usually 4 to 5 m thick. Silicified flow top breccias infilled by white quartz between the fragments occupy 1/5 of the flow thickness. Paucity of intraflow sediment and pillow breccias, the presence of lava septa within pillows, and "pillow budding", as well as, the intimate interdigitation of massive and pillowed cooling units, indicate rather rapid deposition of basalt on a sloping floor at intermediate to proximal distances from the site of extrusion, at depths that permitted vesiculation of the lava but not abundant development of pillow breccias. Water solubility data in silicate melts (Dudas, 1981) indicate that vesiculation in basalts is possible at considerable depths (up to 4000 m).

Geochemistry

The Redrock Lake mafic rocks comprise tholeiitic basalts and basaltic andesites (Figs. 9, 10, Tables 1, 2). The basalts are olivine normative tholeiites with MgO contents in the

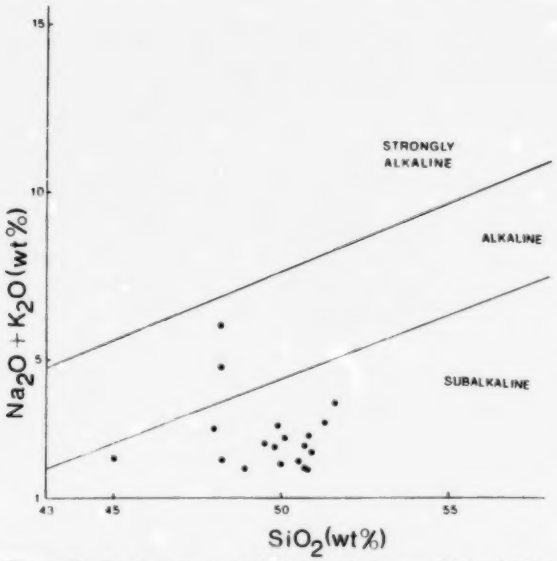

Figure 9: *Total alkalies vs SiO_2 weight % diagram. Redrock Lake basalts.*

range of 5-13 wt%. Andesites and "High Mg" basalts, however, occur infrequently in the studied volcanic section. Fe and Ti contents are moderate to high (FeO 10.5-18.3 wt%; TIO_2 0.6-2.3 wt%). A group of "High Fe-Ti" basalts is discerned in MgO vs TiO_2 space (Fig. 15) but on the AFM diagram the Redrock Lake tholeiites do not show a pronounced trend of Fe-enrichment. Their subalkaline affinity, evident from a total alkalies vs. SiO_2 diagram is taken as an indication of no major resdistribution of the alkalies in the volcanic succession during secondary processes (Fig. 9). K_2O values are variable with an average comparable to those of low-K tholeiites (Table 1).

These basalts have trace and major element characterstics very similar to those of the Point Lake basalts. They show similarly enriched and depleted REE profiles (Fig. 6), spidergrams (Fig. 11) and distribution of HFS elements. On the Ti-Zr-Y (Fig. 12) diagram they plot in fields of "within-plate", arc and back-arc basalts and have HFS element averages and ranges similar to those of arc or back-

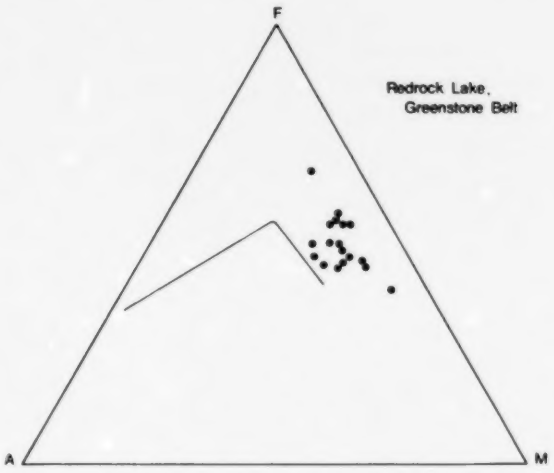

Figure 10: *AFM plot of Redrock Lake basalts.*

arc basalts except for Nb, which is similar to the Nb contents of the continental plate basalts (Fig. 13). The important differences between the two studied basalt populations are that the Redrock Lake popula' n does not include basalt or andesite members with Al_2O_3 > 16 wt% nor do the Redrock tholeiites show a pronounced trend of Fe-enrichment on the AFM diagram.

Compared to the overall composition of island arc basalts and andesites the Redrock Lake mafic rocks have distinctly higher Fe, Ti, Ni and Cr and lower Sr (Pearce and Cann 1973; Gill 1981; Basaltic Volcanism Study Project 1981). These features are also shared by the Point Lake and other Archean andesites (Table 2 and Condie, 1981). In conclusion, the Redrock Lake mafic rocks have geochemistry indicative of deposition in a tectonic regime similar to back-arc and arc within a continental plate where subduction and local rifting were active.

Discussion

One of the major problems in dealing with Archean volcanic rocks is determining the extent to which primary

TABLE 4
Typical Large Cation Abundances in Basalts* (in ppm)

	Type I Morbs	Type II Morbs	Ocean Island Tholeiites	Continent Basalts	Island Arc Basalts	NWT Basalts
K	1064	1854	1600 - 8300	1011 - 17230	900 - 18100	209 - 7756
Rb	1.0	4.5	5 - 12	1 - 65	2 - 61	10 - 60
Ba	12.2	55	70 - 200	51 - 378	55 - 480	40 - 440
Sr	127	105	150 - 400	210 - 440	135 - 540	20 - 310
K/Rb	1046	414	400	111 - 3820	240 - 1000	6 - 258
K/Ba	109	34	25 - 40	15 - 65	13 - 77	1 - 35
Sr/Rb	127	23	20 - 70	1 - 243	67 - 9	1 - 16

*Data other than these referring to NWT mafic rocks are taken from Basaltic Volcanism Study Project (1981). NWT trace element data by XRF on pressed powder pellets. Detection limit: 5 ppm

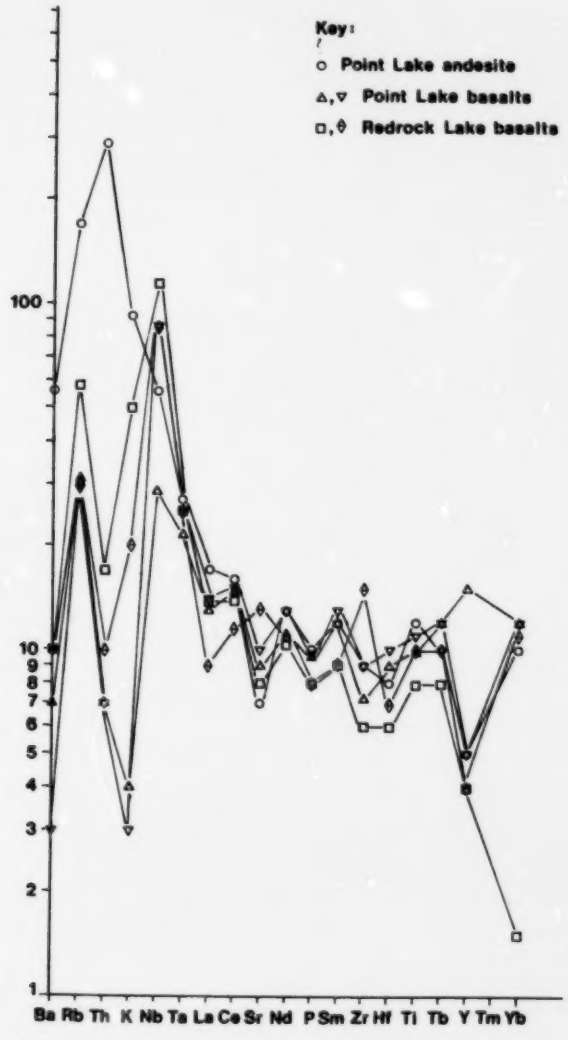

Figure 11: *Spidergram of selected Point and Redrock Lake mafic volcanic lithologies.*

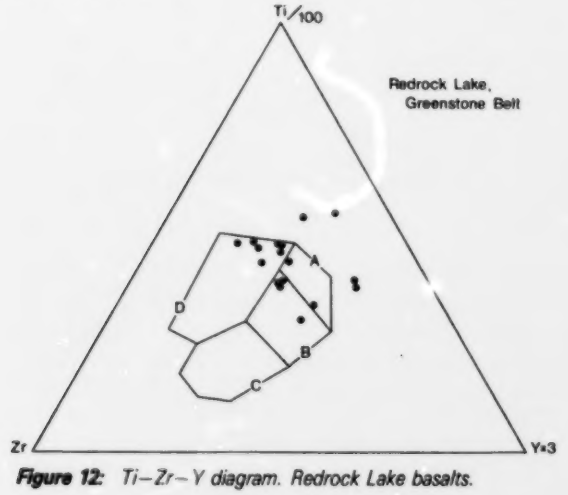

Figure 12: *Ti–Zr–Y diagram. Redrock Lake basalts.*

geochemical patterns have been modified by the secondary effects of sea-floor hydrothermal alteration and subsequent metamorphism. This ambiguity in interpretation can be introduced in any of the previously discussed diagrams in the light of studies of other workers with similar rock systems. MacGeehan and MacLean (1980), for example, discussed the scattering of tholeiitic analyses in the calc-alkaline field due to basalt-sea water interaction assuming constant Fe/Mg ratios in the fluid. Ludden and Thompson (1978) discussed fractionation of the LREE similar to those observed in the NWT (Northwest Territories) rocks and attributed such enrichments to mobility of the LREE during submarine weathering of tholeiitic basalt.

The major alkali elements K, Na are also mobile during halmyrolysis and metamorphism. Some mobility of the large cation lithophile (LIL) elements can be suspected from the scatter of points in the Ti-Zr-Sr plot caused by Sr fluctuations for both Point and Redrock Lake volcanics (Figs 7, 14); however Sr contents remain on the overall consistently low (Table 3). The HFS elements Ti, Zr, and Y, however, are remobilized only under extreme conditions of alteration, i.e., intense carbonatization and stabilization of rutile in the mafic metamorphic assemblage (Hynes, 1980; Murphy and Hynes 1986). Such conditions were *not* encountered in the studied volcanic rocks which are rutile-free. Therefore, the geochemical evidence provided by the HFS absolute contents, ratios, variation diagrams and particularly by the Ti-Zr-Y plot is a valid one and substantiates the arguments derived from the AFM trends and the REE profiles for the Point and Redrock Lake mafic rocks.

The volcanic succession at Point Lake consists of a package of "High Fe-Ti" tholeiites intimately intercalated with "High Al" basalts and overlain by calc-alkaline basaltic andesites and andesites. Tholeiitic basalt overlain by calc-alkaline andesite typifies island arcs but can also be found in anorogenic tectonic environments such as continental rifts, ocean islands and rarely in ocean ridges. Andesites associated with anorogenic domains can be low in K (icelandites) or high in K (trachytes). Contrasted with the compositions of the studied andesites anorogenic andesites display considerably lower Al_2O_3 for similar SiO_2 contents and higher LIL element and Zr contents (Table 2). In comparison to orogenic calc-alkaline andesites from volcanic arcs, the Point Lake andesites have generally higher Ti, Fe, Cr, Ni and lower Sr. These are characteristics shared by many Archean andesites (Condie 1981) and therefore may be indicative of a more Fe-rich Archean mantle; however, these geochemical features are also displayed by a few andesites from younger, immature arcs (Gill 1981). The stratigraphic upwards increase in LIL and REE elements from basalt to andesite, displayed by the Point Lake "High-Al" basalts and andesites (Table 3, Fig. 6) is thought to be a characteristic of a number of recent arcs (Gill 1981).

"High Fe-Ti" tholeiites with varying potassium contents

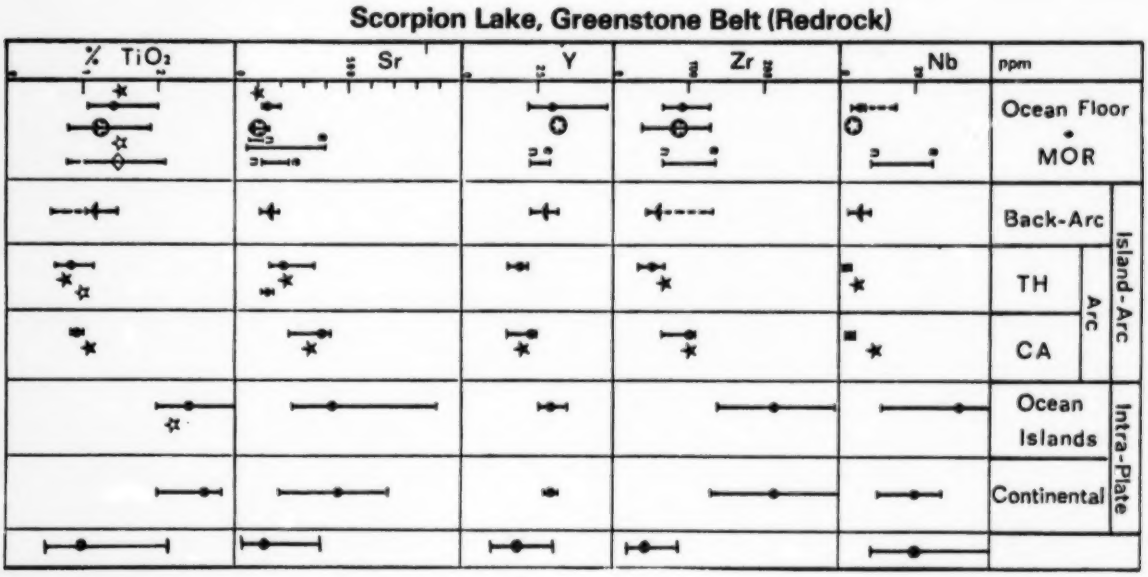

Figure 13a: *Bottom line trace element contents of Point Lake mafic volcanics.*

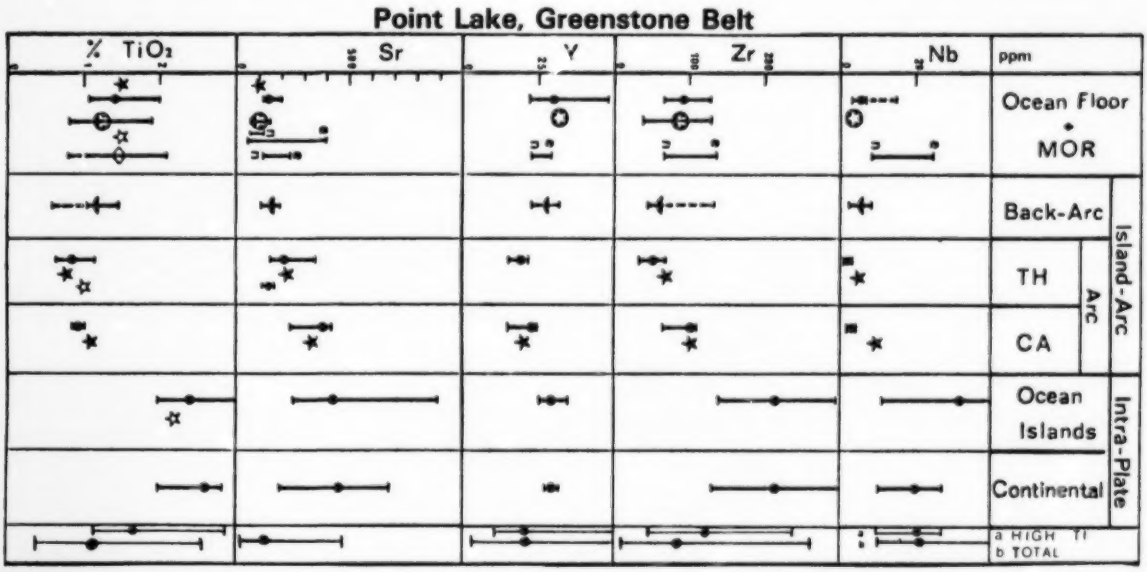

Figure 13b: *Bottom line trace elements contents of Scorpion Lake (Redrock) mafic volcanics.*

Figure 13: *Trace element contents (range and average) of Point and Redrock Lake mafic volcanics compared with ranges and averages of basalts from various recent tectonic regimes (MacLean and others, 1982).*

are known from continental basalt suites. Compared to continental tholeiites (Table 1) the Point and Redrock Lake "High Fe-Ti" basalts show similar major element contents for comparable SiO_2 values. The variability of the potassium contents of the NWT basalts cannot be correlated in the field with any obvious intrusive. However, since the order of mobility of alkali metals increases from Sr to K and since the Sr values (Figs. 7, 14) show mobilization, K contents should be treated with caution. Significantly, however, evidence provided from the elements Ti, Y, Zr, Nb considered to be immobile under non-extreme conditions of alteration, is internally consistent; both Point and Redrock Lake tholeiites display the transitional Y/Nb ratios (Table 3) and high Nb and Ti contents (Fig. 13) which are characteristic of continental basalt suites and Ti-Zr-Y topologies indicate "within-plate" affinities.

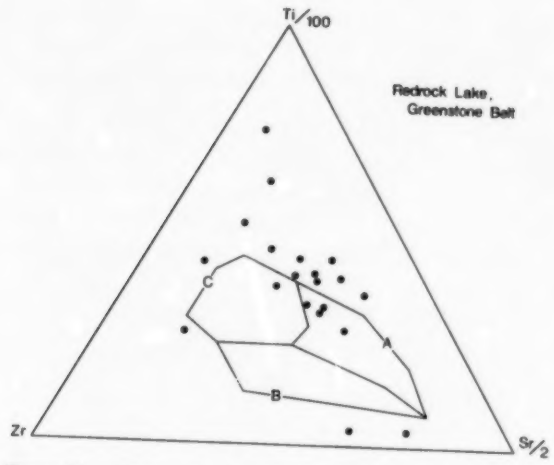

Figure 14: *Ti/100 – Zr – Sr/2 diagram of Redrock Lake basalts.*

This is consistent with independent sedimentological and other evidence arguing for a continental basement to the Yellowknife Supergroup volcanics (Stockwell 1933; Henderson 1975; Henderson and Easton 1977; Easton 1985) for the Point Lake area. However, the absolute Zr contents of the "High Fe-Ti" basalts from Point and Redrock Lakes have averages lower than those expected in continental tholeiites and are similar to ocean floor, arc and back-arc tholeiites. The NWT basalts do not show the intensity of incompatible trace element and Rare Earth enrichments of post-Archean continental tholeiites. Nevertheless, the distribution of such elements in continental basalts is thought to reflect crustal contamination which itself depends on the thickness of the crust (zone refining) or the width of the feeder conduits (Campbell, 1985).

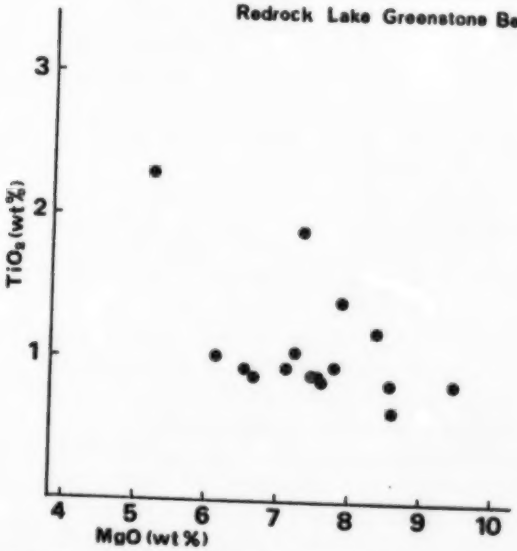

Figure 15: *TiO_2 vs MgO weight % diagram for Redrock Lake mafic volcanic rocks.*

Conclusions

To recapitulate, the "High Fe-Ti" basalts in the studied areas have geochemical features indicative of interaction with continental crust but do not display the extreme incompatible element enrichments (with the exception of Nb) which are characteristic of continental basalt suites and have Zr contents more similar to ocean floor tholeiites.

Thin, rifted continental crust can floor marginal basins. Depending on the degree of rifting and invasion by basaltic magma, such failed continental crustal screens may show properties between continental and oceanic crust (Menard 1967; Dalziel *et al.*, 1974). Basaltic magmas ascending through such a "hybrid" crust are expected to show the geochemical insignia of equilibration with continental crust, but non-extreme incompatible element enrichments. Marginal basins are filled with sedimentary debris derived from a mixed provenance, i.e. the nearby continent and the volcanic arc (Karig and Moore 1975). The CP "High Fe-Ti" basalts at Point Lake are intercalated with conglomerate and overlain by sandstone which is thought to have been subaerially deposited (Henderson 1975). Both the conglomerate and the sandstone have clasts derived from a mixed continental and volcanic provenance. The basalts show frequent hyaloclastic breccias. The CP basalts therefore, may have been, in part, deposited in shallow conditions in proximity to a craton and in a basin that was accepting both continental and volcanic debris; this is an environment not unlike a marginal sea adjacent to a continent and a volcanic arc (Dalziel *et al.*, 1974).

At Point Lake the marginal sea basalts may be represented by the "High Fe-Ti" CP basalts and other tholeiites while the "juxtaposed" island arc volcanic assemblage is represented by the RI "High-Al" basalts, the DP andesites and the rhyodacites and dacites. At Redrock Lake the picture is less than complete since the chemical spectrum of the volcanic compositions is more restricted, sedimentary evidence is missing, and basement-cover relationships are not established. However, geochemical evidence from the Redrock mafic rocks indicates deposition in a back-arc basin or a marginal sea. At Point Lake, the Contoywto turbidites are partly contemporaneous with the volcanics (Bostock, 1980) and may represent the "trench facies" deposited within trenches separating the volcanic arcs. Our field data indicate that rifting must have continued throughout the history of the belt, as evidenced by pretectonic gabbro dykes sills and plugs which cut volcanic and sedimentary units.

Henderson (1981) proposed that the Slave Province may have been under a regime of extension at 2.7 Ga. Easton (1983) further discussed the possible reasons for a continental extension regime, faulting, development of rift basins floored by continental crust and volcanic arcs possibly now represented by tholeiitic and calc-alkaline volcanics of the

greenstone belts (2.67 G.a.) The petrotectonic regime indicated by the geochemical insignia of the mafic volcanic rocks from Point and Redrock Lake greenstone belts substantiates such a hypothesis.

Acknowledgements

This research was supported by NRSEC operating grant A-0634 to Karen St. Seymour. The authors want to express their thanks to DIAND for logistical support and especially to Dr. Bill Padgham for his most helpful attitude during field operations. The manuscript was improved by the suggestions of Drs. Janet King and Bill Kidd; the authors extend their thanks for constructive criticism to the reviewers, but retain full responsibility of interpretations presented in this paper. We appreciate the efficient assistance of R. Fogal, D. Vlassopoulos, R. Roy and typing of the manuscript by Ms. Lori Bertrand. Drs. A. Lalonde, M. St. Onge and J. King kindly introduced the senior author to the idea of working in the Northwest Territories.

References

Basaltic Volcanism Study Project. 1981. Basaltic Volcanism on the Terrestrial Planets. Pergamon Press: New York, 1286 p.

Beaudry, C. and St. Seymour, K. 1986. Dependence of colour index on composition and metamorphic grade of Archean volcanics. N. Jb. Miner. Mh., H.4: pp. 157-62.

Bostock, H.H. 1980. Geology of the Itchen Lake area, District of Mackenzie. Geol. Surv. Can. Mem. 391: 101 p.

Campbell, I.H. 1985. The difference between oceanic and continental tholeiites: a fluid dynamic explanation. Contrib. Mineral. Petrol.: v. 91, pp. 37-43.

Condie, K.C. 1981. Archean Greenstone Belts. Elsevier,Amsterdam: 434 p.

Dalziel, I.W.D., de Wit, M.J. and Palmer, K.F. 1974. Fossil marginal basin in the southern Andes. Nature: 250, p. 291-4.

Dudas, F.O. 1981. The effect of volatile content on the vesiculation of submarine basalts; in Ohmoto, The Kuroko and Related Volcanogenic Massive Sulfide Deposits. H. and Skinner, B.J. (eds.), Econ. Geol. Mon. 5: p. 134-42.

Easton, R.M. 1985. The nature and significance of pre-Yellowknife Supergroup rocks in the Point Lake area, Slave Structural Province, Canada; in Evolution of Archean Supracrustal Sequences. Edited by Ayres, L.D., Thurston, P.C., Card, K.D. and Weber: W. Geol. Assn. Can. Spec. Paper 28, p. 153-167.

Easton, R.M. 1983. Crustal Structure of Rifted Continental Margins: Geological Constraints from the Proterozoic Rocks of the Canadian Shield. Tectonophysics: 94, p. 371-390.

Gill, J.B. 1981. Orogenic Andesites and Plate Tectonics. Springer-Verlag.

Henderson, J.B. 1975. Sedimentological studies of the Yellowknife Supergroup in the Slave Structural Province; in Report of Activities, Part A. Geol. Surv. Can.: Paper 75-1A, p. 325-330.

Henderson, J.B. 1981. Archean basin evolution in the Slave Province, Canada; in Plate Tectonics in the Precambrian. ed. A. Kroner, Elsevier, Amsterdam: p. 213-236.

Henderson, J.B. and Easton, R.M. 1977. Archean supracrustal-basement rock relationships in the Keskarrah Bay map area, Slave Structural Province, District of Mackenzie; in Report of Activities, Part A. Geol. Surv. Can.: Paper 77-1A, p. 217-221.

Hynes, A.J. 1980. Carbonatization and Mobilization of Ti, TY, and Zr in Ascot Formation Metabasalts, SE Quebec. Contrib. Mineral. Petrol: 75, p. 79-87

Jackson, V.A. 1983. Geology of the Keskarrah Bay area, Point Lake, NWT: second preliminary report. Indian and Northern Affairs Canada: EGS 1983-11

Karig, D.E. and Moore, G.F. 1975. Tectonically controlled sedimentation in marginal basins. Earth and Planet. Sci., Lett.: 26, p. 233-238.

Kay, R.W. and Hubbard, N.J. 1978. Trace elements in ocean ridge basalts. E. Plant. Sci. Let.: v. 38, p. 95-116.

Ludden, J.N. and Thompson, G. 1978. Behaviour of rare earth elements during submarine weathering of tholeiitic basalt. Nature: v. 274, no. 5667, p. 147-9.

MacGeehan, P.J. and MacLean, W.H. 1980. An Archean sub-seafloor geothermal system, "calc-alkali" trends, and massive sulfide genesis. Nature: v. 286, p. 761-7.

MacLean, W.H., St. Seymour, K. and Prabhu, M.K. 1982. Y, Zr, Nb, Ti and REE in Grenville amphibolites at Montauban-les Mines, Quebec. Can. J. Earth Sci.: 19, 633-644.

Menard, H.W. 1967. Transitional Types of Crust under Small Ocean Basins. Journal of Geophysical Research. 72, 12, p. 3061-3073.

Murphy, J.B. and Hynes, A.J. 1986. Contrasting secondary mobility of Ti, P, Zr, Nb, and Y in two metabasaltic suites in the Appalachians. Can. J. Earth Sci.: 23, 8, p. 1138-114.

Pearce, T.H. and Cann, J.A. 1973. Tectonic setting of volcanic rocks determined using trace element analysis. E. Plant. Sci. Let.: v. 19, p. 290-300.

Ramsay, J.G. 1967. Folding and Fracturing of rocks. McGraw-Hill.

St. Onge, M.R., Lalonde, A.E., and King, J.E. 1983. Geology, Redrock Lake and eastern Calder River map areas, District of Mackenzie: the central Wopmay orogen (early Proterozoic), Bear Province, and the western Archean Slave Province; in Current Research. Geol. Surv. Can.: Pap. 83-1A, p. 147-52.

Stockwell, C.H. 1933. Great Slave Lake – Coppermine River area, Northwest Territories. Geol. Surv. Can., Ann. Rept. 1932: pt. C, p. 37-63.

Contribution to the Geology of the Northwest Territories, Volume 3, 1988, NWT Geology Division, INAC, Yellowknife

An Archean ultramafic lamprophyre, Yellowknife: implications for tectonics and source regions.*

Dave R. Webb[1] and Robert Kerrich[2]

Abstract

A major lamprophyre dyke intrudes the Yellowknife greenstone belt subparallel to the ore-bearing brittle-ductile shear zones within the NERCO Con Gold Mine. It intruded late in the volcanic-plutonic sequence. The dyke is variably altered, with pargasite partly replaced by phlogopite which in turn is partly replaced by chlorite. The conjunction of low SiO_2 ($\bar{x}$ = 41.9 ± 1.8 wt%, 1σ), and moderate alkalis ($\bar{x}$ = 4.7 ± 2.1 wt%, 1σ), with elevated abudances of the light REE, incompatible (Ba, Zr, Rb, Th, U, P) and mafic-affiliated elements (Cr, V, Ni, Co) justify tentative classification of the dyke as an ultramafic lamprophyre. This is the first Archean ultramafic lamprophyre reported. A characteristic compositional feature is the pronounced troughs, or relative depletions of Nb, Ta, and Ti, on chondrite normalized diagrams, typical of Phanerozoic shoshonitic lamprophyres at convergent plate boundaries. The association of lamprophyres and gold deposits with major structures has also been described from greenstone belts in the Superior Province.

Introduction and Scope of Study

The Yellowknife greenstone belt is in the southwestern portion of the Slave Structural Province. Gold mining since 1938 has accounted for a cumulative production in excess of 11 million ounces of gold. Essentially, all of the gold ore is confined to large brittle-ductile shear zones that transect relatively undeformed tholeiitic volcanic rocks.

Nikic *et al.* (1980) described a diatreme, intersected by the workings of the Con Mine, and characterized by abundant xenoliths of tonalitic, gneissic, granitic, volcanic and vein material. Zircons from these xenoliths yielded U-Pb ages of 3,210 Ma (Nikic *et al.*, 1980). More recent Nd-Sm and U-Pb work on the xenoliths yielded ages up to 3,390 Ma (Bibikova *et al.*, 1986). This along with other lines of evidence has been used to argue for a sialic basement to the Yellowknife supracrustal sequence. Work by Webb (1983, 1986) has redefined the diatreme as a lamprophyre dyke. This contribution describes the geometry, petrography and geochemistry of the lamprophyre. Based on these data, and using the tectonic settings of compositionally similar Phanerozoic counterparts as a possible analogue, we speculate on the source regions and tectonic environment of the lamprophyre dyke. The implications of the lamprophyre dyke for the ore-bearing shear zones at the Con Mine are considered, and possible genetic relationships between the two are discussed.

Geological Setting

The Yellowknife greenstone belt lies in a linear domain on the western margin of the Yellowknife supracrustal basin (Padgham, 1985). The supracrustal sequence is comprised of metavolcanic rocks overlain by metasedimentary rocks, collectively intruded by granitoid batholiths.

The Kam Group is the oldest supracrustal unit of the Yellowknife Supergroup exposed in the Yellowknife mining district, and consists of five formations. The Octopus Formation is a sequence of mafic volcanics and volcaniclastic sediments and is thought to be the oldest formation in the Kam Group. The Octopus Formation is unconformably overlain by the Chan Formation which in turn is conformably overlain by the Crestaurum, Townsite and Yellowknife Bay Formations (Helmstaedt and Padgham, 1986).

The Chan, Crestaurum and Yellowknife Bay Formations are composed of tholeiitic volcanics and intrusive equivalents. The Townsite Formation is a calc-alkaline intermediate volcanic sequence, intruded by gabbroic sills and dykes. The Kam Group is overlain by the Banting Group which is regionally unconformable but locally conformable to the Kam Group. The Banting Group consists of two formations of calc- alkaline mafic to intermediate volcanics and greywacke-argillite successions.

An unsubdivided sequence of turbidites conformably overlies rocks of the Banting Group and is called the Burwash Formation. Helmstaedt and Padgham (1986) show undetermined relationships between the Burwash Formation and the Kam Group, but Padgham (pers com) speculates that they may have been deposited contemporaneously. The Jackson Lake Formation is the youngest unit in the Yellowknife Supergroup at Yellowknife, and is an immature terrigenous clastic sedimentary sequence deposited unconformably on the Kam Group.

Mafic dykes and sills are common in the Kam and Banting Group rocks. Helmstaedt *et al.* (1986) note the presence of multiple or sheeted mafic dyke complexes within the Chan Formation. Dykes and sills of similar composition occur within the Banting Group, but not within the Jackson Lake Formation. Later, feldspar porphyry dykes ± quartz phenocrysts intrude the Kam Group. Sills of similar intermediate to felsic composition with extrusive equivalents are found within the Banting Group (Helmstaedt and Padgham, 1986).

[1] University of Western Ontario, London, Ontario, N6A 5B7
[2] University of Saskatchewan, Saskatoon, Saskatchewan, S7N 0W0.

The Western Intrusive Complex (Padgham, 1985), a felsic intrusion of batholithic proportions, intrudes the Kam Group in the west. Smaller stocks which are thought to be comagmatic with the Western Intrusive Complex intrude the Kam Group northwest of the city of Yellowknife at Stock Lake and 300 m west of the Con Mill at Pud Lake. Two sets of Proterozoic mafic dykes are common in the Yellowknife mining district, and transect all of the previously described units. One set of dykes has been dated by K-Ar techniques at 2.4 ± 0.2 Ga and the other set at 1.2 ± 0.1 Ga (Leech, 1965).

Numerous early faults and associated shear zones transect rocks of the Kam and Banting Groups, as well as the early intrusions. Late transcurrent faults, such as the West Bay fault, offset all lithotypes including the Proterozoic dykes.

Mine Geology

The geology of the Con Mine has been described recently by Bullis *et al.* (1987), and Webb (1983), and can be summarized from these sources as follows. The Con Mine property is on the west-side of the West Bay fault, and is underlain by rocks of the Kam Group. Several laterally continuous flow units ranging up to 200 m in thickness can be mapped on the property. All of the volcanic rocks are tholeiitic basalt to andesite in composition except for the Townsite Formation which is a calc-alkaline dacite. Tuffaceous or interflow sedimentary units are minor to rare. Numerous dykes and sills of gabbroic composition intrude the Yellowknife Bay Formation at the mine site. Felsic dykes of ± feldspar-bearing quartz porphyry intrude the rocks east of the main production shaft (Robertson Shaft).

The Western plutonic complex intrudes the Kam Group and is exposed 1,300 m west of the Robertson Shaft. Small felsic intrusions occur in the mine area. The Pud Lake stock and the Stock Lake intrusion outcrop northwest and north of the Robertson Shaft, respectively, and a small intrusion lying east of the Robertson Shaft, near the Negus workings, is not exposed. Several Proterozoic diabase dykes are exposed on the mine property.

Early faults and attendant shear zones transect all units on the mine property, except the Proterozoic dykes. The major shear zones on the property are the Con, Campbell, Negus and Rycon shear zones. The first two are subparallel curviplanar domains of chlorite carbonate schists striking 007° and dipping 55° west. The Negus and Rycon shear zones are part of a northerly-striking, westerly-dipping fracture system between the Con and Campbell shear zones. Other shear zones occur on the mine property. Some contain auriferous quartz veins, but gold production has been recorded only from the Con, Campbell and Negus-Rycon shear zones. In the Con Mine a large lamprophyre dyke, the subject of this paper, is found parallel to the Campbell shear zone in the hanging wall rocks.

Geometry of the Lamprophyre Dyke

The lamprophyre dyke, throughout much of its length, is a single sheet-like intrusion that strikes 007° and dips to the west at 55°. It has been traced discontinuously by diamond drilling and in mine workings for over 2,800 m along strike and 1,100 m down dip, and is open in all directions. The dyke does not outcrop, probably because upward projection puts it beneath the waters of Yellowknife Bay. The dyke averages 4 m in width, but thicknesses of 30 m have been intersected in the Con Mine.

The lamprophyre dyke is subparallel to, and with rare exception, lies no more than 20 m from the hanging wall of the Campbell shear zone (Figs. 1, 2). Dyke emplacement predates final movement across the Campbell shear zone. Some of the ore in the Campbell shear zone is hosted by chlorite schists derived from the lamprophyre dyke, indicating that the dyke was emplaced prior to ore formation.

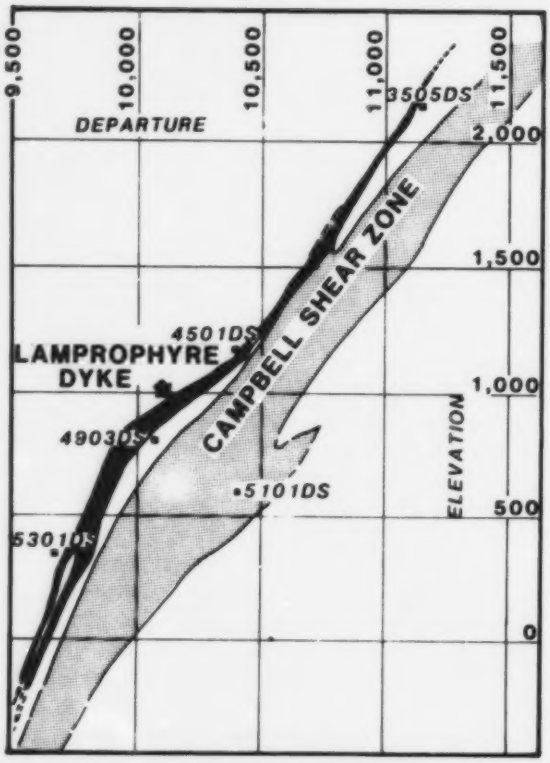

Figure 1: *Cross-section of the Con Mine at latitude 16,750, facing north, showing the lamprophyre dyke relative to the Campbell shear zone. Elevation and departure are in feet, relative to the mine co-ordinate system.*

Petrography of the Lamprophyre Dyke

Macroscopically the lamprophyre dyke is a compositionally and texturally inhomogeneous unit, incorporating xenoliths of exotic and local lithotypes, some of which are partly assimilated. Xenoliths of tonalite, granite, various

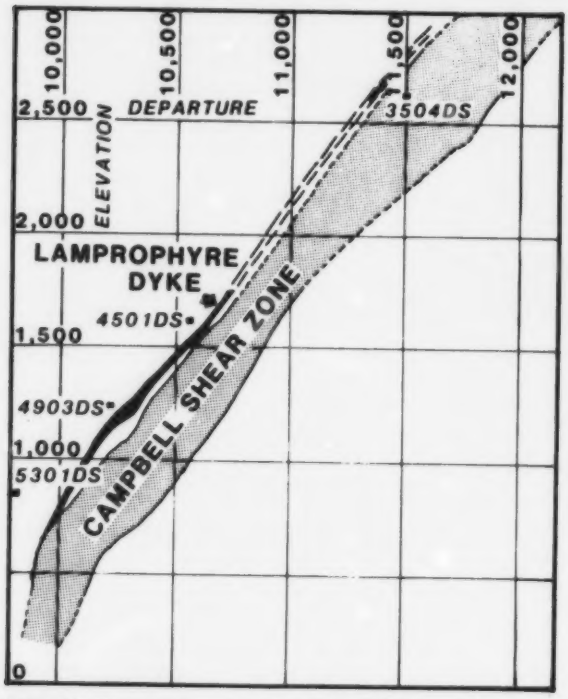

Figure 2: *Cross-section of the Con Mine at latitude 17,800, facing north, showing the lamprophyre dyke relative to the Campbell shear zone. Elevation and departure are in feet, relative to the mine co-ordinate system.*

gneisses, mafic volcanic rocks and quartz vein material have been found distributed medially within the dyke. The felsic xenoliths appear to be more resistant to assimilation than the more mafic xenoliths, and constitute the greatest proportion of the exotic lithotypes observed in the dyke. Xenoliths comprise a major portion of the dyke (~ 30%) in only two localities. The dyke is for the most part xenolith-free (<1%).

The lamprophyre is a medium to coarse-grained panidiomorphic rock. Euhedral to subhedral phenocrysts of phlogopite and pargasite predominate, and locally attain several centimetres in size. The groundmass is composed of feldspar, quartz and calcite, with abundant accessory minerals. Table 1 summarizes the mineralogy of the lamprophyre dyke, and the modal proportions of these minerals within five samples that are representative of the lamprophyre dyke are compiled in Table 2.

Pargasite, an alkali-rich calcic amphibole, occurs ubiquitously as equant euhedral phenocrysts 2 to 3 mm in size. Phenocrysts of pargasite up to 30 mm across have been observed. Pargasite is pale green in plane-polarized light, and is of variable relief. Most phenocrysts show signs of incipient to variable extents of replacement by phlogopite or chlorite. Pargasite analyses, plotted on Deer *et al's.* (1977) Na + K versus Al diagram for calcic-amphiboles are illustrated in Figure 3.

Table 1: Mineralogical composition of the lamprophyre

mineral	phenocryst	major	accessory	secondary
phlogopite	x			x
pargasite	x			
orthoclase		x		
albite-olig.		x		
calcite		x		x
quartz		x	x	x
epidote			x	x
clinozoisite			x	x
allanite			x	x
apatite			x	
prehnite			x	
rutile			x	x
barite			x	
baddelyite			x	x
pyrite			x	x
chalcopyrite			x	x
pyrrhotite			x	x
magnetite			x	
tremolite				x
chlorite				x

Table 2: Relative modal proportions of specific mineral species in representative samples of the lamprophyre.

sample	1	2	3	4	5
mineralogy					
phlogopite	22	40	45	40	60
pargasite	44	20	0	8	6
orthoclase	12	9	8	15	8
plagioclase	6	14	1	18	4
calcite	11	8	10	10	8
quartz	tr	3	3	1	9
epidote	2	4	30	4	1
apatite	1	1	2	3	2
other*	2	1	1	1	2

*includes: pyrite, pyrrhotite, chalcopyrite, barite, rutile, magnetite, prehnite, baddelyite, allanite, chlorite, tremolite, clinozoisite.

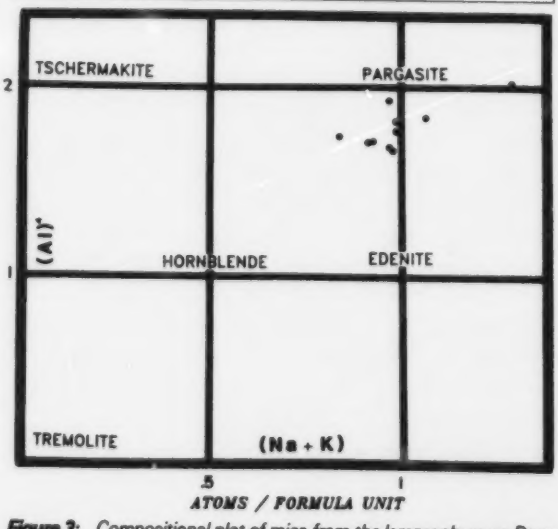

Figure 3: *Compositional plot of mica from the lamprophyre on Deer et. al.'s (1977) Na + K versus $(Al)^{4}$ diagram for calcic-amphiboles.*

Phlogopite, the most common mafic mineral, is present in all samples examined. It occurs in two forms; as corroded primary phenocrysts and, as a secondary alteration product replacing pargasite. Primary phenocrysts of phlogopite appear as euhedral to subhedral grains 2 to 3 mm long by 2 mm wide. They are commonly corroded, showing battlement or ragged terminations. The phlogopite is full of inclusions of rutile, epidote, and allanite. Thin section examination suggests these may constitute up to half the volume of a phlogopite grain. Pleochroic haloes are generally developed around the epidote and allanite inclusions, due to iron diffusion from the inclusions. The phlogopite is often bent or intracrystalline.

The secondary phlogopite is light-brown strongly pleochroic, and generally anhedral. It contains few inclusions, the most abundant of which is epidote. On a compositional diagram from Deer *et al.* (1977), the mica plots within the phlogopite field, midway between the end members phlogopite and eastonite (Fig. 4).

Orthoclase and plagioclase dominate the matrix of the lamprophyre dyke forming optically continuous poikiolitic crystals 6 to 8 mm across. Both feldspars may be twinned and show little evidence, if any, of alteration. Apatite is common in all samples. It appears as acicular to prismatic crystals averaging 8 to 10 mm long by 2 mm wide. Many of the crystals are bent or fractured and they always contain numerous inclusions, dominantly epidote.

Pyrite, pyrrhotite and chalcopyrite form net textures with the mafic minerals in the matrix of the rock. Replacement textures are found only between sulfides. The most common is pyrrhotite replacing pyrite.

Baddelyite is an accessory ZrO_2 phase, and can be found as inclusions within allanite. Commonly a reaction rim has developed between the baddelyite and the allanite. Minor amounts of chlorite are found as an alteration product of pargasite and phlogopite.

Geochemistry of the Lamprophyre Dyke

The lamprophyre dyke is characterized by relatively low SiO_2 (average 41.9 ± 1.8 wt%, 1σ), moderate alkalis (4.7 ± 2.1 wt%, 1σ), and K/Na = 2.2 ± 1.6, 1σ . Elevated LREE (La_{CN} = 920, Ce_{CN} = 850) and relatively low HREE (Yb_{CN} = 8, Lu_{CN} = 7) produce a highly fractionated chondrite-normalized pattern (La_{CN}/Yb_{CN} = 115) (Fig. 5). The lamprophyre possesses elevated abundances of incompatible elements (Ba = 1,400 ppm, Zr = 330 ppm, Rb = 270, Th, U, P and mafic-affiliated trace elements (Cr = 360 ppm, V = 220 ppm, Ni = 190 ppm, Co = 19 ppm). Analyses of representative samples of the lamprophyre dyke are compiled in Table 3.

Table 3: Abundances of major element oxides and selected trace elements in representative samples of the lamprophyre dyke.

	1	2	3	4	5
SiO_2	44.90	44.00	41.70	40.80	39.90
TiO_2	0.66	0.70	0.95	0.86	0.75
Al_2O_3	9.92	10.50	10.40	9.50	12.30
Fe_2O_3	8.33	8.98	8.55	8.50	8.10
MnO	0.12	0.15	0.10	0.14	0.11
MgO	12.50	9.64	10.40	10.60	6.21
CaO	12.50	13.30	10.10	13.80	12.90
K_2O	2.53	2.09	5.15	1.42	2.89
Na_2O	1.72	2.39	1.12	0.32	2.98
P_2O_5	1.01	1.29	1.54	1.19	1.43
L.O.I.	3.85	4.93	7.00	10.40	6.16
Total	98.40	98.30	97.30	98.40	95.00
S	0.11	0.12	0.19	0.10	0.44
Au	2	3	6	13	9
V	208	206	233	277	174
Cr	606	423	311	356	101
Co	40	41	25	35	3
Ni	276	185	230	190	62
Cu	38	41	58	74	60
Zn	100	115	147	160	111
Pb	18	44	156	327	116
Rb	111	706	304	69	166
Sr	1637	1940	843	679	6640
Y	40	49	40	44	45
Zr	313	377	266	271	425
Nb	10	8	9	9	16
Ba	1216	1100	1044	375	3272
Ga	13	13	12	12	17
Ti/Zr	12.6	11.1	21.4	19.0	10.6
Nb/y	0.25	0.26	0.23	0.20	0.36
K/Rb	189	25	141	171	145
K/Ba	17.3	15.8	41.0	31.4	7.3
Rb/Sr	0.07	0.36	0.36	0.10	0.03
Ba/Sr	0.74	0.57	1.24	0.55	0.49
Th/U	6.0	6.5	6.9	6.2	7.0

*all major oxides are in weight percent
*all trace elements are in ppm, except Au in ppb.

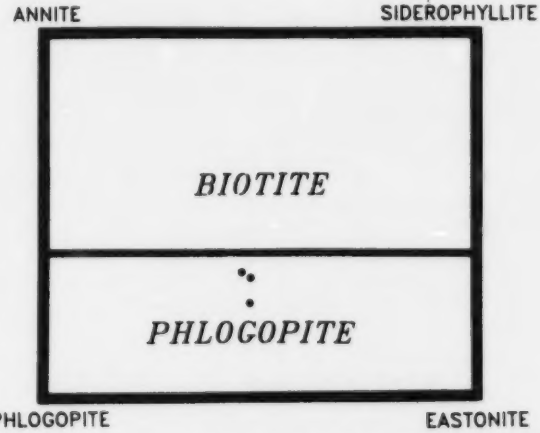

Figure 4: *Compositional plot of mica from the lamprophyre on Deer et. al.'s (1977) biotite-phlogopite diagram revealing phlogopitic compositions midway between pure end-members phlogopite and eastonite.*

Classification of the Lamprophyre Dyke

Attempts to classify the lamprophyre dyke attest to the inhomogeneity of the unit. This inhomogeneity is induced in part by the assimilation of sialic xenoliths, partly by later metasomatism, but also by intrinsic compositional variability. The dyke is a minnette, a vogesite, or a kersantite (after Streckeisen, 1979) depending on which sample is chosen (Table 4). Chemical discrimination of the lamprophyre is equally inconclusive. It plots as an alkaline igneous rock on total alkalies versus SiO_2 diagrams (Irvine and Baragar, 1971) (Fig. 6), and on Rock's (1986) ternary Al_2O_3, MgO, and CaO plot (Fig. 7); but plots as a subalkaline igneous rock on Winchester and Floyd's (1977) Zr/TiO_2 versus Nb/Y diagram (Fig. 8). A ternary $SiO_2/10$, CaO and TiO_2 x 4 plot (after Rock, 1986) reveals the lamprophyre dyke to lie within the fields of both alkaline and ultramafic lamprophyres (Fig. 9).

The lamprophyre dyke is characterized by extreme fractionation of the LIL and compatible elements which generates an extreme negative-slope on extended chondrite-normalized incompatible element diagrams (Fig. 10). There are marked troughs, or relative depletions of Nb, Ta and Ti in this pattern. A relatively low abundance of Sr is a feature noted in the Yellowknife lamprophyre, in all but the most phlogopite-rich, SiO_2-poor sample.

The rare earth element diagrams (Fig. 5, 10, 11) also reveal an enrichment of the LREE relative to the HREE, and conform to the patterns of Rock (1983) and Cullers and Graff (1984) for lamprophyre dykes.

Discussion

The lamprophyre dyke at the Con Mine is adjacent to and subparallel to, a large ore-bearing structure, the Campbell shear zone, which also acts as the host to gold orebodies. The geometry of the lamprophyre dyke indicates emplacement of the dyke in a stress field inconsistent with the stress field suggested by the geometry of the Campbell shear zone.

It is likely that either pre-existing fractures created anisotropic conditions, allowing the lamprophyre dyke to intrude perpendicular to the maximum compressive stress, or that the stress field at Yellowknife evolved and changed over time. The relative age relationships reveal that the emplacement of the lamprophyre predated some ductile deformation and predated mineralization in the shear zone. Dyke emplacement suggests an alkaline-ultramafic magmatic event late in the formation of the Yellowknife greenstone belt. Nikic *et al.* (1980) relate the emplacement of the dyke to the intrusion of the Western Granodiorite, which would confirm the age of the dyke as late Archean, although compositionally they are unlikely to be comagmatic. Rock (1983) reports that some calc-alkaline lamprophyres appear to be spatially, and possibly genetically, related to granitic plutonism. Other workers (Bachinski and Scott, 1980, Thompson *et al.*, 1984) propose a deeper, upper mantle source for lamprophyre dykes, but agree that some crustal modification of the magmas takes place.

Table 4: ***Classification scheme of lamprophyres, based on modal mineralogy (after Streckeisen, 1979).***

dominant feldspar	mica	dominant mafic mineral: amphibole	dominant mafic mineral: Na pyroxene/amphibole
K-feldspar	minnette	vogesite	soda-minnette
plagioclase	kersantite	spessartite	(not known)

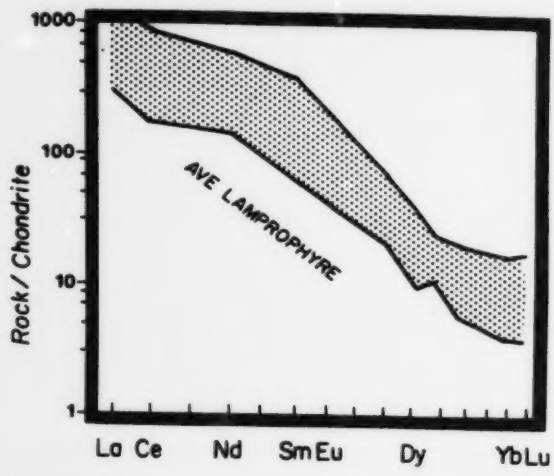

Figure 5: *Envelope of chondrite-normalized REE from Yellowknife lamprophyre revealing extreme light to heavy REE fractionation.*

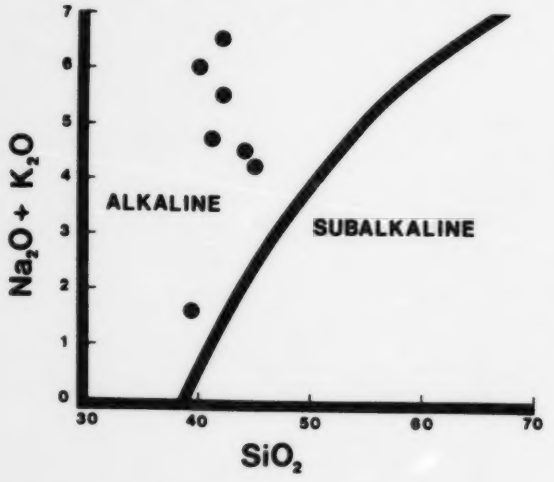

Figure 6: *Total alkalis versus SiO_2 revealing the lamprophyre to be alkaline using the discriminant line of Irvine and Baragar (1971).*

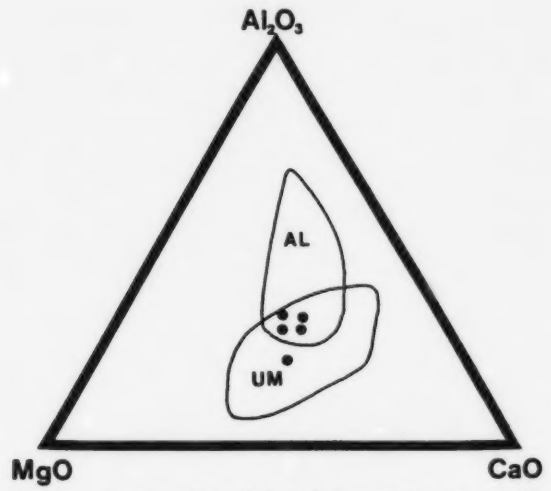

Figure 7: *A ternary Al_2O_3, MgO, CaO diagram (after Rock, 1986) illustrates the ultramafic (UM) to alkaline (AL) nature of the lamprophyre.*

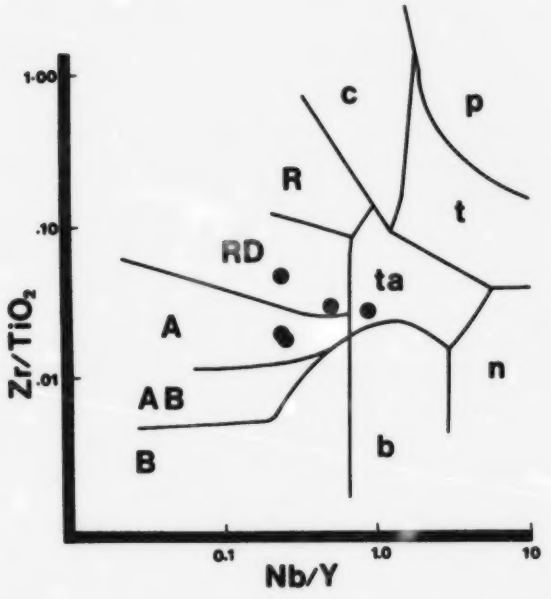

Figure 8: *The lamprophyre dyke is classified as a subalkaline rock on Winchester and Floyd's (1977) Zr/TiO_2 versus Nb/Y diagram for extrusive igneous rocks.*

There is a general concensus that alkaline mafic magmas may be generated in the mantle by low degrees of partial melting, which enriches the melt in LIL-elements relative to the incompatible elements. An alternative hypothesis appeals to the addition of an LIL-enriched "metasomatizing" fluid to the mantle source region, as a precursor to magmatism (see Thompson *et al.*, 1984, for a discussion). A consistent compositional feature of the lamprophyre dyke is the troughs at Ta-Nb and Ti on extended

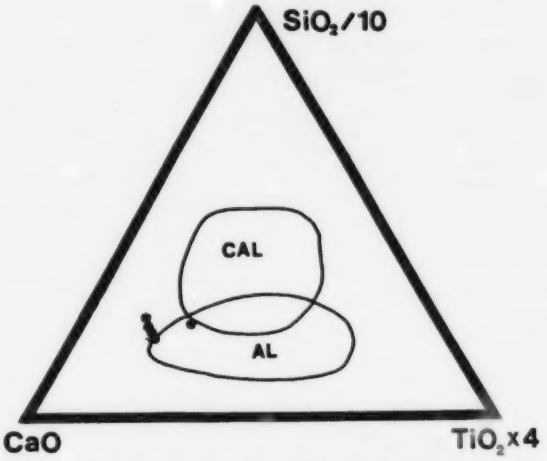

Figure 9: *The lamprophyre plots outside of the alkaline (AL) and Calc-alkaline (CAL) fields on Rock's (1986) ternary $SiO_2/10$, CaO, $TiO_2 \times 4$ plot.*

chondrite-normalized plots. Depletions of Ta and Nb relative to the neighbouring alteration-insensitive elements Th and La has been attributed to two possible processes. First, the incorporation of sediments, which carry a signature of Ta-Nb and Ti depletions, into the source region; or second, stabilization of a Ti-phase in the source region which preferentially retains Ta and Nb relative to Th and La. The latter hypothesis rests in part on the concurrence of troughs at Ta-Nb and Ti, as well as on crystal chemical considerations.

Irrespective of the causal mechanism, Phanerozoic alkaline mafic magmas, characterized by Ta, Nb and Ti troughs, are uniquely associated with destructive plate margins (Thompson *et al.*, 1984). Accordingly, we interpret the tectonic environment of this Archean lamprophyre and its source region to resemble some aspects of a subduction zone. The significance of the lamprophyre, then, may be as a tectonic "probe" of the crust-mantle conditions under which gold deposits were also formed.

The variable degree of alteration in the dyke is due in part to the sensitivity of alkaline igneous rocks to alteration, to its proximity to the Campbell shear zone and consequent potential for deformation and fluid overprint.

The geometric similarities and spatial association of the lamprophyre dyke and the Campbell shear zone must be addressed. Lamprophyre dykes are not rare in gold camps, and in fact may host ore in some deposits (McNeil and Kerrich, 1986). It is likely that for the most part this association reflects the mutual locallization of both lamprophyres and gold deposits near large trans-crustal fractures. Lamprophyre dykes require structures communicating with the upper mantle, and the gold deposits require structures to tap either metamorphic fluids (Kerrich, 1983, Watson and Kerrich, 1983), magmatic fluids (Burrows and Spooner, 1986, Mason and Melnik, 1986), or mixtures of both. A trans-lithospheric fracture could conveniently account for the presence of both lamprophyre dykes and gold deposits.

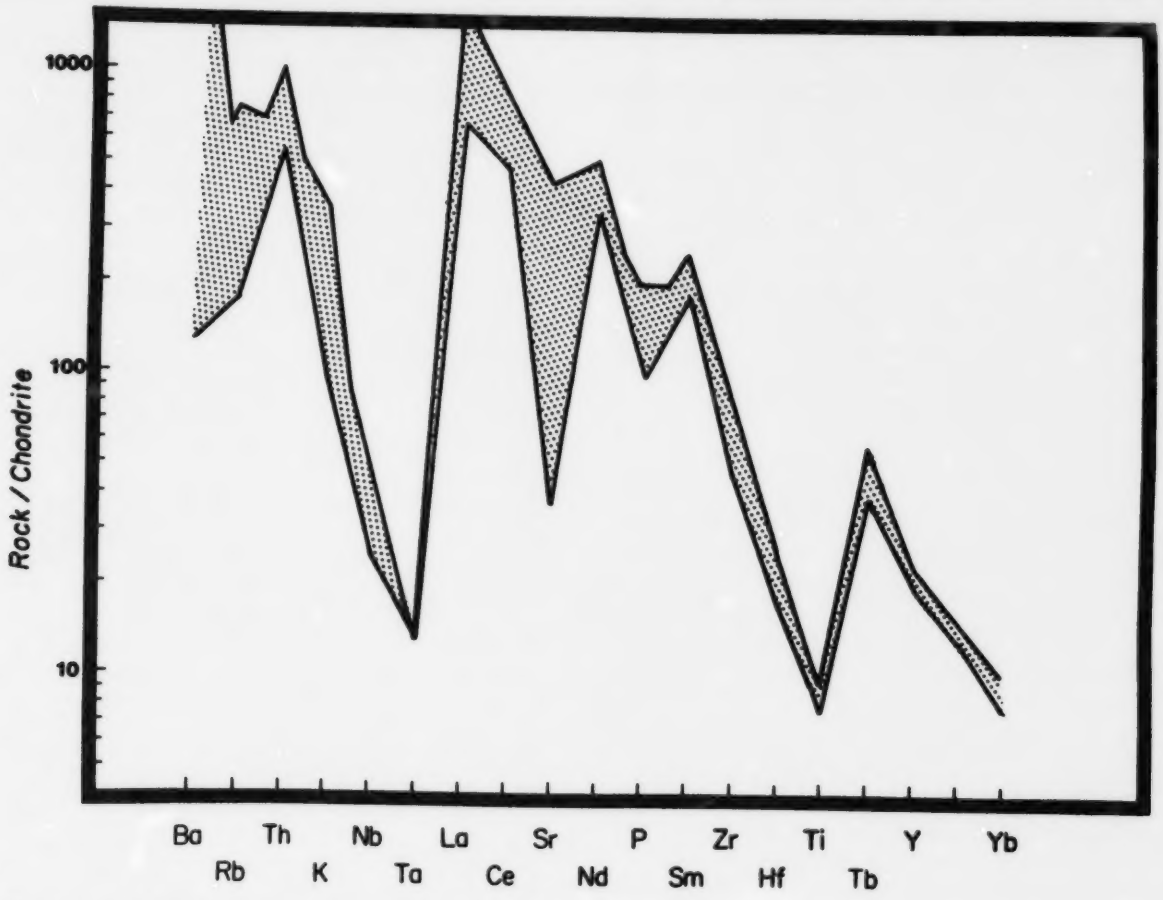

Figure 10: *The lamprophyre reveals a consistent pattern on an extended chondrite-normalized diagram characterized by an extreme negative slope with well developed troughs at Nb-Ta, and Hf-Ti. Normalizing values after Thompson et al (1984).*

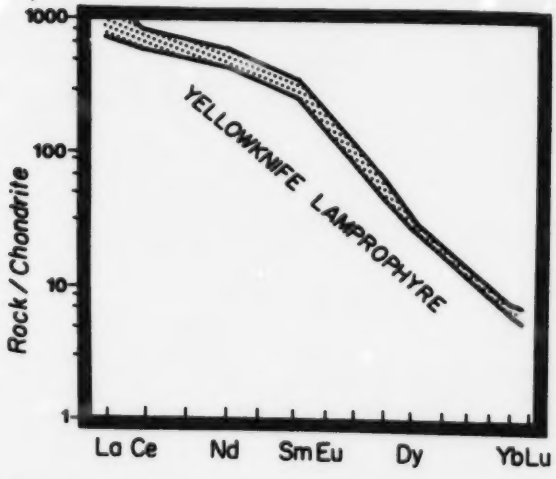

Figure 11: *Chondrite-normalized REE diagram of "average" lamprophyres (after Cullens and Graff, 1984). Compare to Yellowknife lamprophyre, Figure 5.*

In summary, the lamprophyre dyke at Yellowknife appears to be an ultramafic lamprophyre, emplaced late in the volcanic-plutonic history of the Yellowknife greenstone belt. It occupies a pre-existing structure, which is likely why it is so closely associated with the Campbell shear zone. The dyke indicates that the Yellowknife greenstone belt was underlain by granitoid crust through which mantle-derived alkaline magmas intruded the Yellowknife greenstone belt prior to the formation of the gold deposits.

Acknowledgements

We are grateful to W. Padgham for the opportunity to submit this manuscript and to two journal reviewers for helpful critiques of an earlier draft. This work was supported by an NSERC operating grant to R.K., and by Cominco Ltd.'s permission to publish.

References

Bachinski, S.W., and Scott, R.B., 1980. Authors' reply (to a critical comment by N.M.S. Rock). Geochim. Cosmochim. Acta, v. 44, pp. 1389-1392.

Bibikova, E., Baadsgaard, H., and Folinsbee, R.E. 1986. U-Pb and Sm-Nd dating of gneissic tonalite boulders from a diatreme in the Con Mine, Yellowknife, N.W.T., Canada, with South African comparisons. Prepublication abstract presented at the International Conference on Geochronology, Cambridge, England, 1986.

Bullis, H.R., Pratico, V.V., and Webb, D.R., 1987. Geology of the Con Mine, Yellowknife. *in* Padgham, W.A., ed. Field Guide Yellowknife Mining District: Yellowknife Geoworkshop Committee/Geol. Assoc. Can.

Burrows, D.R., and Spooner, E.T.C., 1986. The McIntyre Cu-Au deposit, Timmins, Ontario, Canada. *in* Proceedings of GOLD '86, (ed. A.J. MacDonald), pp 23-39.

Cullers, R.L., and Graff, J.L., 1984. Rare earth elements in igneous rocks of the continental crust: predominantly basic and ultrabasic rocks. *in* Rare earth element geochemistry. (ed. P. Henderson), Elsevier, pp 237-274.

Deer, W.A., Howie, R.A., and Zussman, J., 1977. An introduction to the rock-forming minerals. Longman Group Ltd.

Helmstaedt, H., and Padgham, W.A., 1986. A new look at the stratigraphy of the Yellowknife Supergroup at Yellowknife N.W.T. – implications for the age of gold-bearing shear zones and Archean basin evolution. Can. Jour. Earth Sci., v. 23, pp. 454-475.

Helmstaedt, H., Padgham, W.A., and Prophy, J., 1986. Multiple dykes in the Lower Kam Group, Yellowknife greenstone belt: Evidence for Archean sea-floor spreading. Geology, v. 14, pp. 562-566.

Kerrich, R., 1983. Geochemistry of gold deposits in the Abitibi greenstone belt. Can. Inst. Min. Met., Special Volume 27.

Leech, A.P., 1966. Potassium-Argon dates of the basic intrusive rocks of the District of Mackenzie, N.W.T. Can. Jour. Earth Sci., v. 3, pp 389-412.

Mason, R., and Melnik, N., 1986. The anatomy of an Archean gold system – The McIntyre-Hollinger complex at Timmins, Ontario, Canada. *in* Proceedings of GOLD'86, (ed. A.J. MacDonald), pp 23-39.

McNeil, A.M., and Kerrich, R., 1986. Archean lamprophyre dykes and gold mineralization, Matheson, Ontario: the conjunction of LILE-enriched mafic magmas, deep crustal structures, and Au concentration. Can. Jour. Earth Sci. v. 23, pp. 324-343.

Nikic, Z., Baadsgaard, H., Folinsbee, R.E., Krupicka, J., Leech, A.P., and Sasaki, A., 1980. Boulders from basement, the trace of an ancient crust? *in* Selected studies of Archean gneisses and Lower Proterozoic rocks, Southern Canadian Shield. (ed. G.B. Morey, and G.N. Hanson), Geol. Soc. Am. Special Paper 182, pp. 169-175.

Padgham, W.A., 1985. Observations and speculations on supracrustal successions in the Slave Structural Province In Evolution of Archean supracrustal sequences. (ed. L.D. Ayres, P.C. Thurston, K.D. Card, and W. Webber), Geological Association of Canada, Special Paper 28, pp. 133-151.

Rock, N.M.S., 1983. Nature and origin of calc-alkaline lamprophyres: minettes, vogesites, kersantites, and spessartites. Trans. R. Soc. Edinburgh: Earth Science, v. 74, pp. 193-227.

_____, 1986. The nature and origin of lamprophyres: an overview. prepublication copy.

Streckeisen, A., 1979. Classification and nomenclature of volcanic rocks, lamprophyres, carbonatites, and melilitic rocks. Geology, v. 7, pp. 331-335.

Thompson, R.N., Morrison, M.A., Hendrey, G.L., and Parry, S.J., 1984. An assesment of the relative roles of crust and mantle in magma genesis: an elemental approach. Phil. Trans. R. Soc. London, A310, pp 549-590.

Watson, G.P., and Kerrich, R., 1983. Macassa Mine, Kirkland Lake – production history, geology, gold ore-types and hydrothermal regimes. *in* The geology of gold in Ontario. (ed. A.C. Colvine), Ontario Geological Survey Miscellaneous Paper 110, pp. 56-74.

Webb, D.R., 1983. The relationship of ore to the structural features of the Campbell shear zone and hangingwall stratigraphy in the Con Mine, Yellowknife, Northwest Territories. unpub M.Sc. thesis, Queen's University, Kingston, Ontario, Canada.

_____, 1986. A large Archean lamprophyre dyke at the Con gold mine, Yellowknife, N.W.T. *in* Geological Association of Canada, Program with Abstracts, v. 11 p. 143.

Winchester, J.A., and Floyd, P.A., 1977. Geochemical discrimination of different magma series and their differentiation products using immobile elements. Chemical Geology, v. 20, pp. 325-343.

Phosphate Mineralogy of the Yellowknife Pegmatite Field*

M.A. Wise, R.E. Meintzer and P. Černý

Department of Geological Sciences, University of Manitoba
Winnipeg, Manitoba R3T 2N2

Introduction

The Yellowknife pegmatite field, shown schematically in Figure 1, is populated by pegmatites of the orogenic rare-element class that belong to the barren, beryl and complex types (cf. Černý). They vary from simple homogeneous dikes to complexly zoned ones. The mineralogy ranges from quartz + K-feldspar + albite ± muscovite ± biotite assemblages of the simplest barren pegmatites to more diversified assemblages of the complex dikes. These complex pegmatites contain beryl or beryl plus Nb-Ta oxide minerals, and locally also spodumene; these rare-element minerals are typical of the beryl-columbite and spodumene subtypes. Meintzer *et al.*, (1984) summarized the mineralogical and structural aspects of the pegmatite field and Wise *et al.*, (1985) described the mineralogy and geochemistry of Nb-Ta-Sn mineralization. The present report discusses the distribution, mineralogy and preliminary geochemistry of phosphate minerals from the Yellowknife pegmatite field.

Early and continued interest in the Yellowknife pegmatites focused on minerals of economic importance (e.g. beryl, columbite-tantalite, cassiterite and spodumene), but phosphates have not been considered of economic importance. Consequently, they have received little attention other than nominal mention including reports by Jolliffe (1944), Rowe (1952), Hutchinson (1955), Mulligan (1965) and Kretz (1968). Nonetheless, phosphate mineralization is quite extensive across the Yellowknife field, commonly occurring in the inner intermediate zones and core zones of moderate to well-zoned pegmatites. It is rarely found in the border zone (near the pegmatite-host contact). The most common occurrence is within Li-bearing pegmatites. The phosphate minerals found in the Yellowknife field are listed in Table 1 and the relative abundance of phosphate minerals per pegmatite series is given in Table 2.

Apatite is by far the most abundant phosphate in the Yellowknife region, occurring in both Li-poor and Li-rich pegmatites as well as in certain granites. Members of the

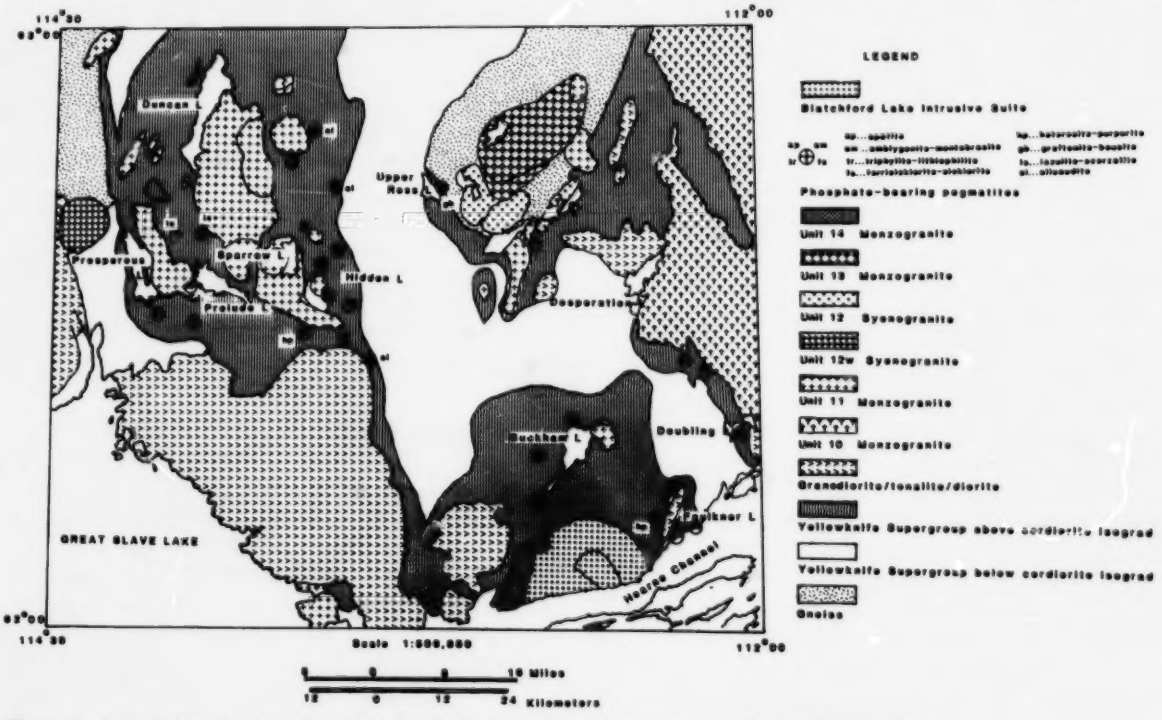

Figure 1: *Schematic map of the Yellowknife pegmatite field showing phosphate bearing pegmatites studied.*

Table 1

Primary Minerals

Apatite	$Ca_5(PO_4)_3(F,OH,Cl)$
Amblygonite-montebrasite	$LiAlPO_4(F) - LiAlPO_4(OH)$
Triphylite-lithiophilite	$LiFePO_4 - LiMnPO_4$
Graftonite-beusite	$(Fe,Ca)_3(PO_4)_2 - (Mn,Ca)_3PO_4)_2$
Wyllieite(?)	$(Na,Ca,Mn^{2+})(Mn^{2+},Fe^{2+})(Fe^{2+},Fe^{3+},Mg)Al(PO_4)_3$
Dickinsonite(?)	$(K,Ba)(Na,Ca)_3(Mn^{2+},Fe^{2+},Mg)_{14}Al(PO_4)_{12}(OH,F)_2$

Secondary Minerals

Ferrisicklerite-sicklerite	$LiFe^{3+}PO_4 - LiMn^{2+}PO_4$
Heterosite-purpurite	$Fe^{3+}PO_4 - Mn^{3+}PO_4$

Metasomatic Minerals

Alluaudite	$(Na,Ca)_4Fe^{2+}{}_4(Mn,Fe^{2+},Fe^{3+},Mg)_3(PO_4)_{12}$
Lazulite-scorzalite	$MgAl_2(PO_4)_2(OH)_2 - FeAl_2(PO_4)_2(OH)_2$
Hagendorfite(?)	$(Na,Ca)Mn(Fe^{2+},Fe^{3+},Mg)_2(PO_4)_3$

Table 2

Pegmatite Series

Mineral	FAULKNER	BUCKHAM WEST	BUCKHAM EAST	DOUBLING	TANCO	BUG	PEG	FLE	BLAISDELL	SPROULE	THOMPSON	SPARROW	HIDDEN	REID	HARDING	BIGHILL	PONTOON	TOM	PETEY	PRELUDE
Apatite	S	R		R	S	R	S		A	A		A	R	R	A	R	A	R		R
Amblygonite-montebrasite	A	A	R		A				R	R	R		R						R	R
Triphylite-lithiophilite	R	R	R		A		A		R		R	R		R		R		R		
Graftonite-beusite							R													
Wyllieite									?											
Dickinsonite																			?	
Ferrisicklerite-sicklerite	R	R	R		A		A		R	R	R	R				R				
Heterosite-purpurite	R													R						
Alluaudite								?	R	R					R					
Lazulite-scorzalite																			R	R
Hagendorfite							?													

A = abundant
S = subordinate
R = rare
? = questionable

triphylite-lithiophilite and amblygonite-montebrasite series are not as common as apatite and are restricted to Li-enriched pegmatites. The occurrence of ferrisicklerite parallels that of triphylite-lithiophilite, while beusite, lazulite-scorzalite, heterosite-purpurite and alluaudite occur only locally.

As a rule, pegmatitic phosphates are a highly diverse and chemically complex group, occurring in a wide variety of paragenetic assemblages. Moore (1973) simplified the paragenesis of pegmatitic phosphates, choosing to classify them into three paragenetic groupings based on their timing of formation: primary, metasomatic and secondary.

Primary phosphates crystallize throughout the period of pegmatite consolidation, although most are typical of the advanced stages of crystallization. Metasomatic and secondary phosphates form at the expense of primary phases. Increased activities of Na^+, K^+, Ca^{2+}, Mg^{2+} and other cations during the later stages of pegmatite consolidation result in the metasomatic replacement of earlier-formed primary phases. Secondary phosphates form as a result of oxidation, alkali leaching, and OH-F exchange during the hydrothermal stage. All three paragenetic types of phosphates occur in the Yellowknife field.

Phosphate Mineralogy

Apatite

Apatite is found as an accessory phase in some granite intrusions of the Yellowknife field and is the most abundant phosphate in the pegmatite dikes. It occurs in all zones of the pegmatites. In the border zone of the Fly pegmatite (Sproule Lake series, cf. Wise *et al.*, 1985 for location), along the pegmatite-schist contact, apatite occurs as stubby, aquamarine, euhedral, hexagonal crystals nearly 5 mm in length. Large crystals, up to 6 cm in length (Fig. 2), occur in the Fern pegmatite (Prelude Lake series, cf. Wise *et al.*, 1985 for location). Anhedral masses, however, are more typical of the apatites from the Yellowknife field. They vary in color from pink and reddish brown to green, bluish green or blue crystals. Color zonation (reddish rims, green cores) is noticeable in some apatites. Dark gray fine-grained apatite is commonly associated with amblygonite-montebrasite as thin rims and cross-cutting veinlets.

Gordiyenko (1970) notes that blue apatites are indicative of at least a Be, Nb-Ta mineralization, although in general, blue apatites appear to be restricted to albite-spodumene and complex pegmatites enriched in Li, Rb and Cs. In the Yellowknife field, pink and reddish apatites are characteristic of simple pegmatites or those with minor Be mineralization. In contrast, blue-green apatites occur in Li- and Ta enriched pegmatites and occasionally in some granites. Blue apatites, on the other hand, are restricted to pegmatites enriched in Li and Ta.

Heinrich (1952) was the first author to note that the F content decreases from early to late members of multigeneration sequences of pegmatitic apatites. Based on their study of the southern Black Hills pegmatite field, Papike *et al.* (1984) suggested the use of F, OH and Cl concentrations in apatites as potential recorders of pegmatite evolution. Their findings showed that apatites crystallizing from zones other than replacement units and fracture fillings, tend to be fluorapatites. In addition, high (OH + Cl)/F ratios in apatites is diagnostic of late-stage, fluid-derived pegmatite units.

Figure 2: *Large apatite crystals (outlined) in the Fern pegmatite.*

Although chemical data are at present insufficient to characterize possible variation across the field, X-ray powder diffraction data indicate that apatite from the Yellowknife field is predominantly close to end-member fluorapatite. Electron microprobe analysis indicate that the Cl content in the Yellowknife apatites is generally minor (< 0.25 wt. % Cl), but is particularly high in apatites associated with lazulite-scorzalite. These Cl-bearing apatites contain 0.80 - 4.10 wt. % Cl. MnO + FeO is generally less than 5% in all apatites examined.

Triphylite-lithiophilite

The second most abundant phosphate in the Yellowknife field is triphylite, the Fe-rich end member of the triphylite-lithiophilite series. No lithiophilite was found in the field by the authors, although it was previously reported by Jolliffe (1944) and Hutchinson (1955). When fresh, triphylite occurs as small anhedral dark green grains, typically less than 1.5 cm in size, but it may reach 6 cm in maximum dimension. In some localities, triphylite displays a dark black submetallic oxidation coating characteristic of incipient weathering. Triphylite commonly occurs in the intermediate zones of spodumene-bearing pegmatites, associated with K-feldspar, albite, muscovite, quartz, spodumene and other phosphates such as apatite and montebrasite. Rare intergrowths of triphylite and beusite occur in pegmatites from the Peg series (cf. Wise *et al.*, 1985 for location).

Microprobe data on triphylite from the Yellowknife field show Mn/(Mn + Fe) ratios which range from 0.11 to 0.40.

These ratios are consistent with the overall Fe-rich pegmatite chemistry suggested by Nb-Ta oxide data of Wise *et al.* (1985).

Amblygonite-montebrasite

Amblygonite-montebrasite ranks second only to triphylite as the most abundant Li-phosphate mineral in the Yellowknife field. Amblygonite-montebrasite occurs as blocky, subhedral crystals or rounded nodules in poorly to well-zoned complex lithium pegmatites. Although most nodules are less than 10 cm in diameter, some amblygonite-montebrasite from the Moose and Bet pegmatites (Faulkner Lake series, cf. Wise *et al.*, 1985 for location) attain a maximum size of 1 m. Commonly associated with spodumene, they are typically found in the inner zones and core of the pegmatite.

Amblygonite-montebrasite is typically gray to white, rarely yellowish, and displays greasy to vitreous luster. Diffuse color banding or zonation is noticeable at many localities. Most of the amblygonite-montebrasite crystals are penetrated by veinlets of late secondary gray to greenish-gray montebrasite or apatite. In addition, an alteration rind composed of fine-grained lithian muscovite and apatite is commonly observed along contacts with silicate minerals.

The main geochemical variable in the amblygonite-montebrasite series is the F-OH substitution. The term amblygonite is applied to members of the series in which the F content exceeds 6.5 wt.%. In general, the F content of the Yellowknife specimens is low with only scattered local enrichment. The overall range determined by the four-peak method of Kallio (1978) is 0.28 to 7.11 wt.%; however most of the individual pegmatite series show much narrower ranges, typically between 1.0 and 2.0 wt. % F (Figure 3). Consequently, most of the specimens studied display F contents less than 6.5 wt. % and are montebrasite. The only true amblygonite occurs at the Riber pegmatite (Petey Lake series, cf. Wise *et al.*, 1985 for location), contains 7.11 wt. % F. Specimens from the Vo (Blaisdell Lake series) (6.31 wt. % F), Mac (Buckham Lake West series) (6.15 % F) and Jo (Tanco Lake series) (5.16 % F) pegmatites may be regarded as fluorian montebrasites (cf. Wise *et al.*, 1985 for location).

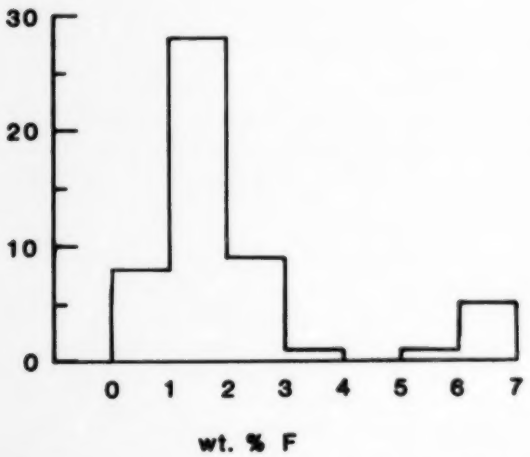

Figure 3: *Histogram of fluorine content in amblygonite-montebrasite. Number of samples analysed plotted against fluorine content.*

In the pegmatite fields or groups examined in sufficient detail, the fluorine content of primary montebrasites ranges from 5 to 6 wt. % (Černá *et al.*, 1972, 1973; Lenton, 1979; Černý, unpubl. data; D. London (White Picacho district, Arizona), pers. comm. 1985). The low F-contents shown by the Yellowknife montebrasites closely correspond to those of secondary montebrasites, generated by F-OH exchange at the expense of the primary composition. However, microscopic examination of the Yellowknife amblygonite-montebrasites reveals only a very limited extent of textures indicative of secondary alteration as follows:

1. Specimens containing > 5 wt. % F lack the abundant secondary veining so typical of extensive OH-F exchange. These specimens are found in the more fractionated pegmatites of the field.
2. The main population (1 - 4 % F) occurs as large, blocky masses in moderately fractionated pegmatites. Incipient OH-F substitution is present, but not extensive.
3. Finally, extremely low F contents (< than 1 % F) are found in medium grained montebrasites associated with saccharoidal albite and metasomatically produced lazulite. As in the other groups, OH-F exchange is minimal.

In all cases, the Yellowknife montebrasites show nearly homogeneous textures with minimal veining by secondary material. In contrast, specimens from other pegmatites such as the Tanco deposit in southeastern Manitoba, or the White Picacho District of Arizona show extensive veining to such a degree that a major portion of the original material is replaced by secondary montebrasite (Černá, 1970; Černá *et al.*, 1972; London and Burt, 1982). The Yellowknife specimens do not show such replacement and consequently must be considered primary.

Beusite

The rare Mn-rich member of the graftonite-beusite series, beusite, has been found in only one pegmatite from the Peg series (dike # 93; cf. Hutchinson, 1955, for location). It occurs as light brown lamellae up to 1.0 mm thick, interlaminated with triphylite (Figure 4). The intergrowths occur in a quartz + perthite + muscovite + plagioclase intermediate zone, associated with beryl, ferrocolumbite, ferrotapiolite, almandine and pyrite.

Optical studies of the intergrowths reveal interesting

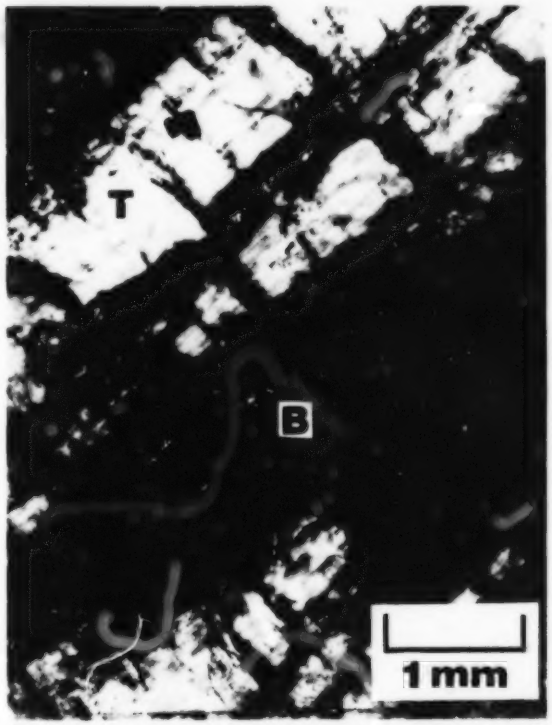

Figure 4: *Photomicrograph of beusite (dark) – triphylite (light) exsolution intergrowths. Photograph taken under cross-nicols in a section nearly parallel to the 001 cleavage of triphylite.*

crystallographic properties. Thin sections show continuous and uniform extinction for the beusite thus indicating a uniform crystallographic orientation. In contrast, the coexisting triphylite is present in at least three different optical orientations. In general, the preferred orientation of triphylite to beusite is such that the [110] of triphylite is parallel to the [100] of beusite.

Chemically, beusite is quite homogeneous under the electron microprobe, showing only minor variations in the Mn/(Mn + Fe) ratio (0.54 - 0.57) (Wise and Černý, unpub. manuscript). In addition, a high Ca content (16 wt. % CaO) characterizes the Yellowknife specimens; beusites from other localities generally contain less than 6 wt. % CaO (Hurlbut and Aristarain, 1968).

Lazulite-scorzalite

Lazulite-scorzalite occurs in three small pegmatite bodies of the Petey Lake series (Petey, Lily, Barbaloo) between the Duncan and Prosperous granites (cf. Wise *et al.*, 1985 for locations). The pegmatites are generally poorly zoned with little albitization and rare-element mineralization, including beryl, montebrasite and locally ferrocolumbite.

Lazulite-scorzalite occurs as dark to sky-blue, fine-grained aggregates intimately intergrown with montebrasite and apatite. Disseminated grains and veinlets of lazulite-scorzalite penetrate white montebrasite giving the specimen a mottled appearance.

Microprobe analyses indicate that single crystals of the Yellowknife lazulite-scorzalite are chemically variable and most lie near the lazulite end of the series. Mg/(Mg + Fe) ratios vary from 0.52 to 0.84. Only one analysis gave results corresponding to scorzalite (analysis # 7, Table 3). The contents of Mn and Ca are low, generally less than 0.5 wt. % oxide. Although Jolliffe (1944) reported the occurrence of lazulite in numerous dikes of the Yellowknife field, it is the opinion of the authors that the mineral he observed was, in many cases, actually blue apatite.

Alluaudite

Alluaudite was previously identified as huhnerkobelite by Mulligan (1965) in the Vo pegmatites (Blaisdell Lake series, cf. Wise *et al.*, 1985 for location) and was subsequently reported by Kretz (1968) in the Casper pegmatites (Sparrow Lake series, cf. Wise *et al.*, 1985 for location). Alluaudite is rare in the Yellowknife field; besides the occurrences mentioned above it has been observed only in the Bill (Blaisdell Lake series) and Jake-Da pegmatites (Harding Lake series, cf. Wise *et al.*, 1985 for locations). It forms fine-grained, dark green to black-green aggregates that may be easily mistaken for triphylite. Specimens range from grains 3 mm in size up to nodules 6 cm long.

Ferrisicklerite

A secondary alteration product of triphylite, ferrisicklerite forms dark brown compact masses commonly pseudomorphing the parent triphylite. It commonly forms as a thin submetallic black alteration rind coating the

Table 3

	1	2	3	4	5	6	7	8
P_2O_5	40.4	41.7	40.7	46.2	41.6	45.4	42.7	39.7
SiO_2	0.0	0.0	0.0	0.0	0.0	0.0	0.0	0.1
Al_2O_3	0.0	0.0	0.0	0.0	0.0	31.9	28.1	1.7
BaO	0.0	0.0	0.0	0.0	0.0	0.0	0.0	5.9
FeO*	2.0	0.0	0.0	27.6	19.8	3.8	15.6	29.7
MnO	3.7	4.0	0.8	18.1	23.1	0.0	0.3	13.4
CaO	50.4	51.2	54.4	0.2	16.1	0.0	0.2	1.6
MgO	0.0	0.0	0.0	0.0	0.0	10.9	3.5	1.6
K_2O	0.0	0.0	0.0	0.0	0.0	0.0	0.0	0.4
Na_2O	0.0	0.0	0.0	0.0	0.0	0.0	0.0	4.0
Cl	4.1	0.0	0.3	0.0	0.0	0.0	0.0	0.1
Total	100.6	96.9	96.2	92.1	100.6	92.0	90.4	98.2
O=Cl	0.9	–	0.1	–	–	–	–	–
Total**	99.7	96.9	96.1	92.1	100.6	92.0	90.4	98.2

Samples **1)** Cl-apatite, Petey pegmatite; **2)** apatite, Fern; **3)** apatite, Moose; **4)** triphylite, Peg # 93; **5)**beusite, Peg # 93; **6)** lazulite, Petey; **7)** scorzalite, Rose; **8)** dickinsonite (?), Barbaloo.

* Total Fe as FeO.

** H_2O and F account for totals lower than 100%.

triphylite; it achieves its characteristic brown color only with further oxidation. In many cases, the primary cleavages of triphylite may be evident even when the parent phase is completely replaced.

Minor phases

Several minor secondary phosphates were noted in the Yellowknife field but at present are not fully characterized. Heterosite-purpurite was found as a small purplish mass with ferrisicklerite in the Tan pegmatites (Faulkner Lake series) near Drever Lake and Pancho Villa pegmatites (Reid Lake series) near Reid Lake (cf. Wise *et al.*, 1985 for locations). Phosphates resembling wyllieite and hagendorfite have been identified from the Bill pegmatite (Blaisdell Lake series) and the Peg series, respectively, by X-ray powder diffraction methods. In addition, electron microprobe analysis suggests the presence of a Ba-rich secondary phosphate similar in composition to dickinsonite from the Barbaloo pegmatite (Petey Lake series). Further examination of these phases is in progress.

Summary

In general, the Yellowknife pegmatite fields can be ranked with the phosphate-poor spodumene-bearing fields of the world, such as the Preissac-Lacorne field in Quebec (Mulligan, 1965). The P_2O_5 content of the leucogranites associated with the Yellowknife pegmatites, however, is quite variable; some leucogranite plutons have less than average contents of P_2O_5 for granitic rocks, while some are above average.

The principal control on the bulk P_2O_5 content of differentiated granitoid complexes is the abundance of P_2O_5 in the metamorphic source region. Whatever the initial concentration, phosphorus evidently tends to accumulate in late members of granite-pegmatite sequences. This is shown by the examples of suites that start at average P_2O_5 levels in the granites, but grade into phosphate-rich pegmatites such as the Harney Peak Granite (with 0.04 - 0.19 wt. % P_2O_5) and the surrounding pegmatite field of the southern Black Hills, South Dakota (Černý, 1982, and Walker, 1984). In other cases, the fertile granites have high P_2O_5 contents themselves (e.g. 0.20 - 0.65 wt. % P_2O_5 in the granites of the phosphate-rich Northern Oberpfalz field in Bavaria; Strunz, 1974). Pegmatite swarms "depleted" in phosphorus are rather exceptional (as the Greer Lake group in southeastern Manitoba which carries only microscopic accessory apatite, and is associated with granite containing P_2O_5 in the 0.04 - 0.11 wt. % range; Černý *et al.*, 1981).

In the Yellowknife field, granites probably comagmatic with the pegmatites display variable P_2O_5 contents. The highest contents are in the two-mica leucogranites of the Prosperous Granite (Henderson, 1985) in which the average P_2O_5 wt.% in individual plutons varies from 0.01 to 1.12 wt. %. The relatively high phosphorus content is borne out by the presence of light, blue-green apatite grains, visible in hand-samples. The leucogranites of the Redout Granite (Henderson, 1985) situated in the northeastern part of the field immediately east of the Peg pegmatite series have, on the other hand, a range of 0.02 - 0.16 wt. % P_2O_5; the maximum is found in the Redout pluton which borders on the Peg series.

Despite the trends repeatedly observed in pegmatite fields worldwide, the details of phosphorus behavior in the granite-pegmatite sequences are far from being properly understood. The available experimental work applies to peralkaline rather than peraluminous melts (Watson and Capobianco, 1981), and experimentation on phosphates in fractionated pegmatite melts is only in its infancy (Shigley and Brown, 1986). Considering the variety of cations entering primary pegmatite phosphates (Li, Na, K, Be, Mg, Ca, Fe, Mn, Al) and the complexity of factors that may influence the phosphate-building components indirectly, the story of primary phosphates will require extensive field observation, crystallochemical consideration and experimental work before it matches the degree of understanding reached in the study of metasomatic and secondary phosphate assemblages (e.g., Moore, 1982).

Conclusion

The primary phosphates of the Yellowknife pegmatite field include apatite, triphylite, montebrasite and an unknown graftonite-like phase. Crystallization of primary phases occurred throughout the pegmatite's consolidation history, with apatite presumably crystallizing first. The pegmatitic fluids from which these phosphates crystallized were generally F-poor and enriched in Fe relative to Mn as indicated previously by Nb-Ta oxide geochemistry (Wise *et al.*, 1985). Crystallization of fluorapatite resulted in further depletion of F in the pegmatite fluid. Consequently, later-formed primary phosphates such as montebrasite are low in F and enriched in OH. A high-temperature, Li-rich, graftonite-like parent phase was the most probable precursor of the beusite-triphylite exsolution intergrowths (Hurlbut and Aristarain, 1968). Segregation of Li and Ca with decreasing temperature resulted in the interlaminated texture exhibited by the beusite-triphylite aggregates.

Through metasomatic processes, oxidation and alkali leaching, phosphates such as lazulite, alluaudite and ferrisicklerite are formed. Introduction of Na^+, Ca^{2+} and Mg^{2+} coupled with simultaneous leaching of Li^+ resulted in the formation of alluaudite from triphylite, and lazulite from montebrasite.

Oxidation of Fe^{2+} to Fe^{3+} in triphylite results in the formation of ferrisicklerite. Heterosite-purpurite subsequently forms by the leaching of Li^+. Veinlets of secondary montebrasite form from primary amblygonite-montebrasite

as a result of OH-F exchange in the primary phase (London and Burt, 1982). Leaching of Li^+ along with Ca-metasomatism produces the fine-grained secondary apatite veinlets which rim and transect the parent montebrasite.

Acknowledgements

The authors gratefully acknowledge the financial support provided by the NWT Geology Division of Indian Affairs and Northern Development, Yellowknife.

References

Černá, I. 1970. Mineralogy and paragenesis of amblygonite-montebrasite with special references to the Tanco (Chemalloy) pegmatite, Bernic Lake, Manitoba. Unpublished M.Sc. Thesis: University of Manitoba, Winnipeg.

Černá, I., Černý, P. and Ferguson, R.B. 1972. The Tanco pegmatite at Bernic Lake, Manitoba. III. Amblygonite-montebrasite. Canadian Mineralogist: v. 11, 643-659.

——, 1973. The fluorine content and some physical properties of the amblygonite-montebrasite minerals. American Mineralogist: v. 58, 291-301.

Černý, P. 1986. Rare-element granitic pegmatites: in Monograph series on mineral deposits geology. In press.

——, 1982 Petrogenesis of granitic pegmatites, in Černý, P.,ed.,Granitic Pegmatites in Science and Industry: Mineralogical Association of Canada Short Course Handbook, v. 8, p. 405-461.

Černý, P., Trueman, D.L., Ziehlke, D.V., Goad, B.E. and Paul, B.J. 1981. The Cat Lake-Winnipeg River and the Wekusko Lake pegmatite fields, Manitoba. Manitoba Dept. Energy and Mines: Mineral Resources Division Economic Geology Report ER80-1, 234 pp.

Gordiyenko, V.V. 1970. Mineralogy, geochemistry and genesis of the spodumene pegmatites. Nedra Lenigrad: 237 pp., in Russian.

Heinrich, E.W. 1952. Chemical differentiation of multi-generation pegmatite minerals. Geological Society of America Bulletin: v. 63, p. 1261.

Henderson, J.B. 1985. Geology of the Yellowknife-Hearne Lake Area, District of Mackenzie: A segment across an Archean basin. Geological Survey of Canada Memoir: 414, 135 p.

Hurlbut, C.S., Jr. and Aristarain, L.F. 1968. Beusite, a new mineral from Argentina, and the graftonite-beusite series. American Mineralogist: v. 53, p. 1799-1814.

Hutchinson, R.W. 1955. Regional zonation of pegmatites near Ross Lake, District of Mackenzie, Northwest Territories. Geological Survey of Canada Bulletin: 34, 50 p.

Jolliffe, A.W. 1944. Rare-element minerals in pegmatites, Yellowknife-Beaulieu Area, Northwest Territories. Geological Survey of Canada: Paper 44-12, 23 p.

Kallio, P. 1978. A new X-ray method for the estimation of fluorine content in montebrasites. American Mineralogist: v. 63, 1249-1251.

Kretz, R. 1968. Study of pegmatite bodies and enclosing rocks, Yellowknife-Beaulieu Region, District of Mackenzie. Geological Survey of Canada Bulletin: 159, 105 p.

Lenton, P.G. 1979. Mineralogy and petrology of the Buck Claim lithium pegmatite, Bernic Lake, southeastern Manitoba. Unpublished M.Sc. Thesis: University of Manitoba, Winnipeg.

London, D., and Burt, D.M. 1982. Alteration of spodumene, montebrasite and lithiophilite in pegmatites of the White Picacho District, Arizona. American Mineralogist: v. 67, p. 97-113.

Meintzer, R.E., Wise, M.A., and Černý, P. 1984. *Distribution and structural setting of fertile granites and related pegmatites in the Yellowknife Pegmatite Field*, District of Mackenzie, in Current Research, Part A. Geological Survey of Canada Paper 84-1A: p. 373-381.

Moore, P.B. 1973. Pegmatite phosphates: descriptive mineralogy and crystal chemistry. Mineralogical Record: v. 4, p. 103-130.

——, 1982. Pegmatite minerals of P(V) and B(III): in P. Cerny, ed., Granitic pegmatites *in* Science and industry. Mineralogical Association of Canada Short Course Handbook: v. 8, p. 267-291.

Mulligan, R. 1965. Geology of Canadian lithium deposits. Geological Survey of Canada Economic Geology Report 21: 131 p.

Papike, J.J., Jensen, M., Shearer, C.K., Simon, S.B., Walker, R.J. and Laul, J.C. 1984. Apatite as a recorder of pegmatite petrogenesis. Geological Society of America Abstracts with Programs: v. 16, p. 617.

Rowe, R.B. 1952. Pegmatite mineral deposits of the Yellowknife - Beaulieu Region, District of Mackenzie, Northwest Territories. Geological Survey of Canada Paper 52-8: 36 p.

Shigley, J.E. and Brown, G.E., Jr. 1986. Lithiophilite formation in granitic pegmatites: A reconnaissance experimental study of phosphate crystallization from hydrous aluminosilicate melts. American Mineralogist: v. 71, p. 356-366.

Strunz, H. 1974. Granite and pegmatites in eastern Bavaria: Fortschr. Mineral: v. 52, p. 1-32.

Walker, R.J. 1984. The Origin of the Tin Mountain pegmatite, Black Hills, South Dakota. Unpublished Ph.D. Thesis, State University of New York at Stony Brook.

Watson, E.B. and Capobianco, C.J. 1981. Phosphorus and the rare earth elements in felsic magmas: An assessment of the role of apatite. Geochimica et Cosmochimica Acta: 45, p. 2349-2358.

Wise, M.A., Meintzer, R.E. and Černý, P. 1985. The Yellowknife Pegmatite Field: Mineralogy and geochemistry of Nb-Ta-Sn oxide minerals, in Contributions to the Geology of the Northwest Territories, v. 2. Geology Div., Yellowknife, Canada, Department of Indian Affairs and Northern Development, Northern Affairs Program: EGS 1985-6, p. 15-25.

Contribution to the Geology of the Northwest Territories, Volume 3, 1988, NWT Geology Division, INAC, Yellowknife.

Geophysics and Permafrost[1]

by W.J. Scott
Hardy BBT Limited, Calgary

Introduction

The purpose of this paper is to describe the influence of permafrost on standard geophysical prospecting techniques for mining exploration and then to describe the use of geophysics for the mapping of permafrost. The influence of permafrost on geophysical measurements can be assessed by looking at the dependence on temperature of geophysical properties such as resistivity, susceptibility, density and seismic velocity. These temperature dependences also demonstrate the particular utility of seismic and electric techniques for mapping permafrost.

Influence of Permafrost on Prospecting Methods

Figure 1 shows the common geophysical prospecting techniques arranged in order of ascending susceptibility to influence by permafrost. For each method the parameter measured is shown as well. The range of temperature variation considered is limited to that seen in near-surface soils and rocks in northern Canada. Typical temperatures range from +10°C to -20°C

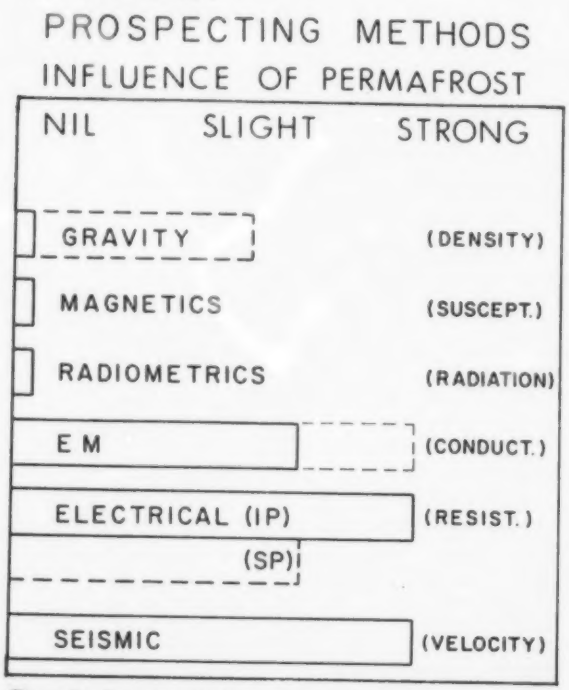

Figure 1: *Common geophysical prospecting techniques and their susceptibility to permafrost influences.*

Because measurements of susceptibility are not influenced by the transition from positive to negative temperatures, magnetic measurements are not significantly influenced by permafrost. Magnetic surveys map variations in magnetic field strength related to changes in concentration of magnetic minerals, or to changes in orientation of remnant magnetization. Within the specified temperature range, magnetic properties of common rocks and minerals are essentially invariant.

Since freezing of a rock or soil makes almost no difference to its radioactive characteristics, radiometric methods are also free of permafrost influences. However, permeability of rocks and soils to gases is reduced when the materials are frozen. Thus, radiometric methods dependent on the detection of diffusing radon gas or its daughter products may be less sensitive in permafrost terrains.

The freezing of a rock or soil makes very little difference to its density provided that excess water is not present. Consequently gravity measurements in dry rock areas are essentially independent of temperatures. If, however, the material has significant porosity, and if excess water is available during the freezing process, then ground ice can be formed under the appropriate conditions and the density of the material can be significantly reduced. (Rampton and Walcott, 1974)

In seismic and electrical methods, however, the influence of freezing is considerable. Figure 2 after Aptikaev (1964) shows the dependence of seismic velocity on temperature for a temperature range from +10°C to −10°C. Above 0° seismic velocities are essentially constant. As temperature decreases through 0°, however, there is a large and rapid increase in velocity. As temperatures continue to decrease, velocity increases more slowly. Figure 3 after Hoekstra *et al.*, (1974) shows a corresponding dependence of resistivity on temperature. Resistivity is essentially independent of temperature for values above freezing, but at or just below 0° there is a large increase in resistivity and for further decrease in temperature there is a corresponding regular increase in resisti[illegible]. Both velocity and resistivity increase when temperatu[illegible]s decrease through 0°C. However, while seismic velocity may double or triple with decreasing temperature, resistivity may increase by several orders of magnitude over the same decrease in temperature.

The temperature dependence of resistivity and velocity of a material can be explained in terms of the water in the pores. Most soils and rocks are composed of minerals which

[1]*Presented at Yellowknife Geoscience Forum, December, 1988. Revised: December 1987*

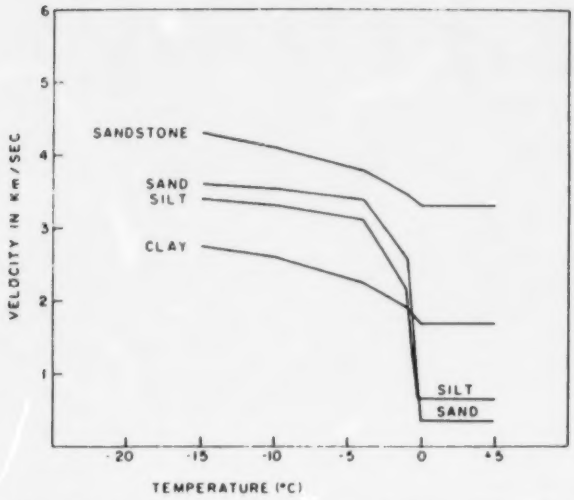

Figure 2: *Seismic velocity as a function of temperature, after Aptikaev (1964).*

are electrical insulators. The conduction of electircity is primarily through the water which fills the pores. Seismic energy on the other hand, travels through both the solid materials and the pore fluids, and the velocity is an average of the higher velocity in the solid minerals and the lower velocity in the fluids.

At temperatures above 0° Celcius the pore water is present as a liquid, and relatively low values of resistivity and velocity reflect this situation. At temperatures below freezing, however, a large part of the water in the pores turns to ice, which has both higher resistivity and higher velocity than liquid water. Thus both resistivity and velocity of the material increase. As mentioned above, for a given drop in temperature, resistivity increases are greater than velocity increases.

At sub-zero temperatures a significant fraction of the pore-water remains liquid. Figure 4, after Anderson and Morgenstern (1973), shows the unfrozen water content of clay-containing materials as a function of sub-zero temperatures. Note that some water remains unfrozen even below – 20° Celsius. At low temperatures the amount of unfrozen water depends on the clay content of the material. Once freezing has taken place in sands and gravels, resistivity and velocity vary only slightly with decreasing temperature. For silts and clays, however, resistivity and velocity show strong temperature dependence even below – 20° Celsius.

Figure 2 shows that seismic velocities are much higher in permafrost than in non-permafrost regions. This fact has serious repercussions in the use of seismic techniques for hydrocarbon exploration in permafrost regions. Variation of

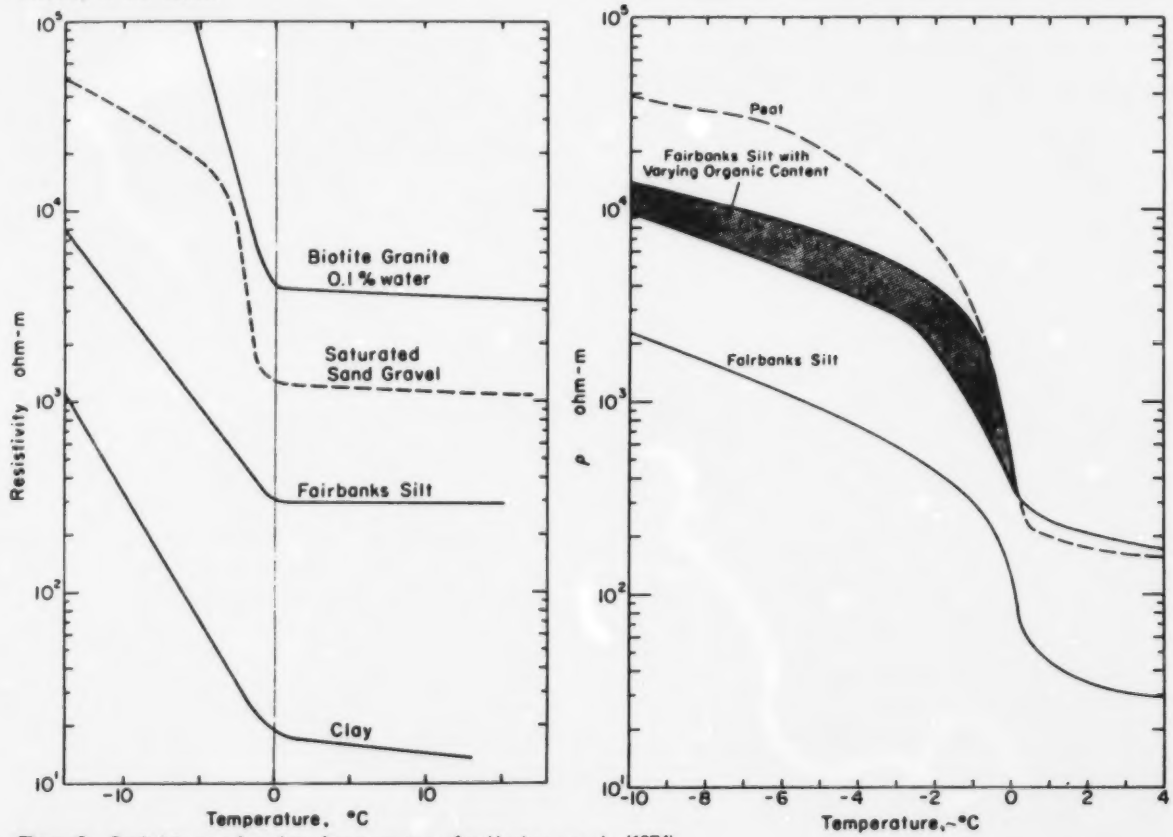

Figure 3: *Resistivity as a function of temperature, after Hoekstra et al., (1974).*

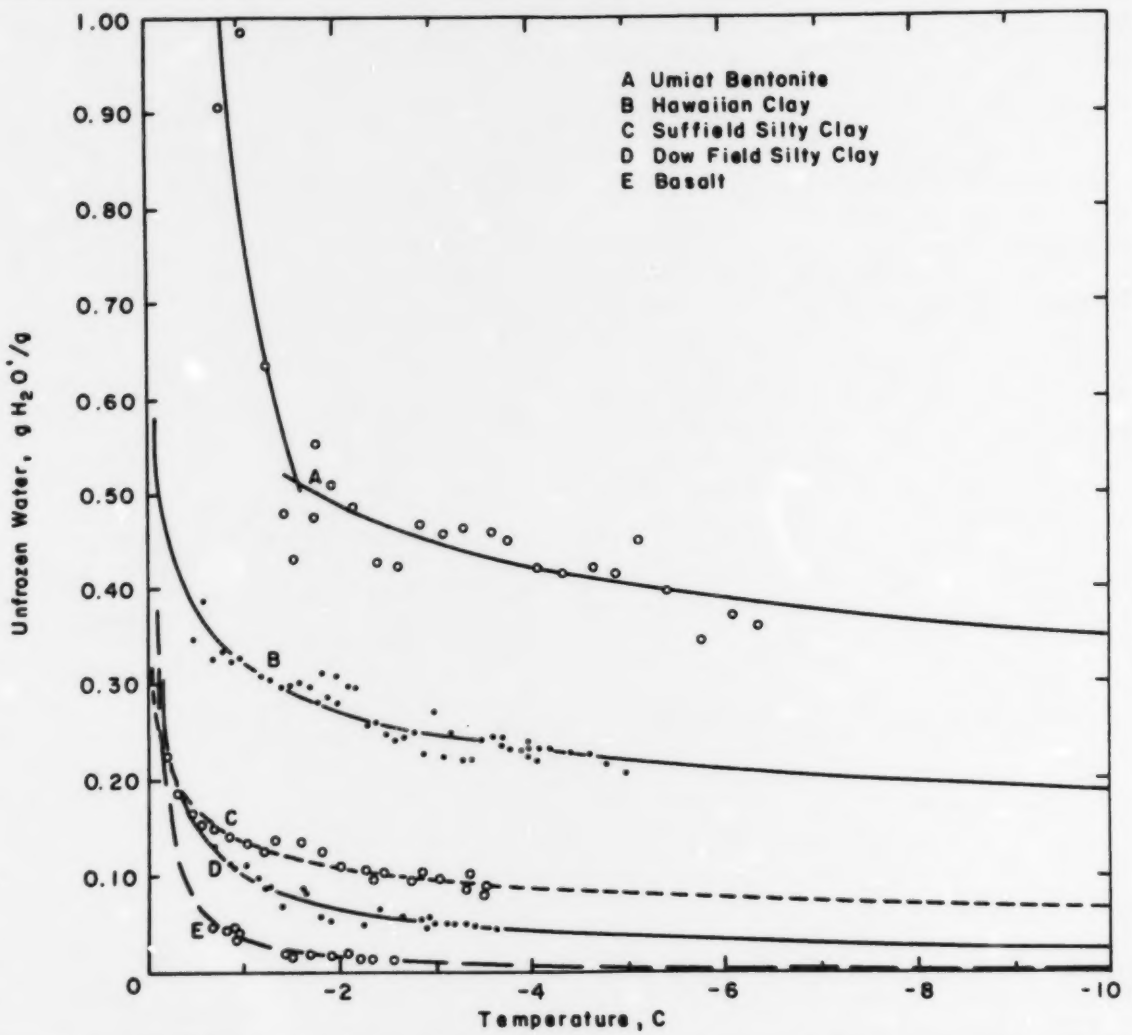

Figure 4: *Unfrozen water content of materials containing clay, as a function of sub-zero temperatures, after Anderson and Morgenstern, 1973.*

permafrost thickness in a seismic survey area requires the use of large static corrections to obtain undistorted reflections from below the base of permafrost, (Hatlelid and MacDonald, 1982). Because this paper is primarily concerned with mineral exploration geophysics, however, no further considerations will be given to the static-correction problem.

Decreasing temperatures below 0° increases background induced polarization (IP) responses due to membrane effects. Membrane polarization arises when pores in a material are so narrow that the mobility of charged ions in the pores is restricted by charges accumulated on particles in the pore walls. (Telford et al, 1976, p. 703-706). Membrane effects are most pronounced when the pores contain some clay minerals. As the temperature decreases, progressively more of the pore water freezes. Dissolved ions diffuse from the ice into the liquid water, which consequently increases in ionic content. The formation of ice also restricts the pores, thus increasing the number of places which are narrow enough to restrict the passage of ions. The combination of increased ion content and increased ion-blockage strongly increases membrane polarization effects. Figure 5, after Olhoeft (1975), shows the dependence of resistivity on frequency for a frozen natural-clay specimen. In the frequency range of interest for IP (.01 to 10Hz), this specimen shows an IP effect of about 40% per decade. Figure 6, shows some values of IP responses for this and other specimens, calculated from results in Olhoeft (1975) and Pandit and King (1979). Although these specimens contain no metallic mineralization, at permafrost temperatures they show large IP effects due to membrane polarization. These results suggest that IP measurements in permafrost regions can be strongly influenced by the presence of clay in the overburden or bedrock. Rocks in emergent arctic shorelines can contain brine in their pores. The presence of brine can lead to

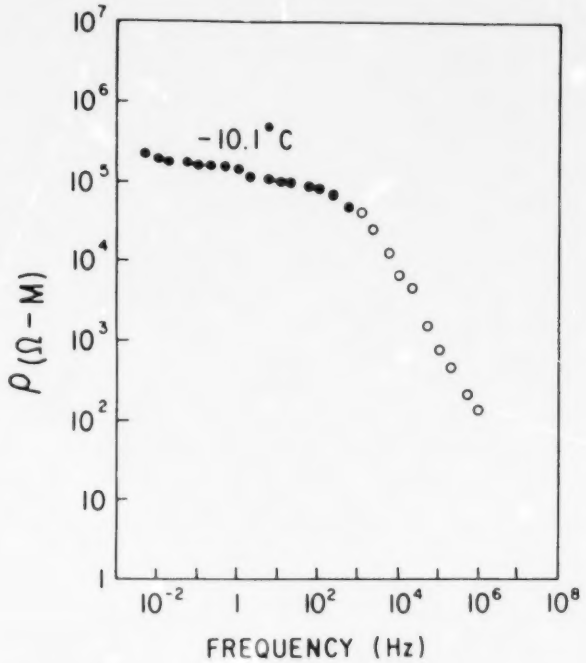

Figure 5: *Resistivity as a function of frequency for a sample of clay from near Tuktoyaktuk, N.W.T., after Olhoeft (1975).*

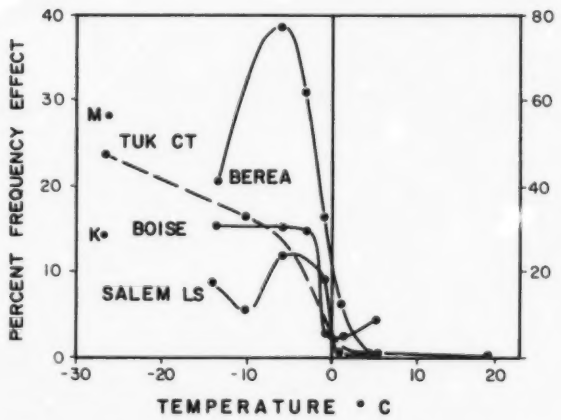

Figure 6: *IP responses as a function of temperature. Salem limestone, after Pandit and King (1979). Boise and Berea sandstone, after Pandit and King (1979) (use RH Scale for Berea). Tuk CT, the sample of Fig. 5, after Olhoeft, 1975. M: frozen montmorillonite, after Olhoeft, 1975. K: frozen kaolinite, after Olhoeft, 1975.*

lower resistivities than expected (McLaren *et al*, 1975), and possibly to higher background IP effects as well.

Kay (1981) has shown that IP effects in frozen rocks, arising from metallic mineralization, can also be very pronounced. Thus both background and anomalous responses can be considerably higher in permafrost regions. Furthermore, the generally higher resistivities lead to operational difficulties in making measurements of induced polarization and caution must be exercised to ensure that the data are reliable.

Spontaneous polarization (SP) anomalies have been observed over sulphide deposits in permafrost. These presumably arise from oxidation-reduction cells set up as result of near-surface oxidation which was established at some warmer period in the past. The strength and shape of an SP response over a sulphide zone can be strongly influenced by permafrost.

Significant freezing potentials can develop across an interface between frozen and unfrozen ground (Petera, 1973 and Yarkin, 1973). Thus SP effects could be observed at the edge of frozen ground in the discontinuous region. Since freezing potentials are created by the process of freezing, existence of such SP effects would indicate that the permafrost was either aggrading or degrading.

Electromagnetic (EM) techniques can also be strongly influenced by permafrost. The degree of influence depends on the source of conductivity giving rise to the electromagnetic anomaly. Figure 7 shows in a schematic way the dependence of permafrost influence on source-type for EM anomalies. If the anomaly arises from massive or well-connected sulphides or from graphite, then the conductivity is not particularly affected by freezing of the rock. For sources of this sort the influence of permafrost is slight. If the conductivity anomaly arises from sulphides which are not well connected then somewhat more influence can be

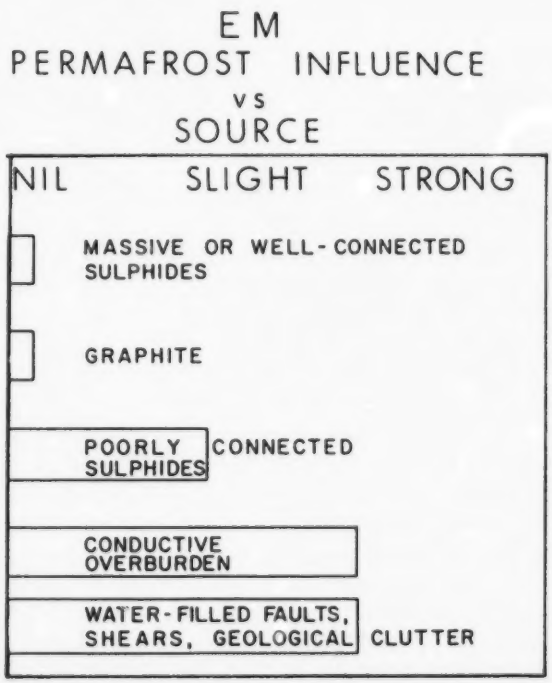

Figure 7: *Influence of permafrost on EM responses from various types of source.*

observed. In temperate zones such bodies achieve part of their conductivity from the fluids which interconnect the sulphides. In a permafrost region these pore fluids will be partly frozen and thus there will be some decrease in conductivity, (Clayton, 1966).

EM anomalies arising from conductive overburden, however, can be significantly reduced in permafrost regions, since the resistivity of frozen soils is considerably higher than if the same soils are unfrozen. It should be remembered that conductive sediments in a lake bottom will not necessarily be frozen in permafrost terrain and can still give rise to EM anomalies.

In EM surveys, anomalies are also observed which arise from water-filled faults, shear zones and similar features, which are generally grouped together as geologic noise. Since these anomalies generally depend on the presence of liquid water, their amplitudes in permafrost terrain can be significantly reduced.

In general then, magnetic and direct radiometric methods are not particularly influenced by the presence of permafrost. Gravity techniques are influenced only if some ground ice is present in the permafrost terrain. Electrical resistivity and seismic measurements are strongly influenced by the presence of permafrost, as are induced polarization measurements. Electromagnetic measurements can be strongly influenced by the presence of permafrost as well.

Prospecting Geophysics Field Example

Figures 9, 10 and 11 illustrate some geophysical responses from a well-connected sulphide body in permafrost terrain. The body is shown at "S" in the map of Figure 8. In the neighbourhood of this body permafrost is about 300 metres thick.

Figure 9 shows VLF-EM responses over the body. The dip-angle anomaly is much as one would expect in unfrozen terrain. There is a significant reversed-quadrature response which suggests that the host rock to some depth has a significant conductivity. The VLF resistivity profile in Figure 9 shows a strong resistivity low over the sulphide body and other auxiliary lows which may correlate with secondary mineralization or changes in rock type. Figure 10 shows the SP response observed over the body. Since SP responses are unpredictable in any case, it is difficult to say whether this response is different from that which would be observed

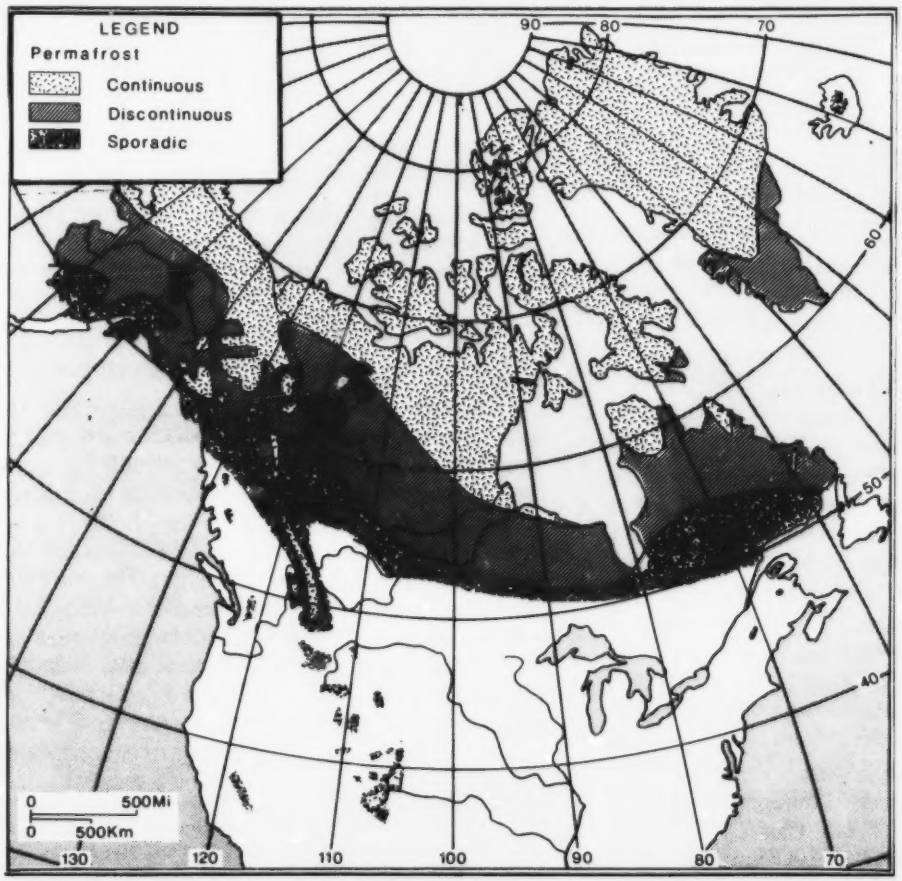

Figure 8: *Map showing the distribution of permafrost and sites mentioned in the text. (Map after Harris, 1986). F-Fairbanks, C-Canol Road, W-Willow Lake River, S-Sulphide Body.*

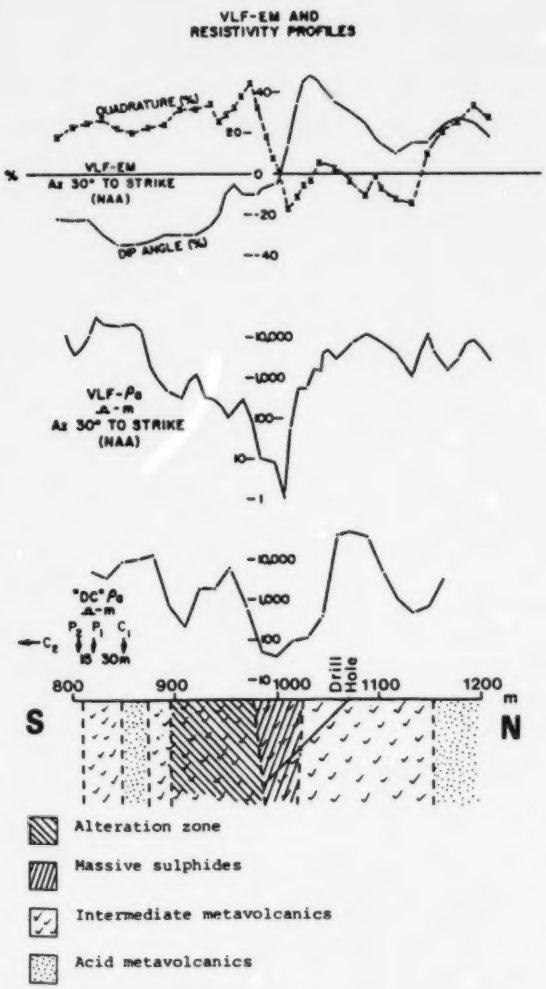

Figure 9: *Responses over sulphide body in permafrost: VLF EM, VLF resistivity and DC resistivity.*

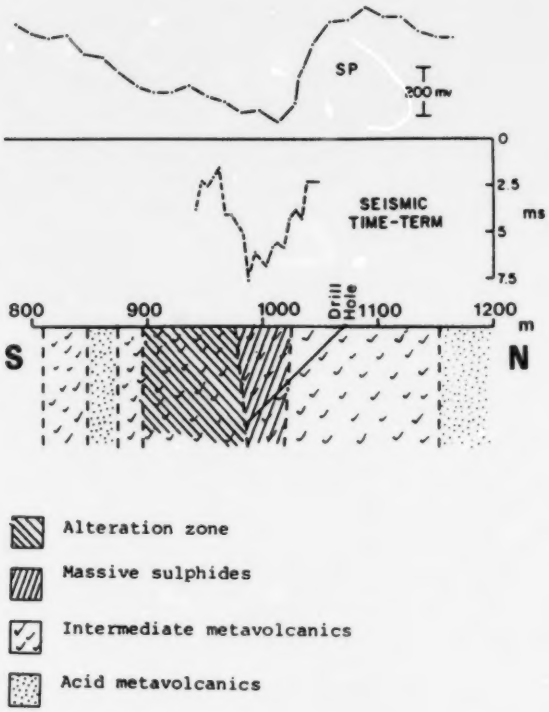

Figure 10: *Responses over sulphide body in permafrost: SP and refraction seismic (interpreted depth of late-summer thaw).*

in an unfrozen region. Figure 10 also shows an interpretation based on refraction seismic measurements which shows an increased depth of thaw in the region of the sulphide body. Since these measurements were taken in late summer, it is likely that the greater thaw is related to the high thermal conductivity of the sulphides. There is a good correlation between the seismically-interpreted depth of thaw and the variation of the apparent resistivity. Figure 11 shows induced polarization responses in both frequency domain and time domain obtained on the same line over this body. The IP responses over the sulphides are of the magnitude to be expected even in unfrozen ground. There is, however, a second IP response to the north which could arise from clay mineralization in faulting, or from presently-unrecognized disseminated mineralization. To the south there is considerable variation in the IP response which could result from frozen clays in the overburden, or from small sulphide concentrations in the bedrock.

Most geophysical techniques can be used in permafrost for prospecting for metallic sulphides. In interpreting the data, however, one must bear in mind the possible influences of frozen ground on the observed responses.

Mapping Permafrost with Geophysics

Since sub-zero temperatures exert a large influence on electrical and seismic properties of geologic materials, it is possible to use geophysical techniques to map the distribution of permafrost, to estimate the depth to the top and also to estimate the thickness and ice content. Figure 12 after Hoekstra (1978) shows measurements of electrical resistivity in a region of discontinuous permafrost. The data were obtained by means of inductive resistivity measurements with the Geonics EM 31 and by Radiohm measurements (VLF and LF magnetotelluric measurements) with the Geonics EM16R and EM 32. There is a clear correlation between the high resistivities and the presence of frozen ground. The inductive resistivity technique has become the standard method for mapping permafrost distribution in the discontinuous zone. (Kay et al, 1983).

If high resistivity bedrock comes near the surface in a zone of discontinuous permafrost, its presence can interfere

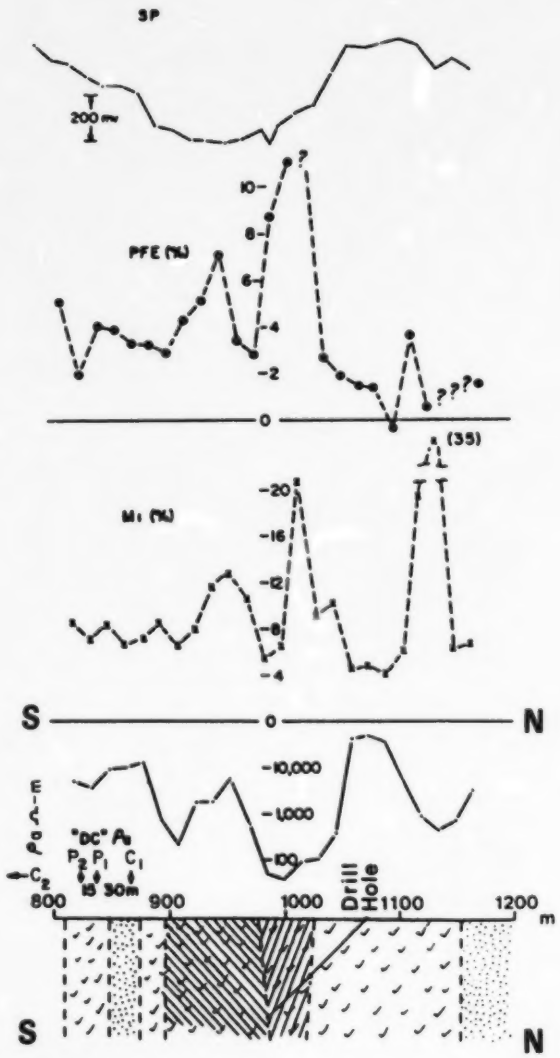

Figure 11: *Responses over sulphide body in permafrost: SP, induced polarization in frequency and time domains, and DC resistivity.*

with the interpretation of simple electromagnetic resistivity data. Figure 13 shows data obtained on a profile between Willow Lake River and River Between Two Mountains in the Mackenzie Valley, (area "W" in Figure 8). Measurements were made using DC resistivity techniques, VLF resistivity

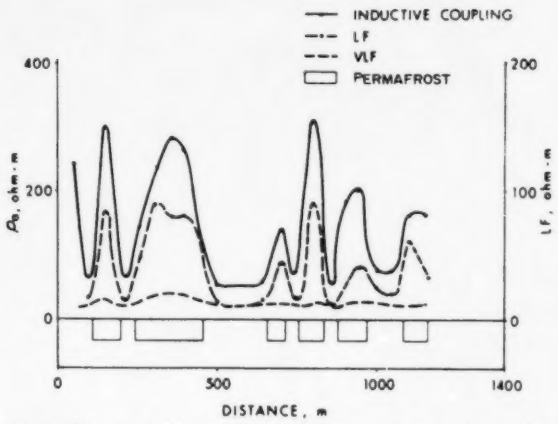

Figure 12: *Resistivity profiles in discontinuous permafrost, after Hoekstra (1978).*

techniques and refraction seismic. The phase angle measured in the VLF technique gives an indication of the sense of resistivity change with depth. Phase angles greater than 45° imply a decrease in resistivity with depth, such as occurs when near-surface permafrost overlies unfrozen soils. Phase angles less than 45° imply an increase in resistivity with depth. Thus the phase angle can be used to discriminate between shallow, high-resistivity features such as frozen ground and deep, high-resistivity features such as bedrock. The correlations among the electric and seismic measurements in the section of Figure 13 have been used to map the distribution of permafrost. Figure 14 shows drilling used as control for the interpretation.

Thus electrical, electromagnetic and seismic techniques can be used to map the distribution of permafrost. In simple cases, electromagnetic resistivity measurements will suffice but in areas of complicated geology, complementary measurements allow a greater sophistication of interpretation.

Measurements of depth of thaw can also be undertaken electromagnetically or seismically. Figure 15 after Sellmann *et al.*, (1979) shows electrical measurements over a test area near Fairbanks ("F" in Figure 8) in which systematic disturbance of the ground surface has resulted in a large variation in depth of thaw. Higher apparent resistivities correlate with shallower thaw depths. On the basis of these measurements, an estimate of variation of thaw depth can be obtained.

Figure 16 after Scott and Hunter (1977) shows results of DC resistivity measurements in the region of the Canol Road, across the Mackenzie River from Norman Wells ("C" in Figure 8). The Canol Road was built in the period from 1942 to 1945 and was abandoned in 1945. The road is associated with a marked decrease in apparent resistivity which correlated with an increased depth of thaw. Figure 17 shows the results of seismic refraction measurements across the Canol Road to estimate the depth of thaw. The reliability of the seismic and electrical measurements is borne

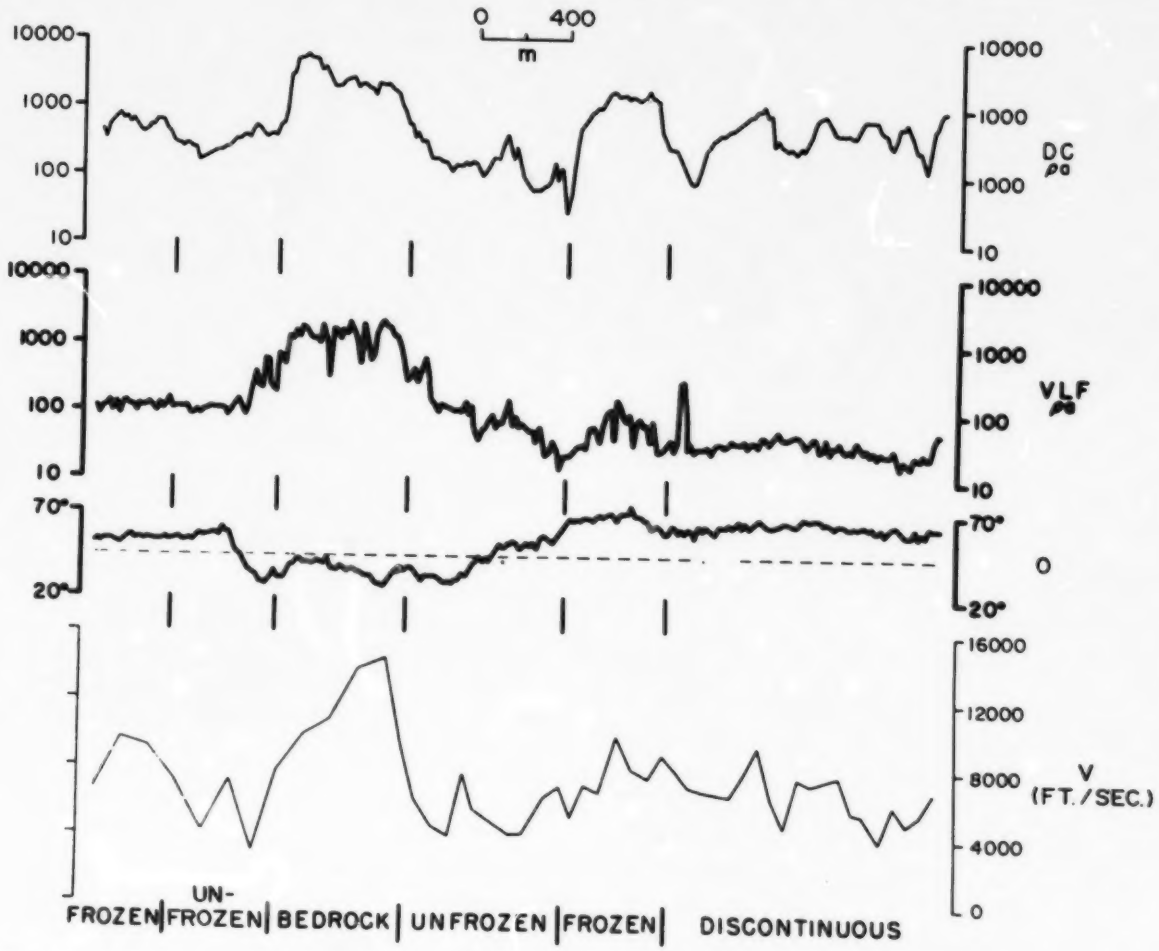

Figure 13: *Profiles in discontinuous permafrost: DC resistivity, V.L.F resistivity and phase angle, and seismic velocity.*

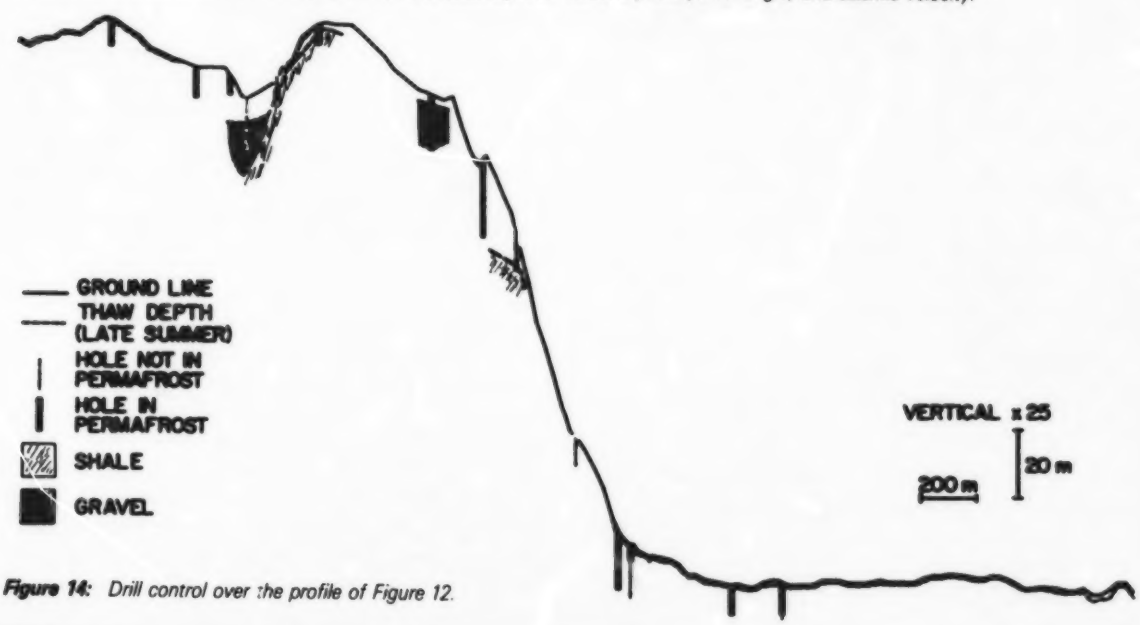

Figure 14: *Drill control over the profile of Figure 12.*

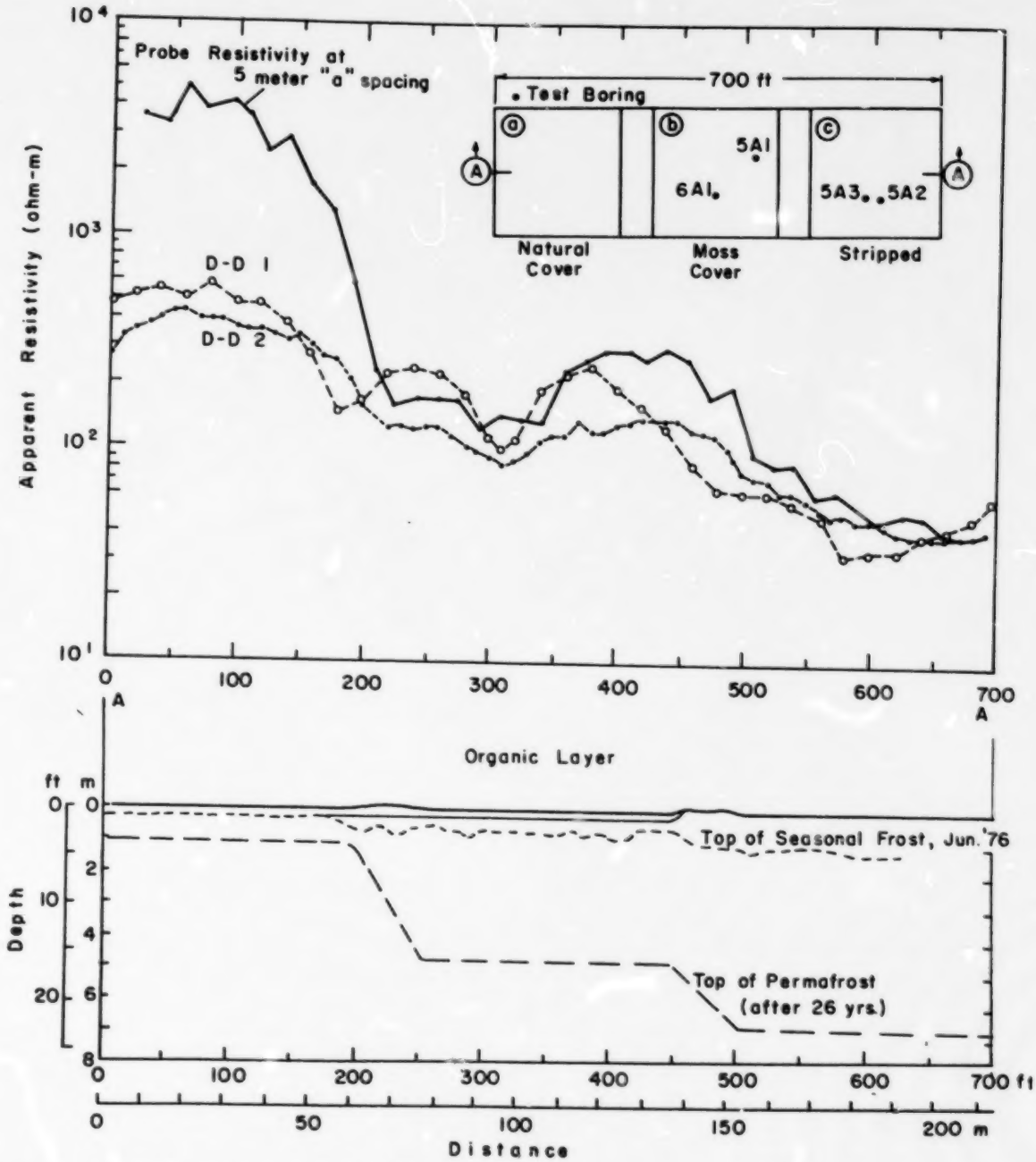

Figure 15: *Profiles over varying depths of thaw, after Sellmann et al., (1979).*

out by the results of drilling on one profile shown in Figure 18.

The ice content of frozen ground can be inferred from measurements of seismic velocity and electrical resistivity. Figures 19a and b show the dependence of velocity and resistivity respectively on ice content for a range of geologic materials. From these results, it is obvious that if a reliable estimate of velocity or resistivity can be obtained and if the geologic material is known then an estimate of ice content can be made.

Current practice in mapping permafrost distribution and estimating depth of thaw is to employ electromagnetic resistivity measurements. The use of non-contracting electromagnetic instruments such as the Geonics EM 31 and EM

Figure 16: *Contours of apparent resistivity over part of the Canol Road, N.W.T., after Scott and Hunter (1977). Grid over which values are contoured on left is shown in Figure 17.*

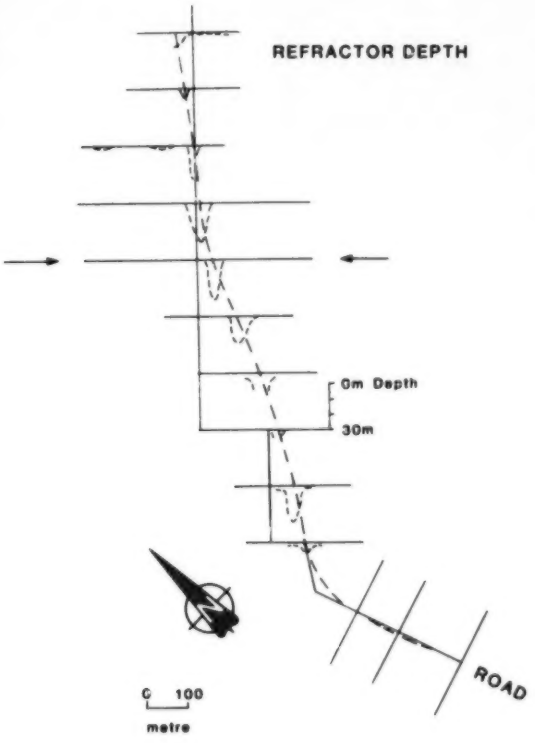

Figure 17: *Grid over which apparent restivity shown in Figure 16 was obtained. Seismically interpreted depths of thaw are shown for part of the grid. After Scott and Hunter (1977).*

34 allows efficient rapid survey over considerable distances. With adequate drilling control, depth of thaw can be estimated from these results as well. Figure 20 after Kay *et al.*, (1983) shows a typical set of results from a winter survey with EM 31 and 34. Where geologic complexity warrants, further geophysical techniques can be employed to improve the accuracy of interpretation.

Ground-probing radar can be used to map depth of thaw with high resolution, providing soils are coarse-grained enough to permit penetration to the frozen interface, (Pilot *et al*, 1980, Kovacs and Morey, 1985).

In areas where permafrost thickness is several hundreds of metres, estimates of thickness can be obtained by DC resistivity soundings or by electromagnetic measurements in time domain or frequency domain. D.C. resistivity soundings are limited because a great lateral distance is required to achieve the required penetration, and permafrost rarely remains constant in thickness over the distance involved (Scott and Mackay, 1977). Frequency-domain soundings have been applied in Alaska, (Daniels *et al*, 1976), to provide static connections for seismic interpretations. Similar surveys have been performed with a time-domain electromagnetic system in the Mackenzie Delta, N.W.T. with reasonable success, (Rozenberg *et al*, 1985).

Summary

This paper has considered the influence of permafrost on geophysical prospecting techniques and conversely the geophysical techniques which can be used for the mapping of permafrost. Magnetic and radiometric techniques are

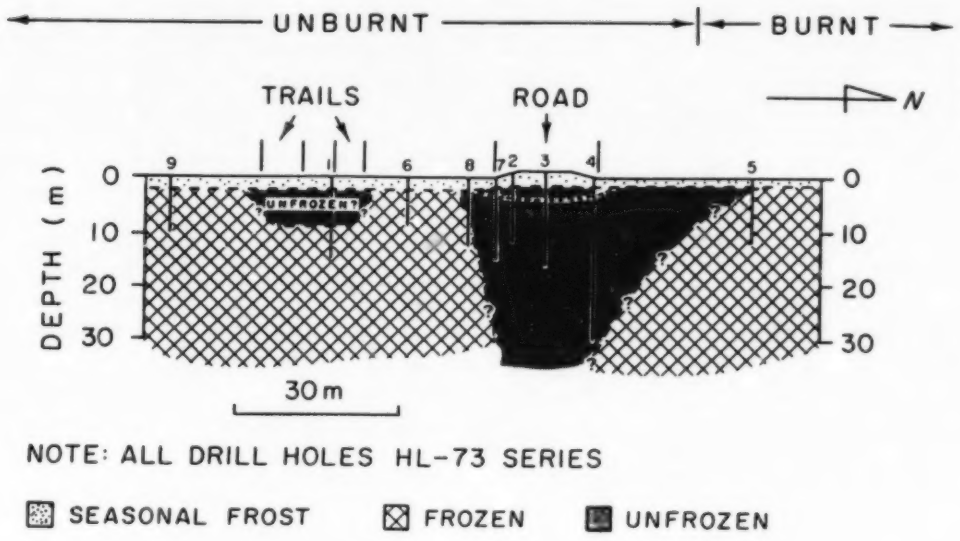

Figure 18: *Drilling results over profile marked with arrow in Figure 17.*

NOTE: ALL DRILL HOLES HL-73 SERIES

SEASONAL FROST FROZEN UNFROZEN

UPHOLE WAVE FRONT DIAGRAMS

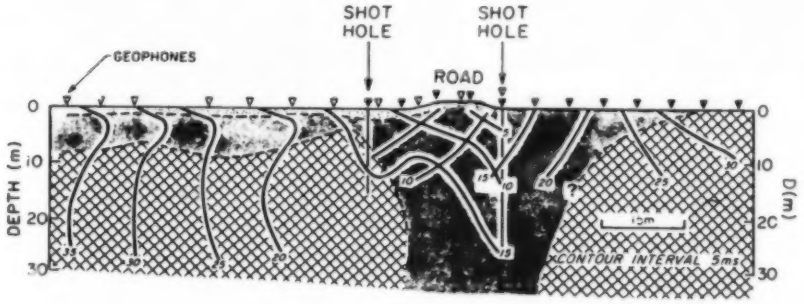

DETAILED RESISTIVITY

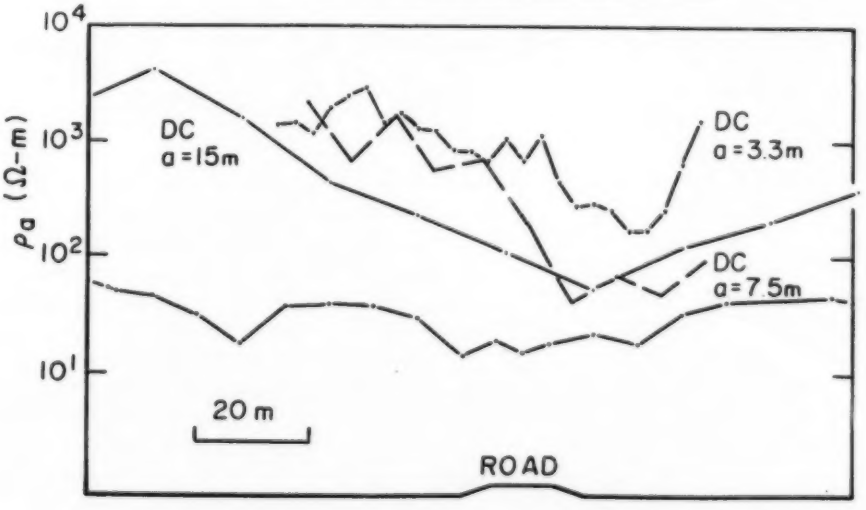

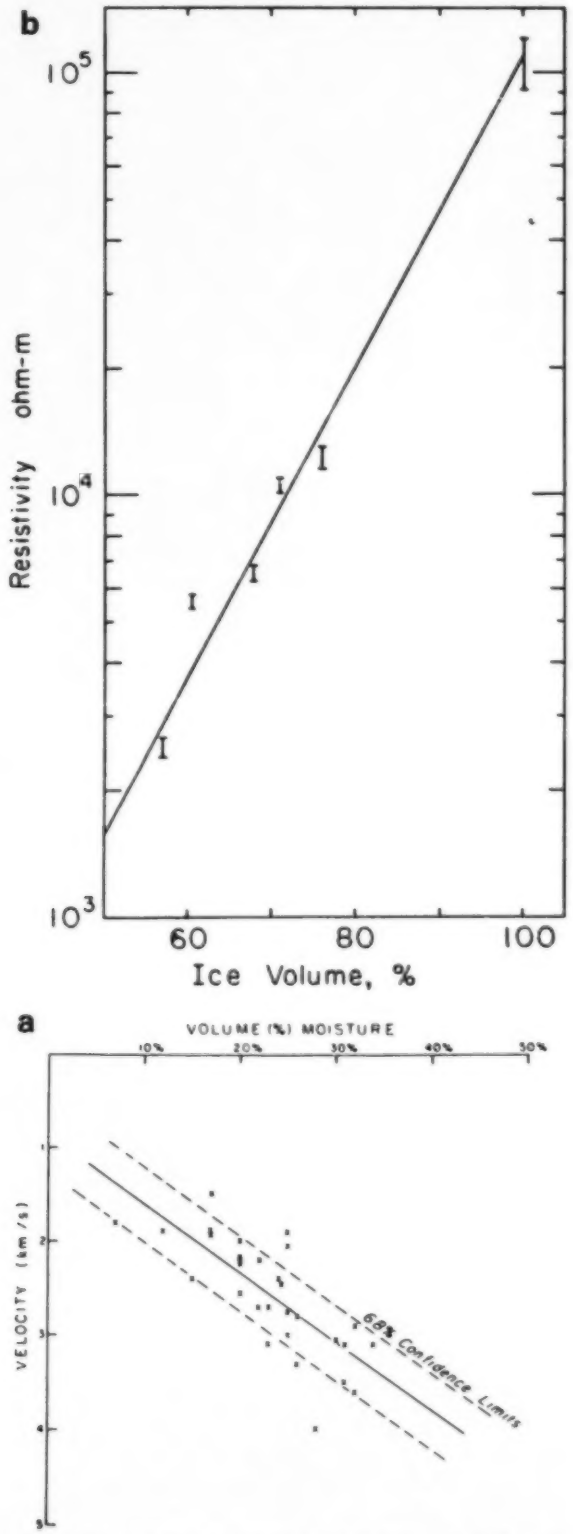

Figure 19: ***a)*** *Velocity (after Scott and Hunter, 1977)* ***b)*** *Resistivity (after Hoekstra et al., 1973) as a function of ice content.*

essentially independent of the presence of permafrost. Gravity measurements are also independent of permafrost unless significant ground ice is present. Seismic, electric and electromagnetic measurements, however, can be strongly influenced by permafrost. An understanding of such influences is necessary for the proper employment of these techniques for prospecting in permafrost regions. The sensitivity of these techniques to the presence of permafrost, however, enhances their utility for mapping permafrost distribution and for estimating the depth to its top and its ice content.

References

Anderson, D.M., and Morgenstern, N.R., 1973. Physics, chemistry and mechanics of frozen ground: a review. Proceedings of the Second International Permafrost Conference, p. 257-288.

Aptikaev, F.F., 1964. Temperature field effect on the distribution of seismic velocities in the permafrost zone: Akad Nauk SSSR Sibjrskoe otd-ie. Inst. Merzlotovedeniia. Teplovye protesessy v merzlykh porod.

Clayton, R. Hugh, 1966. A ground survey at Strathcona Sound, N.W.T. in Mining Geophysics, Volume 1: Case Histories, p. 142-150. Society of Exploration Geophysicists, Tulsa, Oklahoma.

Daniels, J.J., Keller, G.V. and Jacobson, J.J. 1976. Computer-assisted interpretation of electromagnetic soundings over a permafrost section. Geophysics, 41, pp. 752-765.

Harris, S.A., 1986, Permafrost distribution, zonation, and stability along the eastern ranges of the cordillera of North America. Arctic, vol. 34, p. 29-38.

Hatlelid, W.G. and MacDonald, J.R., 1982, Permafrost determination by seismic velocity analyses, Jour. CSEG, Vol. 18, no. 1.

Hoekstra, P., 1978. Electromagnetic methods for Mapping Shallow Permafrost, Geophysics, vol. 43. no. 4, p. 782-787.

Hoekstra, P., and McNeill, J.D., 1973. Electromagnetic Probing of Permafrost. North American Contribution – Permafrost Second International Conference, p. 517.

Hoekstra, P., Sellmann, P.V., and Delaney, A.J., 1974. Airborne resistivity mapping of permafrost near Fairbanks, Alaska: U.S. Army Cold Regions Research and Engineering Laboratory, Research Report 324.

Kay, A.E., 1981. The effects of low temperature on the induced polarization response of Mississippi Valley-type Ore samples. M.Sc. Thesis, Dept. of Geology and Geophysics, University of Calgary.

Kay, A.E., Allison, Andrea M., Scott., William J. and Botha, Willem J., 1983. Continuous Geophysical Investigation for mapping permafrost distribution, Mackenzie Valley, N.W.T., Canada. Proc. IV Int. Conf. on Permafrost, p. 578-583.

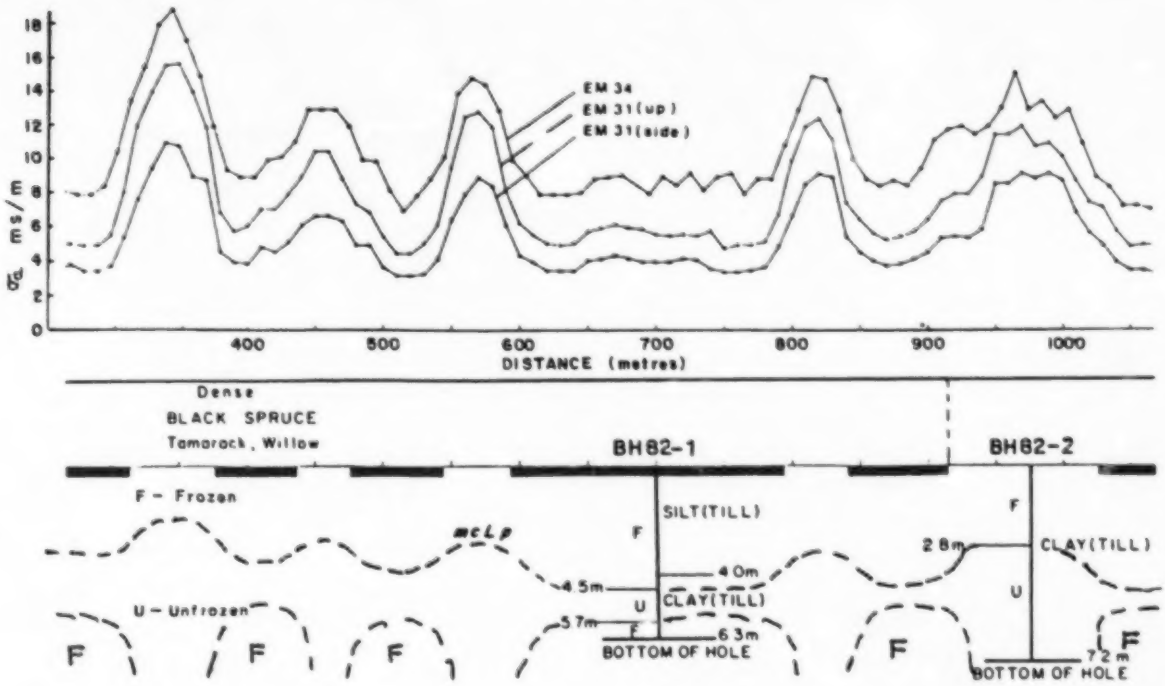

Figure 20: *Typical results in mapping permafrost with EM31 and 34 in discontinuous zone (after Kay et al, 1983).*

Kovacs, A., and Morey, R.M., 1985. Impulse radar soundings of frozen ground, *in* Proc. Workshop on Permafrost Geophysics, October 1984, US Army Corps of Engineers Spec. Rep. 85-5, p. 28-40.

McLaren, P., Scott, W.J., and Hunter, J.A., 1975. The implications of geophysical studies on the permafrost regime and surficial geology. Melville Island and Byam Channel, N.W.T in Geol. Survey Canada Paper, p. 343-351.

Olhoeft, G.R., 1975. The electrical properties of permafrost: Ph. D. Thesis, Dept. of Physics, University of Toronto.

Pandit, B.I. and King, M.S., 1979. A study of the effects of porewater salinity on some physical properties of sedimentary rocks at permafrost temperatures: Can. J. Earth Sci., vol. 16, no. 8, p. 1566-1580.

Petera, V., 1973. The problem of studying charge generation on the phase interface of 10^{-3} molar sodium chloride solution undergoing directed freezing: *in* Physical Methods of Studying Ice and Snow, V.V. Bogordoskii, ed. p. 79-87.

Pilon, J., Annan, A.P., Davis, J.L., and Gray, J.T., 1980. Comparison of thermal and radar measurements of the active layer thickness in the Leaf Bay area, New Quebec. Proc. Symp. Permafrost Geophysics, Nov., 1978. National Res. Counc. Can., Tech. Man. 128, p. 70-83.

Rampton, V.N. and Walcott, R.I., 1974. Gravity profiles across ice-cored topography: Can. J. Earth Sci., vol. 11, no. 1, p. 110-122.

Rozenberg, G.S., Henderson, J.D., Sartorelli, A.N., and Judge, A.S., 1985. Some aspects of transient electromagnetic soundings for permafrost delineation, *in* Proc. Workshop on Permafrost Geophysics, October, 1984. US Army Corps of Engineers, Spec. Rep. 85-5, p. 74-90.

Scott, W.J., and Mackay, J.R., 1977. Reliability of permafrost thickness determination by D.C. resistivity sounding. Proc. Symp. Permafrost Geophysics, Oct. 1976. Nat. Res. Counc. of Can., Tech. Man. No. 119, p. 25-38.

Scott, W.J., and Hunter, J.A., 1977. Applications of Geophysical Techniques in Permafrost Regions, Can. Jour. Earth Sci., vol. 14, no. 1, p. 117-127.

Sellmann, P.V., Delaney, A.J., Arcone, S.A., 1979. An electromagnetic geophysical survey at an Interior Alaska Permafrost Exposure. U.S. Army, CRREL Special Report. S.R.-79-14.

Telford, W.M., Geldart, L.P., Sheriff, R.E., and Keys, D.A., 1976. Applied Geophysics. Cambridge: Cambridge University Press, 860 p.

Yarkin, I.G., 1973. Effect of natural electric potentials on water migration in freezing soils in 2nd International Conference on Permafrost, Translation published by National Academy of Sciences, Washington, D.C. 1978, p. 359-361.